For Reference

NOT TO BE TAKEN FROM THIS ROOM

For Reference

NOT TO BE TAKEN FROM THIS ROOM

Ex LIBRIS
UNIVERSITATIS
ALBERTAENSIS

UNIVERSITY OF ALBERTA
QUAECUMQUE VERA

University of Alberta
Printing Department

Digitized by the Internet Archive
in 2018 with funding from
University of Alberta Libraries

https://archive.org/details/rheologicalbehav00prow

esis
1964
#62

THE UNIVERSITY OF ALBERTA

# THE RHEOLOGICAL BEHAVIOR OF A THIXOTROPIC MODEL

by

D.R. Prowse, B.Sc.

A THESIS

SUBMITTED TO THE FACULTY OF GRADUATE STUDIES

IN PARTIAL FULFILLMENT OF THE REQUIREMENTS FOR THE

DEGREE OF MASTER OF SCIENCE

DEPARTMENT OF CHEMICAL ENGINEERING

EDMONTON, ALBERTA

MARCH, 1964

ABSTRACT

Using the Alberta rotational viscometer contained within a modified temperature control cabinet, the rheological behaviour of a non-Newtonian thixotropic model has been investigated at 60°F.

The model, a commercial light oil into which a partially refined wax fraction was dissolved, owes its rheological characteristics at test temperature to a loosely bonded network of wax crystals or wax clusters. The network structural properties, and hence, the rheological behaviour of the model, were shown to be markedly dependent upon (i) temperature, (ii) sample handling procedure, including rate of cooling to test temperature, and (iii) duration of curing at test temperature.

Utilizing the influence of the above variables on network formation characteristics, two distinctly different networks were prepared at test temperature. The first network was prepared by quick quenching a test sample from 85°F to 60°F and then curing the sample at this temperature for four hours; the second network was prepared by slow cooling a prepared sample from 85°F to 60°F at 0.43°F/minute and then curing the sample for four hours.

The resultant networks were subjected to each of several constant shear rates, ranging from 20 $sec^{-1}$ to 320 $sec^{-1}$, and the structural shear degradation characteristics measured for periods of up to four hours.

Subsequently, the experimental data was processed and correlated on the basis of a theory of thixotropic behaviour proposed by R.A. Ritter (i.e. Theory of Thixotropic Behaviour: Ph.D. Thesis, University of Alberta, Edmonton (1961) ).

# ABSTRACT

Using the Alberta rotational viscometer contained within a modified temperature control cabinet, the rheological behaviour of a non-Newtonian thixotropic model has been investigated at 60°F.

The model, a commercial light oil into which a partially refined wax fraction was dissolved, owes its rheological characteristics at test temperature to a loosely bonded network of wax crystals or wax clusters. The network structural properties, and hence, the rheological behaviour of the model, were shown to be markedly dependent upon (i) temperature, (ii) sample handling procedure, including rate of cooling to test temperature, and (iii) duration of curing at test temperature.

Utilizing the influence of the above variables on network formation characteristics, two distinctly different networks were prepared at test temperature. The first network was prepared by quick quenching a test sample from 85°F to 60°F and then curing the sample at this temperature for four hours; the second network was prepared by slow cooling a prepared sample from 85°F to 60°F at 0.45°F/minute and then curing the sample for four hours.

The resultant networks were subjected to each of several constant shear rates, ranging from 20 $sec^{-1}$ to 320 $sec^{-1}$, and the structural shear degradation characteristics measured for periods of up to four hours.

Subsequently, the experimental data was processed and correlated on the basis of a theory of thixotropic behaviour proposed by R.A. Hitter (i.e. Theory of Thixotropic Behaviour: Ph.D. Thesis, University of Alberta, Edmonton (1961) ).

Correlation of the slow cooled sample thixotropic curves proved most satisfactory with an average deviation of only 1.8 percent between experimentally measured and predicted curves. However, primarily due to a reproducible "hump" on otherwise regularly defined experimental curves, correlation of the quick quenched sample experimental results was less satisfactory. For this latter case maximum deviations between predicted and experimental results were as high as 13.2 percent (i.e. overall average deviation of 5.0 percent) which was more than double the estimated cumulative experimental and correlative error of 5 percent.

Thus, it was concluded, that at its present stage of development, the Theory of Thixotropic Behaviour correlates and predicts the shear degradation characteristics of specific thixotropic networks only. To include behaviour such as was measured for quick quenched sample networks, further development and extension of the Theory is required.

ACKNOWLEDGEMENTS

The author wishes to express his sincere appreciation to Dr. R.A. Ritter whose supervision, criticism and assistance has been invaluable throughout this investigation.

# TABLE OF CONTENTS

ABSTRACT

TABLE OF CONTENTS i

LIST OF TABLES iv

LIST OF FIGURES v

INTRODUCTION 1

INTRODUCTION TO RHEOLOGICAL CLASSIFICATION OF FLUIDS 4

EXPERIMENTAL DETERMINATION OF RHEOLOGICAL PARAMETERS 15

ANOMOLOUS BEHAVIOUR, STRUCTURE FORMATION AND THIXOTROPIC BEHAVIOUR 23

MATHEMATICAL THEORIES OF THIXOTROPIC BEHAVIOUR 28

Theory of Thixotropic Behaviour (Ritter) 31

TYPICAL THIXOTROPIC SYSTEMS

Hydrocarbon Systems 39
Plastic Fats 47

PHYSICAL PROPERTIES OF WAX-SOLVENT SYSTEMS 49

EXPERIMENTAL PROGRAM

I. RHEOLOGICAL TEST APPARATUS
Redesign and Reassembly of the Auxilliary Equipment Associated with the Alberta Rotational Viscometer 52
Description of the Alberta Rotational Viscometer and Associated Temperature Control Equipment 53
Operational Characteristics of the Alberta Viscometer 62
(1) End Effect of the Bob 63
(2) Flow Stability in the Viscometer Annulus 65
(3) Test Sample Heating Effects During Shear 69

II. SELECTION OF A THIXOTROPIC MODEL
Selection of a Thixotropic Model 72
Physical Properties and Treatment of the Components of the Thixotropic Model 82
(1) Parawax 82
(2) CWO Oil 83
(3) Thixotropic Model Preparation 83

III. RHEOLOGICAL BEHAVIOUR OF THIXOTROPIC MODEL
Network Formation Characteristics of the Thixotropic Model 83
Selection of the Experimental Test Program 95
Rheological Test Sequence and Viscometeric Testing Procedure 98
Experimental Results 100

CORRELATION OF EXPERIMENTAL DATA 119

I. DATA PROCESSING AND CORRELATION OF THE SLOWLY COOLED SAMPLE THIXOTROPIC DECAY CURVES
Data Processing of Slowly Cooled Sample Decay Curves 120
Correlation of Thixotropic Decay Data for Slowly Cooled Samples 125

II. DATA PROCESSING AND CORRELATION OF THE THIXOTROPIC DECAY CURVES FOR THE QUICK QUENCHED SAMPLES
Data Processing of the Thixotropic Decay Curves for the Quick Quenched Samples 132
Correlation of Thixotropic Decay Curves for Quick Quenched Samples 133

DISCUSSION OF EXPERIMENTAL PROGRAM AND EXPERIMENTAL RESULTS 144

CONSIDERATIONS INVOLVING PIPELINE FLOW OF THE EXPERIMENTAL MODEL 149

RECOMMENDATIONS FOR FUTURE STUDIES 152

CONCLUSIONS 153

NOMENCLATURE 154

BIBLIOGRAPHY 157

APPENDICES

APPENDIX ONE - Air Circulation and Refrigeration Systems

APPENDIX TWO - Cabinet Temperature Control System

APPENDIX THREE - Experimental Equipment Calibrations

APPENDIX FOUR - Sample Heating Effects During Shear

APPENDIX FIVE - Preliminary Testing Schedules and Test Results Involving Test Sample Reproducibility

APPENDIX SIX - Considerations During Sample Preparation

APPENDIX SEVEN - Tabulated Experimental Rheological Test Data

APPENDIX EIGHT - Sensitivity Analysis of Correlation of Experimental Data Using THEORY OF THIXOTROPIC BEHAVIOUR (Ritter)

APPENDIX NINE - Processed and Computed Rheological Data

APPENDIX TEN - Tabulated Calculations for Pipeline Flow of Thixotropic Model

# LIST OF TABLES


| Table Number | Title | Page |
|---|---|---|
| 1. | Summary of Recent Theories of Thixotropic Behaviour | 30 |
| 2. | Experimental Thixotropic Test Reproducibility | 116 |
| 3. | Evaluation of Rate Decay Constant for Slowly Cooled Sample Thixotropic Decay Curves | 131 |
| 4. | Error Analysis in Prediction of Experimental Shear Stress of Slowly Cooled Test Samples | 132 |
| 5. | Evaluation of Rate Decay Constant for Quickly Quenched Sample Thixotropic Decay Curves: I - Smoothed Data | 138 |
| 6. | Evaluation of Rate Decay Constant for Quickly Quenched Sample Thixotropic Decay Curves: II - Unsmoothed Data | 138 |
| 7. | Error Analysis in Prediction of Experimental Shear Stress of Quickly Quenched Test Samples | 142 |

# LIST OF FIGURES


| Figure Number | Title | Page |
|---|---|---|
| 1 | Rheological Flow Curves for Time Independent Fluids | 8 |
| 2 | Rheological Behaviour of a Thixotropic Fluid | 12 |
| 3 | Comparison Between Rate of Shear Stress Growth for Thixotropic and False-Body Materials | 13 |
| 4 | Correlation of Experimental Thixotropic Data in Terms of Theory of Thixotropic Behaviour - Ritter(1) | 37 |
| 5 | Typical Thixotropic Decay Curves of Residual Fuel Oil at $52^{o}F$ and 13.18 $Sec^{-1}$ Shear Rate - Ackroyd(16) | 41 |
| 6 | Increase in Initial Shear Stress With Time of an Oil Sheared to Equilibrium - Ackroyd(16) | 43 |
| 7 | Typical Thixotropic Decay Curve and Shear Stress Growth Curves - Ritter(1) | 45 |
| 8 | Thixotropic Shear Stress Versus Shear Rate with Time as a Parameter - Ritter(1) | 46 |
| 9 | Schematic Drawing of Cabinet Addition and Air Flow System | 54 |
| 10 | Back View of Cabinet Showing Cooling Coils, Louver and Louver Drive Motor | 55 |
| 11 | Refrigeration System | 56 |
| 12 | Cabinet Air Temperature Control System | 57 |
| 13 | Cup Speed Measuring System | 58 |
| 14 | Alberta Rotational Viscometer | 60 |
| 15 | Illustration of Flow Stability in Alberta Viscometer Annulus | 68 |
| 16 | Initial Sample Handling and Rheological Test Sequence | 76 |

| | | |
|---|---|---|
| 17 | Illustration of Non-Reproducible Thixotropic Behaviour With Continued Re-use of Only One Test Sample | 77 |
| 18 | Illustration of Thixotropic Reproducibility Using Developed Sample Preparation Sequence | 80 |
| 19 | Sample Preparation and Handling Sequence | 81 |
| 20 | Viscosity of CWO Oil Versus Reciprocal of Absolute Temperature | 84 |
| 21 | Incremental Volume Change in Thixotropic Model Versus Temperature | 86 |
| 22 | Illustration of Dependence of Model Rheological Behaviour on Temperature | 87 |
| 23 | Static Test Behaviour of Thixotropic Model Network at 60°F | 89 |
| 24 | Yield Value of Thixotropic Model Versus Temperature | 91 |
| 25 | Influence of Cure Time on Rheological Behaviour of Slowly Cooled Test Samples | 93 |
| 26 | Influence of Cure Time on Rheological Behaviour of Quick Quenched Test Samples | 94 |
| 27 | Experimental Test Program | 97 |
| 28 | Thixotropic Shear Stress Decay Curve- Slowly Cooled Sample Test: Cup Speed = 0.300 RPS | 101 |
| 29 | Thixotropic Shear Stress Decay Curve- Slowly Cooled Sample Test: Cup Speed = 0.800 RPS | 102 |
| 30 | Thixotropic Shear Stress Decay Curve - Slowly Cooled Sample Test: Cup Speed = 2.00 RPS | 103 |
| 31 | Thixotropic Shear Stress Decay Curve - Slowly Cooled Sample Test: Cup Speed = 4.50 RPS | 104 |
| 32 | Thixotropic Shear Stress Decay Curve - Quick Quenched Sample Test: Cup Speed = 0.300 RPS | 105 |
| 33 | Thixotropic Shear Stress Decay Curve- Quick Quenched Sample Test: Cup Speed = 0.800 RPS | 106 |

| | | |
|---|---|---|
| 34 | Thixotropic Shear Stress Decay Curve - Quick Quenched Sample Test: Cup Speed = 2.00 RPS | 107 |
| 35 | Thixotropic Shear Stress Decay Curve - Quick Quenched Sample Test: Cup Speed = 4.50 RPS | 108 |
| 36 | Shear Stress Growth Curve - Slowly Cooled Sample Test: Cup Speed = 0.300 RPS | 109 |
| 37 | Shear Stress Growth Curve - Slowly Cooled Sample Test: Cup Speed = 0.800 RPS | 110 |
| 38 | Shear Stress Growth Curve- Slowly Cooled Sample Test: Cup Speed = 2.0 RPS | 111 |
| 39 | Shear Stress Growth Curve - Quick Quenched Sample Test: Cup Speed = 0.300 RPS | 112 |
| 40 | Shear Stress Growth Curve - Quick Quenched Sample Test: Cup Speed = 0.800 RPS | 113 |
| 41 | Shear Stress Growth Curve- Quick Quenched Sample Test: Cup Speed = 2.0 RPS | 114 |
| 42 | Shear Stress Versus Cup Speed With Time as a Parameter - Slowly Cooled Sample Tests | 123 |
| 43 | Shear Stress Versus Shear Rate With Time as a Parameter - Slowly Cooled Sample Tests | 124 |
| 44 | Determination of Newtonian Component by Viscosity Extrapolation | 126 |
| 45 | Correlation of Experimental Data Using Theory of Thixotropic Behaviour (Equation 30) - Slowly Cooled Sample Tests | 130 |
| 46 | Shear Stress Versus Cup Speed With Time as a Parameter - Unsmoothed Experimental Data: Quick Quenched Sample Tests | 134 |
| 47 | Shear Stress Versus Shear Rate With Time as a Parameter - Unsmoothed Experimental Data: Quick Quenched Sample Tests | 135 |
| 48 | Shear Stress Versus Cup Speed With Time as a Parameter - Smoothed Experimental Data: Quick Quenched Sample Tests | 136 |

| | | |
|---|---|---|
| 49 | Shear Stress Versus Shear Rate With Time as a Parameter - Smoothed Experimental Data: Quick Quenched Sample Tests | 137 |
| 50 | Correlation of Experimental Data Using Theory of Thixotropic Behaviour (Equation 30) - Unsmoothed Experimental Data: Quick Quenched Sample Tests | 139 |
| 51 | Correlation of Experimental Data Using Theory of Thixotropic Behaviour (Equation 30) - Smoothed Experimental Data: Quick Quenched Sample Tests | 140 |
| 52 | Comparison Between Experimental and Predicted Shear Stress Using Evaluated Rate Constants - 300 $Sec^{-1}$ Shear Rate | 143 |
| 53 | Calculated Pipeline Flow Behaviour of Thixotropic Model for Various Flow States | 150 |


APPENDIX


| | | |
|---|---|---|
| 1-A | Schematic of Assembled Refrigeration System | 1-4 |
| 1-B | Dynamic Cooling Characteristics of Air Bath System | 1-6 |
| 2-A | Diagram of Air Bath Temperature Control System | 2-2 |
| 3-A | Calibration Curve of Cup Speed Versus Digital Voltmeter Output | 3-7 |
| 5-A | Preliminary Testing Schedule and Test Results | 5-2 |
| 8-A | Influence on Correlation of Test Data by Error in Determination of Initial Shear Stress | 8-6 |
| 8-B | Influence on Correlation of Test Data by Error in Determination of Limiting Shear Stress | 8-7 |
| 8-C | Influence on Correlation of Test Data by Error in Determination of Newtonian Component | 8-8 |
| 10-A | Growth of Shear Stress in a Test Sample at $60^{\circ}F$ After Slowly Cooling and Continuously Shearing Test Sample From $85^{\circ}F$ to $60^{\circ}F$ | 10-2 |
| 10-B | Shear Stress Versus Cup Speed With Temperature as a Parameter: Slowly Cooled and Continuously Sheared Test Samples | 10-3 |

# INTRODUCTION

Rheology, by definition and in scope, is concerned with the study of deformation and flow of matter. The rheological range of interest includes hydro- and aerodynamics, and in diversity, extends from the creep properties of concrete columns to the lubrication characteristics of air. In practice, however, the term has generally been used to refer to a somewhat narrower field; namely, the study of the rheological properties of those materials, mainly of industrial importance, which show a behaviour intermediate between those of solids and simple liquids. In this latter sense, rheology is concerned with the stress-strain-time relations in such materials and with the influence of such factors as temperature upon them.

Rheological behaviour and rheological measurements have generally been interpreted by, and are of interest to; the physical chemist, whose primary interest is at the submicroscopic level dealing with molecular interactions; the mathematician, who attempts to formulate ideal flow models with properties similar to those observed in rheological experiments; and the engineer who, from necessity, must develop design equations which accurately predict rheological behaviour.

Considering only the requirements of the last mentioned profession, it is interesting to note that the rate of progress in developing suitable rheological design equations has been remarkably slow. In fact, the only notable recent achievements (2,3,4) have been restricted to that class of anomolous fluids (i.e. non-Newtonian fluids) whose flow behaviour is independent of time.

Recently, however, a state equation has been presented*(1) for anomolous fluids whose flow characteristics include time as a pertinent variable. This equation, based on a mechanistic mathematical flow model, defines the rheological behaviour of thixotropic fluids; that is, fluids whose consistency, under prolonged shear, decreases with time. The usefulness of this equation was subsequently demonstrated(1) when experimental thixotropic shear stress measurements obtained from a naturally occurring thixotropic material, Pembina crude oil, were correlated within $\pm 3$ percent.

However, since only the thixotropic decay curves from one material (Pembina crude oil) had been correlated, the general applicability of the design equation with respect to other thixotropic substances was unknown. As well, one of the assumptions of the theory, that of a limiting thixotropic shear stress, had not been experimentally verified. Therefore, strong incentives existed for the experimental examination of other thixotropic materials and thereby, of further examination of the proposed state equation.

To this end, an experimental program was designed with the following objectives: (i) to prepare an artificial thixotropic substance which, since its constituents would be predetermined and varied as desired, could, for all practical purposes, be considered a thixotropic model; (ii) to measure the rheological behaviour of the model with specific emphasis on the measurement of thixotropic decay curves; and, (iii) to correlate the measured thixotropic curves on the basis of the proposed state equation (1). An additional and pre-requisite objective was the modification of existing rheological testing apparatus.

---

* Ritter, R.A.: "Theory of Thixotropic Behaviour"; Ph.D. Thesis, University of Alberta, Edmonton, Alberta (1961).

During the subsequent program, a suitable thixotropic model was prepared and tested using modified experimental equipment. The test results were interesting since although one set of experimental thixotropic curves was correlated satisfactorily by the proposed equation, a second set was not. In addition, several interesting observations were made concerning the preparation and rheological behaviour of the model which undoubtedly will be of interest to following investigators.

## INTRODUCTION TO RHEOLOGICAL CLASSIFICATION OF FLUIDS

Deformation is a movement or displacement of parts or particles of a material body relatively to one another such that the continuity of the body is not destroyed. The term is used both for a relative displacement in progress and for the state of displacement reached at any instant of time.

If under the actions of a constant finite force, the deformation of a body increases with time continuously and indefinitely, the material is said to flow. For such a condition, acceleration of body parts will continue until a steady rate of deformation is reached. If at this state, the body does not require forces to maintain deformation for a finite period, then the body may be classed as an "ideal" liquid.

Dependent solely upon the force field and environmental conditions, any material may be caused to flow. Real materials, of which the "ideal" liquid may be considered as the limiting case, exhibit a whole spectrum of rheological behaviour, ranging from dependence upon the rate of deformation and the deforming force to dependence only upon the extent of deformation (i.e. an elastic solid). There is an infinite variety of intermediate types of rheological behaviour, and in general, any classification of such behaviour in a rheologically consistent pattern must remain inadequate and arbitrary.

However, rheologists have often found convenience in categorizing materials in terms of their rheological equation of state, or in short, their rheological equation. Such a classification requires that the rheological behaviour of a material be approximated by an equation between stress, deformation, and their derivatives with respect to time. Parameters

appearing in the equation of state as coefficients or constants characterize the material, while stress and deformation are rheological variables.

As an introduction to specific rheological equations, consider for example, a thin layer of fluid between two parallel planes (of area A), a distance "y" apart, as illustrated below:

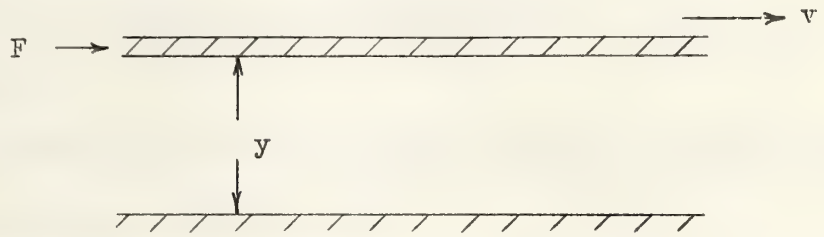


The bottom plane is fixed while the upper plane is being subjected to a constant force, F. At steady state conditions, the moving plate will reach a constant velocity, v, since the force F will be balanced by an opposite and equal force at the fluid-moving plate interface. If the fluid alone is considered, then a specific relationship will exist between the applied shear stress (i.e. where shear stress, $\tau = F/A$) and the fluid deformation. In view of this specification, rheologists(5) have found the following fluid classification convenient:

Category 1:

Fluids for which shear rate (i.e. dv/dy) depends only upon the imposed shearing stress, $\tau$.

where: $dv/dy = d(d\delta/dt)/dy$

$\delta$ = deformation, ft.

t = time, seconds

Category 2:

Fluids for which shear rate depends upon shear stress and the duration of the stress, t.

Category 3:

Fluids for which shear rate depends upon shear stress and the extent of the deformation, $\delta$.

Category 4:

Fluids for which shear rate depends upon shear stress and the intensity of an imposed magnetic field, H.

Category 5:

Fluids which must be considered as made up of discrete particles rather than continuous media.

Since the latter two categories are not of further interest in this manuscript, only the first three classifications shall be described.

Fluids of the first category have rheological properties independent of time, and may be described by a rheological equation of the form:

$$\frac{dv}{dy} = f(\tau) \qquad (1)$$

This equation implies that the rate of shear at any point in the fluid is a function only of the shear stress at that point. Conventionally, fluids with such behaviour have been further subdivided into three distinct types, dependent solely upon the nature of the function $f(\tau)$ in Equation (1). In order of increasing complexity, these types are:

(1) Newtonian fluids;

(2) Pseudoplastic fluids;

(3) Dilatant fluids.

For a Newtonian fluid, the shear rate is directly proportional to the applied shearing stress, the functional relationship between these two

variables being expressed as:

$$\tau = \mu_N \left(\frac{dv}{dy}\right) \qquad (2)$$

where the constant of proportionality $\mu_N$ is called the Newtonian viscosity. It should be noted that this constant completely characterizes the rheological behaviour of the fluid. Examples of Newtonian fluids include most monatomic fluids, light petroleum oil fractions, etc.

The flow behaviour of a pseudoplastic fluid is characterized by a marked non-linearity between shear rate and shear stress; that is, as shear rate increases, the ratio of shear stress to shear rate decreases. Usually this ratio, sometimes called the "apparent viscosity", $\mu_A$, attains a limiting value at very high shear rates, dependent of course, on the individual fluid being sheared. A typical example of such behaviour is shown in Figure (1). It should be noted that pseudoplastic behaviour occurs in many long chain polymer-solvent systems.

On a logarithmetic plot of shear stress versus shear rate (Figure 1), the flow curve of a pseudoplastic material is often found to be linear over a fairly wide range of shear rates. Consequently, an empirical power law functional relationship has often been used(2,6) to approximate such behaviour. The assumed relation may be written as:

$$\tau = k \left(\frac{dv}{dy}\right)^n \qquad (3)$$

The theoretical significance of such an equation has been extensively debated(6) but for polymer-solvent systems, this phenomenon appears related to shear alignment and intermolecular interaction of long chain molecules

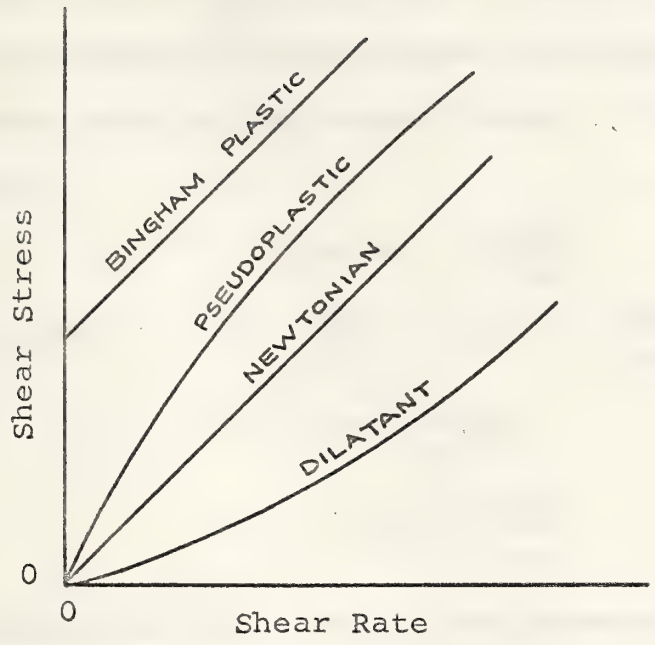


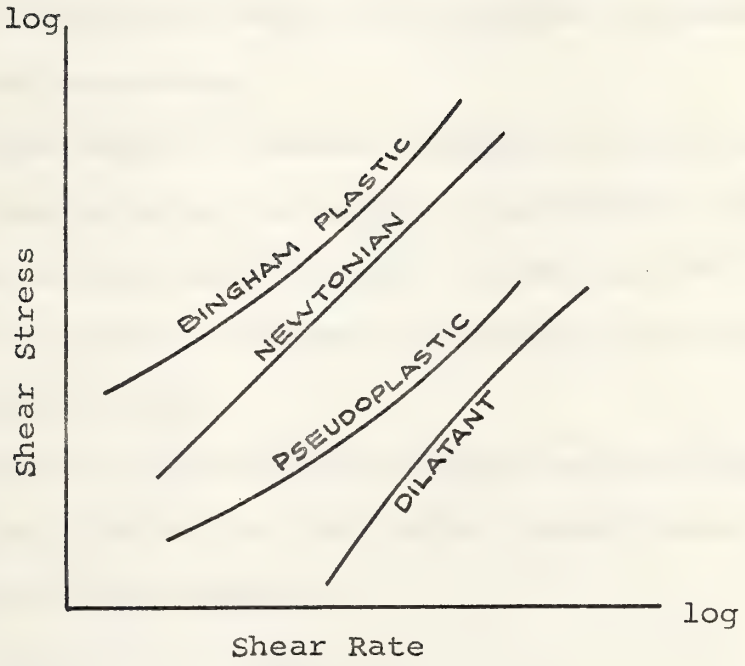


FIGURE 1 Rheological Flow Curves For Time-Independent Fluids

extending through a series of streamlines of flow. Because of such complex behaviour, a significant number of equations have been formulated to correlate experimental measurements on pseudoplastic fluids. A few of the more common equations are:

Eyring(7) $$\tau = A \operatorname{arcsinh} \left(-\frac{1}{B}\frac{dv}{dy}\right) \quad (4)$$

Powell - Eyring(8) $$\tau = A \left(\frac{dv}{dy}\right) + B \sinh^{-1} \left(C \frac{dv}{dy}\right) \quad (5)$$

Prandtl(9) $$\tau = A \sin^{-1} \left(\frac{dv}{dy}/B\right) \quad (6)$$

Ellis(10) $$\tau = \left[A + B(\tau)^{c}\right]\left(\frac{dv}{dy}\right) \quad (7)$$

In these equations, A, B and C are positive parameters which must be numerically determined from experimental data. As such, the only criterion which can generally be used in selection of an appropriate flow equation is to determine, by trial and error methods, which equation reproduces the experimental data most accurately.

Dilatant fluids exhibit an increase in apparent viscosity as shear rate increases. These fluids are very uncommon, and therefore, have received limited experimental or theoretical attention. In practice, the behaviour of these fluids could probably be defined by a suitable modification of a pseudoplastic equation of state.

Before proceeding, one additional flow model has been proposed which satisfies the Category 1 definition. This is the Bingham Plastic which is characterized by the following equation:

$$\tau - \tau_y = \mu_p \left(\frac{dv}{dy}\right) \quad (8)$$

where $\tau_y$ is an elastic yield stress and $\mu_p$ is the plastic viscosity.

The actual existence of a fluid displaying these flow characteristics has never been proven, but since many real fluids (i.e. clay slurries) approximate this behaviour, the concept is very convenient in practice. In explanation of this concept, it is assumed that a three-dimensional structure exists within the fluid of sufficient rigidity to resist any shear stress less than $\tau_y$; when this stress is exceeded, the structure breaks down instantaneously and the system behaves similar to a Newtonian fluid under a shear stress of $(\tau - \tau_y)$. Such behaviour is illustrated schematically in Figure (1).

Classifying this model in Category 1 may be criticized since the existence of a yield value implies that the material is dependent upon the deformation, $\delta$. As well, the use of such an equation in practice appears limiting since actual physical systems to which the equation has been applied(11) are almost always simultaneously thixotropic(12,13).

Fluids of Category 2, as defined,have rheological characteristics dependent upon the magnitude and duration of shear rate. Conventionally, fluids in this category have been classified as thixotropic (decrease in shear stress at constant shear rate) or conversely, rheopectic. In fact, however, some thixotropic materials(13,14) are also dependent upon the extent of deformation, $\delta$. Actually, as shall be discussed in a following section (Experimental Determination of Rheological Parameters), the classification is arbitrary depending solely upon the experimental technique.

When a thixotropic material is subjected to a constant shear rate, the measured shear stress decreases with time in a manner similar to that shown in Figure (2). Further, if experimental data at several shear rates

is cross-plotted, as indicated in Figure (2), then it is seen that the material is usually markedly non-Newtonian. A complete discussion and mathematical interpretation of this behaviour is reserved for subsequent sections (Anomolous Behaviour, Structure Formation and Thixotropic Behaviour; Mathematical Theories of Thixotropic Behaviour); however, it is generally believed that thixotropic behaviour is a result of shear degradation of a loosely bonded molecular network.

One additional aspect of thixotropic behaviour which has been observed(1,15,16) is that if, after shearing for a long period of time, the shear rate is suddenly reduced to a lower value, then the shear stress associated with the lower shear rate will increase over a period of time. Actually two characteristic shear stress growth phenomena have been noted; 'false-body' behaviour and thixotropic growth behaviour. This fact is suitably illustrated in Figure (3) which reveals the difference in the two types of growth behaviours.

Thixotropic and 'false-body' materials are not distinguishable from initial shear stress decay curves, since both exhibit a decline in shear stress at constant shear rate. However, the two materials can be separately distinguished if the rate of shear stress growth at lower shear conditions is measured. True thixotropic materials break down completely under the influence of significant stress, and behave similar to true liquids after the stress has been removed until such time as the structure starts reforming. On the other hand, 'false-body' materials exhibit a rapid increase in consistency immediately upon cessation of stress. Such behaviour has been attributed(15) to elastic stress rebound within the sheared molecules which is not present in thixotropic molecular systems.

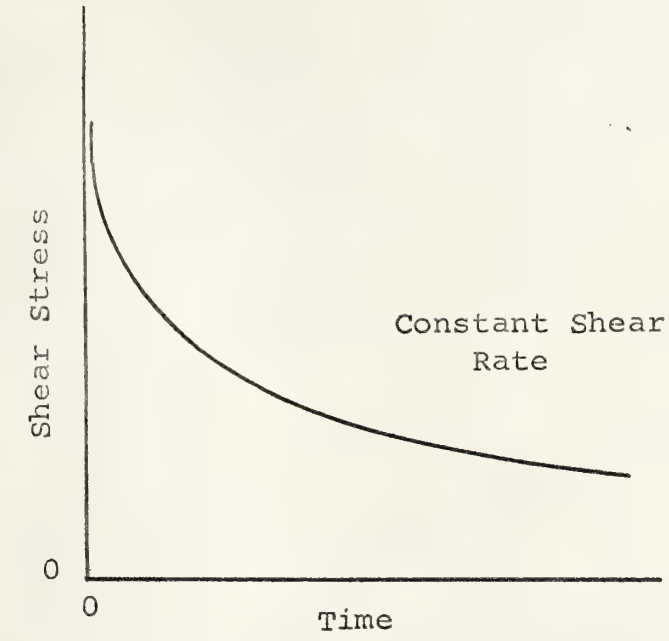


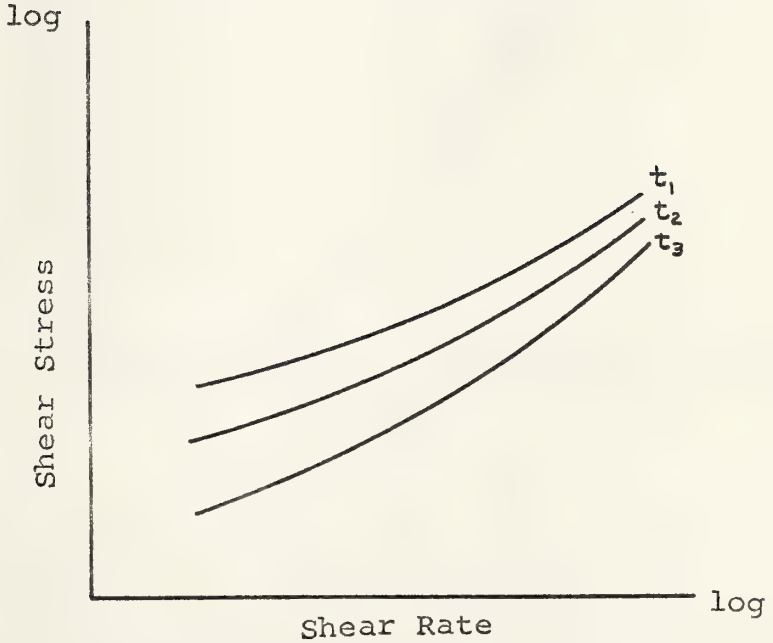


FIGURE 2 Rheological Behavior of a Thixotropic Fluid

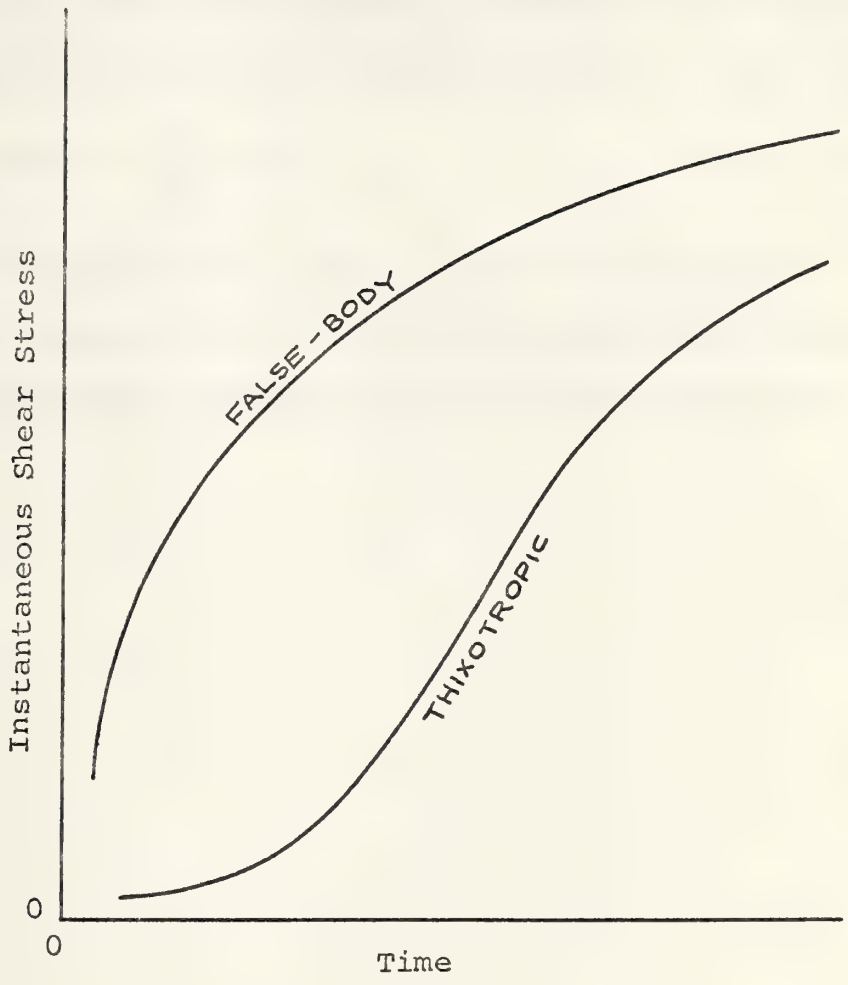


FIGURE 3 Comparison Between Rate of Shear Stress Growth for Thixotropic and False-Body Materials

The previous discussion of 'false-body' elasticity leads naturally to an abbreviated discussion of Category 3 type fluids. Normally these fluids are classified as viscoelastic, since they possess both viscous and elastic properties. As a consequence of both of these latter properties, the rheological equations describing viscoelastic behaviour are differential equations. The general equation describing such behaviour may be written as:

$$\sum_{i=0}^{n} \alpha_i D^i \tau = \sum_{j=0}^{M} \beta_j D^j \delta \qquad (9)$$

where: D is the differential operator, d/dt; $\delta$ is the fluid deformation. For actual fluids, this equation is very difficult to solve, even assuming that the values of the relative parameters ($\alpha$, $\beta$) could be obtained from experiment.

## EXPERIMENTAL DETERMINATION OF RHEOLOGICAL PARAMETERS

The experimental determination of rheological parameters is a pre-requisite to characterization of a fluid. To determine the necessary parameters, two experimental techniques have been consistently employed: (1) the capillary method and (2) the coaxial cylinder method. The relative merits and characteristics of these methods shall be discussed in sequence.

The analysis of flow through a cylindrical tube for the measurement of rheological parameters was introduced by Poiseuille(18) and has been used extensively since. The predominant characteristic of this instrument is that fluid shear rate is not constant, but varies linearly from zero at the center of the conduit to a maximum value at the conduit wall. Consequently, the relationship between shear stress and shear rate must be deduced indirectly from experimental measurements of pressure gradient and volumetric flow rate. The interpretation of such results is not always so obvious, requiring in general a prior knowledge of the fluid rheological behaviour. However, such instruments have been used successfully to determine the rheological parameters of Newtonian, pseudoplastic(2) and, with certain assumptions, of viscoelastic(19,20) fluids. The application of this instrument to the study of thixotropic behaviour has, to the knowledge of this investigator, never been successfully accomplished.

Perhaps the most versatile instrument for determining rheological parameters is the rotational coaxial cylinder viscometer. Use of this instrument permits a relatively direct determination of the experimental relationship between shear rate and shear stress. To do so experimentally, the entire sample is subjected to either, (i) uniform rate of shear, or

(ii) uniform shear stress, depending on the design of the individual instrument. Since the methods of determining rheological parameters through use of this instrument are of further importance to the present study, the basis of such procedures shall be investigated in detail. As a preliminary step in such an investigation, consider the schematic view of a coaxial viscometer illustrated below:

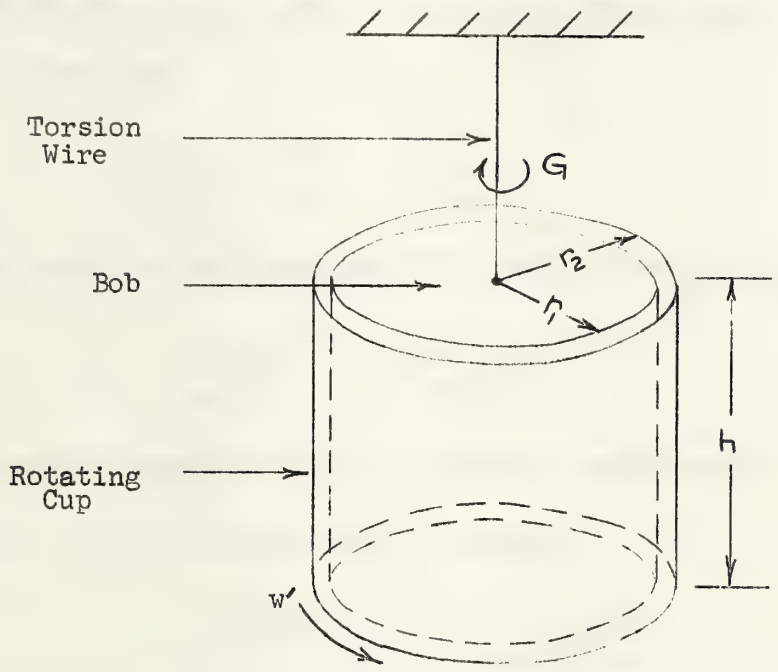


Initially, consider the annular space $(r_2 - r_1)$ to be filled with an anomolous fluid which can be described by the rheological equation:

$$\frac{dv}{dy} = f(\tau) \qquad (1)$$

In use, the cup is rotated at constant speed (w') and the deflection of the torsion wire used to suspend the bob is measured. Subsequently, knowing the calibration constant of the wire, the moment (G) required to maintain constant fluid velocity against the fluid viscous resistance may be calculated. The shear stress at any point, r, across the annulus follows directly as:

$$\tau(r) = \frac{G}{2\pi r^2 h} \tag{10}$$

By definition, shear rate is a function of the rheological behaviour of the fluid in the annulus. Consequently, a relationship must be developed to calculate shear rate as a function of the measured parameters (G,w') and the geometric dimensions of the viscometer. The conventional(21) development of such a procedure is as follows: the rate of shear across the annulus at a point"r"is given by:

$$\frac{dv}{dy} \Rightarrow r\frac{dw}{dr} = r\frac{d}{dr}\left(\frac{v}{r}\right) \tag{11}$$

Therefore, substituting Equations (10) and (11) into (1) gives,

$$r\frac{d}{dr}\left(\frac{v}{r}\right) = f\left(\frac{G}{2\pi r^2 h}\right) \tag{12}$$

Integrating this equation with the boundary conditions v = 0 at r = $r_1$ and v = $r_2 w'$ at r = $r_2$, the following is obtained;

$$\frac{V(r_2)}{r_2} = \int_{r_1}^{r_2} f\left(\frac{G}{2\pi r^2 h}\right)\frac{dr}{r} \tag{13}$$

which by suitable manipulation may be reduced to:

$$w' = -\int_{\tau_1}^{\tau_2} \frac{f(\tau)}{2\tau}\, d\tau \tag{14}$$

The solution of this equation is dependent upon the function $f(\tau)$. However, a general solution to this equation has been derived by Pawlowski(22) and Krieger and Maron(23). Using the latter investigators result, the solution of Equation (14) may, for most practical cases (i.e. $r_2/r_1 < 1.2$), be be simplified to:

$$\left(\frac{dv}{dr}\right)_w = \frac{4\pi N r_2^2}{r_2^2 - r_1^2}\left[1 + B_1\left(\frac{1}{n} - 1\right) + B_2\left(\frac{1}{n} - 1\right)^2\right] \qquad (15)$$

where:

$$B_1 = \frac{r_2^2 - r_1^2}{2r_2^2}\left[1 + \frac{2}{3}\ln\left(\frac{r_2}{r_1}\right)\right]$$

$$B_2 = \frac{r_2^2 - r_1^2}{6r_2^2}\ln\left(\frac{r_2}{r_1}\right)$$

and:

$\left(\frac{dv}{dr}\right)_w$ = shear rate at bob wall, $sec^{-1}$

$N$ = rotational cup speed, RPS

$r_2$ = radius of cup, ft.

$r_1$ = radius of bob, ft.

$n$ = slope of a logarithmic plot of shear stress versus cup speed, at N

Thus, if the geometrical parameters and dynamical measurements are available, the rheological curve of shear stress versus shear rate may be determined for any fluid exhibiting time independent shear behaviour.

For the case of a Newtonian fluid (i.e. n = 1), Equation (15) reduces to:

$$\left(\frac{dv}{dr}\right)_w = \frac{4\pi N r_2^2}{r_2^2 - r_1^2} \qquad (16)$$

which upon substitution into the Newtonian rheological equation of state (Equation 2) gives the Margules(6) Equation:

$$\mu_N = \frac{G}{4\pi h w'}\left(\frac{1}{r_1^2} - \frac{1}{r_2^2}\right) \qquad (17)$$

The characterization of a fluid with time-dependent flow behavior is considerably more complex than that of a time-independent fluid. This complexity is a consequence of the requirement that the fluid must be characterized in terms of three variables (time, shear rate and shear stress), whereas, in general, only two variables (of which time is one) may be experimentally determined. Hence, rheological experiments must be so designed, and data interpretation techniques simultaneously developed as to permit indirect evaluation of the third variable (either shear rate of shear stress). A few of these techniques, as have been applied to thixotropic systems will be discussed.

Traditionally, three experimental methods have been used to measure thixotropic behaviour in a coaxial viscometer:

(1) Measurement of thixotropic decay at constant rotational cup speed (i.e. nearly constant shear rate)(1,16,24);

(2) Measurement of increase in shear rate using a constant shear stress(14,25);

(3) Measurement of a hysteresis shear stress-shear rate curve by means of a programmed cup speed(26,27).

Each has its own individual characteristics, but either of the first two methods is considered to be significantly superior to the third method. Two reasons supporting this conclusion are that (i) an inordinately complex mathematical expression is required to interpret results, and by necessity, such an expression must assume a pre-determined concept of thixotropic behaviour; (ii) the continually changing bob inertial effects impose a limitation on early time measurements of thixotropic decay. This latter aspect has been discussed at considerable length in a recent publication(28), and

an "inertial" criterion proposed, but the assumptions (i.e. Newtonian - thixotropic behaviour) severely limit its usefulness.

Of the first two methods, neither would appear to possess any superior qualities. However, constant cup speed is more easily attainable for long testing periods than the provision of constant shear stress, and, as shall be shown, interpretation of experimental measurements is facilitated by this method.

One difference does exist between rheological parameters as measured by the two methods. This difference arises from the fact that some thixotropic materials have a yield value similar to that described for a Bingham plastic. If in a constant shear stress experiment, the experimental shear stress is much less than the yield value, then thixotropic behaviour will not be measured. Such a parallel comparison is not possible with the constant cup speed technique, since thixotropic behaviour would be measured at any finite shear rate.

Assuming that the shear stress decay curve of a thixotropic material is measured as a function of time at constant cup speed, a fundamental problem is the determination of the instantaneous shear rate associated with the measured shear stress values. This problem arises since, as previously described, shear rate is a function of the rheological behaviour of the sheared fluid, which in turn is a function of time. The problem is especially difficult since the measured variables (time, shear stress) do not permit definition of the fluid rheological behaviour. Consequently, many previous investigators(16,24,25) have assumed that the thixotropic fluid is a time-dependent Newtonian fluid and calculated shear rate directly from the Margules

Equation (Equation 17). However, as shall be described below, a method has recently been developed(1) which permits the determination of instantaneous shear rate from the measured rheological behvaiour of a thixotropic material.

In essence, the method is based on the Krieger-Maron procedure (Equation 15) for non-Newtonian fluids as adapted for time-dependent non-Newtonian fluids. That is, the behaviour of a thixotropic fluid, at any instant, is not unlike that of pseudoplastic fluid. The effect of time is merely that the fluid is converted from one characteristic pseudoplastic to another. The method requires measurement of thixotropic decay curves at each of several cup speeds. Shear stress values are then selected from the experimental data for each cup speed at a specific shear time. These stress values are plotted on logarithmic co-ordinates as a function of cup speed and a regular curve is drawn through the data points. The drawn curve is considered to representative of the rheological behaviour of the fluid at the selected shear time. The procedure is repeated for a number of representative shear times until a series of curves of shear stress versus cup speed have been constructed*. Selection of the chosen shear times is completely arbitrary, but usually the times are chosen so as to provide a representative description of the original decay curve.

To determine the instantaneous shear rate associated with the experimentally measured shear stress and time, the Krieger-Maron procedure (Equation 15) is used directly. That is, the slope of a constant-time curve is determined at a specific cup speed. This slope, n, and the corresponding cup speed, N, are then substituted into Equation (15) and the shear rate is

---

* Such a procedure was used to treat experimental data in this manuscript; for examples of such plots, the reader is referred to Figures (42),(46) and (48).

calculated directly. The resultant shear rate then completes a data sub-set of "shear rate-shear stress-time".

The resultant subsets of data may then be plotted on logarithmic co-ordinates in terms of the variables, shear stress-shear rate, with time as a parameter.* To obtain shear stress values which would have been measured if the experiment had been conducted at constant shear rate, the desired vertical ordinate is chosen and the desired values of shear stress-time are selected at the intersections of this ordinate with the smoothed curves.

---

* Figures (43, (47) and (49).

## ANOMOLOUS BEHAVIOUR, STRUCTURE FORMATION AND THIXOTROPIC BEHAVIOUR.

The qualitative aspects of anomolous behaviour and the consequences of structure formation shall be discussed in this section. Such discussion will not include specific theoretical results but will provide background which will be useful in following sections.

The fundamental unit in rheological analysis and behaviour is the particle, an arbitrary term denoting the discrete members of a dispersed phase within a continuous carrier vehicle. The dependence of rheological behaviour on the particle has been experimentally determined as due to the following particle factors(29):

1. The shape, size and mass of the particle or solute molecule;
2. The size and molecular weight distribution of the particles;
3. The hydrodynamic volume actually occupied by the particles;
4. The internal flexibility and ease of deformation of the particles;
5. The thermodynamic conditions in the system;
6. The concentration of particles.

To abbreviate and direct discussion along pertinent lines, consider a system of asymetrical particles of colloidal size for which the first five factors described above are fixed, with particle concentration as the only variable. For an arbitrary constant particle concentration, the resultant flow behaviour of the suspension may be characterized as being typical of the behaviour associated with one of three concentration ranges. The three ranges are (i) the extremely dilute suspension, (ii) the dilute suspension, and (iii) the concentrated suspension. Before proceeding to a

discussion of suspension flow behaviour within each range, it should be noted that boundaries between these concentration ranges may only be determined from interpretation of rheological measurements.

Considerable theoretical effort, beginning with Einstein's(30) original treatment of a suspension of spherical particles, has been devoted to the description of the flow behaviour of infinitely dilute suspensions of particles. Subsequent investigators(31,32) have extended this treatment to macromolecular and non-spherical particles, but all have retained the concept that during flow, neither the particles nor their hydrodynamic flow patterns interact. Consequently, from the point of view of rheology, the effect of each particle is additive and their cumulative effect is simply to raise the viscosity of the suspension. This increase in viscosity may be regarded as a consequence of the perturbation of the flow of the carrier liquid around the particle which ultimately results in increased heat generation.

As particle concentration increases to the dilute range, the perturbations produced by the solvent flowing about the particles are no longer independent. Individual flow patterns now overlap and become interdependent. In addition, because of the increased particle concentration, interparticle interaction in the form of aggregation effects may occur. This latter condition suggests that interparticle forces exist (i.e. van der Waals-London) which may influence the hydrodynamic flow character of the particles. These effects may be permanent or short-lived, but in any case, suspended particles may form simple aggregates which can act as compact, larger single particles. Such behaviour may, among other things, destroy the Newtonian behaviour of the suspension.

Concentrated suspensions represent that concentration range wherein interparticle aggregation effects predominate flow behaviour. Particle structures are formed, such as nets and three-dimensional networks, which have flow immobilizing effects far exceeding the simple aggregates of dilute suspensions. At this stage, the superposition of individual flow patterns is no longer a suitable approach for investigating the flow behaviour. In view of this complexity, the concentrated suspension region has been relatively little explored either by theory or experiment.

Thixotropic behaviour is one of the more interesting characteristics of concentrated suspensions. Such behaviour is generally conceded(6) to be a result of stress cleavage of a loosely aggregated network. The form of the network is not specified, only that it be amenable to shear degradation.

Theoretical predictions of thixotropic behaviour are almost exclusively precluded due to ignorance of both (i) the detailed structure within the thixotropic system, and (ii) the nature of the forces, hydrodynamic and otherwise, exerted by the particles on each other. The two effects are clearly interdependent.

From a mechanistic point of view, thixotropic behaviour might be explained in the following manner.

Consider a particle network dispersed throughout a carrier liquid at rest; the structure may or may not be continuous, but in any case is composed of particles linked together in the form of aggregated chains. If the structure is continuous in three dimensions, then an overall rigidity will be imparted to the suspension.

If a stress of sufficient magnitude is applied to the suspension such that deformation and flow commences, then a differential stress will be imposed across the network structure. When this differential stress is greater than the structural bonding forces, stress cleavage occurs, resulting in the formation of network segments. Such breakdown will continue until the individual network segments have reached a state of degradation compatible with the imposed stress. If it is assumed that the hydrodynamic stress contribution of a set of individual segments in a chain is less than that of the continuous chain, i.e.

$$\sum_{i=1}^{n} f_i < f \qquad i = 1,2,3, \ldots, n$$

where $f_i$ is the flow resistance due to the $i^{th}$ network segment; f is the flow resistance of a chain of network segments;

then it is easily deduced that as the initial network is broken, the shear stress associated with a given shear rate will decrease. Further, since bond cleavage requires work input, in general the bond breaking process will be a function of time and the magnitude of the aggregative effects. It follows that experimental shear stress will also be a function of these variables.

Two points in the previous discussion should be emphasized: (i) the existence of thixotropic decay implies that aggregation effects are present, and (ii) aggregation effects are not eliminated by a stress condition, although their overall contribution to rheological behaviour may be modified by the magnitude of imposed stress. For example, if during flow, two network segments collide or interact in some specified manner, the possibility of formation of an aggregated doublet will largely be determined by the

compatibility of this doublet in the imposed stress field.

Using the background outlined in this discussion, some thixotropic flow models which have been used to correlate experimental measurements on thixotropic materials will be described in the following section. As previously emphasized, the complex behaviour of thixotropy precludes attempts at studying the network on a hydrodynamic basis. Consequently most investigators have restricted their efforts to mechanistic rather than microrheological considerations. Such considerations usually involve the formulation of an idealized mathematical model to account for the measured rheological behaviour.

## MATHEMATICAL THEORIES OF THIXOTROPIC BEHAVIOUR

The formulation of an adequate mechanistic model to define the flow behaviour of a thixotropic material has been amazingly slow. In fact, it was only recently (1958) that a theory(33) was proposed which satisfied the dual requirements of being (i) based on a plausible molecular model and (ii) capable of direct experimental verification. Prior to this date, experimental verification of acceptable molecular flow models(34) was not possible. As a result of this prior lack of development, those thixotropic measurements which had been made had generally been presented directly as graphical data or, in some cases, in terms of correlation coefficients(35). The theoretical value of the latter technique is questionable(1) but it does provide a suitable classification procedure.

Since the above date, a number of theories have been presented (1,27,36) which are based on acceptable structural models and which have been tested with experimental measurements. A summary of the pertinent features of each theory is shown in Table I.

Upon inspection of Table I, it may be noted that all investigators are in agreement as to the basic thixotropic decay process. That is, all the flow models assume the existence of a network destruction process which ultimately results in an equilibrium flow state within the sheared fluid. However, as shall be discussed, the individual formulations of a theory depicting this decay process are significantly different.

Before proceeding, it should be pointed out that the four theories listed on Table I may be subdivided into two subsets, each of which constitutes a different formulation procedure. The Eyring et al(27) and

Denny-Brodkey(36) approach has been to consider network destruction on the basis of the Theory of Rate Processes(37); the Storey-Merril(33) and Ritter(1) approach has been that of investigation of the macroscopic features of network destruction. The pertinent aspects of each approach shall be discussed.

After reinspection of Table I, it may be seen that the Eyring formulation assumes that thixotropic behaviour is due to the transition process, non-Newtonian structural unit $\rightleftharpoons$ Newtonian flow unit. The final thixotropic equation of state is expressed in terms of an instantaneous equilibrium condition between these two flow units and in terms of their instantaneous concentrations ($X_2$ and $X_1$ respectively). It may be noted then that the state equation is expressed in terms of molecular parameters. In actuality, such an equation cannot be explicitly verified since these latter parameters are to all practical purposes indeterminable by rheological experiments.

Eyring et al(27) have correlated experimental measurements by their proposed equation. To do so, however, required a transformation of the molecular flow parameters into experimentally derivable parameters; these latter parameters were then evaluated by trial and error best-fit-data techniques. The arbitrary nature of both the transformation sequence and the parameter evaluation step appears limiting and has been questioned(36); as yet, justification for these processing techniques has not been forthcoming.

The approach taken by Denney-Brodkey(36) has been to modify Eyring's (37) flow concept in such a manner that the final thixotropic equation is on a mechanistic basis, i.e. in terms of measurable rheological variables. However, as with the Eyring et al (27) formulation, certain aspects limit the usefulness of the final flow equation.

TABLE 1 THEORIES OF THIXOTROPY

Mathematical Models Based on Mechanistic Flow Models

| | Eyring and Co-Workers (27) (1960) | Denny and Brodkey (36) (1962) | Storey and Merrill (33) (1958) | Ritter (1) (1961) |
|---|---|---|---|---|
| Experimental System | Silica Gel Grease | General | Amylose - Amylopectin | Pembina Crude Oil |
| Assumed Molecular Structure | Colloidal Particles of Two Types (i.e. Newtonian and Non-Newtonian) | Entangled Polymer Molecules in Cohesive Structure | Scaffolding Network in Newtonian Solvent | Scaffolding Network in Newtonian Solvent |
| Assumed Flow Model | Non-Newtonian Unit ($X_2$) $\underset{K_2}{\overset{K_1}{\rightleftharpoons}}$ Newtonian Unit ($X_1$) | Unbroken Link ($X_2$) $\underset{K_2}{\overset{K_1}{\rightleftharpoons}}$ Broken Link ($X_1$) | Unbroken Link $\underset{K_2}{\overset{K_1}{\rightleftharpoons}}$ Broken Link | Unbroken Link $\underset{K_2\ (K_B)}{\overset{K_1\ (K_A)}{\rightleftharpoons}}$ Broken Link |
| Structure Decay Mechanism | $-\frac{dX_2}{dt} = K_1 X_2 e^{\frac{\mu\omega}{kT}} - K_2 X_1 e^{-(1-\mu)\omega'/kT}$ | $-\frac{d(X_2)}{dt} = K_1'(X_2)^n - K_2'(X_1)^m$ | $\frac{dN}{dt} = K_1 N\left(\frac{dv}{dx}\right) - K_2(N_0 - N)$ | $\frac{dN}{dt} = \frac{K_B(N_0-N)^2}{t} - \frac{K_A(N)}{t}$ |
| Final Equation of State | $\tau = (1-X_2)\frac{\beta_1}{\alpha_1}\left(\frac{dv}{dx}\right) - X_2 \sinh^{-1}\beta_2\left(\frac{dv}{dx}\right)$ where: $X_2 = \frac{K_2}{K_1+K_2} + \left(X_2^0 - \frac{K_2}{K_1+K_2}\right)e^{-(K_1+K_2)t}$ | $\frac{2}{A}\left[\tanh^{-1}\left(\frac{2C\mu_0+B}{A}\right) - \tanh^{-1}\left(\frac{2C\mu_\theta+B}{A}\right)\right] = K_2't$ where: $A = \left[\left(\frac{K_1}{K_2}\right)^2\left(\frac{dv}{dx}\right)^{2P} + 4\frac{K_1}{K_2}\left(\frac{dv}{dx}\right)\right]^{\frac{1}{2}}$ $B = -\left[\left(\frac{K_1}{K_2}\right)\left(\frac{dv}{dx}\right)^P + 2\mu_0 C\right]$ $C = 1/(\mu_0 - \mu_\theta)$ | $\frac{\tau}{\left(\frac{dv}{dx}\right)} = \alpha N_0 e^{-\left[K_2 + K_1\frac{dv}{dx}\right]t} + \frac{\alpha N_0}{1+\frac{K_1}{K_2}\left(\frac{dv}{dx}\right)} + \frac{\alpha N_0}{1+\frac{K_1}{K_2}\left(\frac{dv}{dx}\right)} e^{-\left[K_2 + K_1\left(\frac{dv}{dx}\right)\right]t} + \mu$ | $\log\left[\frac{\tau_s - \tau_{s\infty}}{\tau_{s0}^2/\tau_{s\infty} - \tau_s}\right] = -K_A\left[\frac{\tau_{s0}+\tau_{s\infty}}{\tau_{s0}-\tau_{s\infty}}\right]\log t - \log\left[\frac{\tau_{s0}^2/\tau_{s\infty} - \tau_{s1}}{\tau_{s1} - \tau_{s\infty}}\right]$ where: $\tau_s = \tau - \tau_\mu$ |
| Experimental Method | Coaxial Viscometer Experiments Based on Hysteresis Technique | Literature Data on Coaxial Viscometer Experiments | Coaxial Viscometer Experiments | Coaxial Viscometer Experiments |
| Experimental Verification Technique | Flow Parameters Evaluated by Trial and Error Data Processing Techniques | Flow Parameters Evaluated by Trial and Error Data Processing Techniques | Flow Parameters Evaluated on Basis of Proposed Theory Techniques | Flow Parameters Evaluated on Basis of Proposed Theory Techniques |

First, the experimental determination of one of the flow parameters (i.e. $\mu_o$) was obtained "at very low shear rates, where deviation from ideal is at a minimum"(36). This is a direct contradiction of the known behaviour of anomolous fluids, i.e. maximum anomolous behaviour occurs at the lowest shear rates. Further, the author(36) concedes that:

> "The main drawback of the method is that back calculation to reconstruct the basic shear diagram (is required) ... ; the development should be considered to be a means of relating flow to the fundamental properties of materials, rather than a representation of the fluid flow."

In this investigators opinion, only two theories (Storey-Merril(33), Ritter(1) ) have been proposed which are sufficiently self-consistent to warrant further consideration. Of these two, only the theory proposed by Ritter(1) shall be reviewed in detail since this theory is a modified and improved analysis of the basic concepts inherent in the Storey-Merril theory(33).

Theory of Thixotropic Behaviour (Ritter)

Compatible with other proposed theories, the molecular model is considered to be a loosely bonded network structure of long chain molecules dispersed in a Newtonian solvent. The network, in an undisturbed and unsheared condition, is assumed to be composed of individual fragments which are joined together in appropriate linkages or 'links'. Under the influence of stress, the network undergoes destruction at the linkage points, thus, creating network fragments. The destruction process is considered reversible

to the extent that a probability exists that network segments can reform. In reality, the network destruction process is symbolized by the following equation:

$$A \rightleftharpoons i'A \rightleftharpoons i''A \ldots\ldots \rightleftharpoons iB \tag{18}$$

where "A" refers to the original network and "B" the final network fragments.

Since it is impossible to derive an exact mathematical expression to define the consecutive reaction illustrated above in terms of experimentally measured quantities, Ritter(1) assumed the following equation as describing the network destruction process:

$$\underset{(A)}{\text{NETWORK}} \xrightleftharpoons[k_B]{k_A} \underset{(B)}{\text{NETWORK FRAGMENTS}} \tag{19}$$

The formulation of the above equation in terms of measurable experimental quantities (i.e. shear stress, shear rate, time) shall now be described. To do so, consider the development of and the assumptions inherent in the Theory:

(1) The total shear stress in the sheared fluid at any time is considered to be the sum of a Newtonian solvent component and a component due to the presence of structural segments, i.e.

$$\tau(t) = \tau_{NEWTONIAN} + \tau(t)_{STRUCTURAL} \tag{20}$$

(2) The structural stress component is proportional to the product of the number of network links existing at any time and some function of the imposed shear rate. i.e.

$$\tau(t)_{STRUCTURAL} = \alpha'(A)\, f\left(\frac{dv}{dy}\right) \tag{21}$$

where: $\alpha'$ = proportionality constant

$(A)$ = concentration of network links

$f(\frac{dv}{dy})$ = shear rate functional relationship

(3) Under the conditions of stress, the rate of link or network destruction is proportional to the number of network links, but is independent of the shear rate. i.e.

$$\frac{d(A)}{dt} = -k_A' (A) \tag{22}$$

where: $k_A'$ = thixotropic rate decay constant independent of shear rate

(4) For any given concentration of networks, the nature of the function relating structural stress to shear rate is independent of the time of shear. i.e.

$$\frac{d}{dt} \left(f(\frac{dv}{dy}) \right) = 0 \tag{23}$$

With this assumption, the following equations may be derived:

$$\frac{d}{dt} (\tau_s) = \frac{d}{dt} (\alpha'(A) f(\frac{dv}{dy}) )$$

$$= \alpha' \left[ \left\{ \frac{d}{dt}(A) \right\} f(\frac{dv}{dy}) + \left\{ \frac{d}{dt} f(\frac{dv}{dy}) \right\} (A) \right]$$

$$= \alpha' f(\frac{dv}{dy}) \frac{d(A)}{dt}$$

Therefore;

$$\frac{d(A)}{dt} = \frac{d\tau_s}{dt} \frac{1}{\alpha' f(\frac{dv}{dy})} \tag{24}$$

Combining Equations (24) and (21) and substituting into Equation (22), the following is obtained:

$$\frac{d\tau_s}{dt} = -k_A' \tau_s \tag{25}$$

(5) The rate of change of structural stress arising from the rupture or reformation of network links is dependent upon the average size of the network and is assumed to be inversely proportional to time of shearing: i.e. from Equation (25):

$$\frac{d\tau_s}{dt} = -\frac{k_A \tau_s}{t} \tag{26}$$

(6) The network fragment recombination process is analogous to a second order chemical reaction, and is dependent upon shear rate. Considering the assumptions outlined from (1) to (5), the following equation was derived in an analogous manner:

$$\frac{d\tau_s}{dt} = \frac{k_B(\tau_{so} - \tau_s)^2}{t} \tag{27}$$

where: $k_B$ = network recombination constant dependent upon shear rate

$\tau_{so}$ = the shear stress at time zero

The net rate of decay of structural stress at constant shear rate may now be described by combining Equation (26) and (27) to yield:

$$\frac{d\tau_s}{dt} = \frac{k_B(\tau_{so} - \tau_s)^2}{t} - \frac{k_A \tau_s}{t} \tag{28}$$

which with the boundary condition of $\frac{d\tau_s}{dt} = 0$ at infinite shear time, results in simplification to:

$$\frac{d\tau_s}{dt} = \frac{k_A}{t}\left[\frac{\tau_{s\infty}(\tau_{so} - \tau_s)^2}{(\tau_{so} - \tau_{s\infty})^2} - \tau_s\right] \tag{29}$$

This differential equation was then solved with the following boundary conditions:

$$\text{at} \quad t = 0; \qquad \tau_s = \tau_{so}$$

$$\text{at} \quad t = 1 \text{ (minute)}; \quad \tau_s = \tau_{s1}$$

to yield:

$$\log \left(\frac{\tau_s - \tau_{s\infty}}{\tau_{so}^2/\tau_{s\infty} - \tau_s}\right) = -k_A \left(\frac{\tau_{so} + \tau_s}{\tau_{so} - \tau_s}\right) \log t - \log \left(\frac{\tau_{so}^2/\tau_{s\infty} - \tau_{s1}}{\tau_{s1} - \tau_{s\infty}}\right) \quad (30)$$

which represents the final expression for the decay of shear stress at constant shear rate. It may be seen that this equation predicts a straight line relationship on logarithmetic coordinates between:

$$\left(\frac{\tau_s - \tau_{s\infty}}{\tau_{so}^2/\tau_{s\infty} - \tau_s}\right) \qquad \text{and} \quad t$$

The slope of the straight line is:

$$-k_A \left(\frac{\tau_{so} + \tau_{s\infty}}{\tau_{so} - \tau_{s\infty}}\right)$$

In order to verify Equation (30), experimental data in the form of shear stress as a function of time at constant shear rate is required. In addition, a measure of the Newtonian component is necessary. Therefore, for the purpose of correlating experimental data, Ritter(1) made one additional assumption:

(7) That the Newtonian component of the total stress may be evaluated at high shear rates, a condition which is assumed to complete destruction of the network into non-stress contributing fragments. The Newtonian component as evaluated by this method

is applicable at all shear rates and all shear times. Thus, the 'final' network fragment is assumed to be Newtonian in character but does not appreciably add to the Newtonian component. i.e.

$$\tau_{NEWTONIAN} \neq f(t) \tag{31}$$

Subsequent to the development of Equation (30), Ritter made extensive rheological measurements (i.e. three shear rates at each of four temperatures) on a naturally occuring thixotropic fluid, Pembina crude oil. The experimental thixotropic decay curves, as correlated on the basis of Equation (30) are presented in Figure (4).

Except for minor, random deviations, the correlated data confirmed the theoretical analysis that $k_A$, the thixotropic decay constant, was independent of time. Further, utilizing the correlated results, individual decay constants were calculated for each shear rate. The results indicated that, as predicted, $k_A$ was independent of shear rate. In support of an earlier postulate, $k_A$ was also shown to be a function of temperature and appeared to exhibit a temperature dependence analogous to that described by the Arrhenius equation of chemical kinetics. i.e.

$$k_A = Ae^{b/T} \tag{32}$$

where: A,b = correlation constants

T = absolute temperature, $^{o}R$

However, in view of the limited number of experimental points (four), the correlation could not be affirmed.

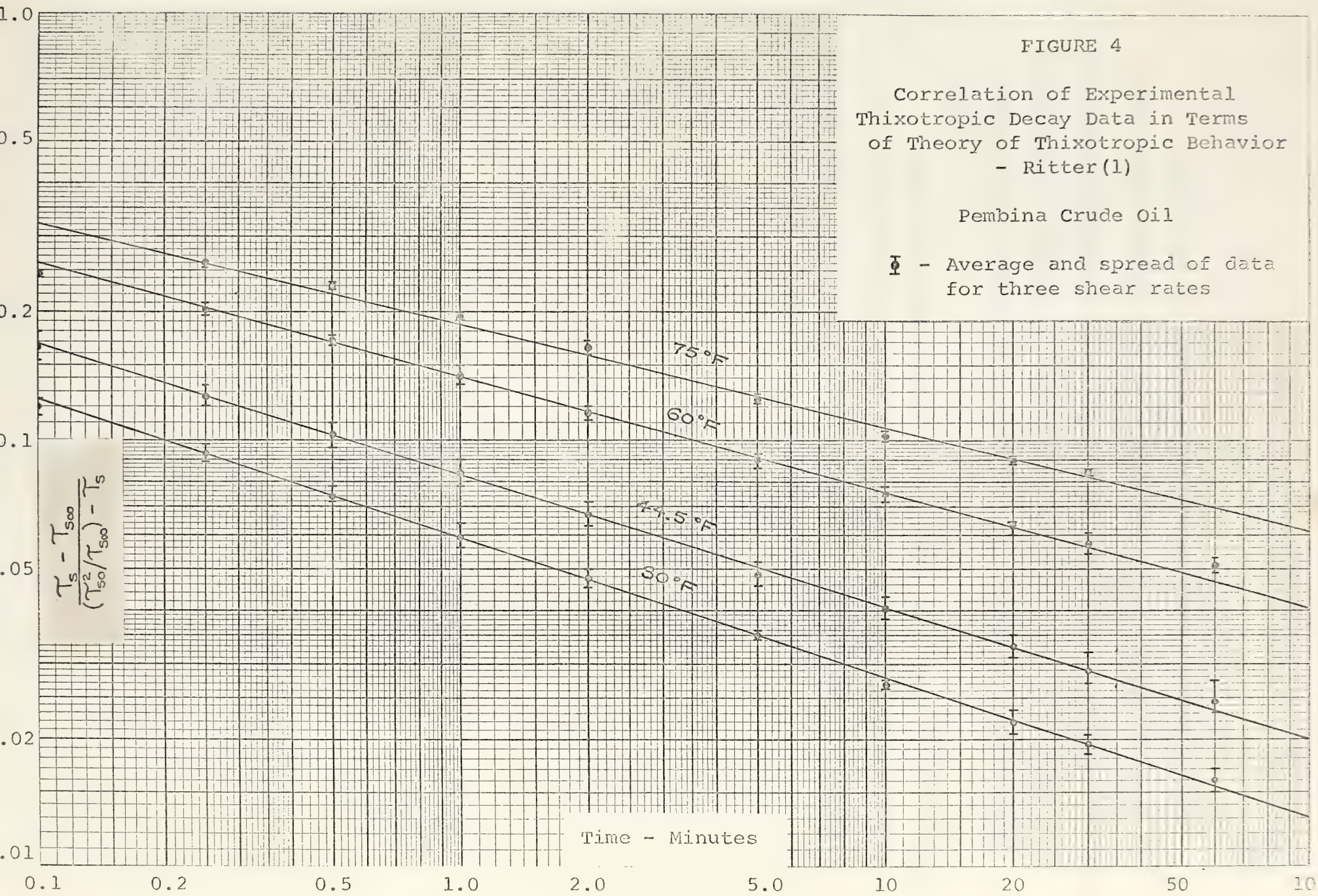
FIGURE 4
Correlation of Experimental Thixotropic Decay Data in Terms of Theory of Thixotropic Behavior - Ritter(1)
Pembina Crude Oil
Φ - Average and spread of data for three shear rates
75°F
60°F
44.5°F
30°F
$\frac{\tau_s - \tau_{s\infty}}{(\tau_{50}^2/\tau_{s\infty}) - \tau_s}$
Time - Minutes
1.0
0.5
0.2
0.1
.05
.02
.01
0.1
0.2
0.5
1.0
2.0
5.0
10
20
50
100

Simultaneous verification of the predicted nature of the reverse reaction rate constant, $k_B$, was attempted but due to the sensitivity of the correlation method and inaccuracies in the data, only a trend was sufficiently well defined. However, it appeared that the reverse rate constant was dependent on both temperature and shear rate as predicted by the theoretical analysis.

Resumé: The most recently published (from 1958) equations describing thixotropic behaviour have been investigated. Of these, the Theory of Thixotropic Behaviour(1) appears to offer the only suitable basis for correlation of experimentally measured thixotropic decay curves.

## TYPICAL THIXOTROPIC SYSTEMS

To this point, the presence of a rheological structure amenable to shear degradation has not been established conclusively. However, detailed investigation of a number of thixotropic systems has provided considerable evidence in support of the concept of a network model. The nature of two of these systems will be discussed.

### Hydrocarbon Systems:

Early investigators(39) recognized that some crude oils, and crude oil derivatives were complex vehicles which could, over a relatively short interval of temperature, display an amazingly wide range of rheological behaviour. Such range in behaviour was generally characterized by (i) a sudden divergence in a normally straight line temperature-viscosity plot, and (ii) the simultaneous change from Newtonian flow behaviour to markedly anomolous behaviour. Since this behaviour was generally noted only when the oil temperature was lowered beneath its natural pour point*, the qualitative conclusion was that such behaviour was linked to crystallization of wax within the oil. However, beyond these observations, the consequences due to such behaviour were not studied carefully until Ackroyd and Aubrey(16) published the results of an investigation on the flow behaviour of a wax-laden residual fuel oil.

These results are particularly interesting, since not only was the flow behaviour of the oil measured, but also the individual effect of the

---

* The lowest temperature at which an oil will pour or flow when it is chilled without disturbance, under prescribed test conditions(40).

components of the oil upon flow behaviour were determined. To aid interpretation of the rheological measurements, an x-ray diffraction study was performed on the oil and its components (i.e. light oil, wax, asphaltene and resin fractions, respectively).

As may be noted from inspection of Figure (5), the fuel oil, after being treated according to a detailed handling procedure*, displayed marked thixotropic behaviour. After about two and one-half hours shearing, the measured shear stress decreased to a value considered to be essentially an equilibrium condition. It should be noted that for the 110°F-reheat thixotropic curve, a peculiar maximum in shear stress was measured; the authors could not explain such a phenomenon.

Shearing tests similar to those illustrated in Figure (5) were conducted on, (i) the residual fuel oil, (ii) the same oil after removal of the asphaltenes and (iii) the same oil after removal of both asphaltenes and resins. Despite the individual removal of constituents, the flow curves of each treated fraction were qualitatively similar to the original oil sample.

On the basis of the rheological studies and an interpretation of the x-ray diffraction results, Ackroyd(16) concluded that the measured flow behaviour was due to the wax fraction. It was proposed that, at test temperature, wax crystallization within the oil resulted in the formation of a rigid structure. The structure was readily destroyed by continuous shearing, but even after an extensive shearing time, the

---

* An oil sample was heated to 170°F, shock chilled to -30°F, reheated to either 110°F or 85°F, and then charged to the viscometer at the chosen temperature (i.e. 110°F or 85°F); the viscometer and oil were then slowly cooled to test temperature (52°F).

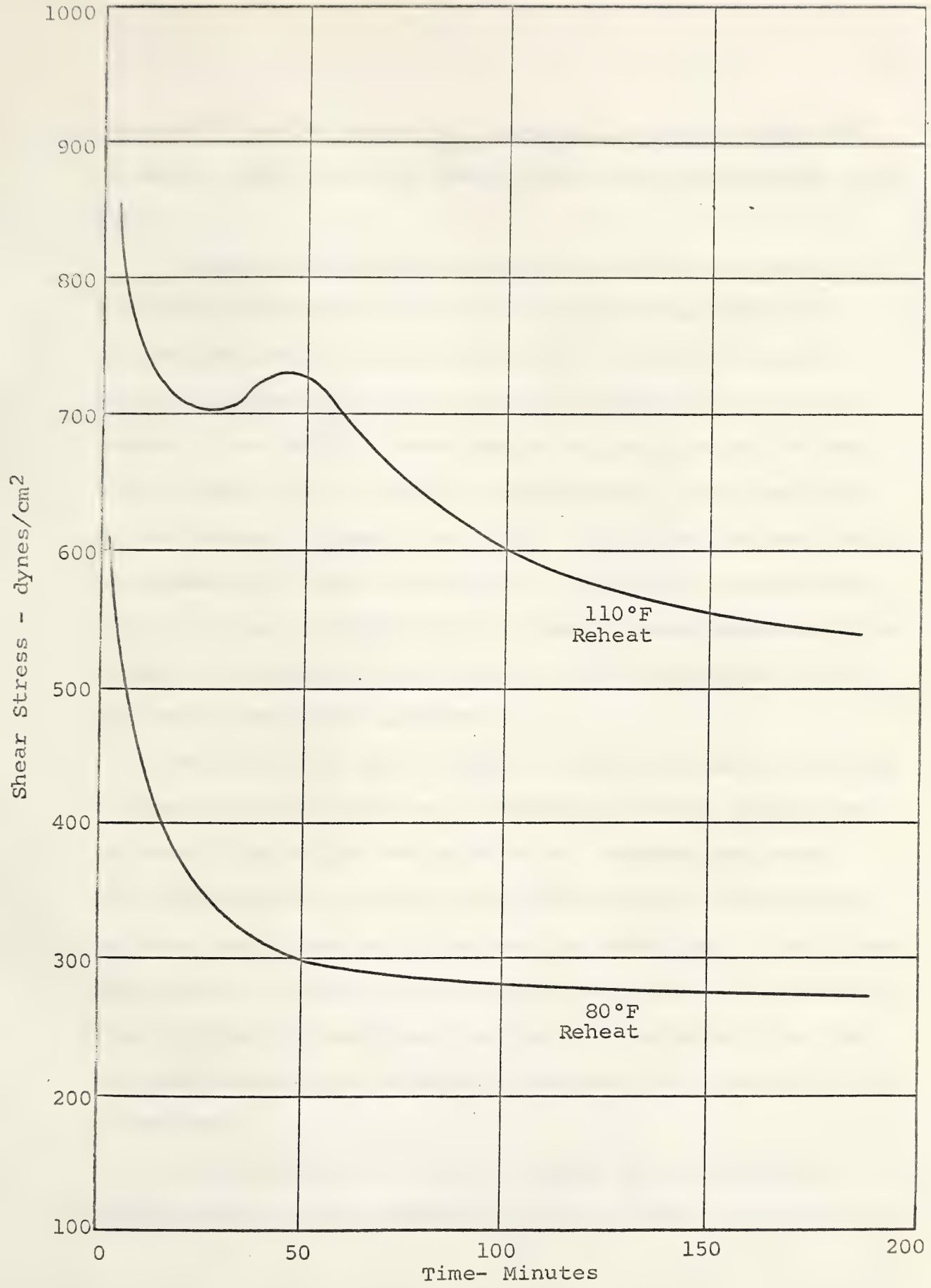


FIGURE 5 Typical Thixotropic Decay Curves of Residual Fuel Oil at 52°F and 13.18 $Sec^{-1}$ Shear Rate - Ackroyd(16)

structural flow effects were still apparent. As shown in Figure (6), the sheared structure did not readily reform even under non-shear conditions.

Slightly preceding the investigation by Ackroyd and Aubrey(16), a separate investigation of the behaviour of wax-laden lubricating oils was performed by Jones and Tyson(25). In this latter work, a lubricating oil was artificially loaded with paraffin wax, the temperature of the solution lowered beneath its pour point and the rheological behaviour of the wax-oil system measured. In all cases, pronounced thixotropic behaviour was noted, which in turn, was ascribed to the degradation of a wax crystal lattice. This latter contention was supported by photomicrographs(41) of a sheared wax-oil suspension which revealed the progressive shear degradation of the aggregated lattice into smaller and smaller aggregates.

One interesting aspect of the rheological measurements conducted by Jones and Tyson(25) was that a significant inflection in shear rate was noted if the samples were subjected to a constant shear stress. Such a phenomenon has also been noted by Billington(14), who measured the thixotropic properties of a natural "wax-containing" oil at constant shear stress. To explain his experimental measurements, Billington(14) considered the thixotropic decay sequence to be comprised of two time dependent components and subsequently correlated the thixotropic curves on that basis.

Before proceeding, it should be stated that the correlation technique employed by Billington(14) has little theoretical justification,

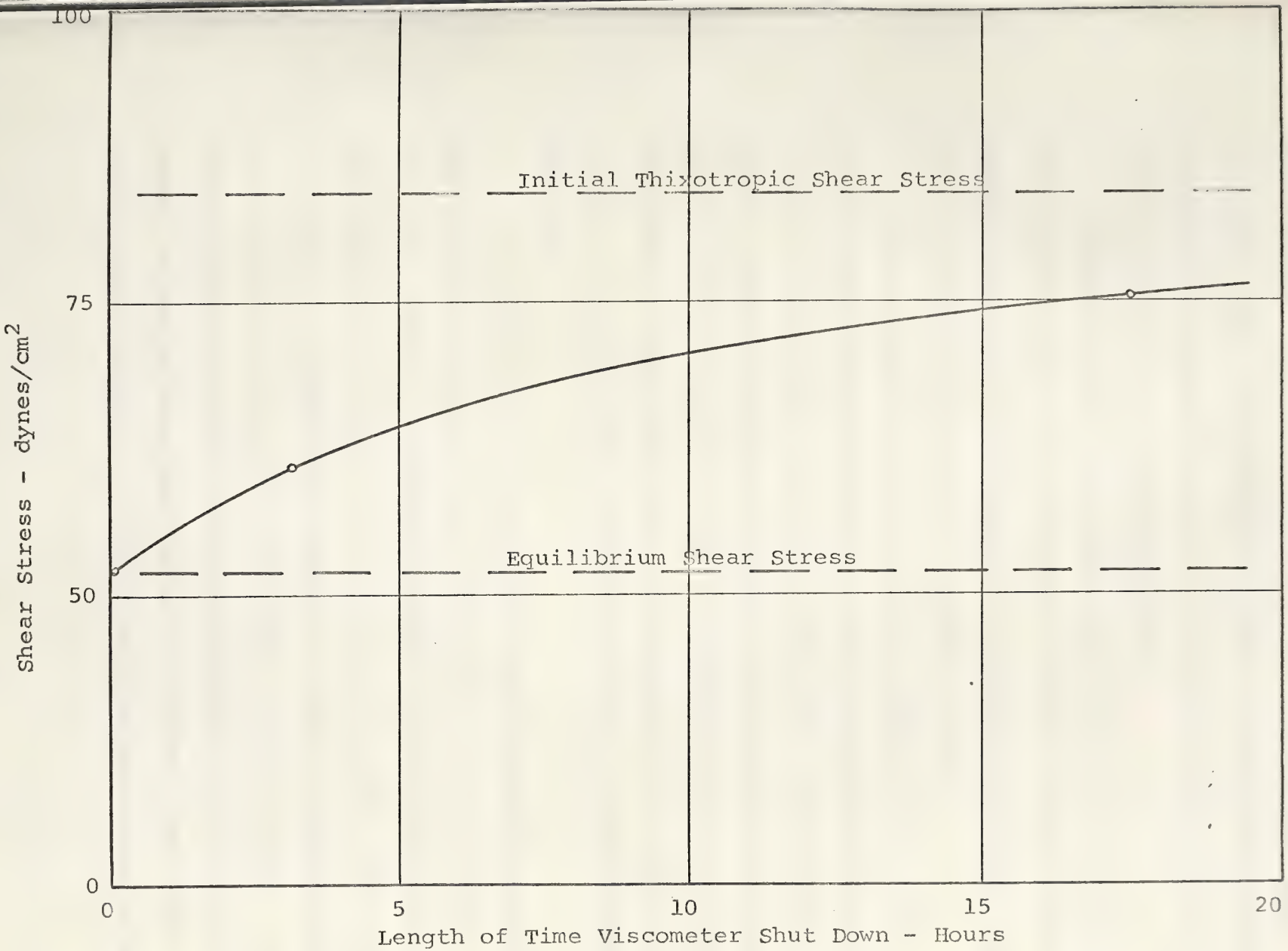


FIGURE 6 Increase in Initial Shear Stress with Time of an Oil Sheared to Equilibrium - Ackroyd (16)

being essentially experimental plots of dimensionless stress versus dimensionless time. In agreement with previous investigators(16,25), Billington(14) attributed the measured thixotropic behaviour as due to an internal structure of wax crystal aggregates.

Recently, Ritter(1) has measured the thixotropic behaviour of Pembina crude oil which, at temperatures below 90°F, displays marked anomolous behaviour. This behaviour was attributed to a loosely bonded network structure dispersed within a Newtonian solvent.

In all, Ritter(1) measured thixotropic decay and shear stress growth curves at three rotational viscometer cup speeds (0.5 RPS, 2.0 RPS, 4.5 RPS) at each of four temperatures (75°F, 60°F, 45°F and 30°F). A typical thixotropic decay curve, together with associated shear stress growth curves is shown in Figure (7). As indicated on the plot, the measurement of these latter curves was accomplished by adjusting the cup speed to a lower value after prolonged shearing at a specified elevated shear rate.

In general, all of the thixotropic curves measured by Ritter(1) were continuous functions of shear rate similar to that indicated in Figure (7). However, considerable variation in the relative amount of thixotropic decay was noted. As indicated in Figure (8), which presents a typical set of cross-plotted thixotropic curves, the relative amount of thixotropic decay decreased as the shear rate was increased. In addition, anomolous behaviour was more pronounced at the lower shear rates. In fact, at shear rates approaching 1500 $sec^{-1}$, the oil was shown to behave essentially as a Newtonian fluid after extensive shearing.

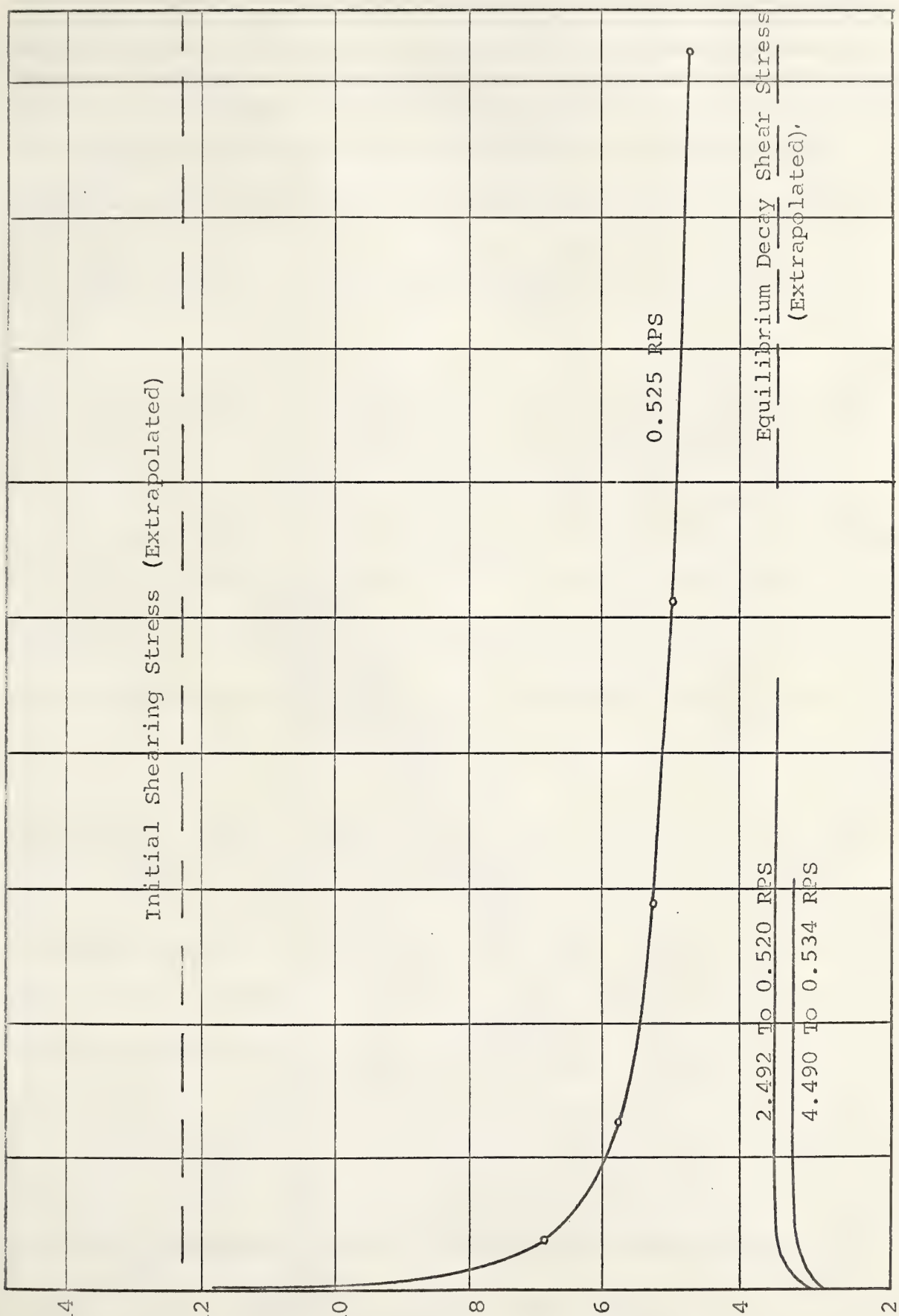
Shear Stress (x $10^2$) - $lbf/ft^2$
Time - Minutes
Initial Shearing Stress (Extrapolated)
0.525 RPS
Equilibrium Decay Shear Stress (Extrapolated)
2.492 To 0.520 RPS
4.490 To 0.534 RPS

FIGURE 7 Typical Thixotropic Decay Curve and Shear Stress Growth Curves - Ritter(1)

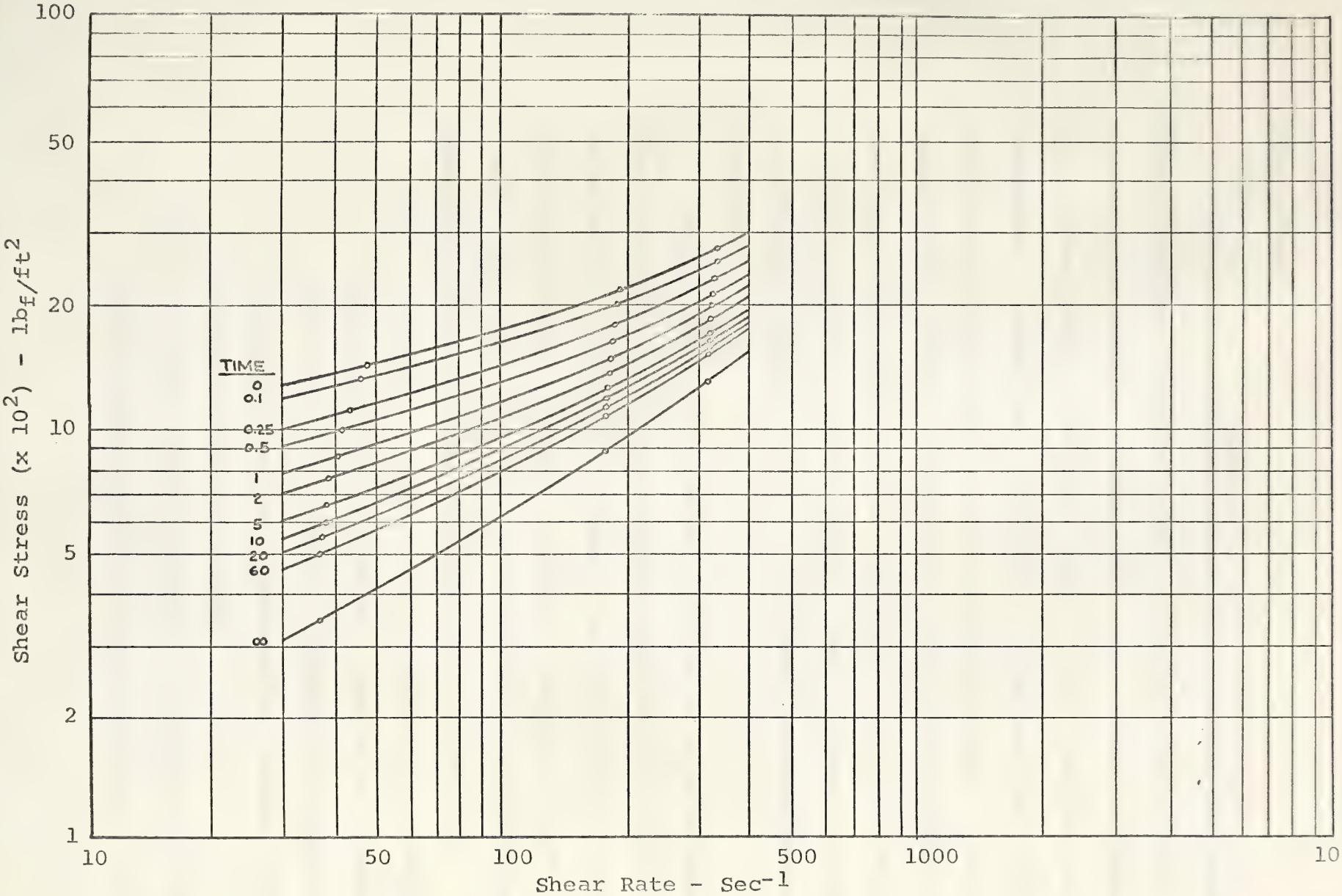


FIGURE 8 Thixotropic Shear Stress versus Shear Rate with Time as a Parameter - Ritter(1)

Plastic Fats:

In plastic fats(42), the crystals of high melting triglycerides form a rigid three dimensional network in the remaining liquid oil. The rheological behaviour of this system shows a strong resemblance to that of other systems containing a network of solid particles, such as dispersions of carbon black in oil(38) or of clay particles in water(13,43). This similarity arises since all of these systems require a finite shear stress prior to continuous deformation or flow; that is, if during a constant shear stress experiment, the applied stress is significantly below the finite shear stress required for flow, the system will display only a deformation characteristic of a solid under comparable testing conditions.

The mechanical, or solid-like properties of the above described plastic fat system have been investigated below the finite 'yield' stress and at stresses near the yield stress by van der Tempel(42). The latter condition resulted in a gradual breakdown of the network structure after a sufficiently long period. Based on rheological measurements, van der Tempel(42) proposed the following description of the network:

(1) The network is composed of a flocculate as an assembly of chains; each chain consists of a linear array of particles placed very close together. The chains are branched and interlinked to form a three-dimensional network, the voids of which are filled by liquid.

(2) The crystal network properties are determined by the density of junction points between the crystals and the strength

of the bonds in these junctions.

(3) Two types of bonds exist in the network; a primary and a secondary bond. The latter are assumed to be due to van der Waals-London attraction between neighboring particles. The nature of the primary bond was not specified, but these were considered to be stronger than the secondary bonds.

Based on this network model, the static network strength of the system was satisfactorily correlated. To do so, however, required estimation of a number of parameters which could not be experimentally measured.

Resumé: All investigators(1,14,16,25) have attributed thixotropic behaviour in hydrocarbon systems as due to a bonded network structure. Three(14,16,25) of these investigators have stated that the network is a consequence of wax crystallization such that the network structural units are wax crystals or wax clusters.

The structural characteristics of a network(42) similar to that proposed for a thixotropic hydrocarbon system have been discussed.

## PHYSICAL PROPERTIES OF WAX-SOLVENT SYSTEMS

In the previous section it was shown that under specific conditions, wax crystallization within a carrier fluid such as a crude oil resulted in the formation of a network structure. Consequently it would appear desirable to investigate some of the physical characteristics of these network structures. However, such investigation has generally been precluded by the complex interdependent behaviour of the waxes and the carrier fluids. As a simpler case then, consider the known physical behaviour of pure waxes and of waxes within industrial solvents.

The crystallization of a mixture of waxes from their melts has been studied(44) both theoretically and by experiment. Generally, attempts have been successful in calculating the solid-liquid equilibrium existing between wax as crystals and wax as liquid. Further, it has been experimentally verified that the addition of an ideal solvent (e.g. heptane, octane, etc) to the wax melt does not alter subsequent equilibrium calculations. For example, the following equation which was originally derived to predict equilibria in wax melts has been found valid over a wide range of temperatures for n-paraffin waxes within 'good' solvents:

$$\log_{10} X_i = -178 N_i \left(\frac{1}{T} - \frac{1}{T_{ni}}\right) \qquad (33)$$

where:

$X_i$ = mole fraction of wax"i" in the liquid phase

$N_i$ = number of carbon atoms per molecule of "i"

$T_{ni}$ = melting point of "i", $^{o}R$

Thus the relationship between wax as crystals and the carrier solvent is a simple function of temperature. For non-ideal solvents, correction factors must be applied to the above equation.

One aspect of wax crystallization in solvents which has been found to be particularly interesting is the crystal habit* of the individual wax crystals. It has been shown experimentally that at least three crystal types form during crystallization: (i) platelets, (ii) needles, and (iii) malcrystalline masses (i.e. irregularly formed masses of microscopically small crystals). To account for such behaviour, at least two explanations have been proposed.

The first(45) attributes crystal habit to the molecular structure of the crystallizing wax and proposes that plate-type crystals represent straight chain hydrocarbons, whereas needles and malcrystalline masses are branched chain hydrocarbons.

The second(46) attributes crystal habit solely to the rate of crystallization. A schematic illustration of this behaviour is shown below:

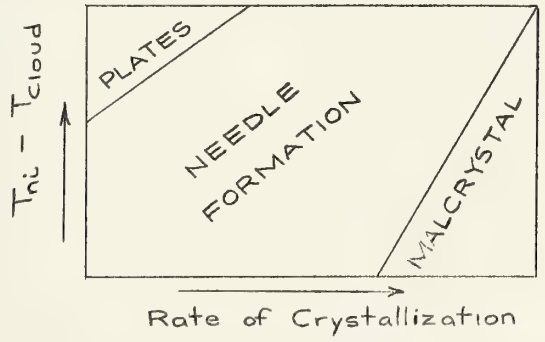


---

* The external shape of a crystal

It might be explained that the rate of crystallization was increased by increasing the cooling rate of the parent solution to final crystallization temperature.

In agreement with the above observations, it was also noted that as the cooling rate increased, the individual crystal size decreased. Further, the presence of resinous materials appeared to accelerate the formation of malcrystalline masses.

# EXPERIMENTAL PROGRAM

In the INTRODUCTION it was pointed out that the experimental program would include (i) modification of the rheological test apparatus, (ii) the selection of a suitable thixotropic model, and (iii) the investigation of the rheological behaviour of the model; the primary direction of the latter objective was towards measurement of the thixotropic behaviour of the model.

Since the chronological progress of the experimental program coincided with the above objectives, it is only logical that each should be considered in sequence as a separate sub-section.

## I. Rheological Test Apparatus

### Redesign and Reassembly of the Auxiliary Equipment Associated with the Alberta Rotational Viscometer

The original air bath temperature control apparatus associated with the Alberta rotational viscometer* occupied the larger portion of one laboratory and, in addition to being bulky and cumbersome, had many undesirable operational characteristics. Consequently, it appeared desirable to redesign and reconstruct the various bath temperature control components.

Specifically, the following equipment alterations and modifications were made:

(1) An air bath recycle flow channel was designed and fitted to the existing viscometer cabinet. This addition (Figure 9) included provision for (i) an internally mounted but externally

---

* This name has traditionally (1,49) been used to describe a rotational viscometer originally designed and constructed by J.V. Fischer(47).

driven air circulation fan, (ii) an air flow control louver and (iii) cooling coils mounted in one of the two available air flow passages. The completed equipment array is shown in Figure (10).

(2) A cold fluid circulation and refrigeration system was designed (APPENDIX ONE) and constructed in the cabinet support framework (Figure 11). The purpose of this system was to provide cold fluid to the air cooling coils.

(3) A temperature control system was designed (APPENDIX TWO) and constructed to regulate the temperature of a recirculating air stream (Figure 12).

In addition to the above, an extremely accurate instantaneous viscometer-cup velocity measuring device was constructed (Figure 13).

Generally, the basic criteria in designing the above equipment were (i) elimination of former operational difficulties, and (ii) formation of a compact, yet portable unit.

Before proceeding further, it shall be advantageous to describe the present form and operational characteristics of the rheological test apparatus.

## Description of the Alberta Rotational Viscometer and Associated Temperature Control Equipment

The Alberta rotational viscometer, illustrated in its present form in Figure (14), consists essentially of a hollow lucite bob, 1.582 inches in diameter and a rotating stainless steel cup, 1.761 inches inside diameter.

The bob has an overall length of 4.860 inches (not including spindle

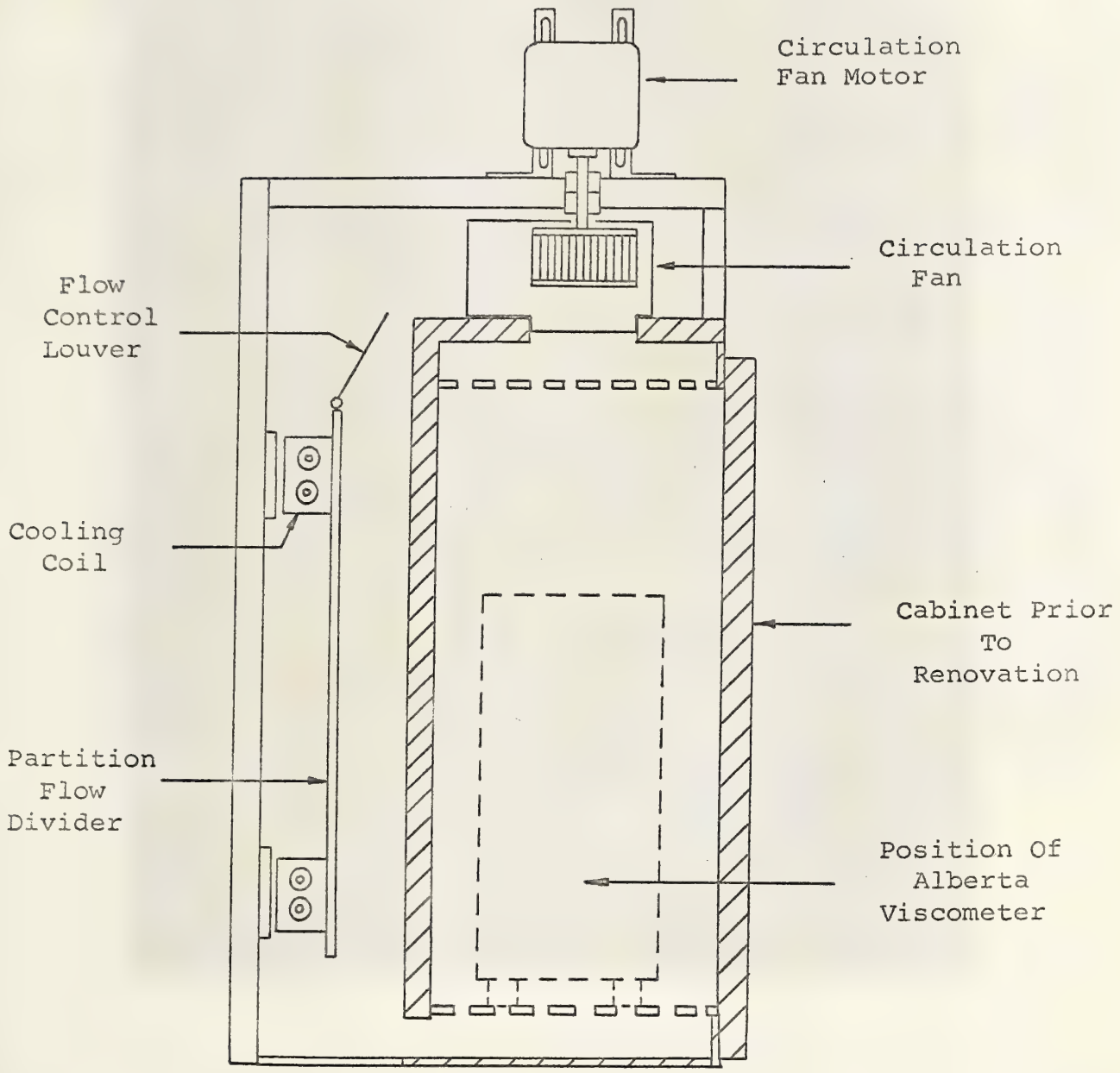


FIGURE 9 Schematic Drawing of Cabinet Addition and Air Flow System

FIGURE 10 Back View of Cabinet Showing Cooling Coils, Louver and Louver Drive Motor

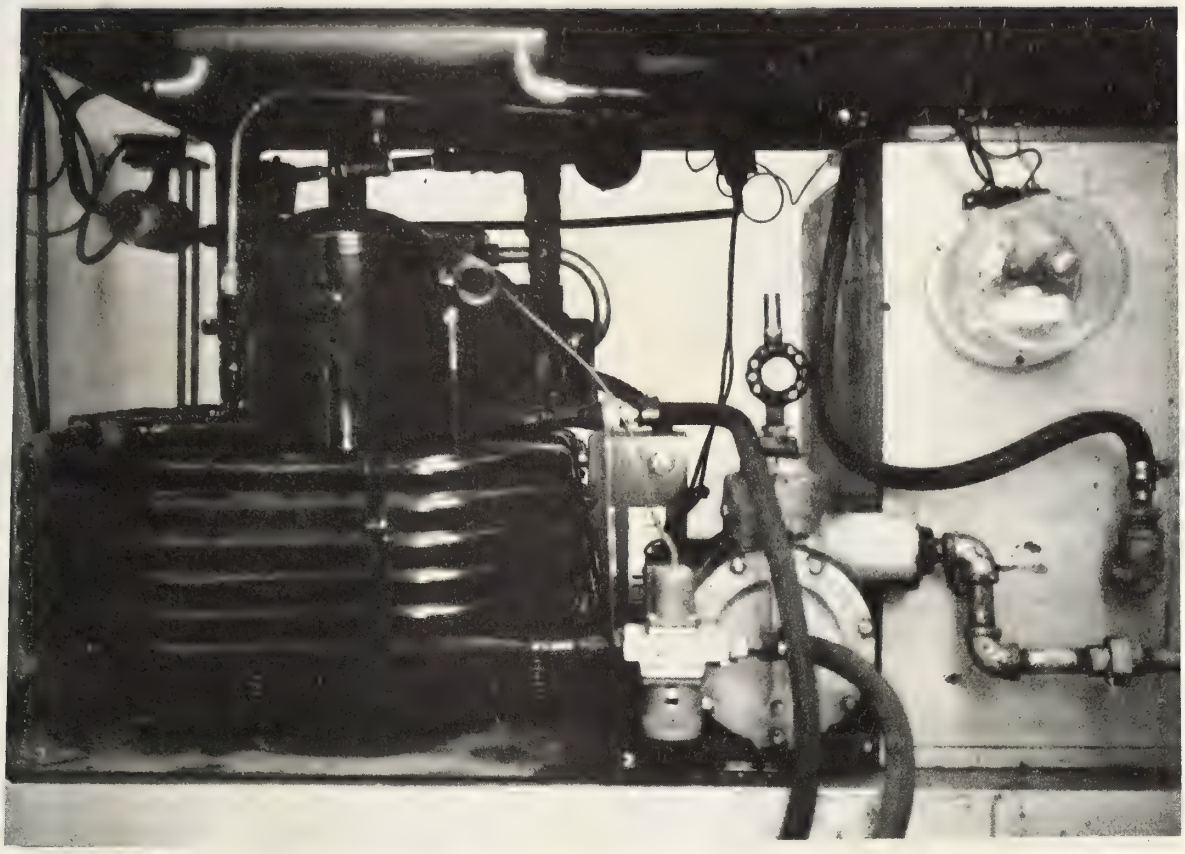

FIGURE 11 Refrigeration System

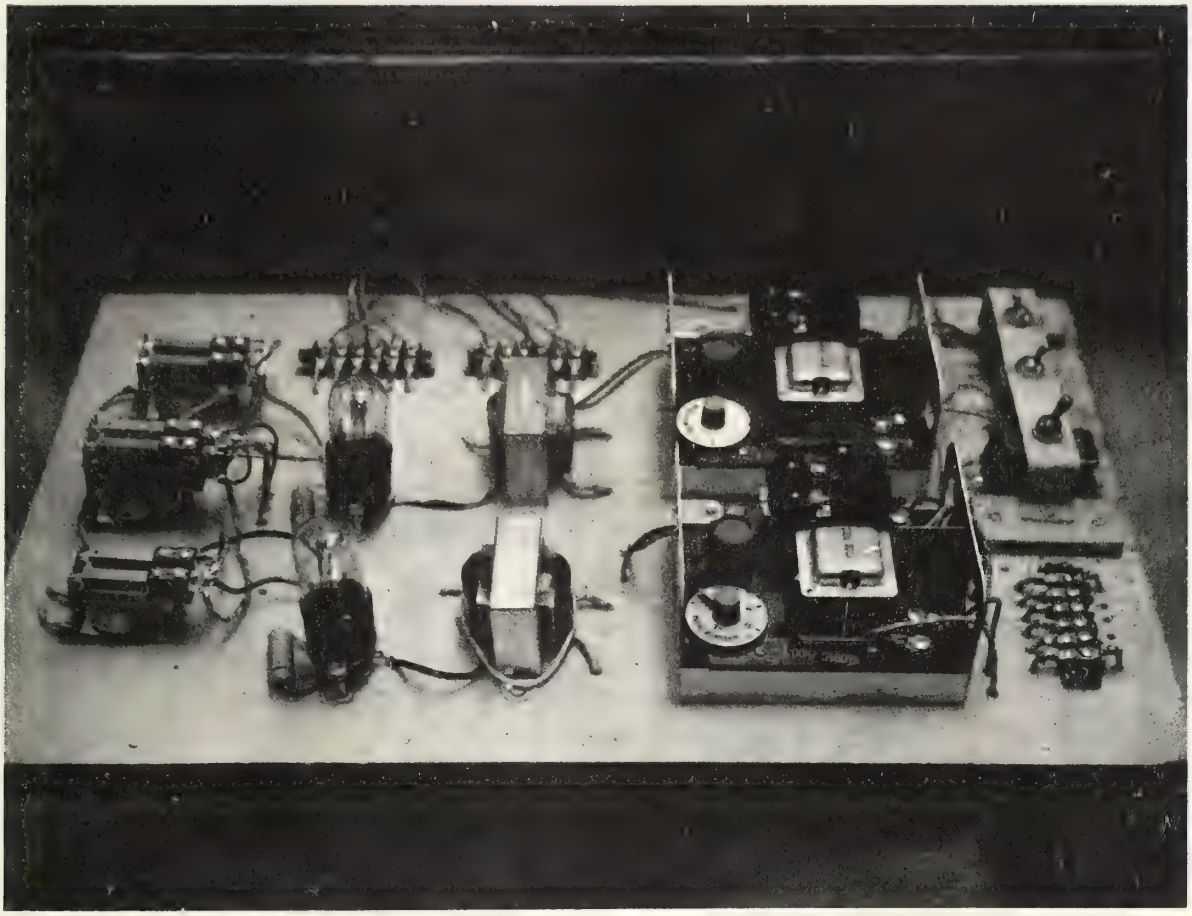

FIGURE 12 Cabinet Air Temperature Control System

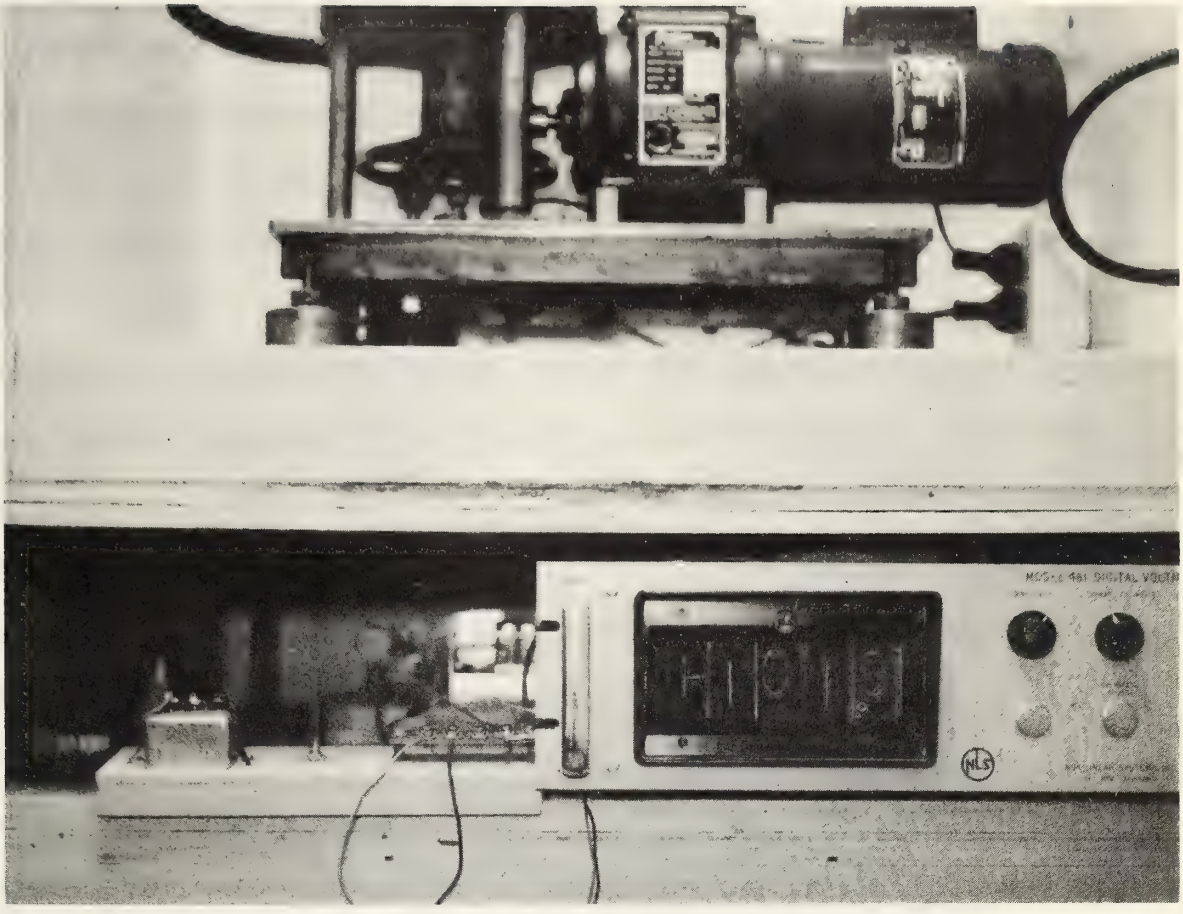

FIGURE 13 Cup Speed Measuring System

and chuck) and has a conical bottom with an apex angle of 151 degrees. Two copper-constantan thermocouples are located on the bob wall 1.344 inches apart and permit accurate measurement of the test sample temperature. The bob is further provided with a concentrically mounted protractor which in conjunction with a stationary indicator is used to measure bob deflection.

During operation, the bob is suspended from the upper chuck support mechanism of the viscometer by means of any one of several 10 inch long calibrated torsion wires. The bob may be coaxially aligned within the cup via an overhead centering platform which contains the upper chuck support mechanism; the vertical position of the bob may be adjusted by means of the viscometer elevator. In all experiments conducted, the bob extended 4.0 inches (as measured from the base of the conical bottom) into the cup. This depth represents maximum possible bob immersion and is most desirable since the end effect of the bob is minimized.

The inside depth of the cup, as measured from the cup lip to its conical base ($151^{\circ}$ apex angle) is 4.625 inches. Thus, a constant end gap of 0.625 inches exists between the bottoms of the bob and cup. The cup is further provided with a bottom inlet line for introduction of samples.

Test sample temperature control is obtained via a concentrically mounted copper bath which surrounds the cup and through which glycol-water is circulated from an Aminco constant temperature bath ($\pm 0.05^{\circ}F$). This test sample temperature control arrangement, as shall be shown in a latter section, performed extraordinarily well.

The motive force necessary for rotation of the cup is provided by a 1/4 HP synchronous motor coupled through a variable speed Graham transmission

FIGURE 14 Alberta Rotational Viscometer

and gear train to the cup bottom. The gear train-transmission combination allows selection of any desired cup speed within the range 0 to 500 RPM. Concentric to cup and mounted on the cup-drive gear is an eccentric cam which upon cup rotation, actuates an electrical counter for measurement of total cup revolutions.

Mounted coaxially with, but beneath the cup drive gear, is a 120 tooth gear which drives an eccentrically supported 24 tooth gear. Suspended from the bottom of the support shaft of this smaller gear is a small D.C. generator whose electrical output passes through a filter (a resistance-capacitance network) to an industrial digital volt meter. The visually displayed voltmeter output, when used in conjunction with a calibration graph(APPENDIX THREE) provides an extremely accurate ($\pm$0.5%) method for determining angular cup velocity.

The entire viscometer assembly just described is mounted within an insulated, thermostatically controlled air bath to reduce the temperature gradient between the ambient air and the test sample. During operation, circulating air is withdrawn from the main cabinet body through a perforated false cabinet roof into the eye of a 1/2 HP driven circulation fan and discharged into the false back of the cabinet. Dependent upon the relative position of a flow control louver located in the false cabinet back, the air either flows over a finned tube cooling coil (surface area of 60 $ft^2$) or by-passes the coil to return to the main cabinet body.

Adjacent to the viscometer and mounted in the circulating air stream is a temperature sensing thermistor which is directly connected to the air bath control system. This control system is a differential gap on-off controller which determines the rotational direction of a 1/20 HP reversing

motor. The motor is ratio gear-coupled (250:1) to the air flow control louver.

In operation, when the air temperature drops below the control band ($\pm 0.1^{\circ}F$), the louver motor is actuated and rotates the louver, effectively closing the cooling coil air passage and permitting the circulating air to bypass directly back to the main cabinet body. When the air temperature rises above the control band, the louver is rotated to uncover the cooling coil air passage while simultaneously blocking the air bypass duct.

The cooling fluid (varsol) necessary for supplying the cooling coils is obtained from a refrigeration system which is located beneath the main cabinet in the cabinet support framework. The major piece of equipment in this system is a Tecumseh 2 HP Low Temperature refrigeration unit with a heat load capacity of 8325 BTU/hr at an expansion coil temperature of $-20^{\circ}F$. The expansion coil associated with the refrigerator is composed of 100 feet of 3/8 inch copper tubing (surface area of 13.1 $ft^2$) and is located in a 10 gallon insulated varsol bath. From the bath, a 1/4 HP driven turbine pump circulates varsol directly to the air cooling coils. The circulating varsol temperature and the operation of the refrigerator is controlled by a thermostat in the varsol bath (APPENDIX ONE).

## Operational Characteristics of the Alberta Viscometer

Three operational characteristics of the Alberta viscometer have been examined by former investigators. They are:

(1) End effect of the bob;

(2) Flow stability in the viscometer annulus;

(3) Test sample heating effects during shear.

These are not characteristics unique to the Alberta viscometer alone, but rather are of varying degrees of importance in every coaxial viscometer. As such, the above characteristics could be adequately investigated on a theoretical basis alone, and could have been discussed earlier in this manuscript; however, since no two coaxial instrument designs are identical, each of the above characteristics shall be discussed as pertaining primarily to the operation of the Alberta viscometer.

(1) End Effect of the Bob

End effect is due to viscous drag by the test sample on the bottom surface of the bob. Unless a viscometer is so designed so as to effectively eliminate it, end effect is of importance in all coaxial viscometers.

The actual consequences of end effect are complex since, due to the test sample flow pattern on the bob bottom, the stress distribution on the finite cylindrical bob surface differs from that of an infinitely long cylinder. As a result, standard formulae which are normally used in coaxial cylinder viscometry are invalid if end effect is excessive. This is a significant problem since analytical derivation of formulae to include end effect are, to all practical purposes, impossible. One investigator(48) has attempted to treat this problem analytically, but the resultant flow equations are intractable for even the most simplified case.

Fortunately, an experimental method has been devised which does permit measurement of, and correction for, end effect. In essence, the stress contribution due to end effect is considered as equivalent to an increase in the length of the cylindrical bob surface. Thus, as applied

to Equation (17), the following equation has been proposed:

$$G = \frac{4\pi(h + \Delta h)}{\left(\frac{1}{r_1^2} - \frac{1}{r_2^2}\right)} \mu_n W \qquad (36)$$

where $\Delta h$, the end effect correction, is stated to be a function of h (the total bob immersion) and the end-gap distance between the bottoms of the bob and cup.

This end effect correction is usually obtained experimentally by plotting (G/w) versus (h) to obtain a linear relationship between these variables which then permits direct evaluation of ($\Delta h$). An account of this method, together with experimental results as ascertained for the bob-cup combination of the Alberta viscometer has been given in a recent publication (1). Specifically, for the experimental bob immersion (4.00 inches) used during the current investigation, an end effect correction of 0.225 inches has been determined(1). The relative magnitude of this correction (equivalent to an additional 5.3% of cylindrical bob surface) has been confirmed by previous investigators (47,49).

Actually, end effect corrections, as determined utilizing Equation (36), are suitable only for Newtonian fluids, since due to the complex inter-relationship of shear rate and consistency of a non-Newtonian fluid, end effect should be a function of the characteristics of the non-Newtonian fluid being sheared. Hence, certain inadequacies exist if an end effect as determined for Newtonian fluids is used in calculations involving non-Newtonian fluids. However, to quote a previous investigator(1);

"The situation is not as serious as it might initially seem.

The largest variation in viscosity will likely occur in the region approaching the apex of the cone, which also represents a region of reduced torque due to both lower shear rate and radius. Hence, the net deflection of the bob will not be materially influenced ..."

In view of this qualification, errors in the end effect correction were assumed to be tolerable and the afore-mentioned experimental technique was adopted.

(2) Flow Stability in the Viscometer Annulus

In all equations pertaining to concentric cylinder viscometry, it is inherently assumed that the basic flow pattern is laminar. However, this condition is not guaranteed at all shear rates, since ring-shaped vortices, characteristic of a turbulent flow process, develop at a specified viscometer "Reynold's" number. For the coaxial arrangement of a stationary inner cylinder and a rotating outer cup, the critical "Reynold's"number, as given below, is strongly dependent upon the ratio of annular thickness to the outer cylinder radius:

$$\frac{W r_2^2 \rho}{\mu_n} = f\left(\frac{r_2 - r_1}{r_2}\right) \qquad (37)$$

A graphical correlation of "Reynold's" number versus $(r_2 - r_1)/r_2$ has been given by Schlichting(50). For the geometrical arrangement of the Alberta viscometer, a critical transition equation of the following form is indicated:

$$\frac{W\rho}{\mu_n} = 12.85 \times 10^6 \qquad (38)$$

Thus, considering typical properties of a 10.0 cp. oil with a density of 45 $lbm/ft^3$, a critical transitional speed of about 300 RPS (about 30 times faster than maximum possible experimental speed) is indicated. Further, a recent publication(51) has shown that shear of a non-Newtonian fluid does not significantly alter this value.

From the above calculations, it would appear that considerations involving unstable flow behaviour would be unwarranted in view of the limited range of cup speeds available (i.e. maximum of 10 RPS). However, an earlier investigator(47) noted that when low viscosity (5 to 20 cp) oils were being sheared in the Alberta viscometer, a deviation from Newtonian behaviour occurred above a specific cup speed. This investigator has also noted such behaviour and feels that such deviations demonstrate the onset of an unstable flow process.

Such behaviour is rather puzzling since other viscometers with which the transition correlations were developed do not display this phenomenon until extremely high shear rates are attained. However, in one respect, the Alberta viscometer differs from these viscometers - having a relatively large end-gap beneath the bob. It is thought that this flow region is responsible for the apparent onset of instability.

It has previously been indicated that the flow pattern in the end-gap space is, to all practical purposes, impossible to describe on an analytical basis. As such, this flow area has never been extensively investigated and a stability criteria to include end effect has never been developed.

Experimentally, the only qualitative observations on such a process have been made by Fischer(47), who noted that as the clearance between the

bob and the bottom of the cup decreased, the apparent onset of instability advanced to progressively higher cup speeds. If a superficial analogy between Couette flow and the flow pattern at the cup bottom may be used, then this phenomenon should occur, since in effect the 'annular' width is being decreased, thereby tending to stabilize laminar flow.

Unfortunately, this problem was not recognized until completion of the experimental program and, as such, a detailed study of this phenomenon was not conducted. However, it is possible with existing available data to make some comments on the stability problem which exists in the Alberta viscometer, and to qualitatively indicate a safe operational cup speed range.

Perhaps the most difficult problem in ascertaining the stability limit is the actual detection of the onset of instability, since in all cases, the contribution of end effect is a small (5.3%) portion of total shear stress. This statement may be exemplified by examination of Figure (15), in which a number of curves have been plotted, one of which illustrates the gradual onset of instability. The difficulty of detecting instability is readily apparent since deviations from Newtonian behaviour attain only about 4% of the total shear stress even when cup speed has exceeded the critical speed by twice. Further, considering all of the data available to this investigator, a positive onset of instability could only be identified for the 4.511 and 8.5 centipoise oils shown. This was primarily due to the limited range of the data available (generally only up to about 3.0 RPS) and the uncertainty in detection of an actual onset of instability.

As may be noted from Figure (15), as the viscosity of the sheared oil increases, the onset of instability is progressively increased to higher

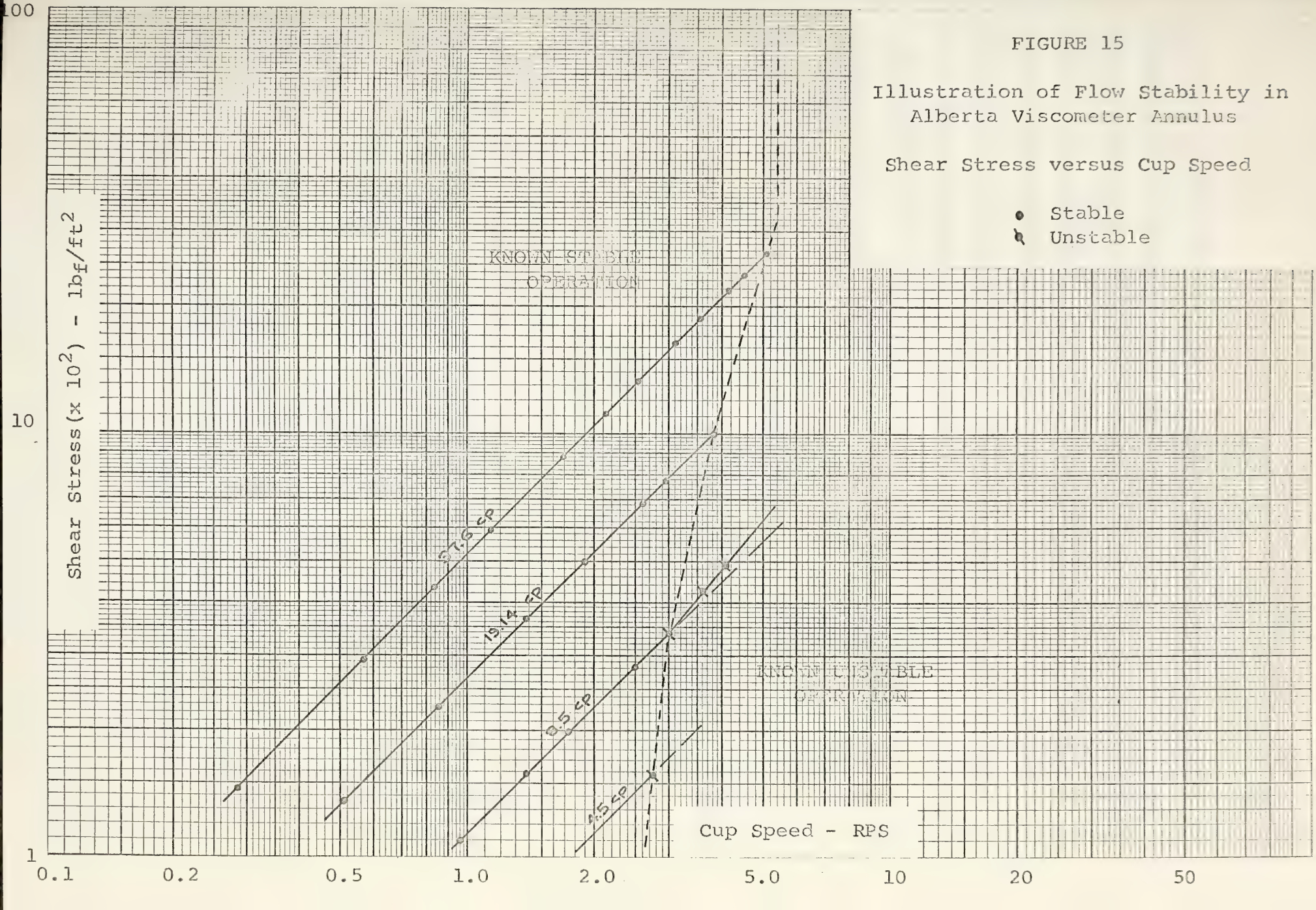


FIGURE 15

Illustration of Flow Stability in Alberta Viscometer Annulus

Shear Stress versus Cup Speed

● Stable
◔ Unstable

cup speeds. This fact was also noted by Fischer(47); thereby, a qualitative stability limit (indicated by the sloping dotted line in Figure (15) ) has been presented. This line is not intended to serve as a rigorous determination of a generalized stability limit but rather to serve as a guide line during interpretation of experimental results. Despite the limitations of such a plot, it may be noted that, in general, stability would not appear to be a crucial factor in interpretation of experimental results, since in the majority of the experimental runs, the apparent oil viscosity was greater than 35 centipoises.

(3) Test Sample Heating Effects During Shear

During the early stages of the experimental program it was necessary to determine the magnitude of the temperature rise in a sheared sample. This was a matter of some importance since if the sample temperature continually increased during the test period, then it might have been impossible to differentiate between sample degradation and shear heating effects near the end of a long sample-test period. A previous investigator(1) had reported a maximum temperature increase of $0.5^{\circ}F$, but no specific reference had been made as to the duration of temperature increase.

The method of approach to this problem utilized two evaluation techniques; (i) a theoretical evaluation and, (ii) an experimental test to determine "average" sheared fluid temperature rise.

The theoretical approach was based on a consideration of the temperature rise in a Newtonian fluid sheared in an annulus similar to conditions experienced in the Alberta viscometer. The evaluation did not

consider temperature effects due to sample shear by the end of the bob, since this source could only contribute a small portion to overall temperature rise. In short, the approach was essentially that of solving the energy equation for a fluid in the annulus in terms of the transport properties of the sheared oil. In cylindrical coordinates, and in dimensionless form, the energy equation may be expressed as (52, APPENDIX FOUR).

$$\frac{1}{E}\frac{d}{dE}\left(E\frac{d\Theta}{dE}\right) = -\frac{4\bar{N}}{E^4} \qquad (39)$$

where E is a dimensionless co-ordinate group; $\Theta$ is a dimensionless temperature group, and $\bar{N}$, a dimensionless group in terms of the transport properties of the fluid and the geometrical configuration of the viscometer.

Applying the proper boundary conditions, Equation (39) was solved to determine the maximum temperature (i.e. at the bob surface) within the viscometer annulus. In terms of the pertinent variables, the final equation was:

$$T_{BW} = T_{CW} + \left(\frac{\mu w^2}{k}\right) 1.96 \times 10^{-3} \qquad (40)$$

where $T_{BW}$ is the bob wall temperature; $T_{CW}$ is the cup wall temperature, and k, the thermal conductivity of the sheared fluid.

It may be noted that Equation (39) predicts the bob wall temperature to be directly proportional to the sheared fluid viscosity, but of more importance, to the square of the cup speed. Furthermore, a complete analysis requires estimation of the cup wall temperature.

In order to provide a check on the magnitude of the temperature bound predicted by Equation (40), an experimental run was conducted by

shearing a heavy Newtonian oil ($\mu$ = 117 centipoises; k = 0.082 BTU/hr.ft$^2$ $^\circ$F) at a cup speed of 4.5 RPS. For this flow system, the bob wall temperature and cup wall temperatures were calculated (APPENDIX FOUR) to be:

$$T_{BW} = T_{CW} + 0.228^\circ F$$

$$T_{CW} = T_{CF} + 0.03^\circ F$$

where $T_{CF}$ is the temperature of the cooling fluid from the Aminco constant temperature bath.

Thus the total bob wall temperature rise would only be 0.26°F. In fact, the magnitude of this temperature bound was confirmed during the experimental run by utilizing the overall decrease in bob deflection to calculate an "average" temperature rise across the annulus (0.15°F average experimental versus 0.26°F calculated maximum). Further, it was noted that the total bob deflection decrease occured within five minutes of the start of the test run.

Since the oil used during the above experimental run approximated the viscosity of the system used during the subsequent experimental program, temperature rise during test sample shear is not of sufficient magnitude or duration to warrant consideration during interpretation of experimental results.

## II. Selection of a Thixotropic Model

### Selection of a Thixotropic Model

One of the objectives of this investigation was the selection of a non-volatile experimental thixotropic model which could be continuously

re-used. This requirement inferred that the model would have reproducible network regenerative capability. If this objective could be met, then two important problems would be solved; namely, (i) the requirement of handling large amounts of test materials would be eliminated and, (ii) during correlation of test results, possible individual sample differences would not have to be considered. The initial stages of the experimental program were, therefore, devoted to selection of a thixotropic system which would provide reproducible thixotropic behaviour from only one sample.

Before proceeding, it should be stated that this objective was not attained. For this reason, it is instructive to follow the experimental developments leading up to the final selection of an experimental model and to the simultaneous selection of the final experimental program.

The initial choice of a thixotropic model was relatively straight forward, since at least three investigators(14,16,25) had surmised that thixotropic behaviour in one experimentally feasible system was due to a loosely bonded wax crystal network. Accordingly, a highly refined sample of eicosane (nC - 12) was diluted to various concentrations in a variety of solvents (acetone, heptane, octane and Diol-34*). These mixtures were then inserted into a constant temperature bath and visually observed over a range of temperatures from 30°F to 70°F. Except for the Diol-34 mixture, in which network structures were formed, the remaining solvent-wax mixtures precipitated wax crystals. Consequently, all base solvents, with the exception of Diol-34 were discarded.

---

* An uninhibited napthenic base lubricating oil with a viscosity of 15 centipoises at 70°F and a pour point of -50°F.

Tests continued with the eicosane-Diol 34 mixtures, but it was generally noted that regardless of the eicosane concentration, once a network formed at a specific temperature level, the network appeared so rigid as to preclude satisfactory viscometer testing. It was tentatively suggested that a longer wax chain fraction might have a wider network formation temperature range and thereby have a "looser" network. Consequently attempts were made to obtain a pure long chain wax fraction.

During the interim period, a few preliminary tests were conducted using a commercial sealing wax, Parawax ($\triangleq$ nC - 26), which was mixed to various concentrations (2.0, 5.0 and 7.0 percent by weight) in Diol-34 and visually observed at various temperatures between 40°F and 90°F. At 60°F, the 5.0 percent mixture appeared to have a "looseness" similar to that desired, so the mixture was subjected to a few rheological tests. These tests merely involved slowly cooling the wax-oil mixture from 120°F to 60°F in the viscometer, allowing the sample to remain undisturbed for an hour at 60°F, and then measuring the rheological behaviour of the sample at a constant cup speed. The subsequent test results indicated that this system appeared to be a very good thixotropic model, displaying both pronounced thixotropic behaviour and shear stress network growth.

Subsequent to these preliminary tests, it became evident that a suitable long chain wax fraction of the purity (99+%) desired could not be readily obtained. Therefore, from lack of a more promising wax fraction, Parawax was used as the wax fraction during the remaining test program.

Since the 5.0 percent by weight Parawax in Diol-34 system appeared to be a most satisfactory thixotropic model, a testing program to measure

the rheological behaviour of this model was begun. Such a test program involved continual re-use of one sample (about 100 c.c.) at a variety of predetermined cup speeds, at which thixotropic decay and shear stress growth curves were to be obtained. However, after a few experimental tests at one constant cup speed, it became evident that the thixotropic decay curves were not reproducible, i.e. the absolute error between shear stress values from the individual thixotropic decay curves, as selected at a specific shear test time, was greater than the desired error limit of $\pm 3$ percent.

Since such non-reproducibility might have been due to sample handling, a standardized experimental procedure was developed. Utilizing this procedure, outlined in Figure (16), additional rheological tests were conducted at predetermined cup speeds. However, as before, the measured thixotropic decay curves were non-reproducible. A few test results, as shown in Figure (17), exemplify this latter statement.

However,one relevant fact was noted; that a comparison between individual shear stress values, as measured after one minute of shear, indicated that this shear stress value decreased as the number of rheological tests increased. Accompanying this decrease in shear stress at one minute was a respective decrease in the measured yield value.

Since the experimental method had been standardized and rigidly conformed to, the non-reproducibility could be attributed only to changes in the physical characteristics of the model. This conviction was further strengthened when it was noted that as the number of tests increased, an increasing number of wax "threads" remained undissolved at $180^{\circ}F$. It was

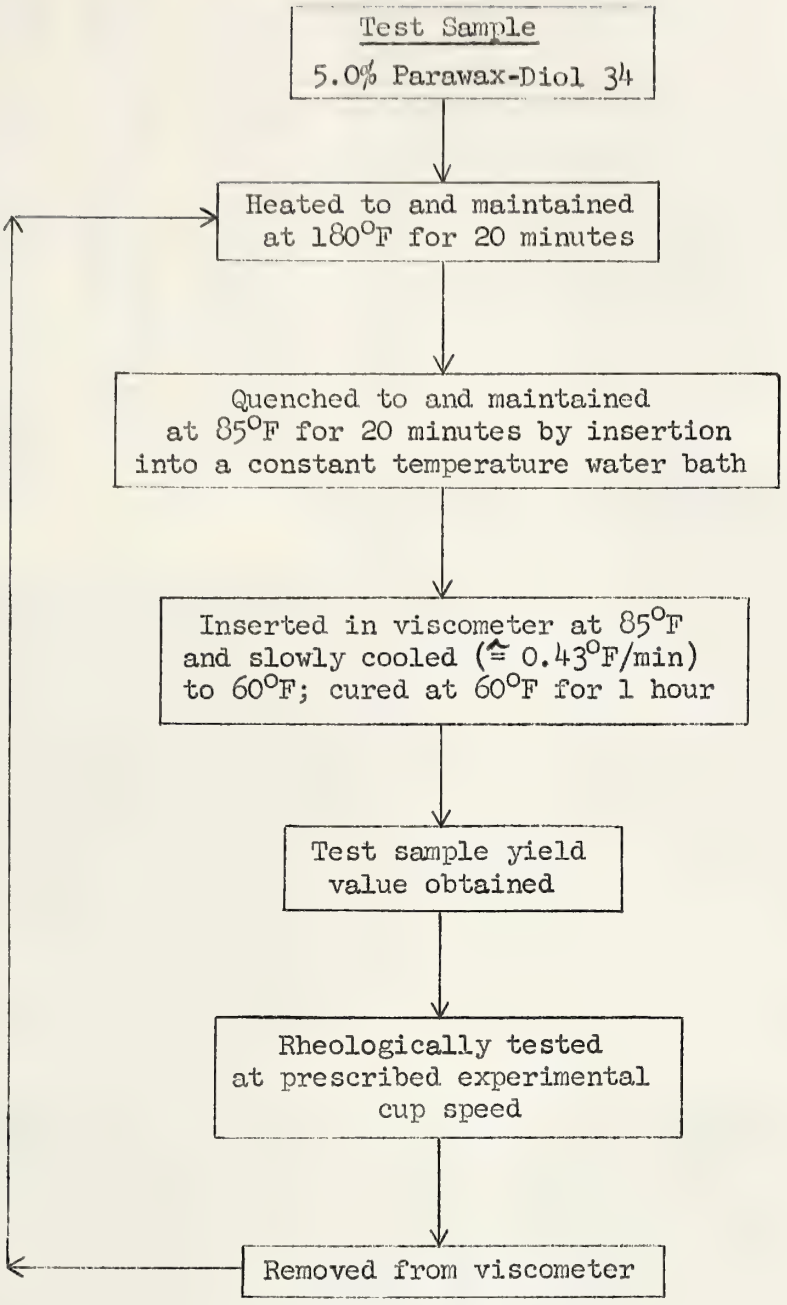
Test Sample
5.0% Parawax-Diol 34
Heated to and maintained at 180°F for 20 minutes
Quenched to and maintained at 85°F for 20 minutes by insertion into a constant temperature water bath
Inserted in viscometer at 85°F and slowly cooled (≏ 0.43°F/min) to 60°F; cured at 60°F for 1 hour
Test sample yield value obtained
Rheologically tested at prescribed experimental cup speed
Removed from viscometer

FIGURE 16

Initial Sample Handling and Rheological Test Sequences

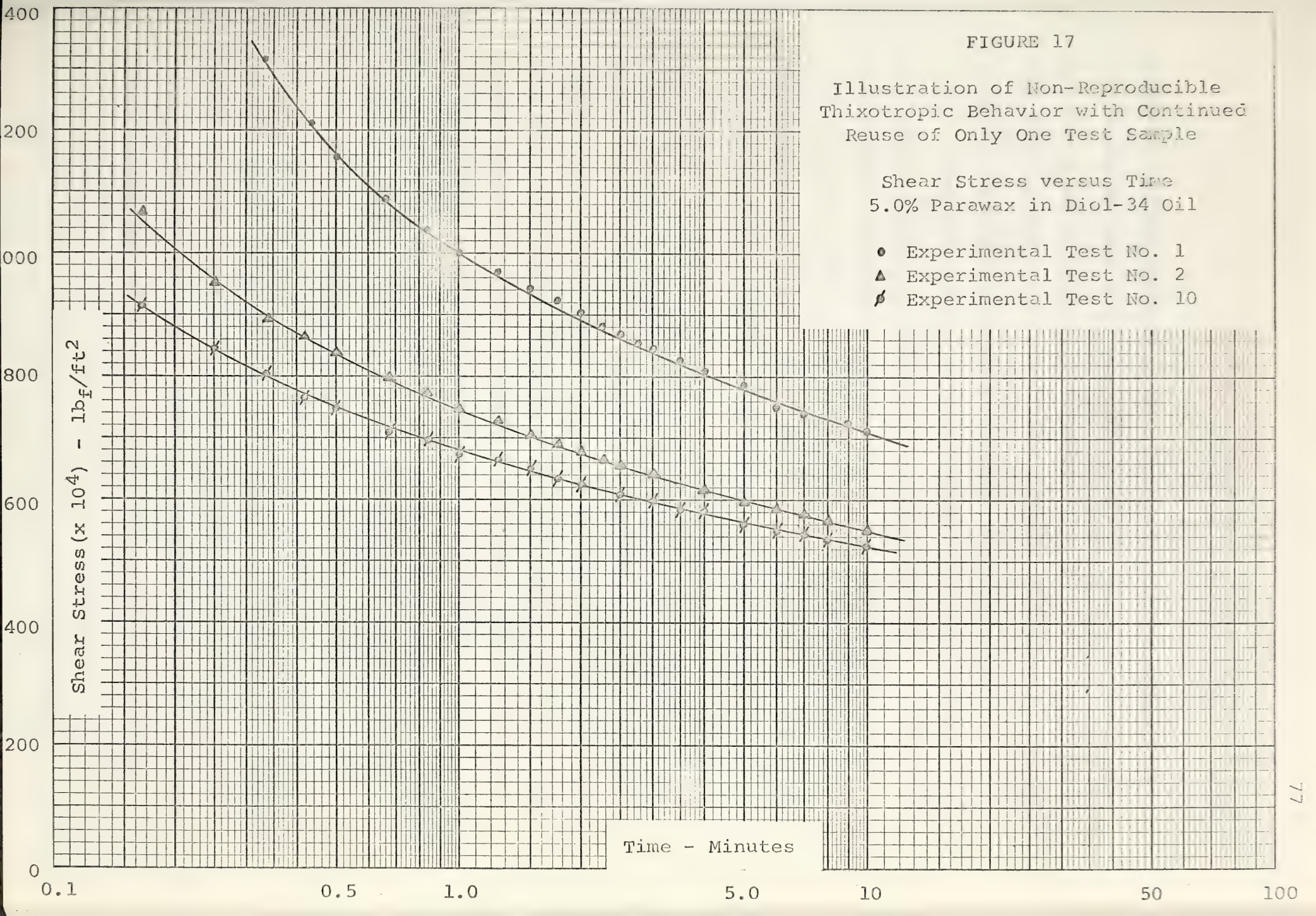
FIGURE 17
Illustration of Non-Reproducible Thixotropic Behavior with Continued Reuse of Only One Test Sample
Shear Stress versus Time
5.0% Parawax in Diol-34 Oil
Experimental Test No. 1
Experimental Test No. 2
Experimental Test No. 10
Shear Stress (x 10⁴) - lb_f/ft²
Time - Minutes
0
200
400
600
800
000
200
400
0.1
0.5
1.0
5.0
10
50
100

suggested that the formation of these threads was, by some unknown manner, influencing the rheological behaviour of the test sample. (Actually, the quantity of wax so involved, as determined by visual inspection, could not have been more than 1/1000 of the total wax initially dissolved. Nevertheless, the phenomenon could not be attributed to any other factor)

Since the formation of these "threads" could possibly be due to chemical combination, a straight distillation-run oil (CWO) without catalytic chains or additives was obtained and a wax refinement procedure instituted (as described in "Physical Properties of the Components of the Thixotropic Model"). With these ingredients, a series of tests (27 in all) were conducted using a 5.25 percent by weight Parawax in CWO solution.

In the interests of brevity, individual test results shall not be discussed here (see APPENDIX FIVE for an abbreviated analysis), but in summary, it may be stated that thixotropic reproducibility using one sample only was not attained. Moreover, it was tentatively concluded that regardless of the experimental technique, re-use of one sample would never yield reproducible results within a reasonable time limit. This conclusion will be given further attention in the "Discussion of Results".

Two alternatives were thus available: (1) to discontinue use of a wax-oil model and replace it with an alternate thixotropic system, or (2) to develop a technique capable of handling test samples on a once-through basis. The first alternative was considered but discarded after an investigation of possible alternate systems (i.e. clay-water suspension, silica gel grease, various concentrated polymeric-solvent systems) revealed that they did not possess any superior experimental advantages; in fact, a wax-oil system appeared to be the simplest of experimental thixotropic

models. Consequently, the 5.25 percent by weight Parawax-in-CWO system was accepted as being the most suitable thixotropic model.

At first it was felt that a new test sample could be individually prepared prior to each rheological test. This approach was attempted but test results were erratic, and reproducibility was not within the desired experimental limits (i.e. 10 percent versus the desired limit of $\pm 3$ percent). This latter erratic behaviour was attributed to the difficulty in obtaining a small individual representative wax sample for preparation of the individual test samples.

Based on the test results of individual sample preparation, a simplified statistical study (APPENDIX SIX) indicated that a gross sample mix equivalent to at least eleven samples would have to be prepared prior to a test; only one sample could be used from this mix and the remainder would have to be discarded. Hence, considerable incentive existed for the development of a technique which would permit storage of a gross sample without attendent physical degeneration.

Gross sample storage was attempted at room temperature, and at intermediate storage temperatures up to , and including, 250°F. However, test results (APPENDIX FIVE) indicated that sample degeneration occurred at all these test temperatures. Hence, a gross sample was prepared, divided into test size increments and stored at -7°F in a commercial refrigerator. The implications inherent in such a procedure will be discussed in a latter section ("Discussion of Results"), but, as may be noted from Figure (18), utilizing this sample storage method, together with a standardized sample handling and rheological test sequence, resulted in reproducible ($\pm 3$ per cent) thixotropic behaviour.

FIGURE 18

Illustration of Thixotropic Reproducibility Using Developed Sample Preparation Sequence

5.25% Parawax in CWO oil
Cured one hour at 60°F

- Sample storage = 22 hours at -7°F
- Sample storage = 74 hours at -7°F

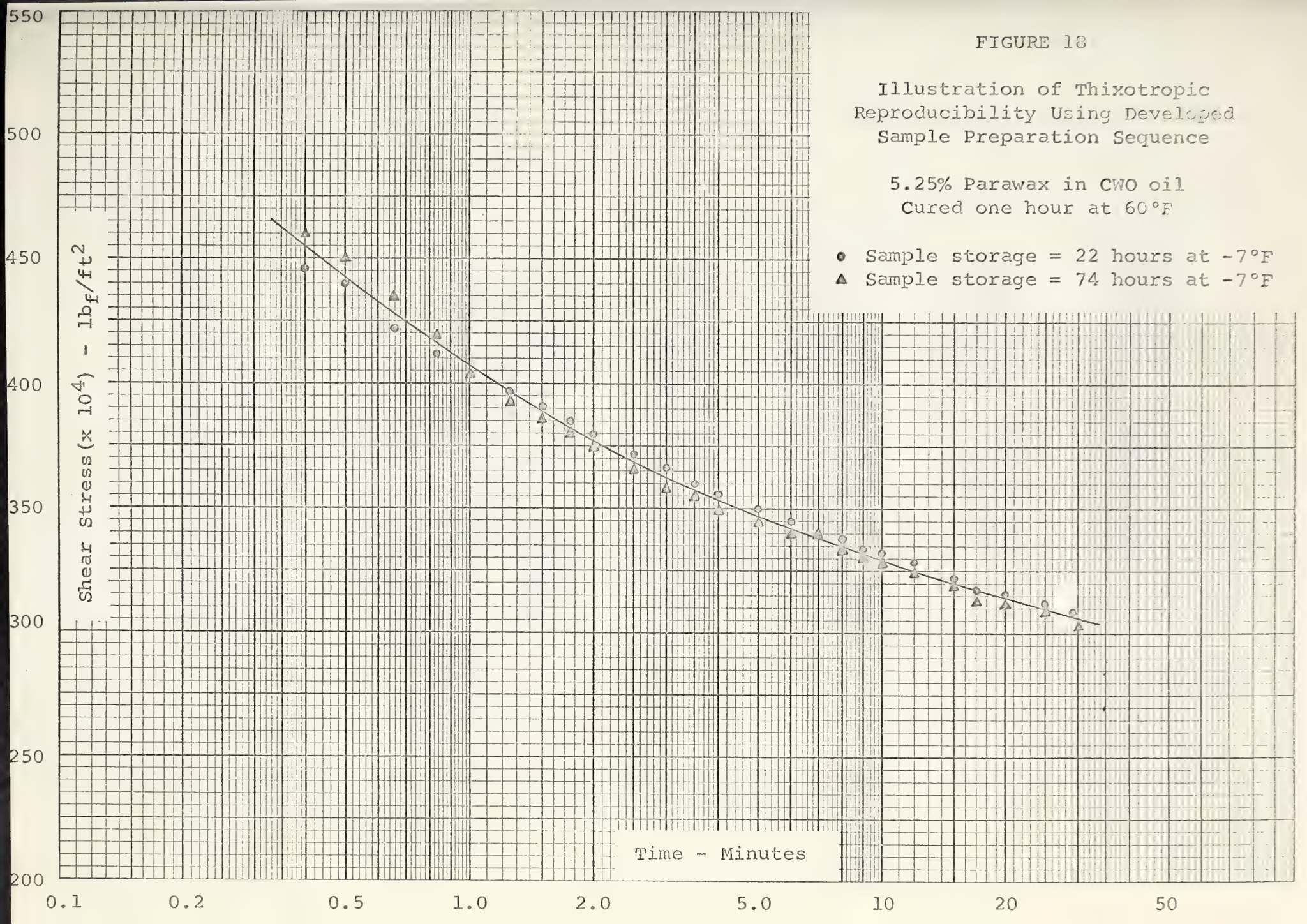

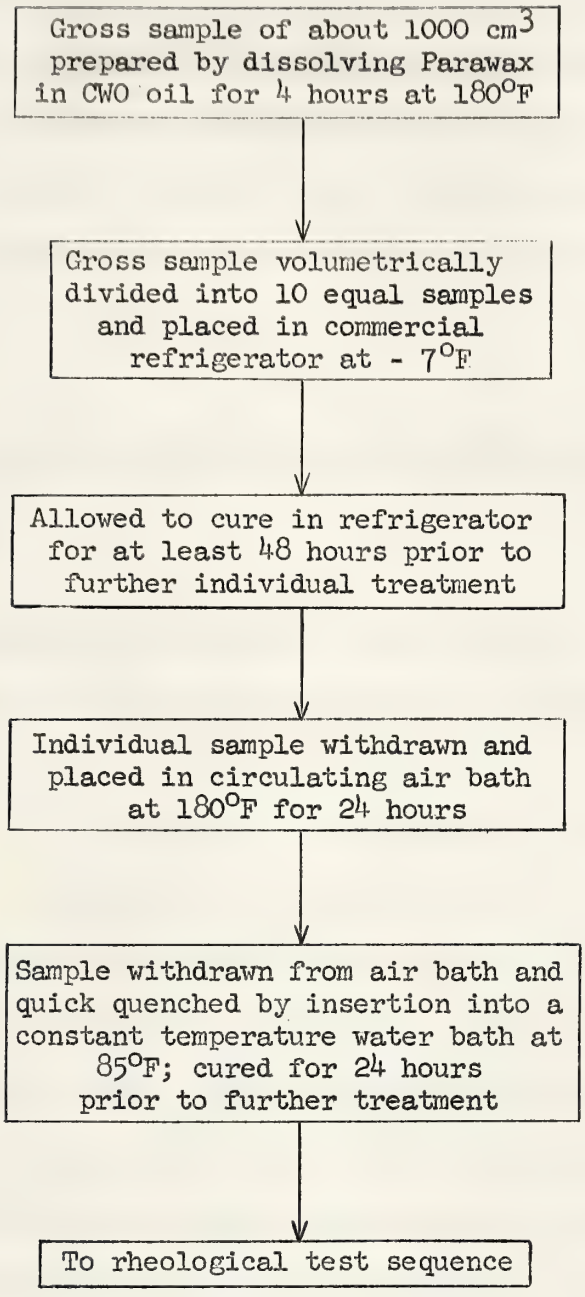
Gross sample of about 1000 cm3 prepared by dissolving Parawax in CWO oil for 4 hours at 180°F
Gross sample volumetrically divided into 10 equal samples and placed in commercial refrigerator at - 7°F
Allowed to cure in refrigerator for at least 48 hours prior to further individual treatment
Individual sample withdrawn and placed in circulating air bath at 180°F for 24 hours
Sample withdrawn from air bath and quick quenched by insertion into a constant temperature water bath at 85°F; cured for 24 hours prior to further treatment
To rheological test sequence

FIGURE 19

Sample Preparation and Handling Sequence
Prior to Rheological Test Sequence

The development of a follow-up sample handling sequence to prepare a test sample for a rheological analysis was relatively straight forward, requiring only that a procedure be used which was easily reproduced and which would minimize possible sample handling errors. The sequence of steps involved, as adopted for the remainder of the test program, is shown in Figure (19).

Physical Properties and Treatment of the Components of the Thixotropic Model

(1) Parawax:

The physical properties of the Parawax, as determined experimentally and as obtained from manufacturers(International Waxes Corporation) specifications are:

Oil content - less than 0.1 percent

Melting point - 133 to 135°F

Although the wax was specified pure, in conformance with the Food and Drug Act, some foreign bodies were visibly present in the wax melt. As a purification step, about 1000 grams of wax was heated to 150°F and then vacuum filtered three times at that temperature. The wax was then cured at 180°F for three days, the temperature lowered to 140°F for 24 hours and then vacuum filtered at this temperature. The resultant wax liquid was poured onto a clean plastic surface to a depth ranging from 1/16" to 1/8" and allowed to solidify at room temperature. The wax sheet was then cut into 1" squares, and subsequently cut into cubes ($\triangleq$ 1/16" per side). The wax cubes were stored in a stoppered glass container prior to usage.

For the final experimental runs, all wax samples were obtained from one 1000 gram batch since experimental studies had shown a marked dependence of rheological behaviour on different batches of wax.

(2) CWO Base Oil:

The oil fraction was a straight distillation-run cut without additives or catalytically produced fractions.

The physical properties, as obtained from the manufacturer (Imperial Oil Limited) were:

| | |
|---|---|
| Flash Point | 300°F |
| Pour Point | -40°F |
| °API | 34° |

The experimentally determined viscosity of the oil as a function of temperature is shown in Figure (20).

(3) Thixotropic Model Preparation

The thixotropic model component fractions were obtained by accurately weighing the individual wax and oil fractions on an analytical and Bouillon beam balance respectively. By this method, when two components were finally mixed, wax concentrations were within $\pm$0.001 weight percent.

## III. Rheological Behaviour of Thixotropic Model

### Network Formation Characteristics of the Thixotropic Model

The fundamental characteristic of the thixotropic model is its inherent ability to form network structure. This is not a characteristic

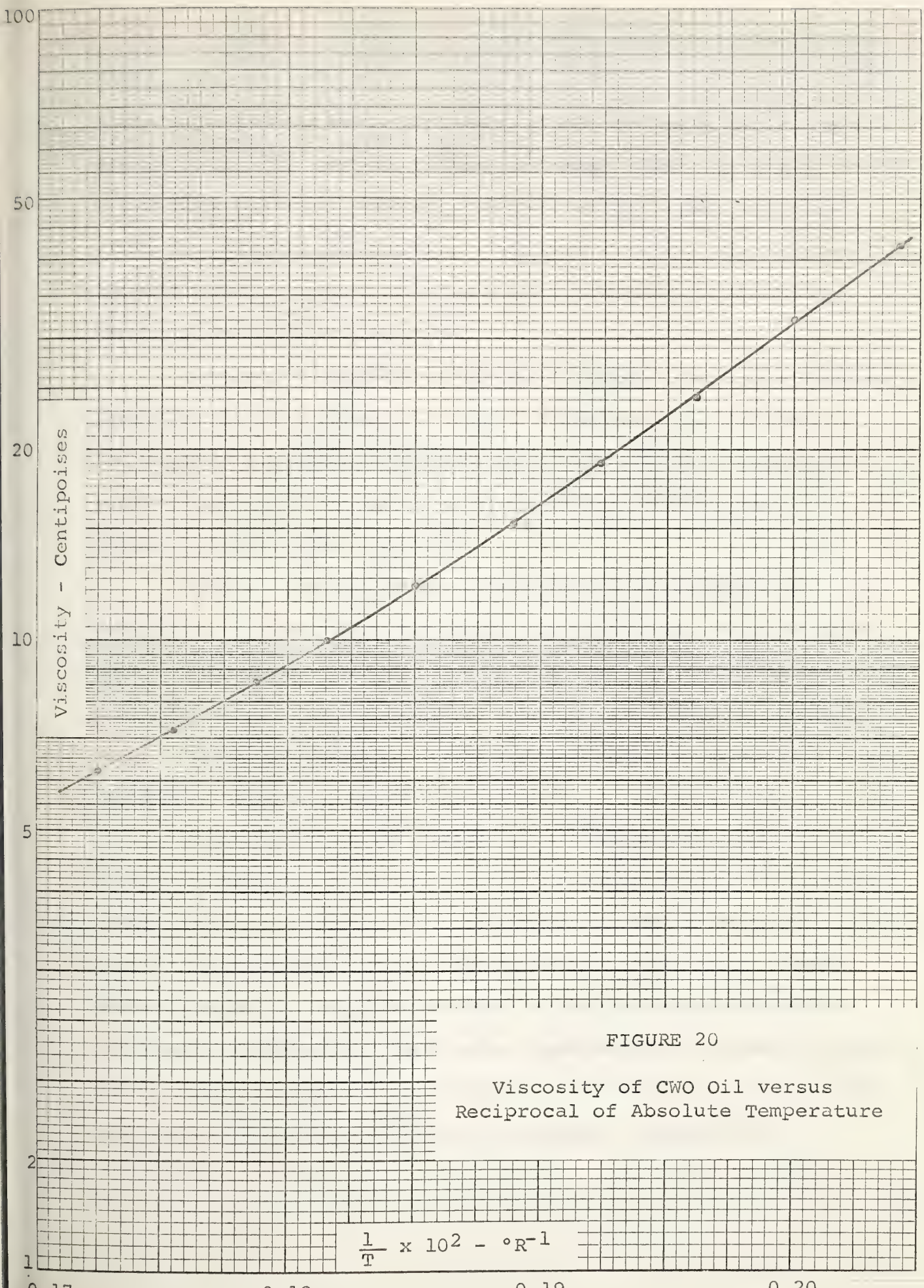


FIGURE 20

Viscosity of CWO Oil versus
Reciprocal of Absolute Temperature

unique to this chosen model, but rather, is demonstrated by similar wax-oil systems (14,16,25). However, for each individual system, the network formation characteristics, and hence, the resultant rheological properties differ from those of other systems. Such being the case, some of the characteristics of network formation and the subsequent rheological behaviour of the model will described.

At elevated temperatures, the wax-oil model displays many physical properties which are essentially those of the solvent oil. For example, the temperature dependent bulk volume coefficient and the temperature dependent viscosity of the wax-oil model are, in most respects, identically similar to those of the solvent oil.

However, once the system temperature is lowered beneath an experimentally determinable temperature, the wax-oil model displays marked anomolous behaviour. The incipience of this behaviour is characterized by a visually discernable "murkiness" or "cloud effect" throughout the liquid phase. This latter behaviour is directly attributable to formation of wax crystals or clusters of wax crystal chains.

The formation of wax clusters has a profound effect upon the physical characteristics of the wax-oil system and subsequently causes abrupt changes in the bulk volume coefficient (Figure 21) and in the temperature-viscosity relationship. Further, the consistency of the system becomes markedly anomolous, being characterized by both non-Newtonian behaviour and shear time dependence. These latter characteristics necessarily require specialized rheological measurements and testing techniques. An example of such rheological behaviour is clearly illustrated in Figure (22).

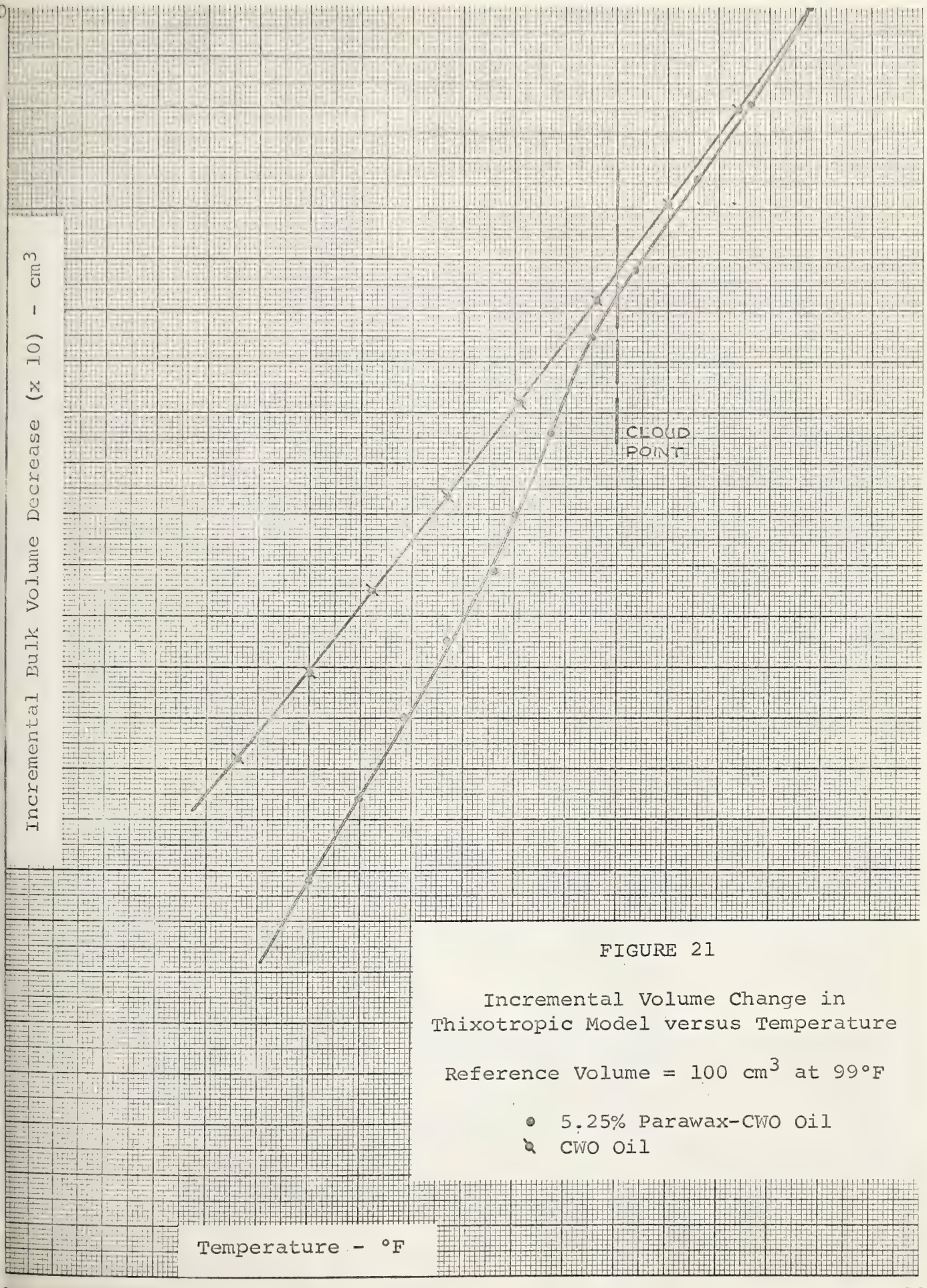


FIGURE 21

Incremental Volume Change in Thixotropic Model versus Temperature

Reference Volume = 100 $cm^3$ at 99°F

- 5.25% Parawax-CWO Oil
- CWO Oil

FIGURE 22

Illustration of Dependence of Model Rheological Behavior on Temperature

Shear Stress after one hour
Shear at 0.3 RPS at test temperature

○ 5.25% Parawax-CWO Oil
△ CWO Oil

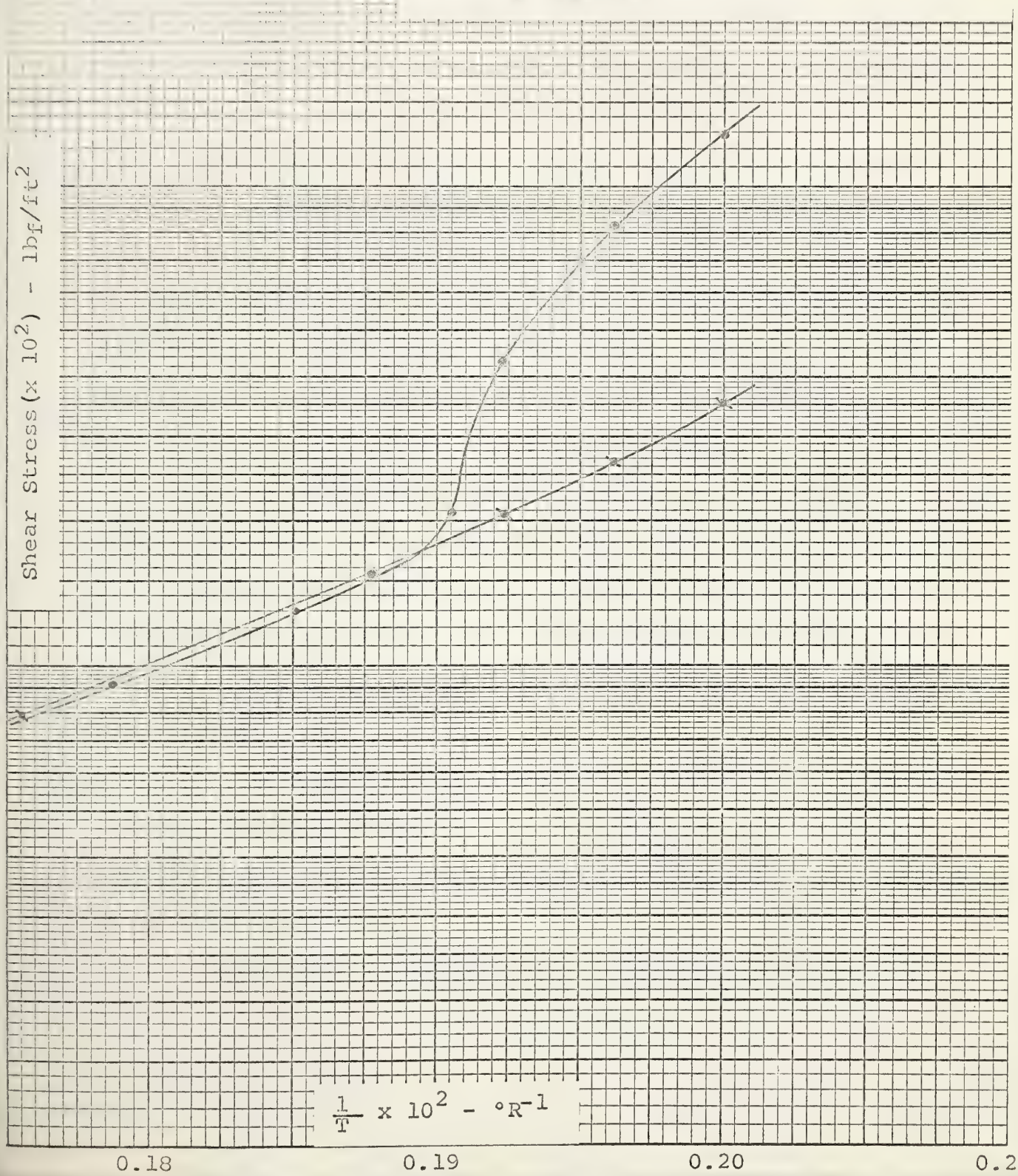

If the temperature of the experimental model is lowered below the cloud point temperature and if the model is allowed to rest undisturbed at this temperature for a prescribed period of time, then the system, if statically tested at low shear stress values, will display solid-like properties. For similar systems (42), this behaviour has been ascribed to a weakly bonded three-dimensional network of colloidal size particles, the bonding forces of which are due to van der Waals-London attraction.

The static strength of the wax cluster network may be measured in a coaxial viscometer in a manner analogous to tensile strength testing of a piece of steel. That is, simply by rotating the viscometer cup and noting the stress and strain in the sample prior to destruction of the network. Such tests have been performed. As may be noted from Figure (23) the strength modulus (i.e. the stress/strain ratio) of the network is variable. This behaviour is typical(42) for systems of this type.

As the shear stress is slowly increased on a test sample, a stress value is reached at which the network bonding forces are overcome; at this point, the network linkages start to break in an almost autocatalytic fashion. As previously described, the stress value at which this behaviour occurs has been arbitrarily called the "yield value", presumably for lack of a more definitive term.

If the shear stress is maintained at a value equal to or greater than the yield value stress, then the test sample, by virtue of the network destruction process, loses its solid-like properties and starts to flow as an anomolous fluid.

In addition to the network strength modulus as measured at 60°F,

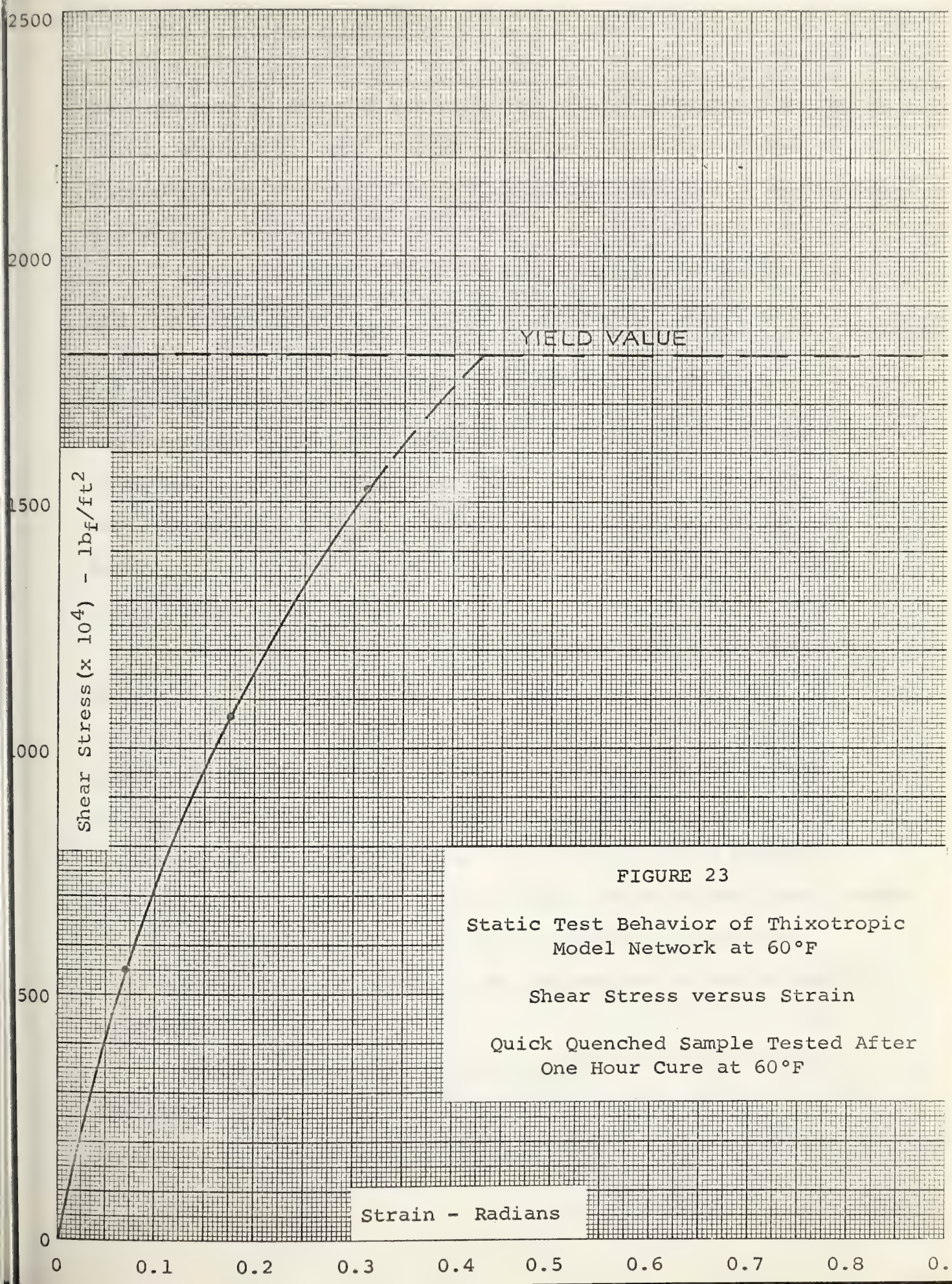


FIGURE 23

Static Test Behavior of Thixotropic Model Network at 60°F

Shear Stress versus Strain

Quick Quenched Sample Tested After One Hour Cure at 60°F

the yield value of the model was measured at other temperatures. The test results, as shown in Figure (24) are highly specific, since, as shall be described, a family of curves, each corresponding to a different rheological test sequence, could have been measured.

To this stage, it has been implicitly assumed that at a specific temperature level, only one characteristic network structure is present. In actuality, this investigator, as well as others(1,16) have noted that the measured thixotropic behaviour in a wax-oil system is drastically influenced by the method used in reaching the test temperature. In addition, it has been noted that the time for which the sample has been allowed to rest undisturbed at the test temperature has a profound influence on subsequent rheological measurements. Such behaviour is attributed directly to the formation characteristics of the basic network structure.

Actually such behaviour is not surprising, since if the fundamental structural unit is a wax crystal or wax cluster, the physical behaviour of the structural units, and hence, the behaviour of the gross structure, should be influenced to some degree by the same variables which govern wax crystal characteristics in simple solvents. In simple solvents, the predominant variables determining wax crystal habit are: (i) temperature, as displayed by its influence on the equilibrium concentration of wax crystals; (ii) rate of cooling, as displayed by its influence on crystal size; (iii) duration of curing, because of the time required to reach an equilibrium state.

Subject to these considerations, it would be suspected that the formation of a network should possibly be a function of all three variables. In fact, as previously illustrated in Figure (24), the relative network

FIGURE 24

Yield Value of Thixotropic Model versus Temperature .

Quick Quenched to Test Temperature and Tested After One Hour Cure

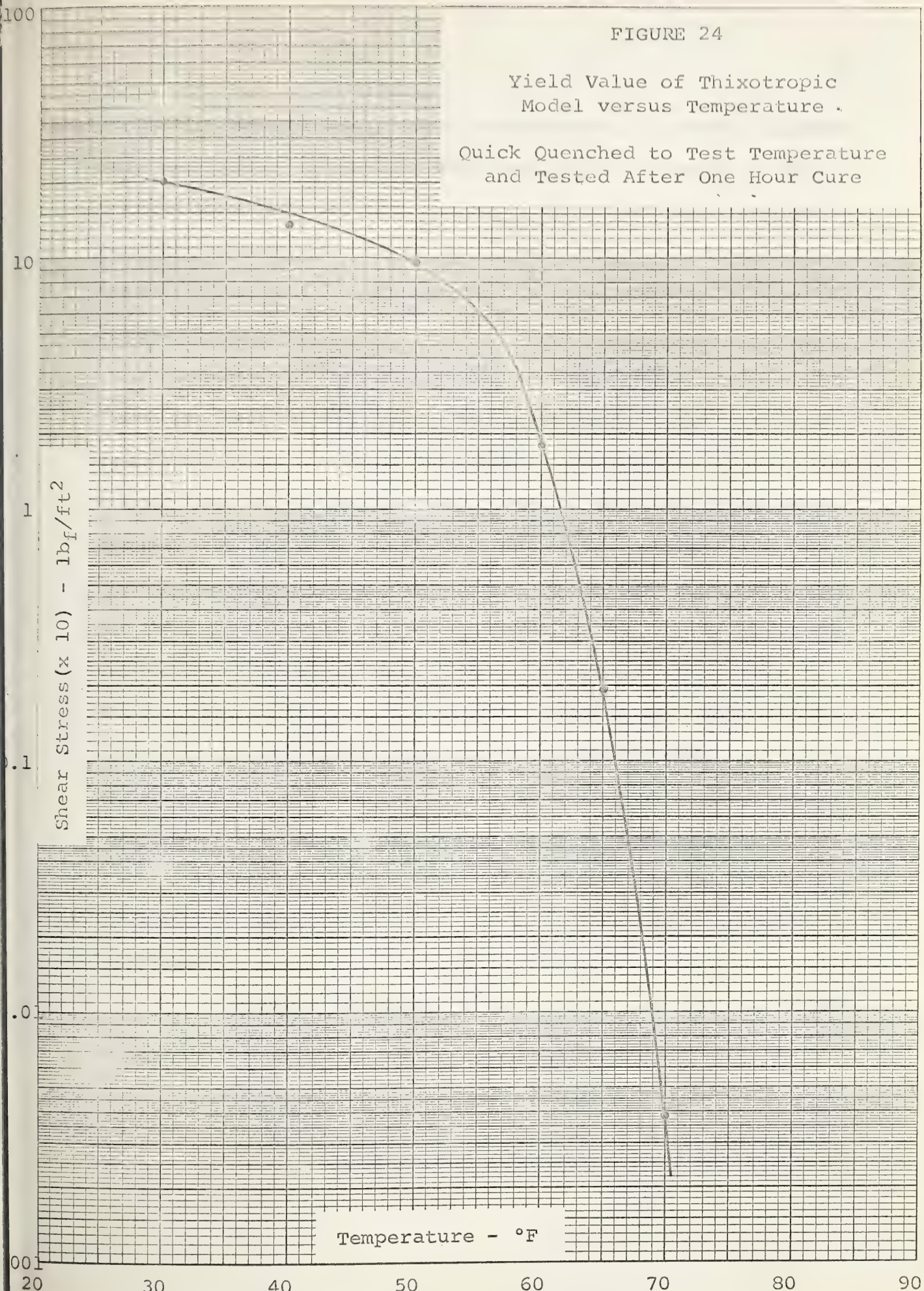

strength (as deduced from yield value measurements) is markedly dependent upon temperature. In addition, at a specified test temperature, the measured thixotropic behaviour and hence, the network properties, are markedly dependent upon rate of cooling and duration of curing before the rheological test. This latter fact is suitably demonstrated in Figures (25)and (26).

Inspection of these Figures reveals several significant features. First, for identical curing times at test temperature, the shear stress as measured at one minute for the quickly quenched samples is significantly greater than the corresponding shear stress of the slowly cooled sample. Secondly, the rate of growth of shear stress (i.e. as measured at one minute of shear) as curing time increases is very slow after one hour for the quick quenched samples. In contrast, growth in shear stress at-one-minute for the slowly cooled samples is markedly significant even after one hour of curing. Such behaviour serves to illustrate the complexity of the rheological properties of the wax-oil model, and further emphasizes the requirement for rigidly standardized rheological testing techniques if rheological measurements are to be compared or correlated.

It is evident from the above considerations that the structural properties of the network may, in general, be described by the following relationship:

$$f(NS) = f(T, CR, t_E) \qquad (41)$$

where: NS = network structural properties;

T = rheological test temperature;

CR = cooling rate sequence from $T_o$ to T, where $T_o$ is a temperature significantly above the cloud point;

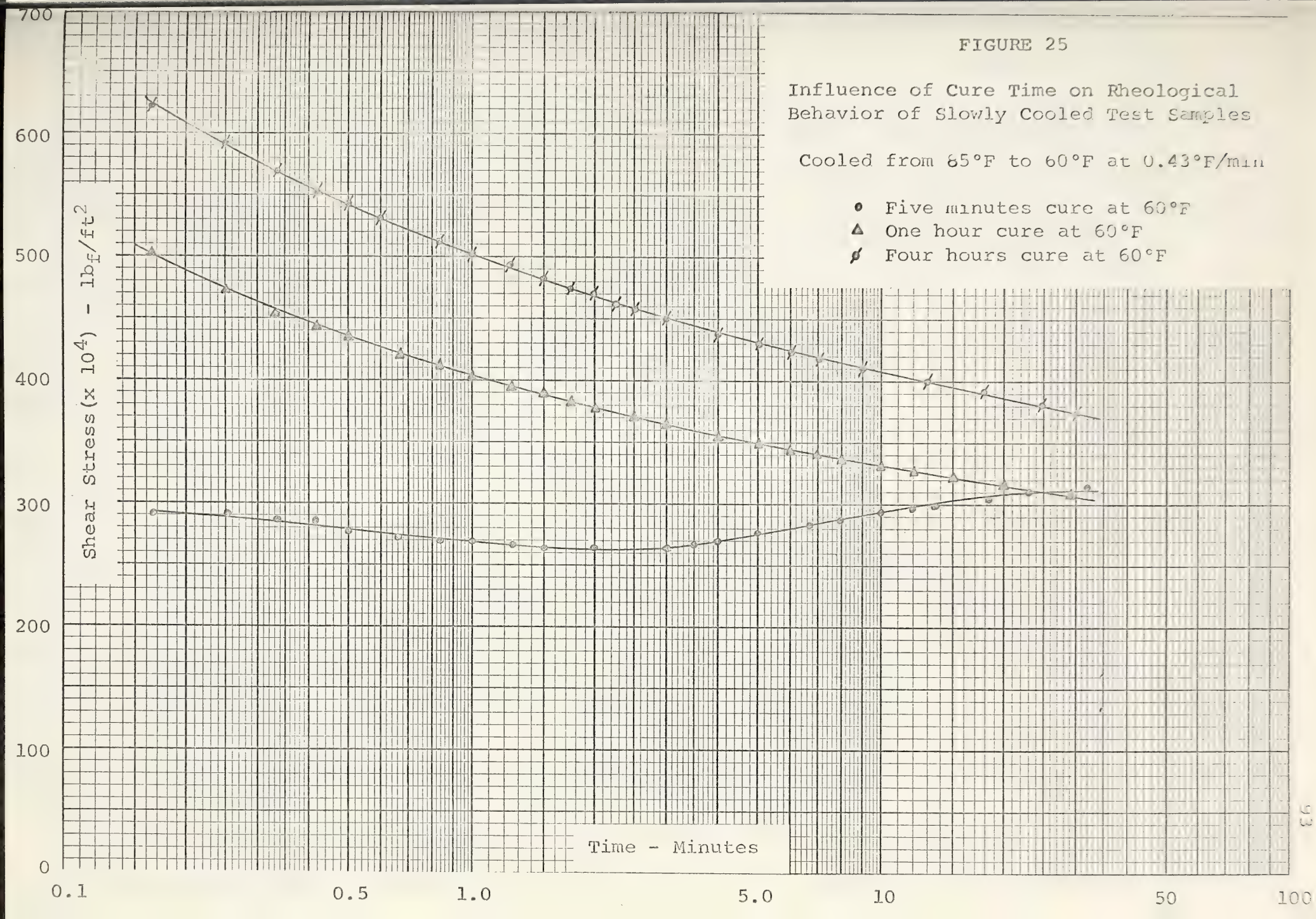
FIGURE 25
Influence of Cure Time on Rheological Behavior of Slowly Cooled Test Samples
Cooled from 65°F to 60°F at 0.43°F/min
Five minutes cure at 60°F
One hour cure at 60°F
Four hours cure at 60°F
Shear Stress (x $10^4$) - $lb_f/ft^2$
Time - Minutes
700
600
500
400
300
200
100
0
0.1
0.5
1.0
5.0
10
50
100

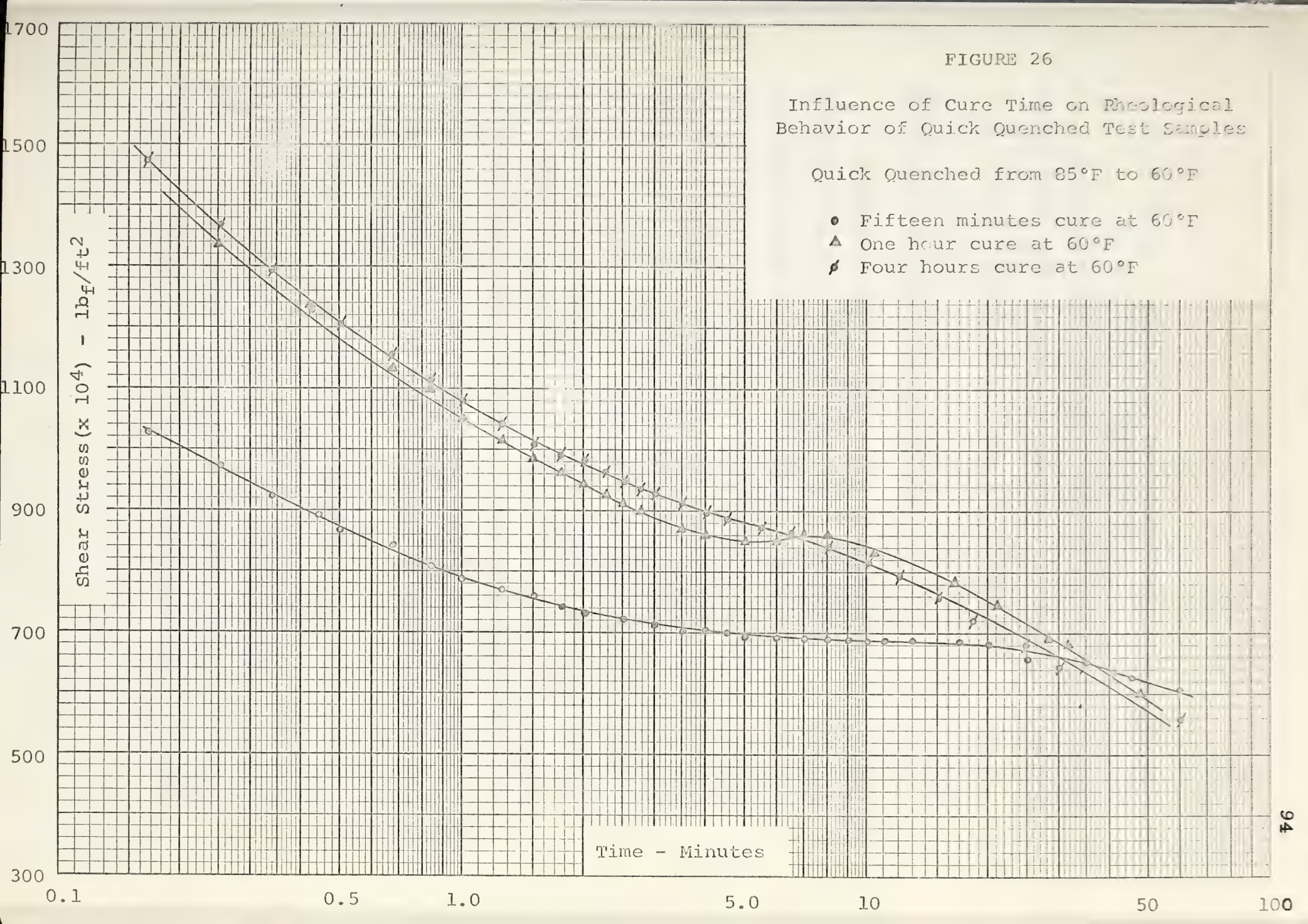


FIGURE 26

Influence of Cure Time on Rheological Behavior of Quick Quenched Test Samples

Quick Quenched from 85°F to 60°F

- Fifteen minutes cure at 60°F
- One hour cure at 60°F
- Four hours cure at 60°F

$t_E$ = elapsed time from start of sample preparation to start of rheological test.

A further extension or clarification of Equation (40) in more definitive terms, such as in terms of the Theory of Thixotropic Behaviour(1) or in terms of molecular interactions, is not available.

Selection of the Experimental Test Program

Initially an experimental program was selected which was essentially identical to that of a previous investigator, Ritter(1). Such a program would have entailed measurement of thixotropic decay curves and complementary shear stress growth curves at four viscometer cup speeds (0.3 RPS, 0.8 RPS, 2.0 RPS and 4.5 RPS) at each of three test temperatures (60°F, 45°F and 30°F). The primary incentives in the selection of such a program were, (i) to obtain sets of thixotropic decay data with which to test the Theory of Thixotropic Behaviour(1), and (ii) to obtain rheological data which would permit a more precise definition of $\tau_\infty$, the thixotropic equilibrium shear stress. Measurement of the latter quantity had not been possible with the thixotropic fluid (Pembina crude oil) used by Ritter(1) because of sample degeneration (loss of volatile hydrocarbons) during shear tests.

However, after analyzing the experiments on reproducible thixotropic behaviour and on network formation characteristics, it was felt that the objectives of the initial program could be met equally as well by an alternate experimental program. Consequently the initial test program was modified to the experimental program schematically illustrated

in Figure (27). The premise underlying the selection of this experimental program was that sufficient complexity of thixotropic behaviour existed at one temperature so as to eliminate the necessity of obtaining additional thixotropic data at other temperatures.

Several salient features of the experimental program are worth noting. First, this program provides only two sets of thixotropic data as opposed to the originally planned three sets. This is not a serious drawback, since in fact the primary aspects of the Theory of Thixotropic Behaviour(1) could be investigated by only one set of data.

Second, as has been previously described, an exact sample handling sequence was required prior to a rheological test. Once an individual test sample was removed from sample storage, a minimum of 52 hours of carefully programmed steps (seven in all) were necessary prior to a viscometric test. Fortunately it was possible to stagger the sample handling sequences such that upon completion of one rheological test, another test sample was generally ready for insertion into the viscometer. In this manner, it was possible to obtain a set of thixotropic data (10 rheological tests) in only nine days.

Regardless of the rheological test sequence, all samples were cured at test temperature for four hours before rheological testing. This cure time was considered quite satisfactory despite the fact that, for the slow cooled samples at least, static network growth would have continued beyond this cure time. It would have been more desirable to test only a finally stabilized network, but in practice(17), rheological tests on network forming systems are almost exclusively conducted at an intermediate stage

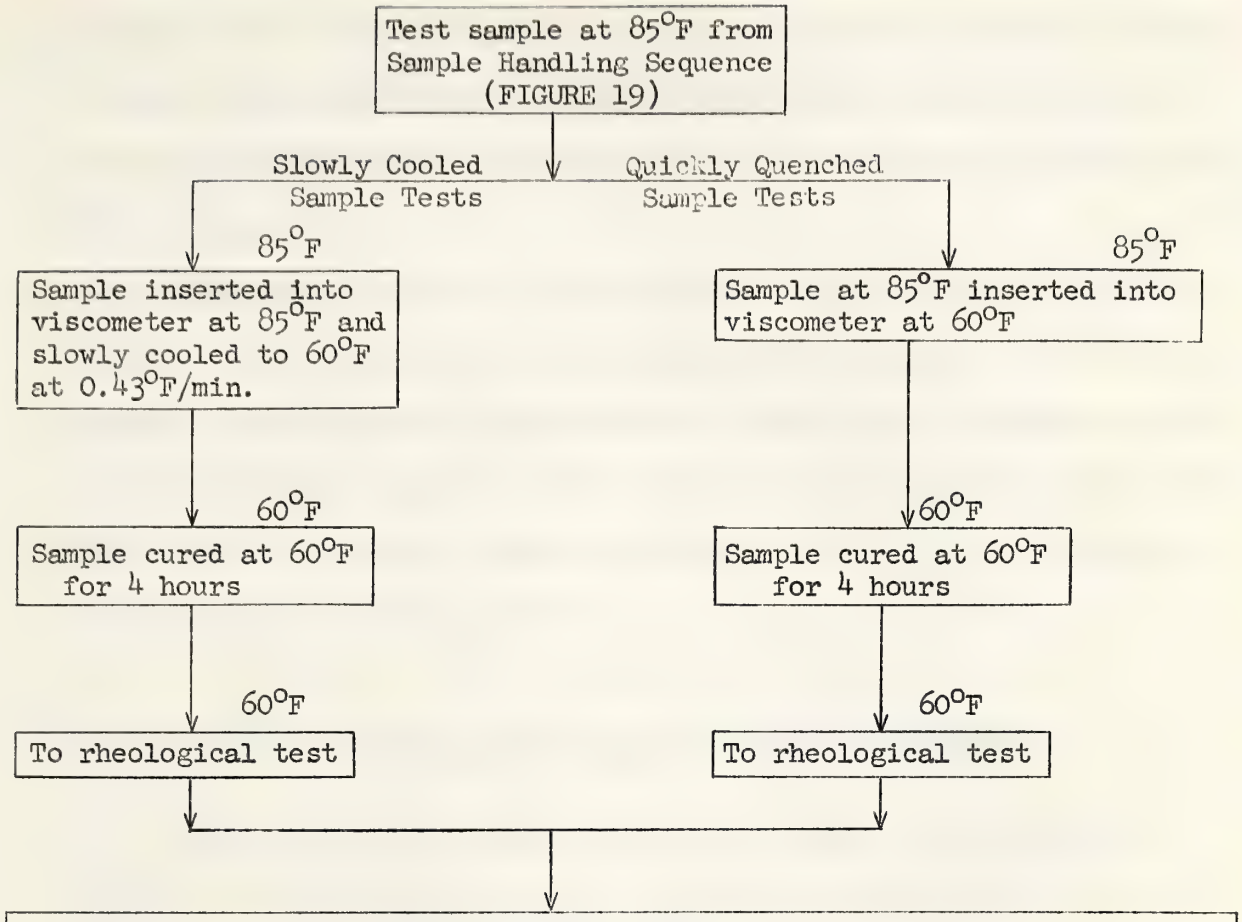
Test sample at 85°F from Sample Handling Sequence (FIGURE 19)
Slowly Cooled Sample Tests
Quickly Quenched Sample Tests
85°F
Sample inserted into viscometer at 85°F and slowly cooled to 60°F at 0.43°F/min.
85°F
Sample at 85°F inserted into viscometer at 60°F
60°F
Sample cured at 60°F for 4 hours
60°F
Sample cured at 60°F for 4 hours
60°F
To rheological test
60°F
To rheological test

RHEOLOGICAL TEST PROGRAM

| Cup Speed (RPS) | Shear Stress Decay Test (Number of tests) | Shear Stress Growth Test (Number of tests) |
|---|---|---|
| 0.3 | 2 | 0 |
| 0.8 | 2 | 1(1) |
| 2.0 | 2 | 2(2) |
| 4.5 | 3 | 3(3) |

(1) 0.8 → 0.3 RPS
(2) 2.0 → 0.3 RPS; 2.0 → 0.8 RPS
(3) 4.5 → 0.3 RPS; 4.5 → 0.8 RPS; 4.5 → 2.0 RPS

FIGURE 27

Test Program For Thixotropic Model

of network development. This arises from the fact that the time required to reach a stabilized network is beyond experimental feasibility, requiring, in some cases(17) constant control of cure conditions for periods up to two years.

Although no specific criteria has been developed to indicate the length of time a sample should be cured prior to testing, it would appear desirable that rheological measurements be taken at as an advanced stage of network growth as possible. The reason is that such measurements will exhibit greater anomolous behaviour and hence, will facilitate interpretation and correlation procedures.

Rheological Test Sequence and Viscometric Testing Procedures

The previously described experimental program (Figure 27) was designed to quantitatively measure thixotropic behaviour of the experimental model. The sample handling sequence (Figure 19) has been adequately described, but the experimental methods used during the rheological test sequences and the viscometric test procedures have not. Consequently a detailed description of these latter steps will be outlined in the following paragraphs.

Prior to insertion of a test sample in the viscometer, the temperature of the cabinet air bath and the viscometer were adjusted to the desired temperature; for the slow sample-cooling sequence, 85°F, and for the quick quench sequence, 60°F. Then the variable speed Graham drive was adjusted to the selected cup rotational speed and tested several times to ensure the external dial setting was correctly positioned (i.e. using this

procedure, cup rotational speeds could be set within ±0.5 percent of the desired speed). The viscometer bob was suspended in position in the cup by an appropriate torsion wire and then levelled and centered via the viscometer elevator and movable support platform. After these preparations a test sample was inserted into the viscometer by gravity flow through a funnel-flexible tube arrangement attached to the sample inlet line at the bottom of the viscometer cup.

For the quick quenched samples, insertion of the sample was followed directly by four hours curing. However, for the slowly cooled samples, after the sample was inserted, the viscometer assembly and cabinet air bath temperatures were simultaneously lowered at a steady predetermined cooling rate of 0.43°F per minute until the test temperature (60°F) was reached; the test sample was then cured for four hours. (The cooling rate of 0.43°F per minute was the maximum cooling rate of the Aminco constant temperature bath attached to the viscometer assembly. Throughout the test program, measured cooling rates did not differ by more than ±0.02°F per minute)

Following four hours of curing, the test sample was ready for a rheological test. The Graham drive motor would be started (i.e. the viscometer cup set in motion) and the resulting bob deflection was noted according to a programmed test time sequence. Generally, the first bob deflection noted was at 10 seconds, followed by a reading at 5 second intervals for the remainder of the first half-minute, every 10 seconds for the second half-minute and at 15 second intervals for the next four minutes. Thereafter, readings were taken every minute up to a total elapsed

time of 30 minutes, after which readings were generally taken at 5 or 10 minute intervals.

Upon completion of a test, the rotational speed of the cup was generally reduced to a lower predetermined cup speed, and the bob deflection again measured as a function of time. This second test sequence permitted measurement of network growth at reduced shear conditions.

Upon completion of the above tests, the sample was removed from the cup and discarded. The viscometer assembly was cleaned and prepared for a subsequent test sequence.

## Experimental Results

Experimental results, as measured in accordance with the experimental program outlined in Figure (27) are presented in graphical form from Figure (28) to Figure (41). The basic experimental data from which these plots were drawn is tabulated in APPENDIX SEVEN.

It may be noted that the experimentally measured thixotropic decay curves have been plotted on semi-logarithmic coordinates rather than conventional arithmetic coordinate plots. Two reasons are given in support of this choice: (i) the relative decreases in shear stress as a function of time are uniformly distributed, and (ii) a closer inspection of the decay curve at pertinent points is afforded. The only disadvantage to this plotting method is that reproducibility errors are distractingly obvious in the first few minutes of the shear test. However, it must be taken into consideration that this time period is the most difficult in which to obtain test measurements.

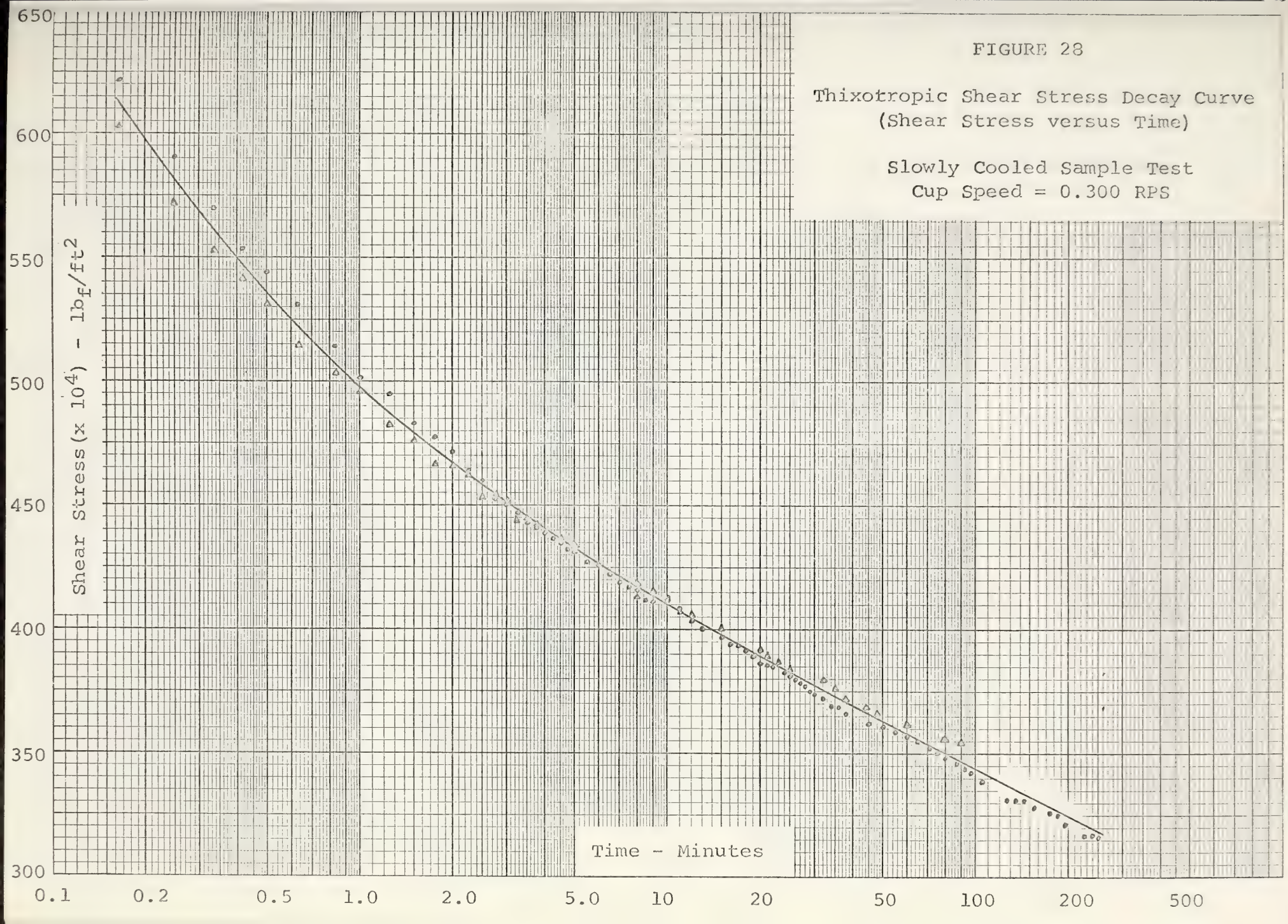
FIGURE 28
Thixotropic Shear Stress Decay Curve
(Shear Stress versus Time)
Slowly Cooled Sample Test
Cup Speed = 0.300 RPS
Shear Stress (x $10^4$) - $lb_f/ft^2$
650
600
550
500
450
400
350
300
Time - Minutes
0.1
0.2
0.5
1.0
2.0
5.0
10
20
50
100
200
500

FIGURE 29

Thixotropic Shear Stress Decay Curve
(Shear Stress versus Time)

Slowly Cooled Sample Test
Cup Speed = 0.800 RPS

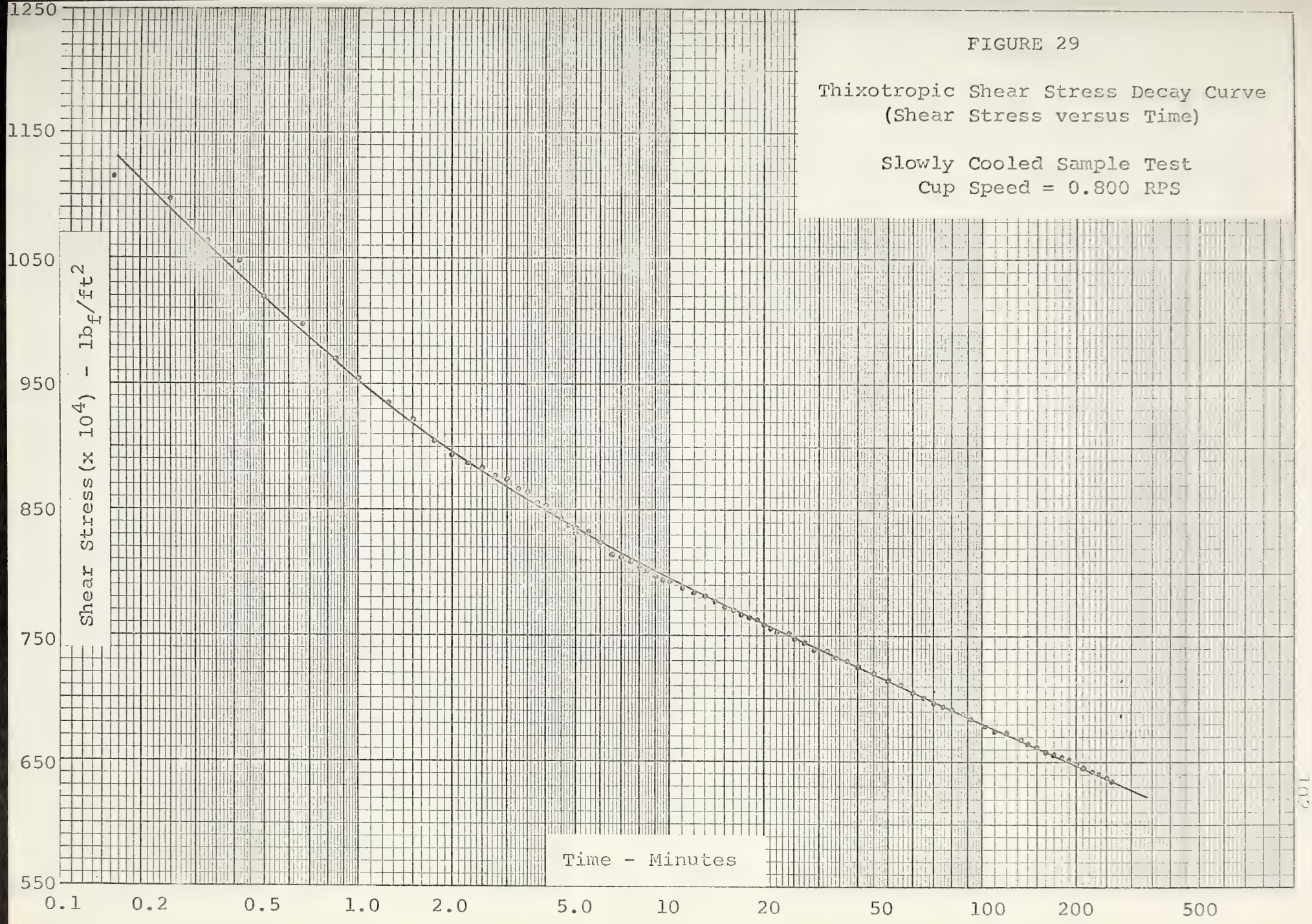

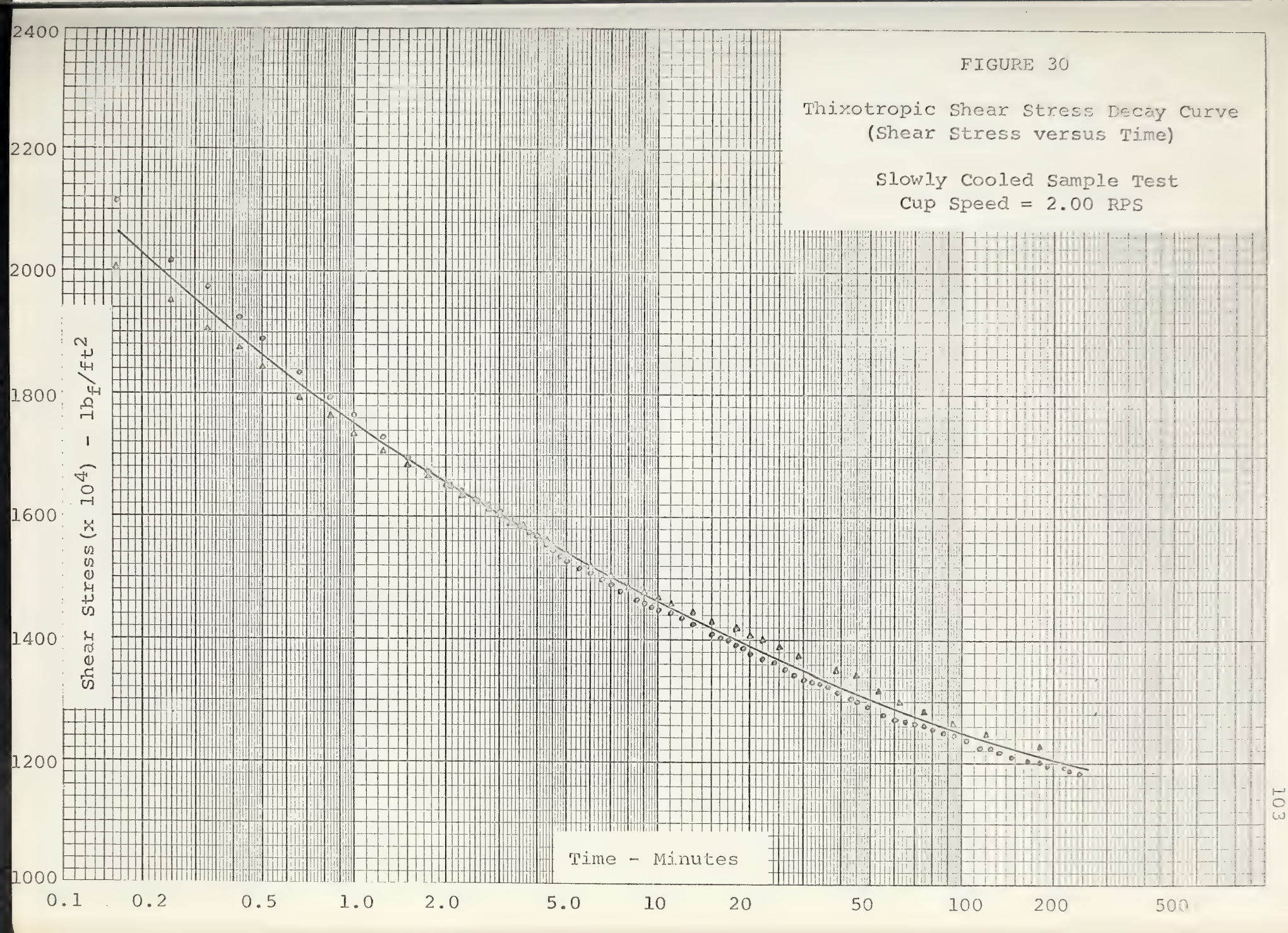
FIGURE 30
Thixotropic Shear Stress Decay Curve
(Shear Stress versus Time)
Slowly Cooled Sample Test
Cup Speed = 2.00 RPS
Shear Stress (x $10^4$) - $lb_f/ft^2$
2400
2200
2000
1800
1600
1400
1200
1000
Time - Minutes
0.1
0.2
0.5
1.0
2.0
5.0
10
20
50
100
200
500

FIGURE 31

Thixotropic Shear Stress Decay Curve
(Shear Stress versus Time)

Slowly Cooled Sample Test
Cup Speed = 4.50 RPS

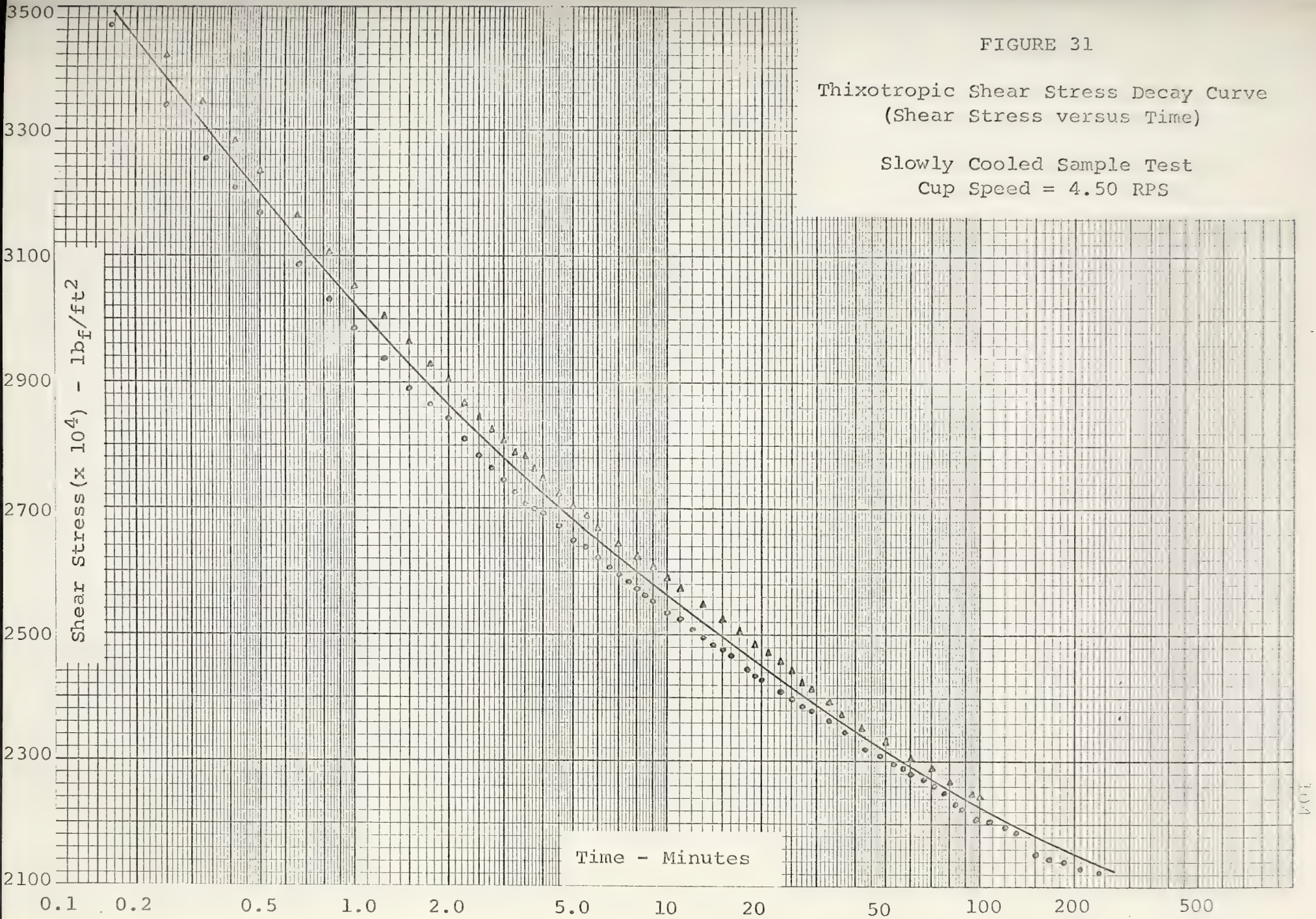

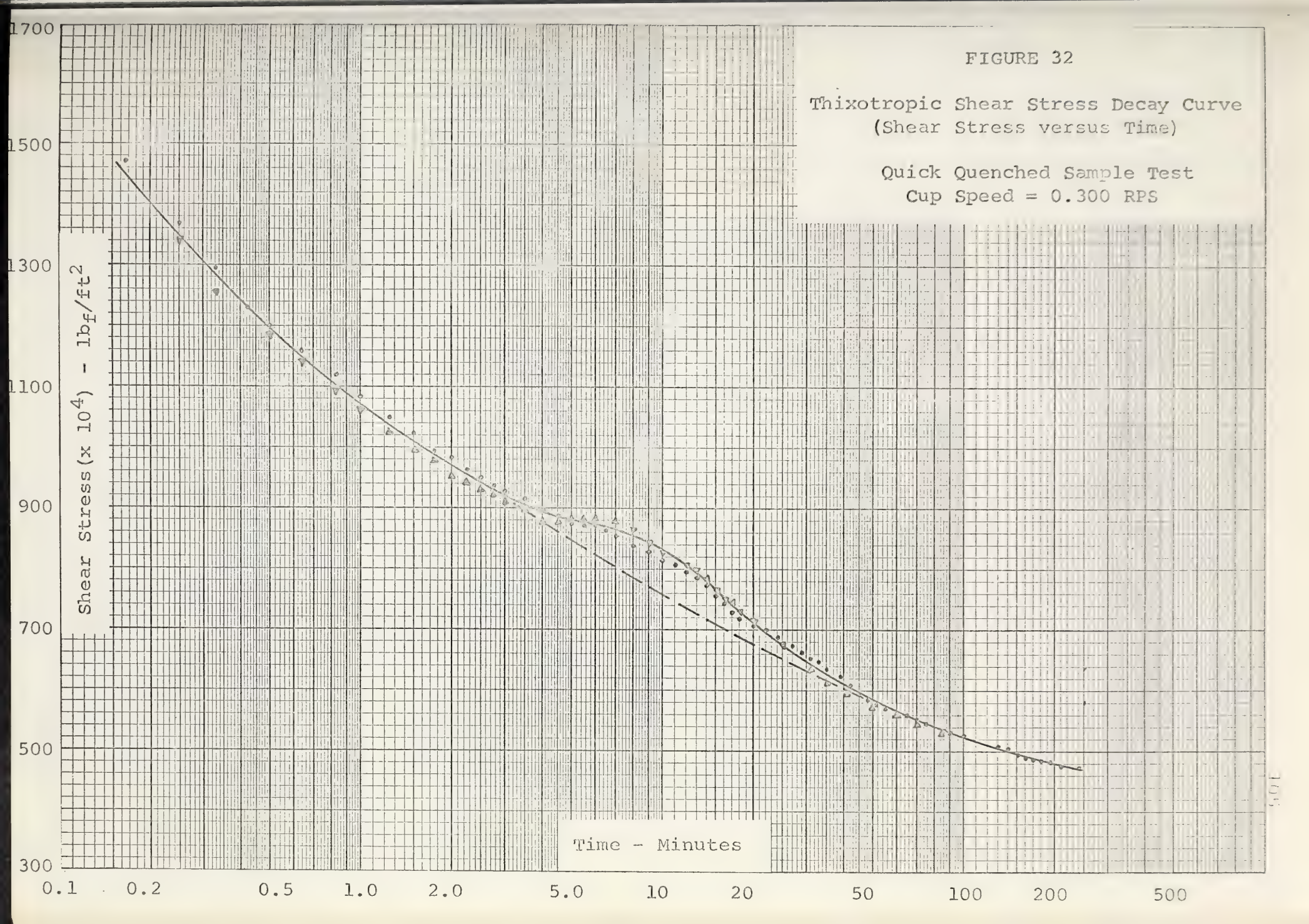
FIGURE 32
Thixotropic Shear Stress Decay Curve
(Shear Stress versus Time)
Quick Quenched Sample Test
Cup Speed = 0.300 RPS
Shear Stress (x $10^4$) - $lb_f/ft^2$
1700
1500
1300
1100
900
700
500
300
Time - Minutes
0.1
0.2
0.5
1.0
2.0
5.0
10
20
50
100
200
500

FIGURE 33

Thixotropic Shear Stress Decay Curve
(Shear Stress versus Time)

Quick Quenched Sample Test
Cup Speed = 0.800 RPS

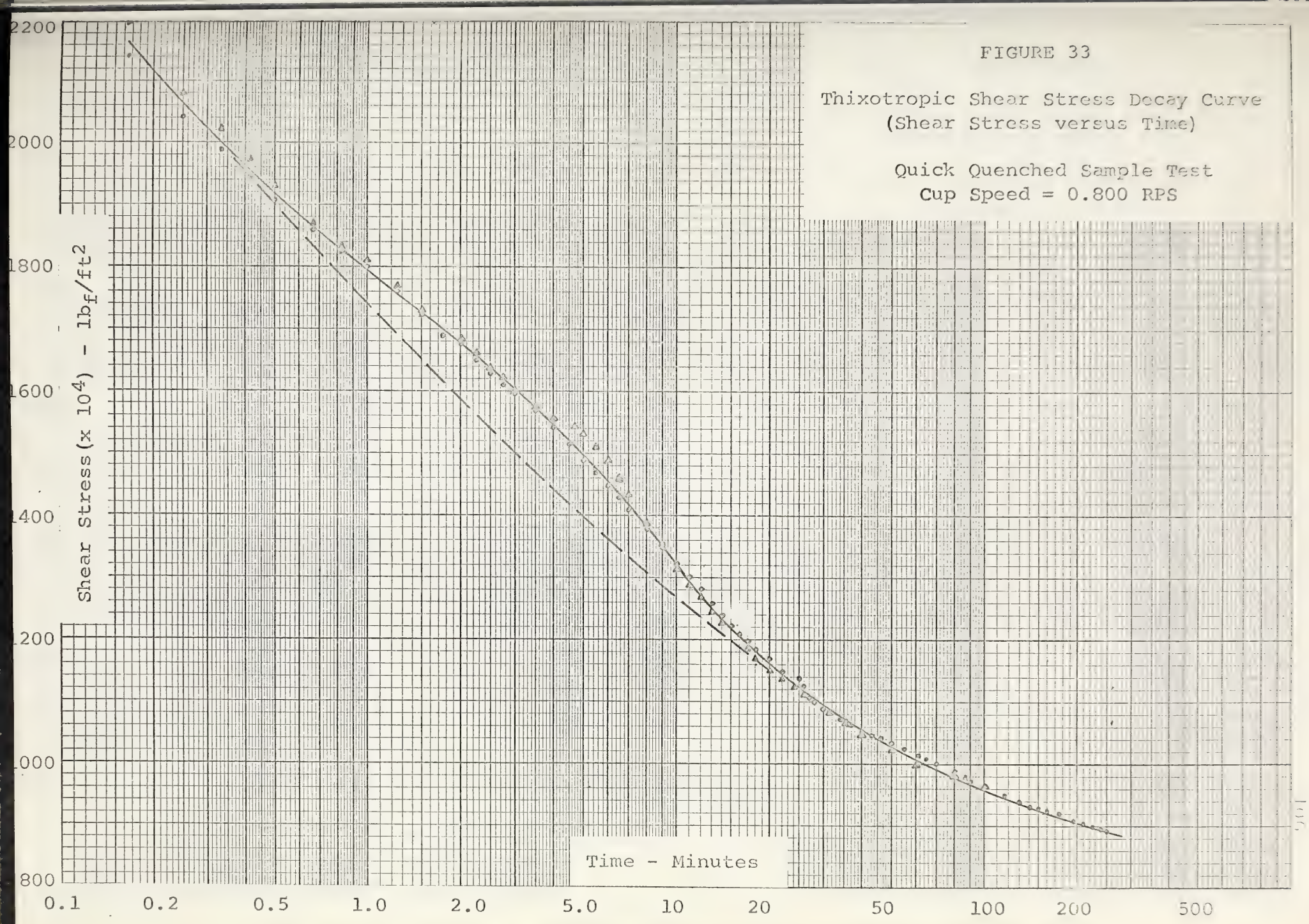

FIGURE 34

Thixotropic Shear Stress Decay Curve
(Shear Stress versus Time)

Quick Quenched Sample Test
Cup Speed = 2.0 RPS

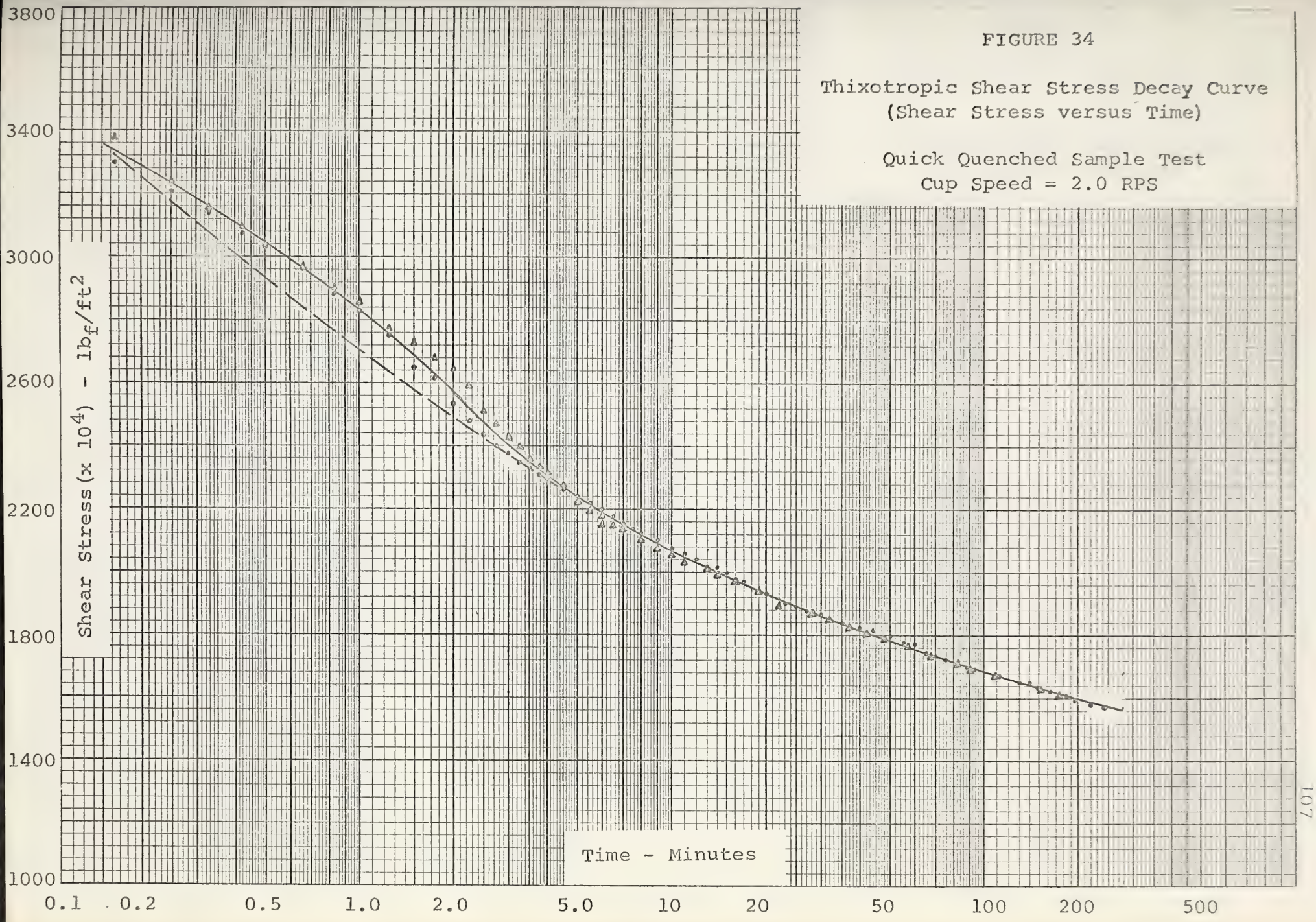

FIGURE 35

Thixotropic Shear Stress Decay Curve
(Shear Stress versus Time)

Quick Quenched Sample Test
Cup Speed = 4.50 RPS

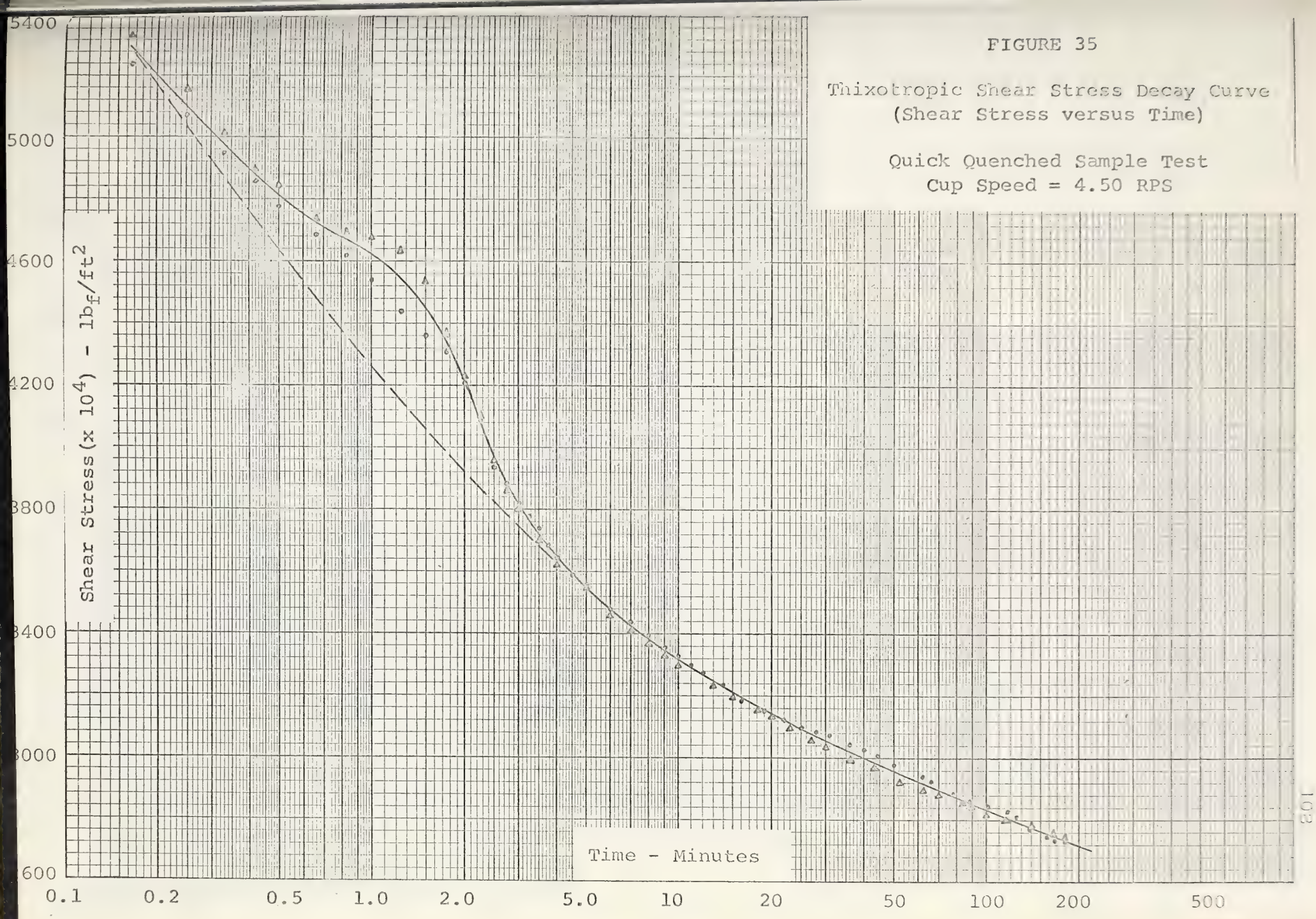

FIGURE 36

Shear Stress Growth Curve
(Shear Stress versus Time)

Slowly Cooled Sample Test
Cup Speed = 0.300 RPS

Shear History

△ - After 260 min. shear at 0.8 RPS
ø - After 250 min. shear at 2.0 RPS
o - After 240 min. shear at 4.5 RPS

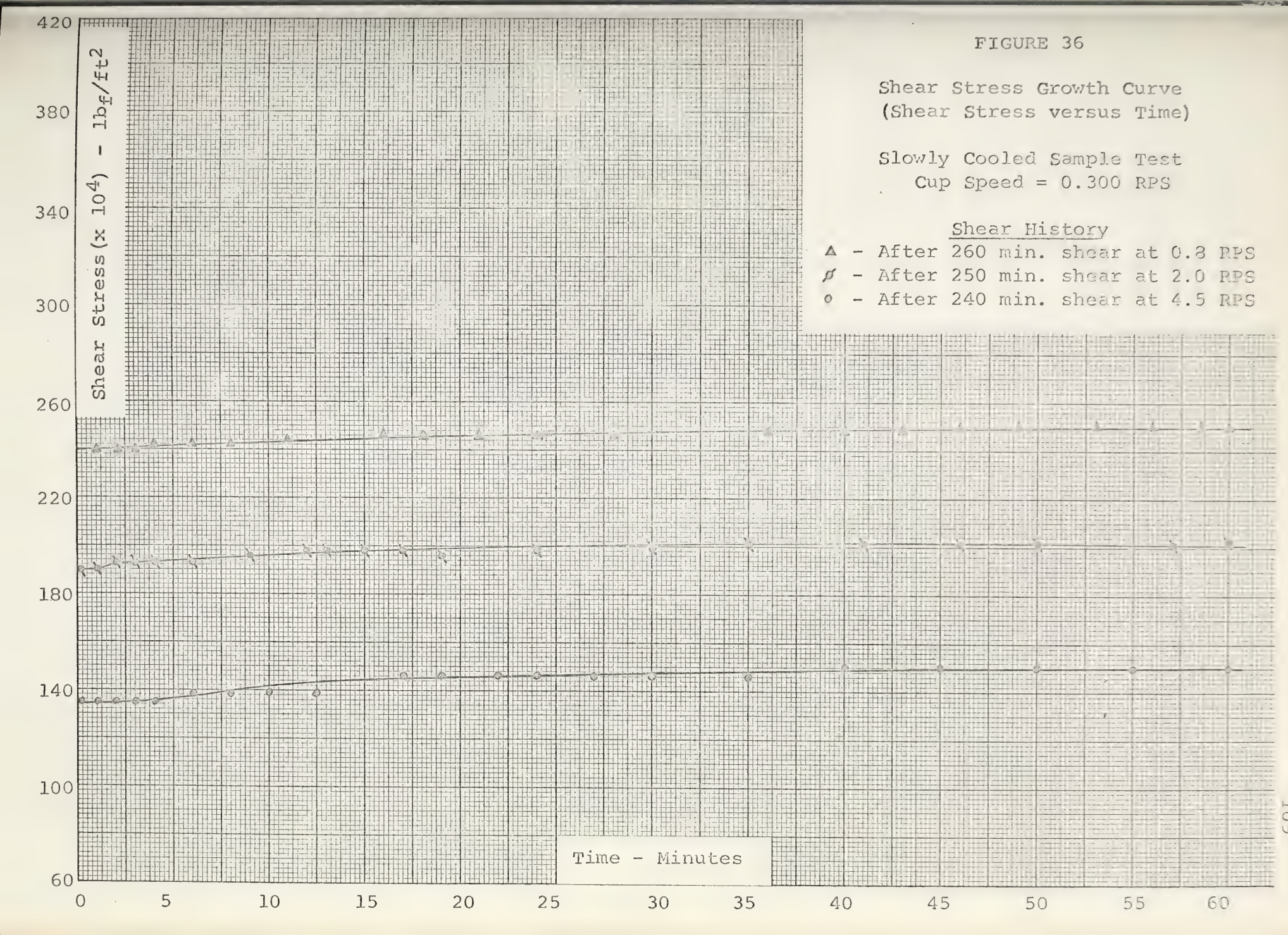

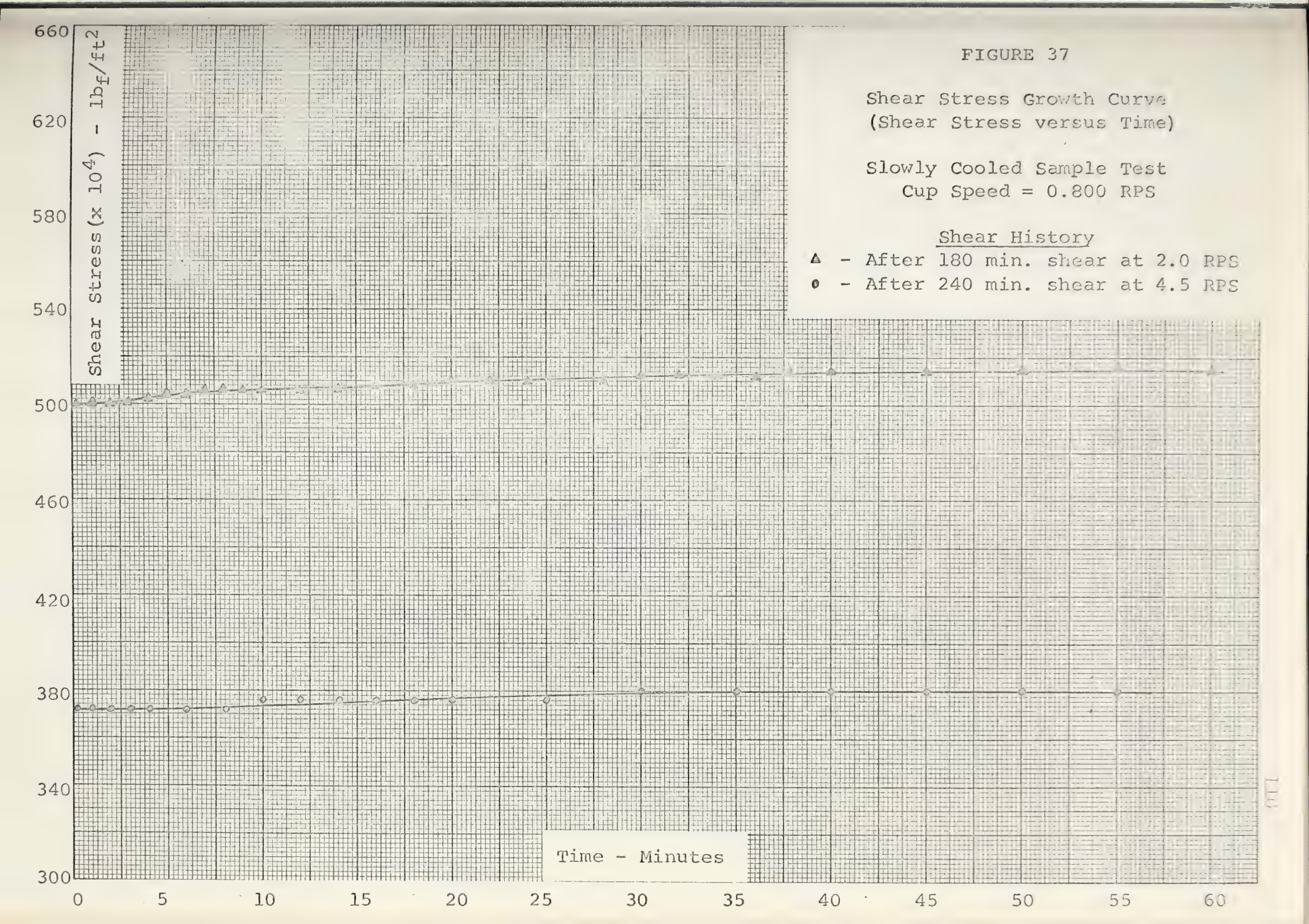


FIGURE 37

Shear Stress Growth Curve
(Shear Stress versus Time)

Slowly Cooled Sample Test
Cup Speed = 0.800 RPS

Shear History

▲ - After 180 min. shear at 2.0 RPS

● - After 240 min. shear at 4.5 RPS

FIGURE 38

Shear Stress Growth Curve
(Shear Stress versus Time)

Slowly Cooled Sample Test
Cup Speed = 2.0 RPS

Shear History
o - After 240 min. shear at 4.5 RPS

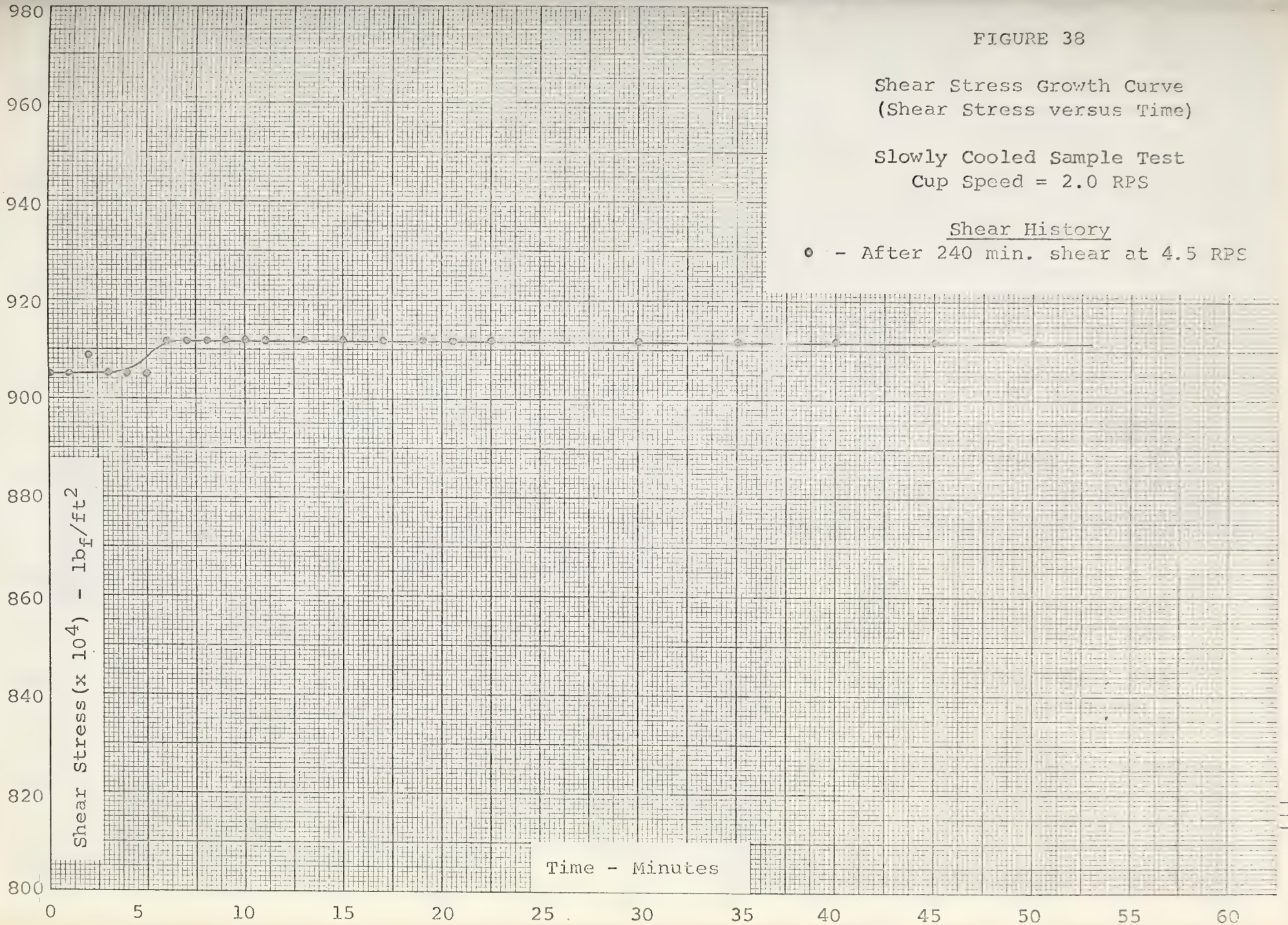

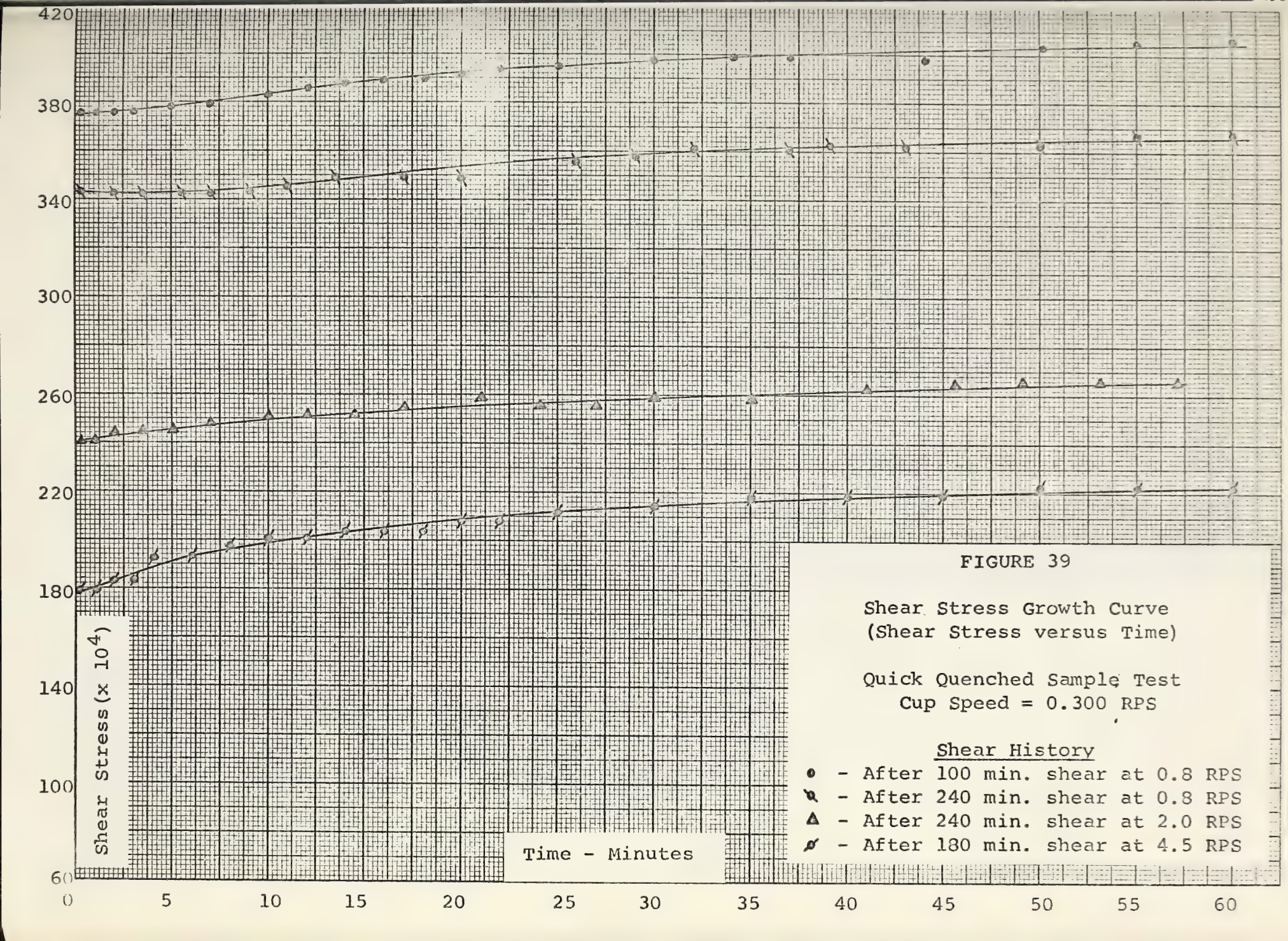


FIGURE 39

Shear Stress Growth Curve
(Shear Stress versus Time)

Quick Quenched Sample Test
Cup Speed = 0.300 RPS

Shear History

- ● - After 100 min. shear at 0.8 RPS
- ⊗ - After 240 min. shear at 0.8 RPS
- △ - After 240 min. shear at 2.0 RPS
- ⊘ - After 180 min. shear at 4.5 RPS

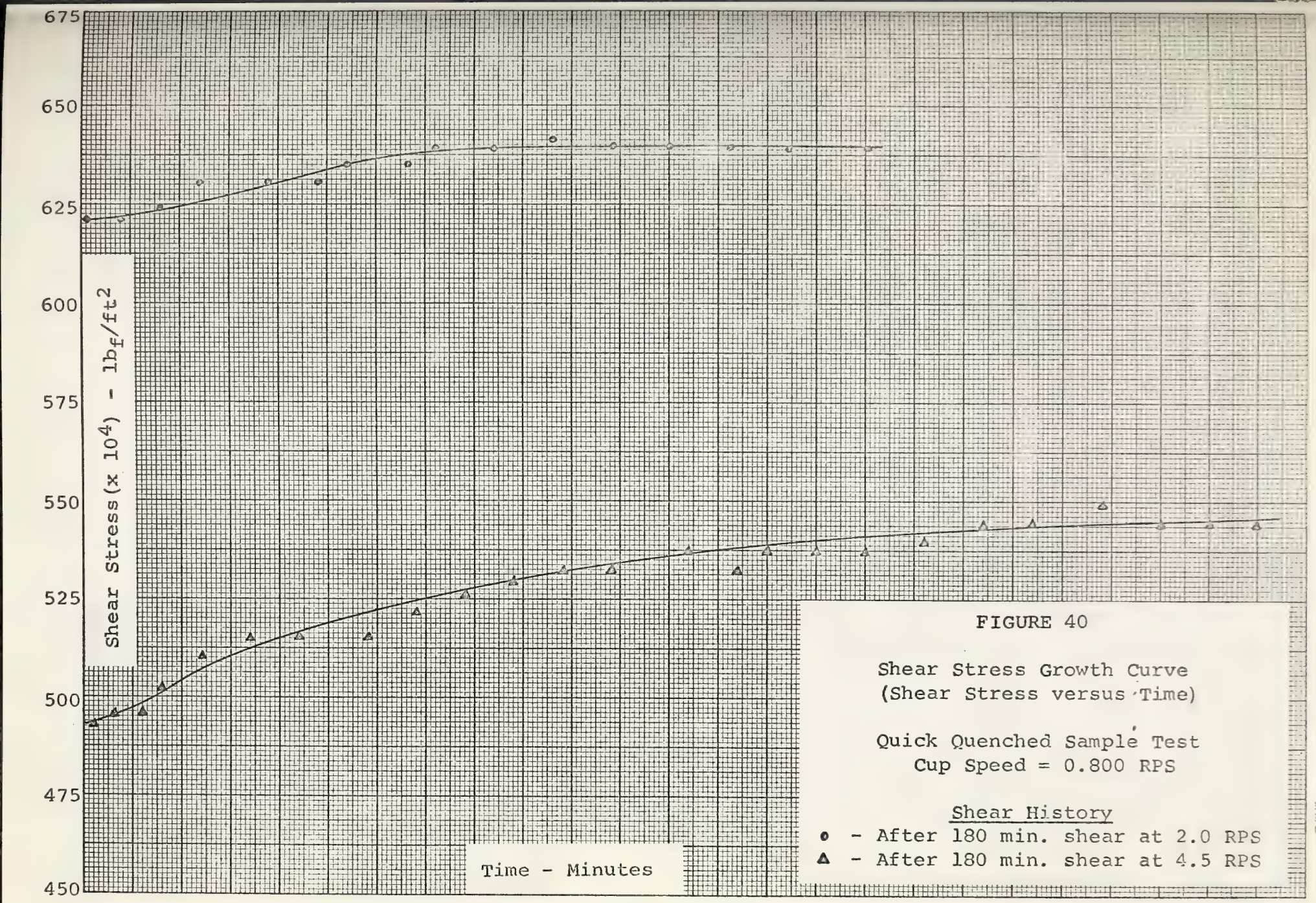


FIGURE 40

Shear Stress Growth Curve
(Shear Stress versus Time)

Quick Quenched Sample Test
Cup Speed = 0.800 RPS

Shear History

o - After 180 min. shear at 2.0 RPS

Δ - After 180 min. shear at 4.5 RPS

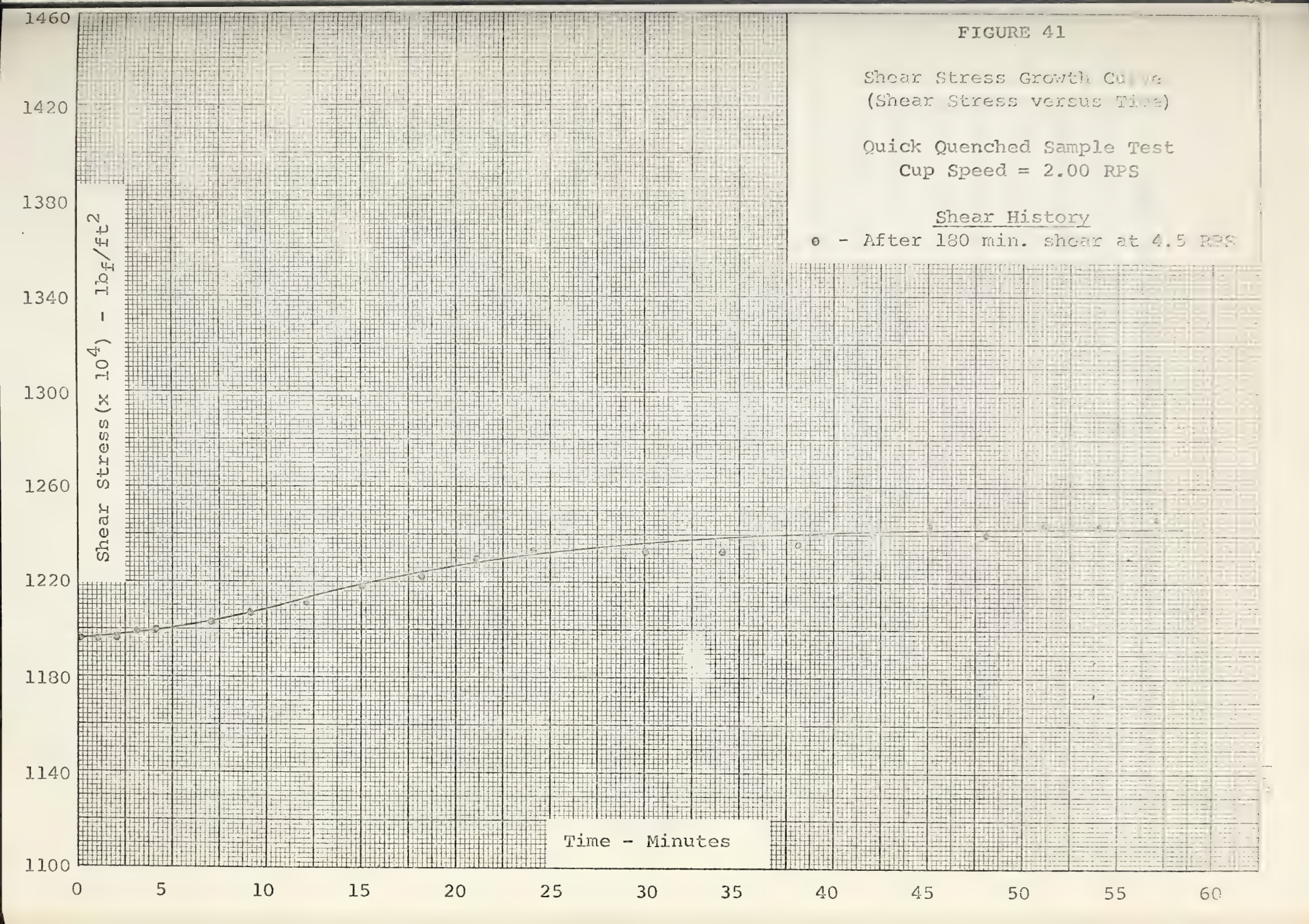
FIGURE 41
Shear Stress Growth Curve
(Shear Stress versus Time)
Quick Quenched Sample Test
Cup Speed = 2.00 RPS
Shear History
o - After 180 min. shear at 4.5 RPS
Shear Stress (x $10^4$) - $lb_f/ft^2$
1460
1420
1380
1340
1300
1260
1220
1180
1140
1100
Time - Minutes
0
5
10
15
20
25
30
35
40
45
50
55
60

Inspection of the thixotropic decay curves (Figures 28 to 35) reveals that the measured shear stress (as converted from actual bob deflection) decreased rapidly during the early stages of shearing. However, as the shearing time increased, the rate of change of shear stress decreased, and continued to decrease until the end of the tests. For all the test conducted, there was never any indication that the rate of stress decrease would become zero within possible experimental time limits. Consequently, in general, the maximum time for an individual viscometric test was four hours. This latter time, as will be discussed, was considered to be an optimal experimental choice.

After approximately 100 minutes of continuous shearing, accurate measurement of change in shear stress became progressively poorer. Such behaviour may be attributed to two complementary effects. First, consider the equation for calculation of shear stress ($\tau$) from bob deflection (D), as measured in degrees:

$$\tau = aD \qquad (42)$$

where "a" is a proportionality constant (APPENDIX THREE). In practice, measurement of bob deflection under steady state conditions, or when the rate of change in shear stress was small, was usually within $\pm 0.1$ degrees Hence, at long test times when the change in bob deflection was only slightly greater than the absolute measuring error, the error involved in ascertaining the actual change in bob deflection became fairly significant.

In addition to the above errors, but of considerably more importance, bob deflections at long test times (i.e. greater than 100 minutes) became subject to unexplainable fluctuations which in most instances were greater

than actual measured bob deflection decreases. The fluctuations appeared to assume the form of a random, but consistently present, oscillation sequence having both long and short time periods. It was possible to estimate an average mean value of the short period fluctuations, but estimation of an average mean value for a long range fluctuation became increasingly difficult. Consequently, the four hour test time represented the maximum time for which a full measure of confidence could be placed on experimental results. The source or cause of these fluctuations was never discovered, but at least one other investigator(53) has experienced similar difficulties with another network type system.

Moreover, even if experimental data had been measured up to 700 minutes shear time (i.e. the maximum testing period for the experimental set-up) such results would not appear to have contributed significantly to determining an absolute value of the limiting shear stress. This fact is readily obvious if any of the measured shear stress decay curves are extrapolated to a possible limiting shear stress, and the corresponding time noted at which this shear stress value is approached.

Generally, experimental reproducibility was within the desired limits of 3 percent and usually better than this value. The following table illustrates this fact to better advantage:

TABLE 2

Experimental Thixotropic Test Reproducibility

Quick Quenched Sample Thixotropic Tests:

| | 0.3 RPS | 0.8 RPS | 2.0 RPS | 4.5 RPS |
|---|---|---|---|---|
| Up to one minute: | 2% | 3% | 2% | 2% |
| After one minute: | 2% | 1% | 2% | 1% |

TABLE 2 (continued)

Slow Cooled Sample Thixotropic Tests:

| | 0.3 RPS | 0.8 RPS | 2.0 RPS | 4.5 RPS |
|---|---|---|---|---|
| Up to one minute: | 3 % | ---* | 3% | 2% |
| After one minute: | 1.5% | ---* | 2% | 2% |

where the percentages are expressed as percent of average instantaneous shear stress.

In all fairness, it must be stated that the above levels of reproducibility are quite good, although it is admitted that comparison with similar data by other investigators is difficult. The only published data on thixotropic reproducibility is by Ritter(1) who quoted maximum deviations between experimental runs of $\pm 3$ percent.

Although the slow cooled sample thixotropic decay curves (Figures (28) to (31)) were regular uncomplicated functions of shear time, the quick quenched thixotropic decay curves (Figures (32)to (35)) were not. Inspection of these latter curves reveals a reproducible "hump" superimposed on an otherwise regular shear stress decay curve. The presence of this "hump", or "secondary effect", is rather startling if reference is made only to those thixotropic measurements made by Ritter(1), but, in fact, other investigators(14,16,25) have noted such behaviour. It is also interesting to note that as the shear rate increased, the "hump" or secondary effect progressively shifted to earlier shear times. This fact may be demonstrated by comparison of Figure (32) to Figure (35).

Before proceeding, it should be pointed out that the "secondary effect" discussed above is thought to be a characteristic of the network destruction process and is not attributable to experimental equipment

---

* One experimental run only.

characteristics. This conclusion is supported by the experimental data of other investigators(14,16,25) who have detected such behaviour with a varied selection of experimental equipment.

Inspection of the shear stress growth curves (Figures (36) to (41)) reveals several interesting features. First, the relative extent of shear stress growth of the slow cooled samples (approximately 4%) is less than half that of the quick quenched sample growth curves (approximately 9.5%) for the same length of test period. Secondly, the shape of the shear stress growth curves is quite different from that reported by Ritter(1). The difference in shape is qualitatively illustrated below:

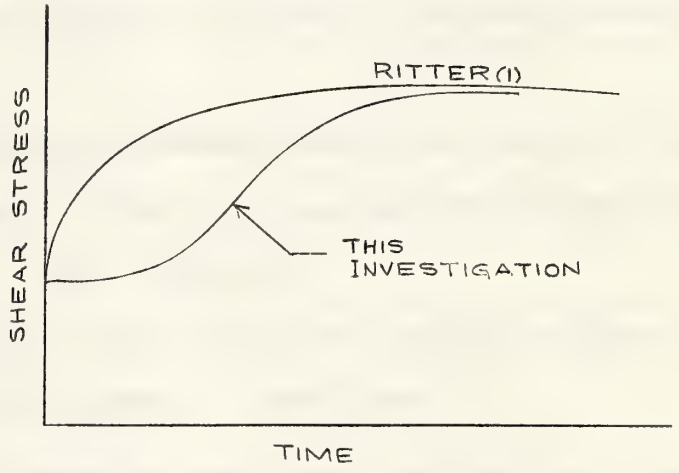


It should be pointed out that the shape of the shear stress growth curves as measured in this investigation generally conformed to the behaviour noted in other thixotropic systems(6).

## CORRELATION OF EXPERIMENTAL DATA

The final objective of the experimental program was correlation of the experimentally measured thixotropic decay curves in terms of the Theory of Thixotropic Behaviour(1). Consequently attention was focussed primarily on the shear stress decay curves and no further data treatment was attempted using the shear stress growth curves.

In view of the different behaviour between the slowly cooled and quickly quenched samples, data processing and correlation of the two sets of thixotropic decay curves was considered as two separate cases. Separate analysis was felt advisable since the form of the quick quenched sample decay curves was different from that of the slowly cooled sample decay curves.

To prepare the raw experimental data for correlation in terms of Equation (30), each set of thixotropic data requires four additional data processing steps. These steps are:

(1) For each thixotropic decay curve, the initial shear stress, $\tau_o$, must be estimated at "zero" time;

(2) For each thixotropic decay curve, the limiting or equilibrium shear stress, $\tau_\infty$, must be estimated;

(3) The measured decay curves at constant cup speeds must be processed to determine the shear rates corresponding to the measured shear stresses;

(4) The stress contribution of the Newtonian solvent, $\tau_\mu$, must be determined.

The subsequent data processing steps used, and the resulting correlation of the two sets of rheological data will be described in the following sections.

## I. Data Processing and Correlation of the Slowly Cooled Sample Thixotropic Decay Curves

### Data Processing of Slowly Cooled Sample Decay Curves

As may be noted from Figure (28) to Figure (31) the thixotropic decay curves for slowly cooled samples were regular uncomplicated experimental functions of shearing time. Consequently, subsequent data processing techniques did not, for the most part, differ from those techniques developed by Ritter(1) for processing similar type experimental data. The techniques used will be described.

Both the shear stress at zero time and that resulting from prolonged shear at constant cup speed were necessarily determined by extrapolation of the data in Figure (28) to Figure (31). Two independent methods were used for the former and gave results which in most cases, differed by less than 3 percent.

In the first of these methods, the incremental change in shear stress from the second to seventh 10-second time interval was obtained directly from experimental data and plotted as a function of the time interval number on logarithmetic coordinates. The resulting straight lines of negative slope were then extrapolated towards the left until they intersected the vertical line coordinate representing the first time interval. This shear stress value was taken as representing the incremental change in shear stress from zero time to 10 seconds;

adding the incremental stress to the experimentally determined 10 second shear stress gave the initial shear stress, $\tau_o$.

In the second method, shear stress was plotted as a function of time (seconds) plus ten seconds on logarithmic coordinates and the resulting curve again extrapolated towards the left. The initial shear stress was provided directly by the intersection of the extrapolated curve with the vertical coordinate corresponding to ten seconds.

The determination of the limiting shear stress proved to be a more difficult problem than that of determination of the initial shear stress and no truly satisfactory method was developed for prediction of this quantity. Initially, three extrapolation techniques were used: (i) that of plotting the experimental data on arithmetic coordinates and estimating the point at which the experimental curves would become asymptotic to a horizontal line representing the final or limiting shear stress, and that of extrapolating the experimental data from (ii) semilogarithmic coordinates, and (iii) from logarithmic coordinates. All three methods required an inordinate weighting on the experimental data near the end of the test period; since the logarithmic and smilogarithmic extrapolations were unduly influenced by slight variations in these end points, these two methods were discarded as unreliable. Consequently only the arithmetic coordinate extrapolation technique was utilized in estimating limiting shear stresses.

Although there was not inconsiderable difficulty in estimating probable upper and lower bounds on an arithmetically extrapolated shear stress, considerable difficulty was encountered in selection of the most

probable limiting shear stress within the bounds. Generally the bounds could be estimated to about $\pm 5$ percent of the bounds mid-point shear stress, but the error involved in the final choice of the most probable limiting shear stress was unknown. The consequences of this latter difficulty shall be thoroughly discussed in a later section.

Although the relationship between bob deflection and shear stress is independent of the rheological properties of a fluid, the relationship between cup speed and shear rate is not, and a somewhat more complicated procedure is required to calculate this latter quantity. The method used to determine instantaneous shear rate has been described in an earlier section (Experimental Determination of Rheological Parameters).

The experimental data plots necessary for the determination of shear stress at constant shear rate are shown in Figures (42) and (43); the constant shear rates chosen were 25 $sec^{-1}$, 60 $sec^{-1}$, 150 $sec^{-1}$ and 300 $sec^{-1}$. The corresponding values of shear stress-time at these shear rates are listed in APPENDIX NINE as part of the computed rheological data.

The stress contribution by the Newtonian solvent was determined by a procedure differing from that developed by Ritter(1). This new technique was used solely because of the difference between the systems in each investigation. The Newtonian solvent characteristics for an artificially loaded system may generally be determined directly from an investigation of the viscosity of the solvent at test temperature; in a naturally occurring system, it is very rare that the solvent or carrier liquid characteristics are known at test temperature.

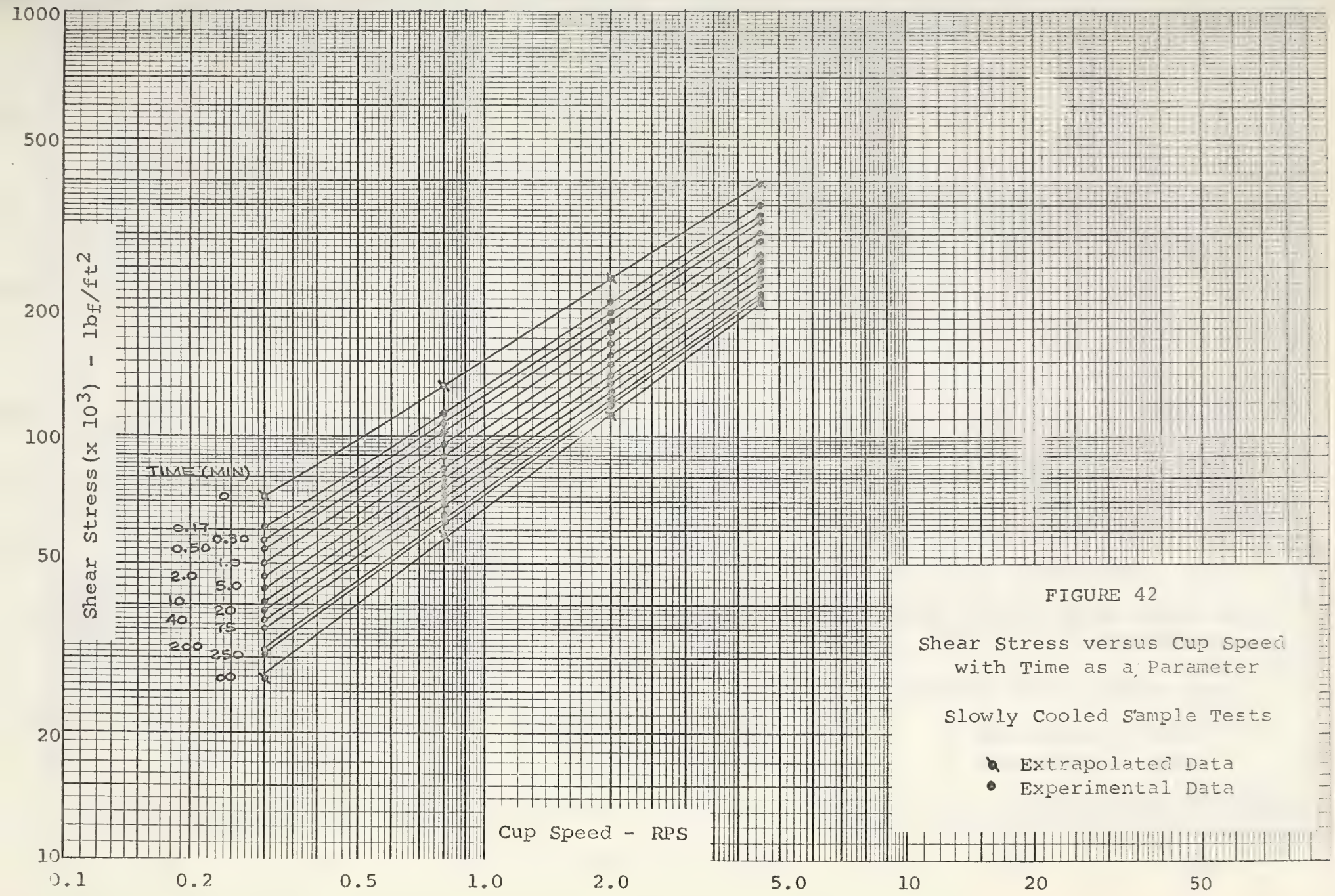


FIGURE 42

Shear Stress versus Cup Speed with Time as a Parameter

Slowly Cooled Sample Tests

Extrapolated Data

Experimental Data

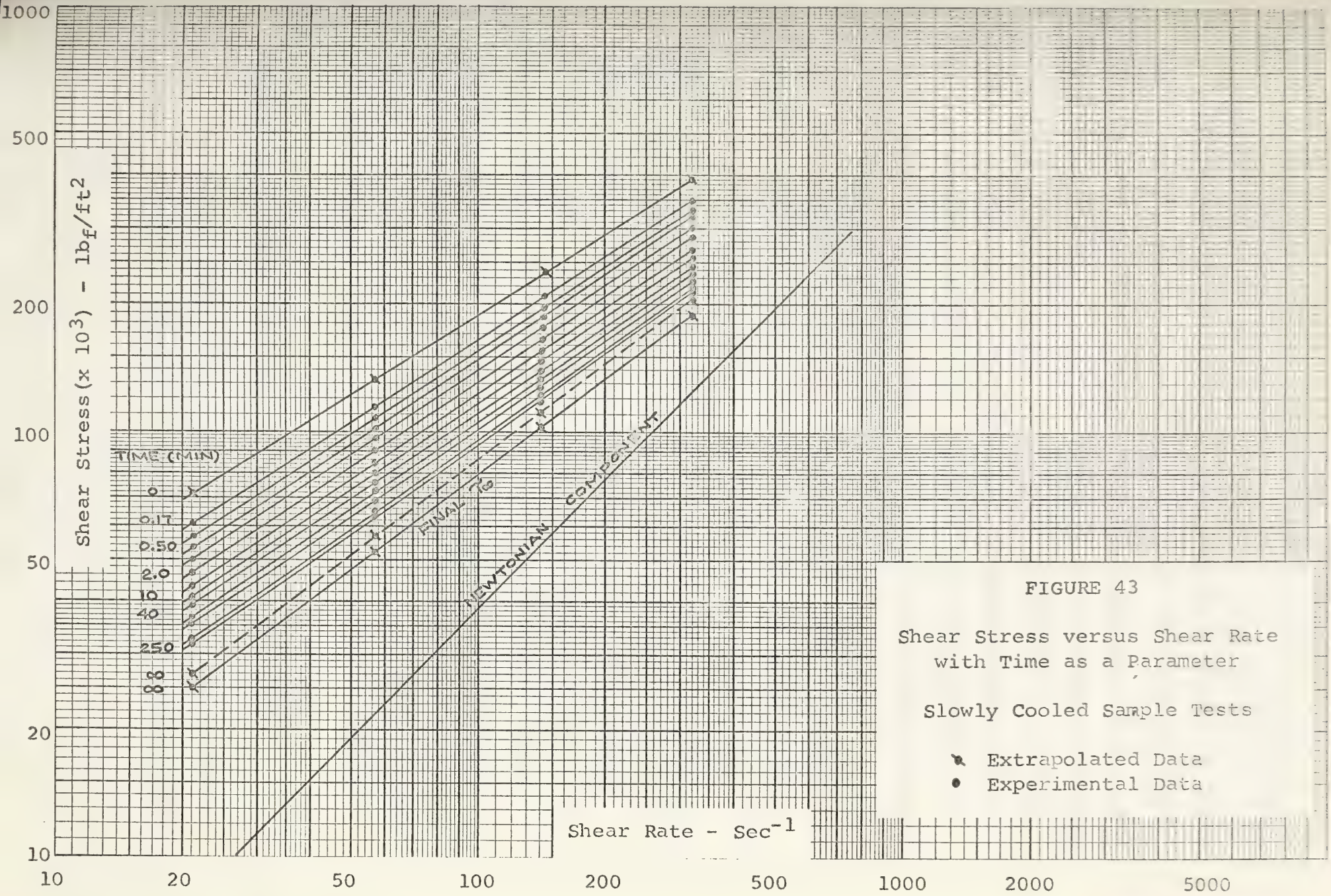


FIGURE 43

Shear Stress versus Shear Rate with Time as a Parameter

Slowly Cooled Sample Tests

- Extrapolated Data
- Experimental Data

The solvent in this investigation was composed of CWO oil and liquid wax. Above 80°F, solvent and model viscosities are identical; below 80°F, since the model rheological behaviour becomes complex, separation of solvent shear stress from total shear stress becomes much more difficult. The considered best method(54) of determining solvent viscosity at test temperature was to extrapolate solvent viscosities, as determined above 80°F, to the test temperature of 60°F. The extrapolation is shown in Figure (44) and, as may be noted, closely parallels that of pure CWO oil which comprised about 95 volume percent of the solvent.

Actually, the true solvent viscosity at 60°F would be somewhat intermediate between that of the extrapolated value and that of the CWO oil, since network formation would alter the oil/liquid-wax volume ratio (i.e. and hence the "solvent" viscosity). However, since such a value is experimentally indeterminable, it was assumed that the quantity of wax involved in network formation would not seriously alter the extrapolated solvent viscosity. As an estimate, based on consideration of both Figure (24) and Equation (33), it is felt that the error involved in such an assumption is less than one percent. In the extreme, if all wax were used during network formation, such an assumption would result in a maximum error in solvent viscosity of 3 percent, which in any case, has almost negligible influence during final correlation of experimental results.

## Correlation of Thixotropic Decay Data for Slowly Cooled Samples

The Theory of Thixotropic Behaviour (Equation 30) predicts that at constant temperature, a straight line relationship exists on logarithmetic

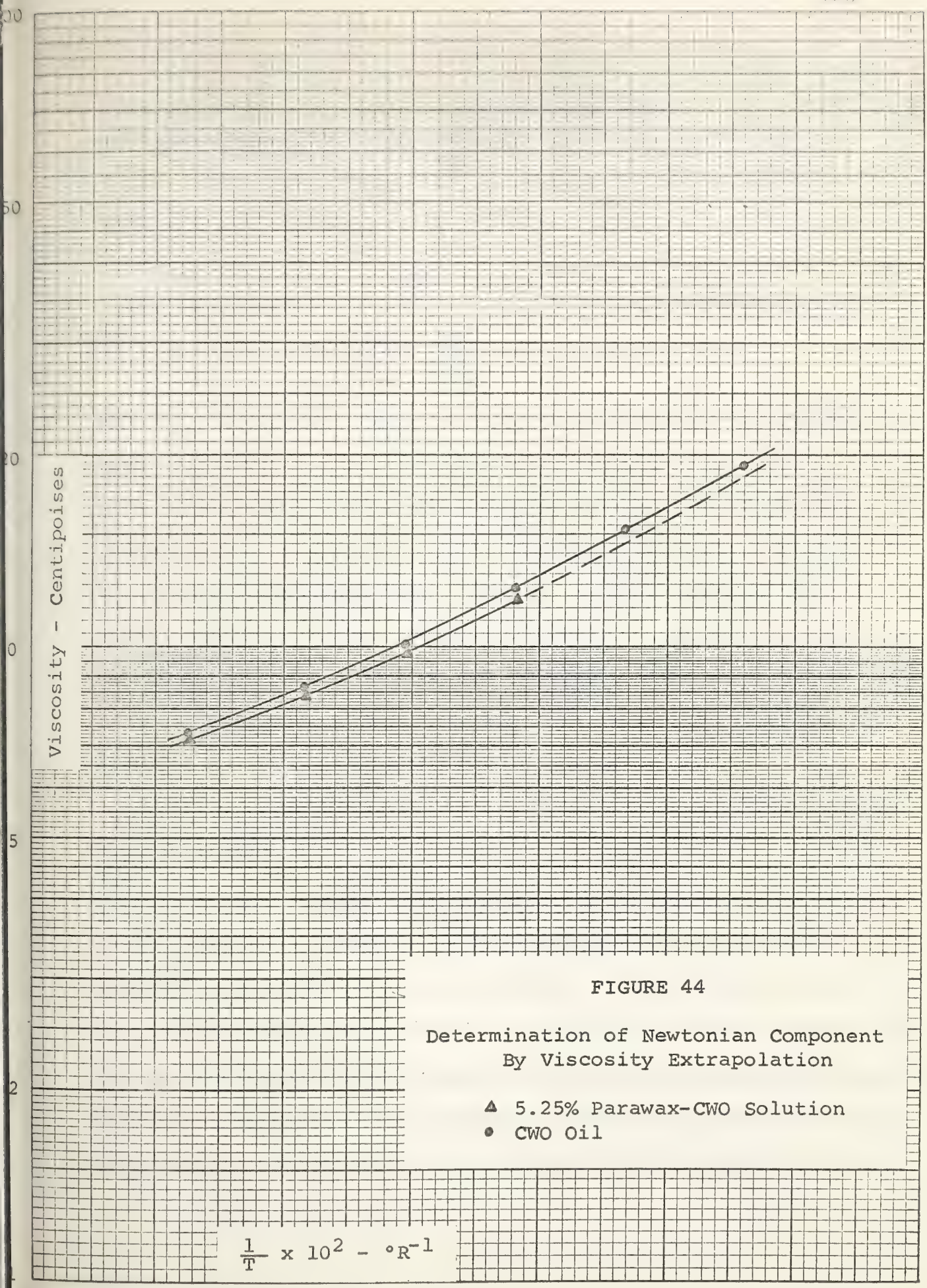


FIGURE 44

Determination of Newtonian Component
By Viscosity Extrapolation

▲ 5.25% Parawax-CWO Solution
● CWO Oil

coordinates between the computed quantity

$$\frac{\tau_s - \tau_{s\infty}}{\tau_{so}^2/\tau_{s\infty} - \tau_s} \qquad \text{and t.}$$

The slope of this straight line, as defined, is:

$$-k_A \left(\frac{\tau_{so} + \tau_{s\infty}}{\tau_{so} - \tau_{s\infty}}\right)$$

where $k_A$, the thixotropic decay constant is independent of time and shear rate.

Consequently, using limiting shear stress values as extrapolated from arithmetic coordinates, a preliminary attempt was made to correlate the processed experimental data in terms of the above variables. The initial result was that at each shear rate (25 $sec^{-1}$, 60 $sec^{-1}$, 150 $sec^{-1}$ and 300 $sec^{-1}$), a fairly straight line of negative slope was defined up to about thirty minutes; past this shear time, the straight lines gradually developed a steadily increasing downward curvature.

At first, the deviation from linearity was considered significant since it appeared to refute the postulated constant behaviour of $k_A$ as a function of time. However, in consideration of the uncertainties inherent in the extrapolation procedures, a simplified sensitivity analysis was performed on Equation (30) using as variables: (1) the initial shear stress, $\tau_o$; (2) the limiting shear stress, $\tau_\infty$ ; and (3) the Newtonian component, $\tau_\mu$. The analysis (APPENDIX EIGHT) indicated that if during extrapolation procedures, the limiting shear stress was estimated too high, then a normally straight line correlation would transform into a curve of the form described above.

Since further extrapolation procedures would have been inherently biased, the required limiting shear stress values were estimated by an alternate, but less justifiable procedure. First, the value of $\tau_\infty$, obtained through extrapolation of the arithmetic shear stress-time plot for the 25 $sec^{-1}$ shear rate, was incrementally decreased until, using the appropriately processed data, a straight line correlation resulted between

$$\frac{\tau_s - \tau_{s\infty}}{\tau_{so}^2/\tau_{s\infty} - \tau_s} \qquad \text{and } t$$

Two incremental decreases were necessary, decreasing the limiting shear stress from 310 $lbf/ft^2$ to 283 $lb/ft^2$ (about a 9 percent decrease). Then, with reference to Figure (43) a line was drawn parallel to the original arithmetically extrapolated limiting shear stress line, but passing through the coordinate (25 $sec^{-1}$, 283 $lbf/ft^2$). This latter line was called the true limiting-shear-stress line; the remaining three individual limiting shear stress values were then obtained at the intersections of this line with the vertical ordinates corresponding to 60 $sec^{-1}$, 150 $sec^{-1}$ and 300 $sec^{-1}$.

Using a procedure such as that described above would appear to be unjustifiable since it forces the data from at least one shear rate (25 $sec^{-1}$) to correlate on the basis of Equation (30). However, the following points should be considered: (i) that only the data for one shear rate was forced into a straight line correlation; and (ii) that the limiting shear stress values so obtained were within the realm of possibility, as was subsequently determined by re-extrapolation to these values on the various experimental data plots. Further, the fact is that some assumptions must be made concerning the rate at which the experimental shear stress is converging

to, or approaching the limiting shear stress. If this assumption is incorrect, then the extrapolated shear stress values would be displaced from the actual limiting shear stresses.

Subsequently, limiting shear stress values, as determined by the method just described, were used to correlate the experimental data. The final correlation, as performed in accordance with Equation (30) is shown in Figure (45). The associated computations are tabulated in APPENDIX NINE.

To this point, considerable emphasis has been placed upon the necessity of a straight line correlation (i.e. $k_A$ independent of time). In fact, an equally demanding requirement of the Theory is that $k_A$, the thixotropic decay constant, must be shown to be independent of shear rate.

Before proceeding, it should be noted that verification of this last condition does not require superposition of the linear correlations at each shear rate. For purposes of explanation, a re-examination of Equation (30), shown below, is useful:

$$\log\left(\frac{\tau_s - \tau_{s\infty}}{\tau_{so}^2/\tau_{s\infty} - \tau_s}\right) = -k_A\left(\frac{\tau_{so} + \tau_{s\infty}}{\tau_{so} - \tau_{s\infty}}\right)\log t - \log\left(\frac{\tau_{so}^2/\tau_{s\infty} - \tau_{sl}}{\tau_{sl} - \tau_{s\infty}}\right)$$

The only requirement of the Theory is that during the evaluation of $k_A$ from experimental data, the product

$$-(\text{slope})\left(\frac{\tau_{so} - \tau_{s\infty}}{\tau_{so} + \tau_{s\infty}}\right)$$

be a constant. However two additional possibilities exist:

$$\log\left(\frac{\tau_{so}^2/\tau_{s\infty} - \tau_{sl}}{\tau_{sl} - \tau_s}\right) = \begin{cases} \log C \neq f\left(\frac{dv}{dr}\right) & (1) \\ f\left(\frac{dv}{dr}\right) \neq \log C & (2) \end{cases} \qquad (43)$$

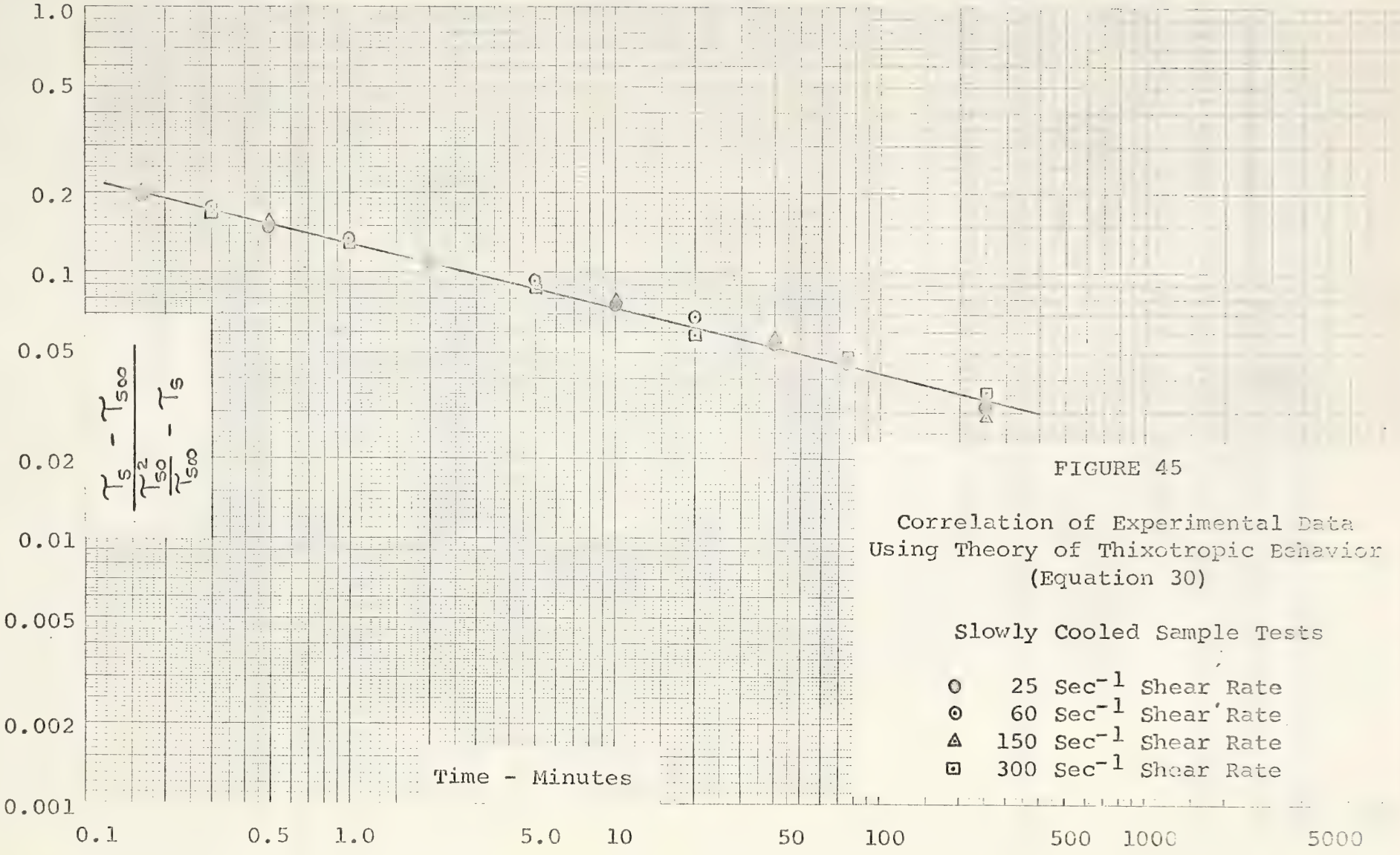


FIGURE 45

Correlation of Experimental Data
Using Theory of Thixotropic Behavior
(Equation 30)

The first of the above possibilities is not inherent in the Theory of Thixotropic Behaviour(1) and must be shown by data correlation. Since within the accuracy of the experimental data, a single linear correlation was obtained, it appears that both the quantities

$$\frac{\tau_{so} - \tau_{s\infty}}{\tau_{so} + \tau_{s\infty}} \qquad \text{and} \qquad \frac{\tau_{so}^2/\tau_{s\infty} - \tau_{sl}}{\tau_{sl} - \tau_{s\infty}}$$

are independent of shear rate. To demonstrate this fact, the values of $k_A$ obtained at each shear rate are tabulated below.

TABLE 3

Evaluation of Rate Decay Constant for Slowly Cooled Sample Thixotropic Decay Curves

| Shear Rate ($sec^{-1}$) | $\left(\frac{\tau_{so} - \tau_{s\infty}}{\tau_{so} + \tau_{s\infty}}\right)$ | Slope | $k_A$ |
|---|---|---|---|
| 25 | 0.575 | -0.242 | 0.139 |
| 60 | 0.570 | -0.242 | 0.138 |
| 150 | 0.577 | -0.242 | 0.140 |
| 300 | 0.602 | -0.242 | 0.146 |
| | | Average | 0.141 |
| | Average Deviation From Average | | 2.1% |
| | Maximum Deviation From Average | | 3.5% |
| | Maximum Deviation Between Two Determinations | | 5.7% |

The final test of the significance of $k_A$ is how well it would re-define the original experimentally measured curves. As may be seen below, the percentage error between predicted and experimental shear stress is clearly within the range of cumulative experimental and correlative error (i.e. estimated at about 5 percent).

TABLE 4

Error Analysis in Prediction of Experimental Shear Stress of Slowly Cooled Samples

| Shear Rate ($sec^{-1}$) | Duration of Shear (minutes) | | | | | |
|---|---|---|---|---|---|---|
| | 0.5 | 5.0 | 20.0 | 75.0 | 250.0 | |
| Absolute Precent Deviation Between Predicted and Experimental Shear Stress | | | | | | |
| | | | | | | Average |
| 25 | 1.2 | 1.5 | 2.5 | 2.8 | 1.7 | 1.9 |
| 60 | 0.5 | 2.2 | 2.9 | 1.7 | 0.9 | 1.6 |
| 150 | 1.4 | 1.6 | 0.9 | 0.2 | 2.2 | 1.3 |
| 300 | 0.2 | 1.3 | 2.0 | 3.4 | 4.4 | 2.3 |
| | | | | | Average | 1.8 |

In view of these results it must be concluded that for the data processing techniques used, the Theory of Thixotropic Behaviour(1) correlates the experimental data to a high degree of accuracy.

## II. Data Processing and Correlation of the Thixotropic Decay Curves for the Quick Quenched Samples

### Data Processing of the Thixotropic Decay Curves for the Quick Quenched Samples

At the outset is was recognized that the relative shape of the decay curves for the quickly quenched samples (Figure (32) to Figure (35)) could only be approximated by Equation (30). Therefore, any serious correlative attempts to verify the Theory of Thixotropic Behaviour(1) were precluded.

However, since it was of interest to see how closely Equation (30) could approximate the measured decay curves, the experimental data was

subsequently processed as two separate cases. In the first case, the experimental data was processed directly; for the second case, the experimental data was smoothed, as indicated by the dashed regular curves in Figure (32) to Figure (35), and then duly processed.

Data processing techniques identical to those described in the previous section were used in both cases.

For each of the above cases, identical values of the limiting shear stresses (as determined from arithmetic coordinate extrapolation procedures) and the Newtonian component were used. However, due to the smoothing procedures in the latter case, initial shear stress values for the smoothed data case were significantly different from those of the unsmoothed data case.

The plotted data associated with these processing techniques is shown from Figure (46) to Figure (49); the associated tabulated data is summarized in APPENDIX NINE.

## Correlation of Thixotropic Decay Curves for Quick Quenched Samples

The processed experimental data was subsequently correlated (APPENDIX NINE) and plotted in terms of the pertinent variables, as indicated in Figure (50) and Figure (51).

It may be noted that correlation of the unsmoothed data (Figure 50) results in a notable "hump" in an otherwise straight-line relationship; the "hump" is absent from the smoothed data correlation (Figure 51).

For the smoothed data, the following thixotropic rate decay constants ($k_A$) were calculated:

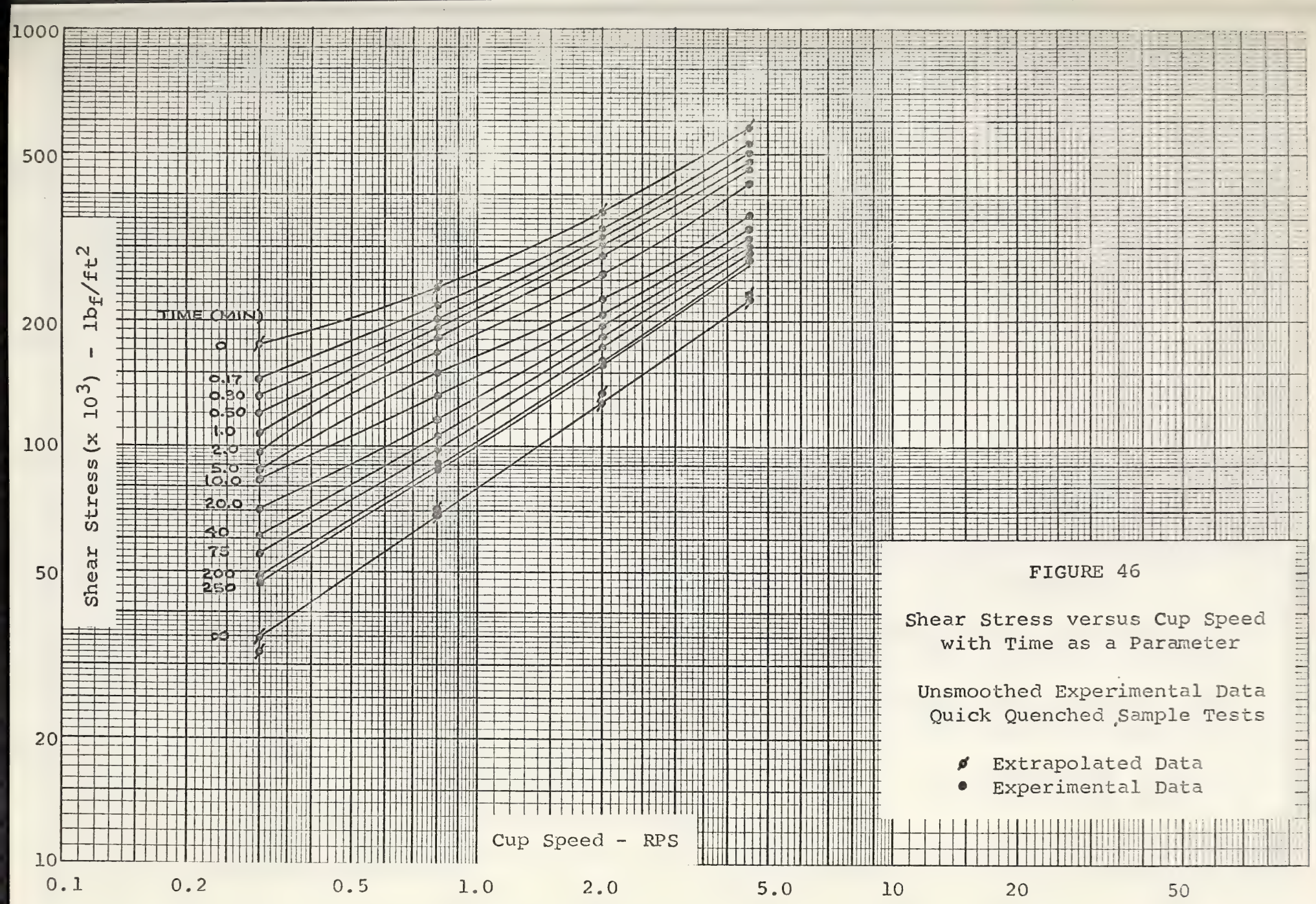


FIGURE 46

Shear Stress versus Cup Speed with Time as a Parameter

Unsmoothed Experimental Data
Quick Quenched Sample Tests

ø Extrapolated Data
• Experimental Data

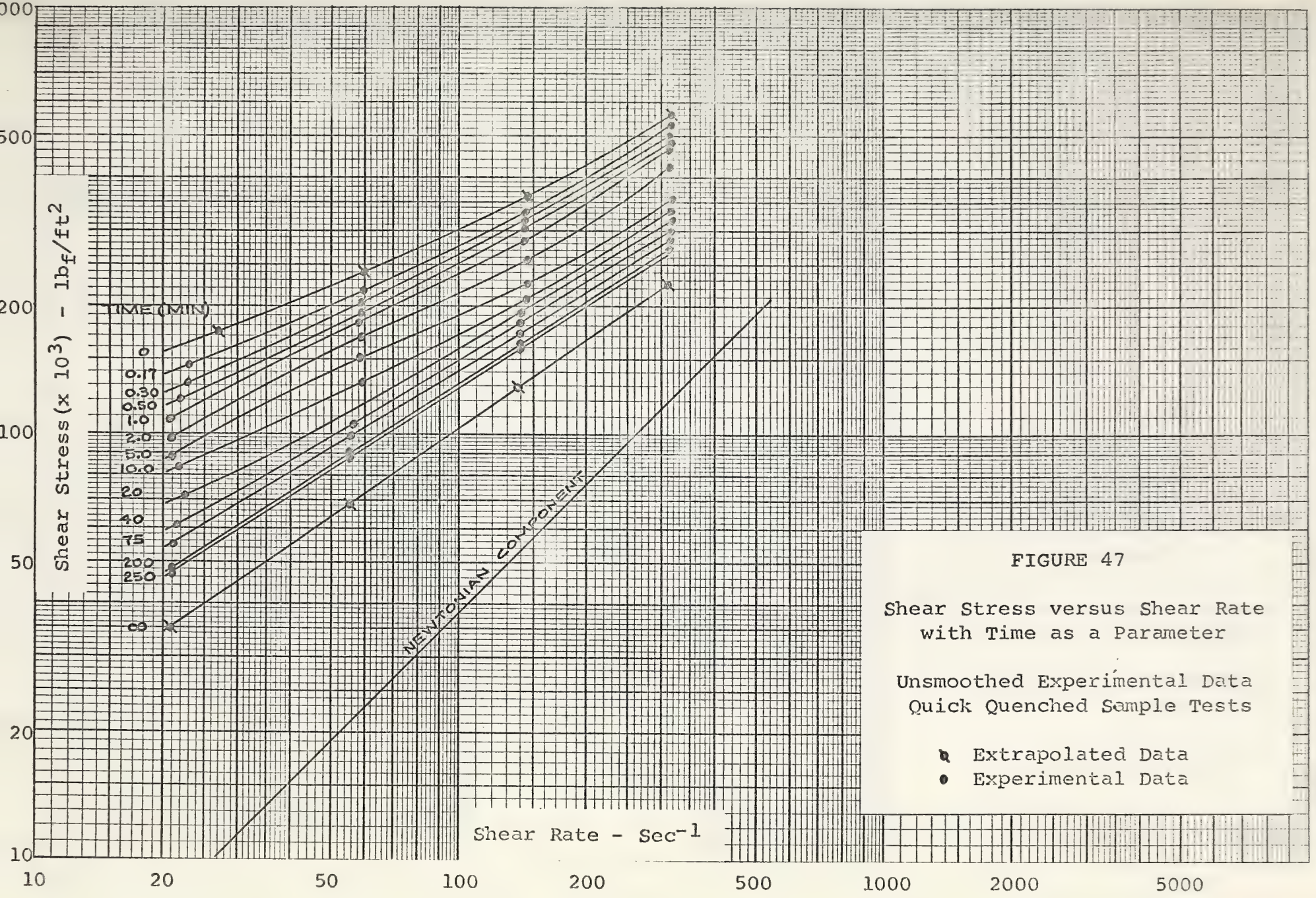


FIGURE 47

Shear Stress versus Shear Rate with Time as a Parameter

Unsmoothed Experimental Data
Quick Quenched Sample Tests

- Extrapolated Data
- Experimental Data

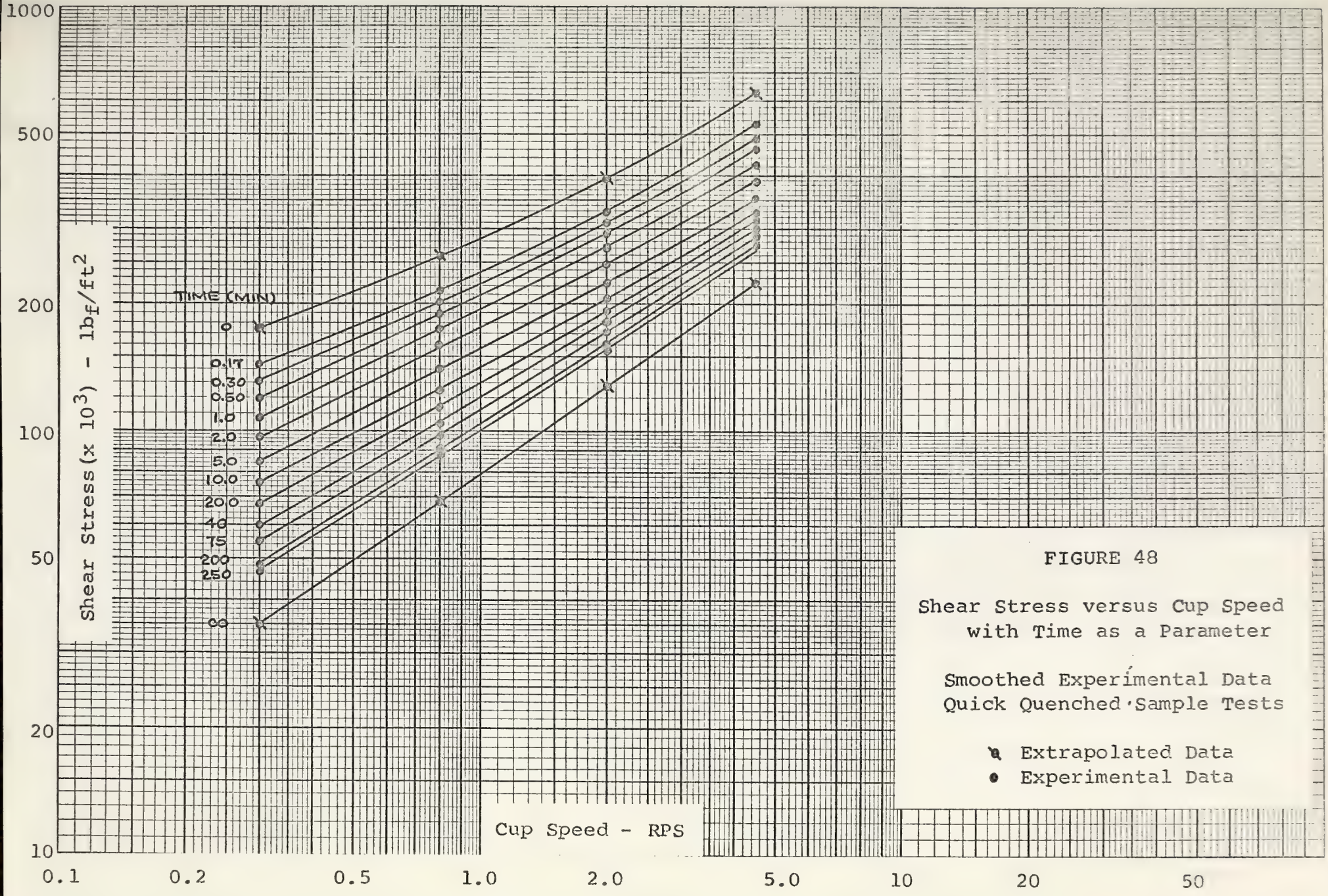


FIGURE 48

Shear Stress versus Cup Speed
with Time as a Parameter

Smoothed Experimental Data
Quick Quenched Sample Tests

Extrapolated Data
Experimental Data

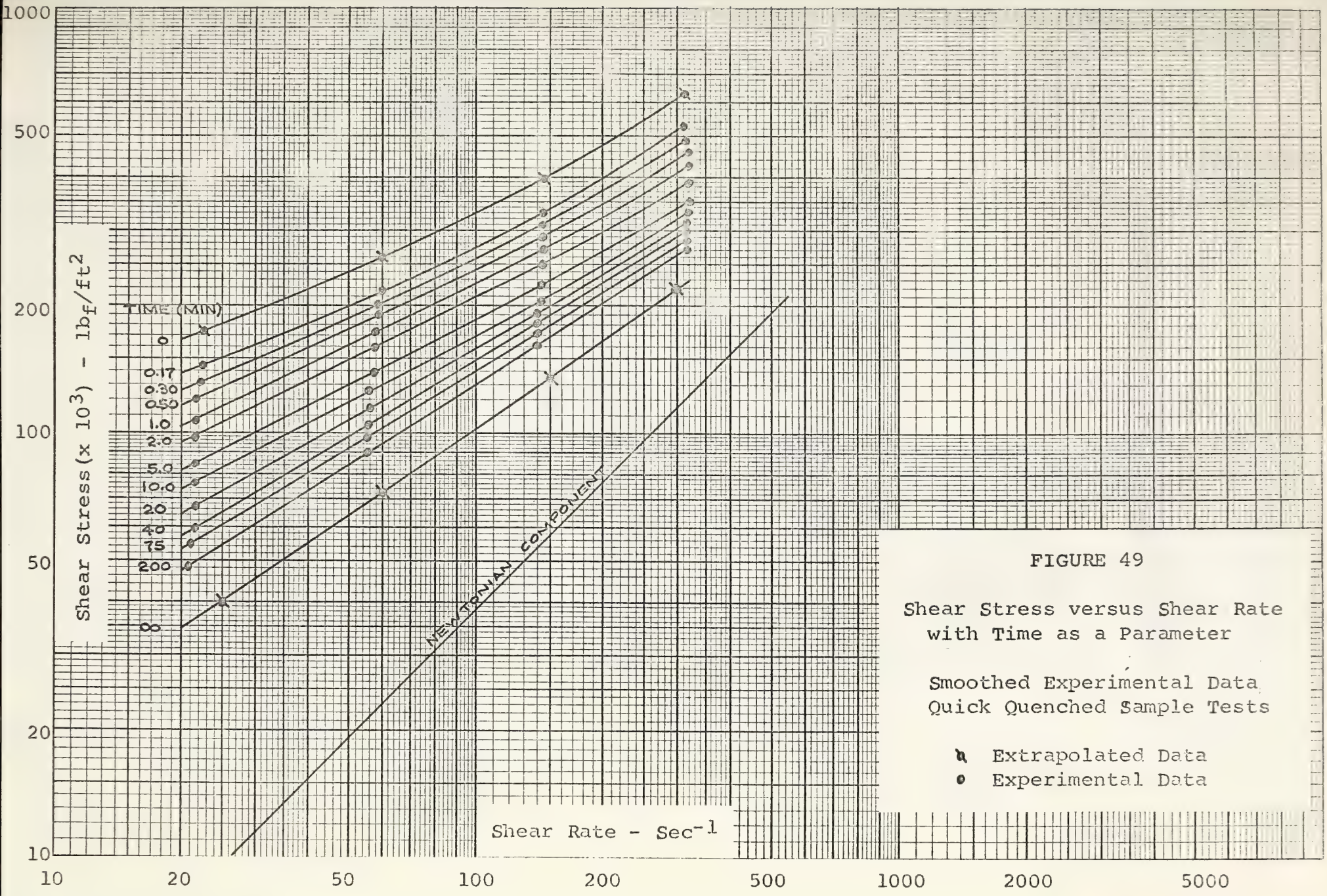


FIGURE 49

Shear Stress versus Shear Rate with Time as a Parameter

Smoothed Experimental Data
Quick Quenched Sample Tests

- Extrapolated Data
- Experimental Data

TABLE 5

Evaluation of Rate Decay Constant for Quickly Quenched Sample Thixotropic Decay Curves:
I - Smoothed Data

| Shear Rate ($sec^{-1}$) | $\left(\frac{\tau_{so} - \tau_{s\infty}}{\tau_{so} + \tau_{s\infty}}\right)$ | Slope | $k_A$ |
|---|---|---|---|
| 25 | 0.697 | -0.286 | 0.199 |
| 60 | 0.654 | -0.286 | 0.187 |
| 150 | 0.633 | -0.286 | 0.181 |
| 300 | 0.662 | -0.286 | 0.189 |
| | Average | | 0.189 |

| | |
|---|---|
| Average Deviation From Average | 2.7% |
| Maximum Deviation From Average | 5.4% |
| Maximum Deviation Between Two Determinations | 10.1% |

For the unsmoothed data, the computed rate constants were:

TABLE 6

Evaluation of Rate Decay Constant for Quickly Quenched Sample Thixotropic Decay Curves:
II - Unsmoothed Data

| Shear Rate ($sec^{-1}$) | $\left(\frac{\tau_{so} - \tau_{s\infty}}{\tau_{so} + \tau_{s\infty}}\right)$ | Slope | $k_A$ |
|---|---|---|---|
| 25 | 0.677 | -0.322 | 0.218 |
| 60 | 0.628 | -0.322 | 0.202 |
| 150 | 0.604 | -0.322 | 0.195 |
| 300 | 0.630 | -0.322 | 0.203 |
| | Average | | 0.204 |

| | |
|---|---|
| Average Deviation From Average | 3.1% |
| Maximum Deviation From Average | 6.2% |
| Maximum Deviation Between Two Determinations | 10.3% |

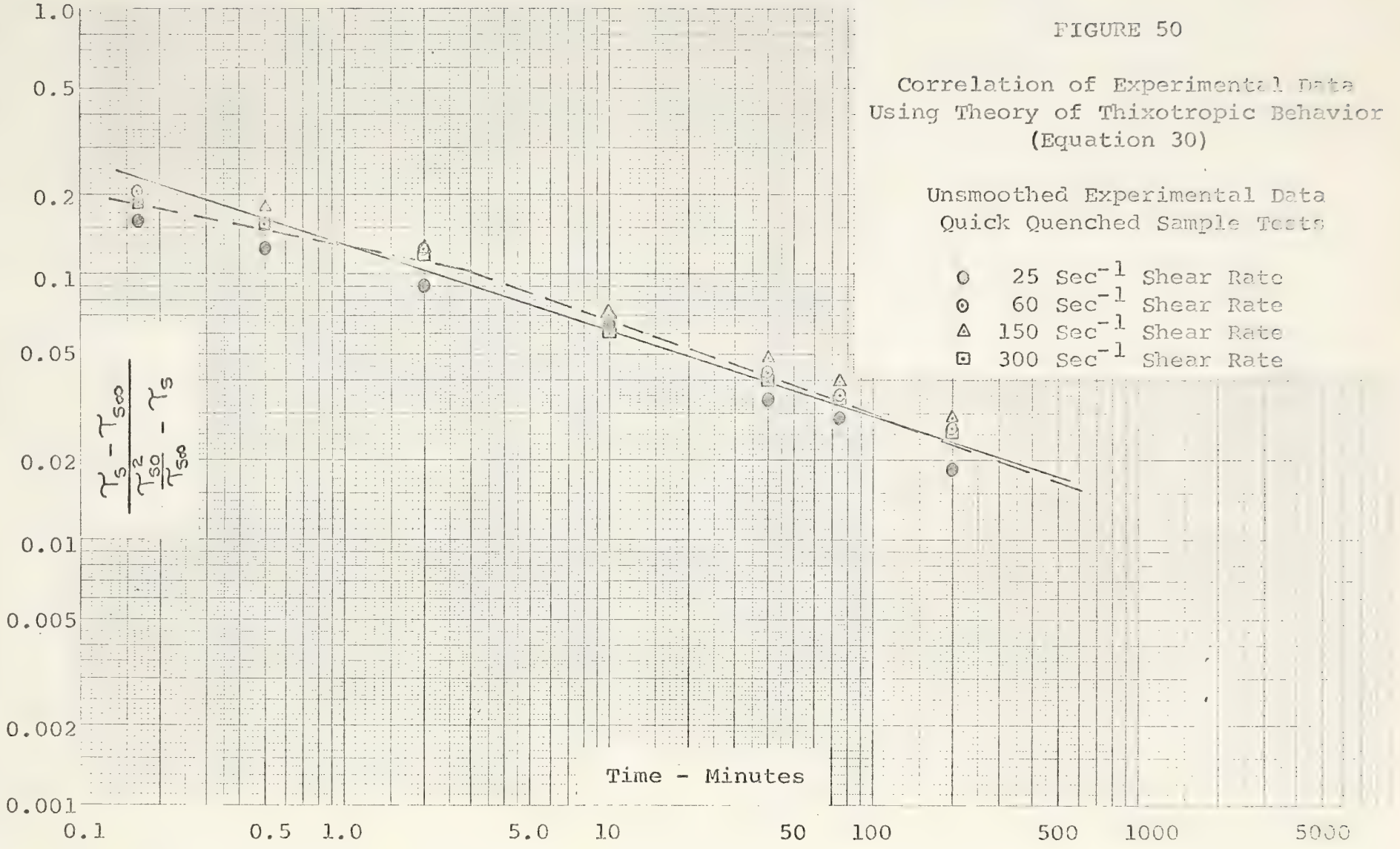


FIGURE 50

Correlation of Experimental Data
Using Theory of Thixotropic Behavior
(Equation 30)

Unsmoothed Experimental Data
Quick Quenched Sample Tests

- 25 $Sec^{-1}$ Shear Rate
- 60 $Sec^{-1}$ Shear Rate
- 150 $Sec^{-1}$ Shear Rate
- 300 $Sec^{-1}$ Shear Rate

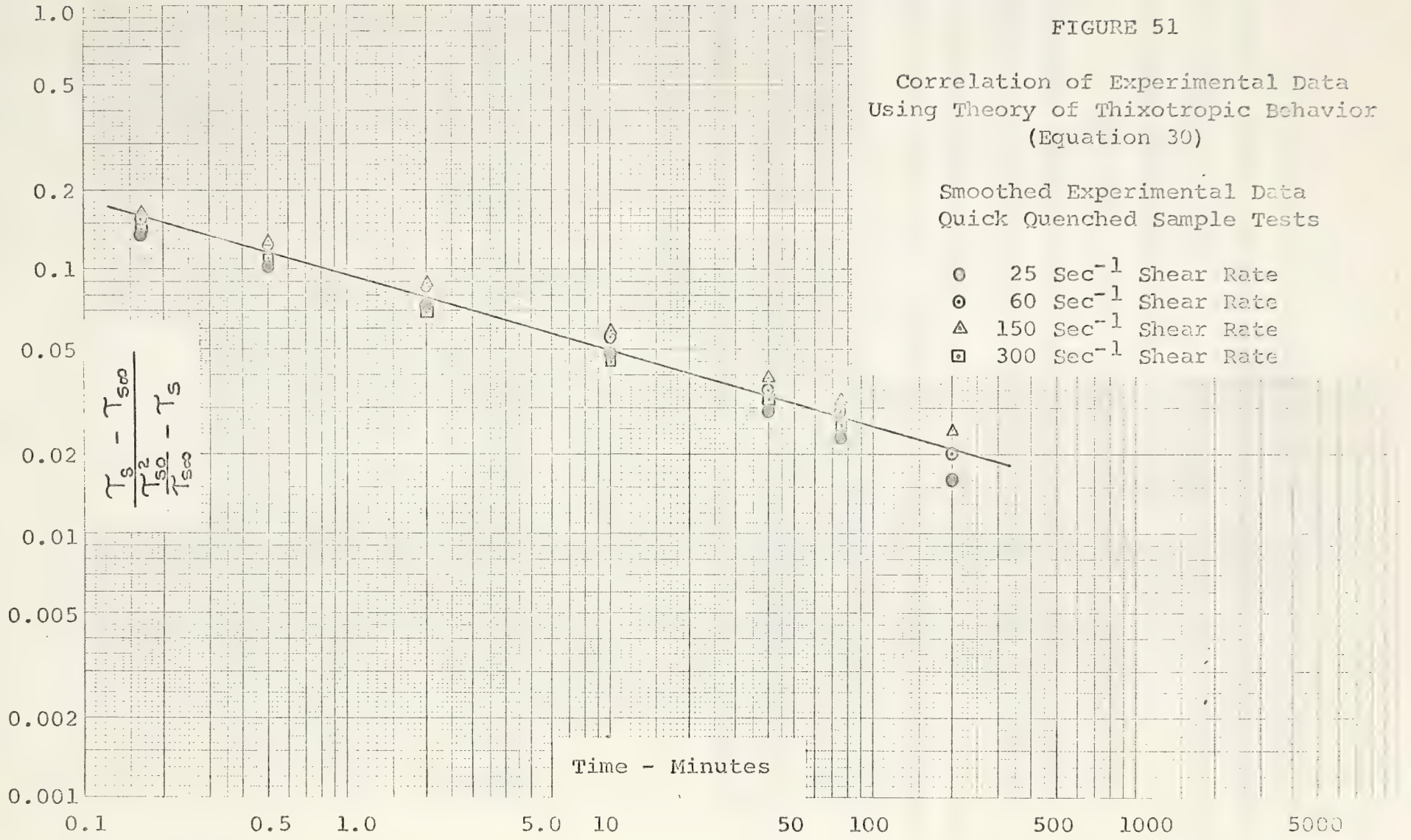


FIGURE 51

Correlation of Experimental Data
Using Theory of Thixotropic Behavior
(Equation 30)

Smoothed Experimental Data
Quick Quenched Sample Tests

As would be expected, the average rate constants are significantly different. Further, maximum deviations between individual rate constants was as high as 10.3 percent (i.e. as compared to 5.7 percent between slowly cooled sample rate constants).

As indicated in Table 6, the average error in predicting the experimentally measured decay curves was only about 5 percent. However, individual deviations were as high as 13.2 percent (i.e. more than twice the maximum permissible error of about 5 percent). The magnitude of this latter error was due to: (i) the inherent error involved during data processing operations; and (ii) the relative shape of the experimental shear stress decay curves.

An illustration of the difference between predicted and experimental shear stress decay curves is shown in Figure (52); the "secondary" effect is readily discernable.

TABLE 7

Error Analysis in Prediction of Experimental Shear Stress of Quickly Quenched Samples

| Shear Rate $(sec^{-1})$ | Duration of Shear - Minutes 0.5 | 5.0 | 20.0 | 75.0 | 200.0 | $t_m$ (1) | Error(2) (Absolute) |
|---|---|---|---|---|---|---|---|
| **I - Smoothed Experimental Data** | | | | | | | |
| 25 | 5.5 | 4.8 | 3.6 | 8.8 | 11.5 | 3.8 | 6.3 |
| 60 | 4.6 | 13.2(1) | 4.5 | 2.1 | 0.3 | $(13.2)^3$ | 5.0 |
| 150 | 8.9 | 6.2 | 6.1 | 4.1 | 3.8 | 10.9 | 6.7 |
| 300 | 0.9 | 1.7 | 0.9 | 0.7 | 1.8 | 7.4 | 2.2 |
| | | | | | | Average = | 5.0 |
| **II - Smoothed Experimental Data** | | | | | | | |
| 25 | 16.5 | 0.5 | 3.7 | 6.1 | 8.3 | 1.8 | 6.1 |
| 60 | 1.1 | 10.6 (1) | 5.6 | 3.4 | 2.9 | $(10.6)^3$ | 4.7 |
| 150 | 4.0 | 6.3 | 8.0 | 6.7 | 5.9 | 8.3 | 6.5 |
| 300 | 0.5 | 1.1 | 0.5 | 1.8 | 2.1 | 5.1 | 1.8 |
| | | | | | | Average = | 4.9 |

(1) Time at which deviation between smoothed and experimental data is a maximum; included in average error.

(2) In percent; (predicted shear stress - experimental shear stress)/experimental shear stress.

(3) Excluded from average error.

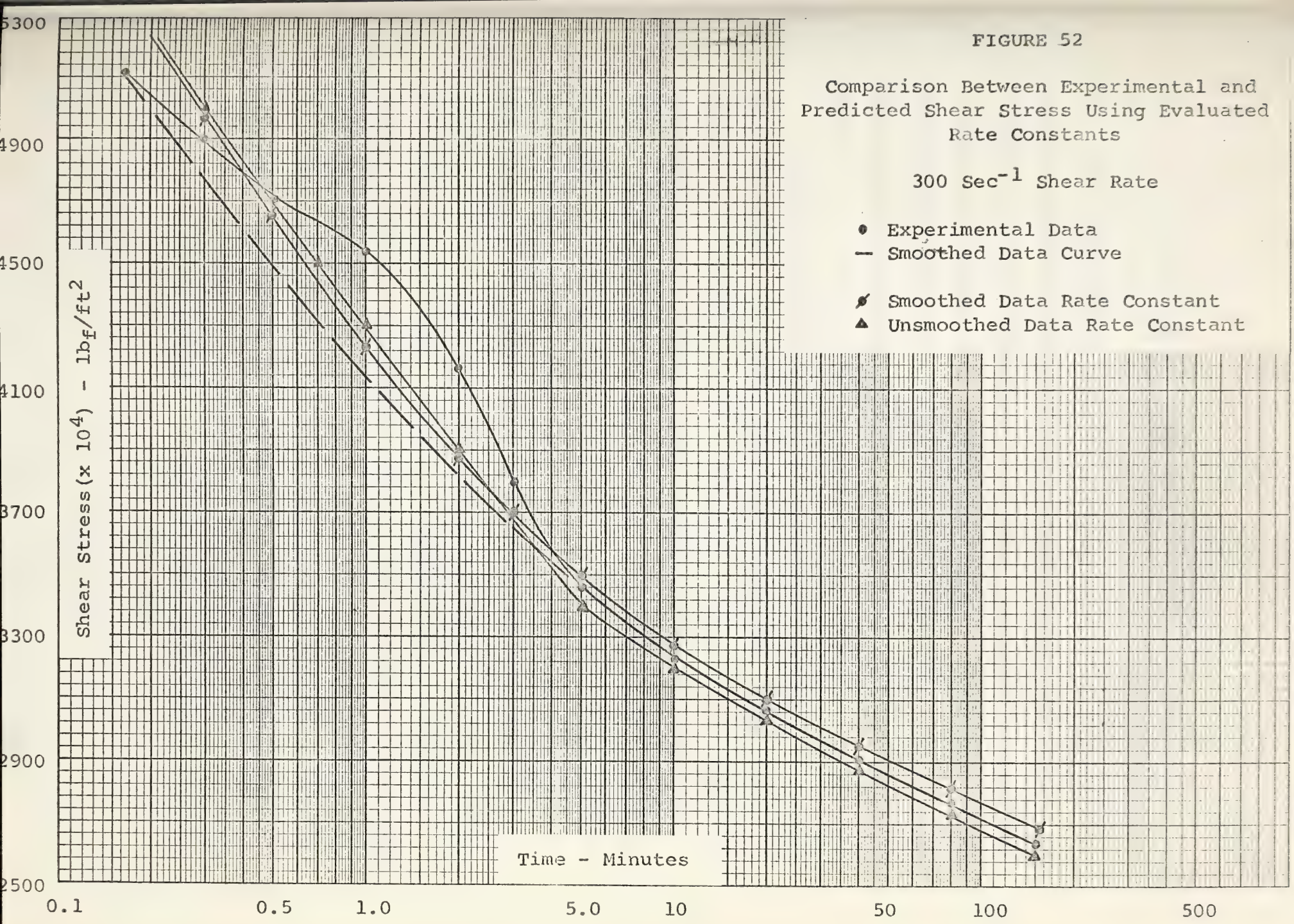


FIGURE 52

Comparison Between Experimental and Predicted Shear Stress Using Evaluated Rate Constants

300 $Sec^{-1}$ Shear Rate

- Experimental Data
- Smoothed Data Curve

- Smoothed Data Rate Constant
- Unsmoothed Data Rate Constant

## DISCUSSION OF EXPERIMENTAL PROGRAM AND EXPERIMENTAL RESULTS

1. The newly modified environmental temperature control cabinet and the auxiliary temperature and speed control apparatus associated with the Alberta Viscometer performed adequately. In all cases, temperature and speed control limits were within the desired control limits of $\pm 0.25^{\circ}F$ (maximum) and $\pm 0.5$ percent, respectively. However, several characteristics of the present experimental set-up require attention prior to a follow-up experimental program.

First, in its present form, the experimental apparatus is limited as to the duration of a test period, since constant supervision during operation of the various equipment components is required. Secondly, since shear stress is directly proportional to bob deflection, and since the absolute measuring accuracy of this latter quantity is constant at any deflection, then as bob deflection decreases, the relative error in shear stress increases. This latter characteristic is particularly critical during measurement of shear stress growth curves and during measurement of the incremental decrease in shear stress near the end of a test period. To overcome these problems, a superior viscometer design is required capable of sustained unsupervised operation and with improved shear stress measuring accuracy.

2. Although the experimental model displayed the requisite features of network degradation under conditions of shear, one important criteria, namely that of regenerative reproducible rheological behaviour from only one sample was never attained. Further, if reproducible behaviour between

discrete samples was to be obtained, a complicated sample handling procedure and standardized rheological test sequence was required. In part, such non-reproducibility may have been accentuated by preparation of a synthetic system, but, as has previously been described, other investigators (1,16,24) have experienced similar test difficulties when using naturally occurring thixotropic systems. A possible explanation for such non-reproducible behaviour, as applied to wax-oil systems, has not previously been advanced. It is to this end that the following discussion is directed.

It is a recognized characteristic of some wax-laden hydrocarbon systems that active "building block" sites are present which have a predominant influence during wax "crystallization" and subsequent network formation. Such sites are believed to be nucleation centers to which, initially at least,wax molecules migrate and crystallize upon. The result is a propogation of crystal chains. (The recognition that such sites exist is the basis of selective blending of wax inhibitor additives into an oil(55); the additives are believed to preferentially adsorb on these nucleation sites, thereby reducing their relative activity and retarding network formation).

In a network forming system similar to that of a wax laden crude oil, namely a crystalline polymeric system, it has been noted(56) that the network junction points have, under comparable environmental conditions, a powerful growth tendency. Such a tendency results in the formation of "crystallites" which can grow to a relatively large size and which are stable within the liquid phase to very high temperatures.

The mechanism described above may be used to describe network formation in the thixotropic model. First, it is assumed that this system

contains active network formation sites. Secondly, it was observed that as time progressed after mixing Parawax with Diol-34, an increasing number of opalescent threads became visually discernable. It is believed that these "threads" were the indication of an active growth process centered about the network promotion sites. The continued existence of this almost-polymeric growth process would have a profound influence on the rheological behaviour of the model system.

Since these threads are relatively stable at elevated temperatures, the active network sites cannot be readily regenerated. Hence, the process of network growth and destruction over a period of time is more or less irreversible. The use of a single sample for repeated rheological experiment is thus precluded.

At temperatures significantly below the cloud point (for example, at -7°F), the network formation sites are effectively stabilized within the network structure and continued growth proceeds very slowly, if at all. Consequently, sample storage at such temperatures appears to be an effective method of eliminating or minimizing sample degeneration.

3. During shear testing of the quick quenched samples, a reproducible "secondary effect" was measured. This effect, which is attributed directly to the network destruction characteristics,results in a localized deviation from the behaviour of thixotropic systems as predicted by Equation (30). An explanation of such behaviour in terms of the present knowledge of the network destruction processes is not readily apparent. However, for a similar network forming system, one investigator(42) has suggested the existence of two characteristic types of network bonding. Presumably then, the shear destruction process would reflect the dissimilar natures of the

two bonding mechanisms.

As an alternate explanation, consider the above behaviour in terms of the general shear degradation process as proposed by Ritter(1):

$$A \rightleftharpoons i'A \rightleftharpoons i''A \ \ldots \ iB \tag{18}$$

which for purposes of mathematical treatment was simplified to:

$$A \rightleftharpoons iB \tag{19}$$

This form inherently assumes that the network decay process may be approximated by a single rate determining step. In an analogous manner to the above simplification, consider a reduction of Equation (18) in terms of the quick quenched sample decay process. In this case, a plausible simplification is:

$$A \rightleftharpoons i'A \rightleftharpoons iB \tag{43}$$

where now the shear destruction process is characterized by two rate determining steps. Such a process appears compatible with the two slope sequence of Figure (50).

It is seen then that the shape of the quick quench sample decay curves may be explained on a qualitative basis by the Theory of Thixotropic Behaviour(1). However, if such behaviour is to be treated on a quantitative basis, that is, if the analytical characteristics of the Theory of Thixotropic Behaviour(1) are to be maintained, additional thixotropic decay equations, similar to Equation (30), but based on more general decay processes (i.e. such as Equation 43) shall have to be formulated. Presumably, such equations would contain provision for two or more thixotropic decay rate determining steps.

4. Considerable difficulty was encountered during extrapolation to a value corresponding to the limiting shear stress, and no truly satisfactory method was developed for prediction of this quantity. This problem is one which will be encountered by future investigators even if a suitable viscometer is constructed to extend the test period. Consequently, it is suggested that a numerical curve fitting and/or curve simulation technique be investigated to provide an alternate and unbiased extrapolation procedure.

5. Ritter(1) observed that for one network preparation method used prior to shear testing, the thixotropic rate decay constant appeared to be a function of temperature as described by:

$$k_A = Ae^{b/T} \qquad (32)$$

However, the significance of the above correlation could never be affirmed(1) due to a meager amount of data and the rather large deviations of the data from the straight line correlation. This experimental investigation has shown that $k_A$ might also be a variable at one temperature, being dependent upon the conditions under which the network is formed. However, this postulate cannot be confirmed since $k_A$ would also appear to be markedly dependent upon data processing techniques.

## CONSIDERATIONS INVOLVING PIPELINE FLOW OF THE EXPERIMENTAL MODEL

Previously Ritter(1), and then Govier and Ritter(57) outlined methods for calculating the pipeline flow behaviour of a thixotropic fluid from rheological data obtained in a coaxial viscometer. Using their procedure, the pipeline flow behaviour of three possible flow conditions of the experimental model have been calculated. The three conditions were: (1) the initial and final (after an infinite length of time) flowing pressure gradient of the model after quick quenching from 85°F to flow temperature (60°F) and curing for 4 hours at this temperature; (2) the initial and final pressure gradient of the model after being cooled at 0.43°F/min to 60°F and cured at this temperature for four hours; (3) the initial and maximum pressure gradients of the model at 60°F after being simultaneously sheared and cooled at 0.43°F/min to 60°F. The results are presented graphically in Figure (53) as pressure drop per mile versus average flowing velocity. The assumed diameter of the pipeline was six inches.

It may be noted that experimental data has not been given previously for the above mentioned condition(3). This data in graphical form, is presented in APPENDIX TEN together with the summarized calculations of the above flow conditions(1),(2) and (3). As a pertinent observation, corresponding to condition (3), it was noted that the measured shear stress would gradually increase from an initial to a maximum value after about an hour, before slowly starting to decay. For the purposes of calculation, maximum shear stress values after one hour of shear at 60°F were used to calculate the corresponding flow behaviour of the model.

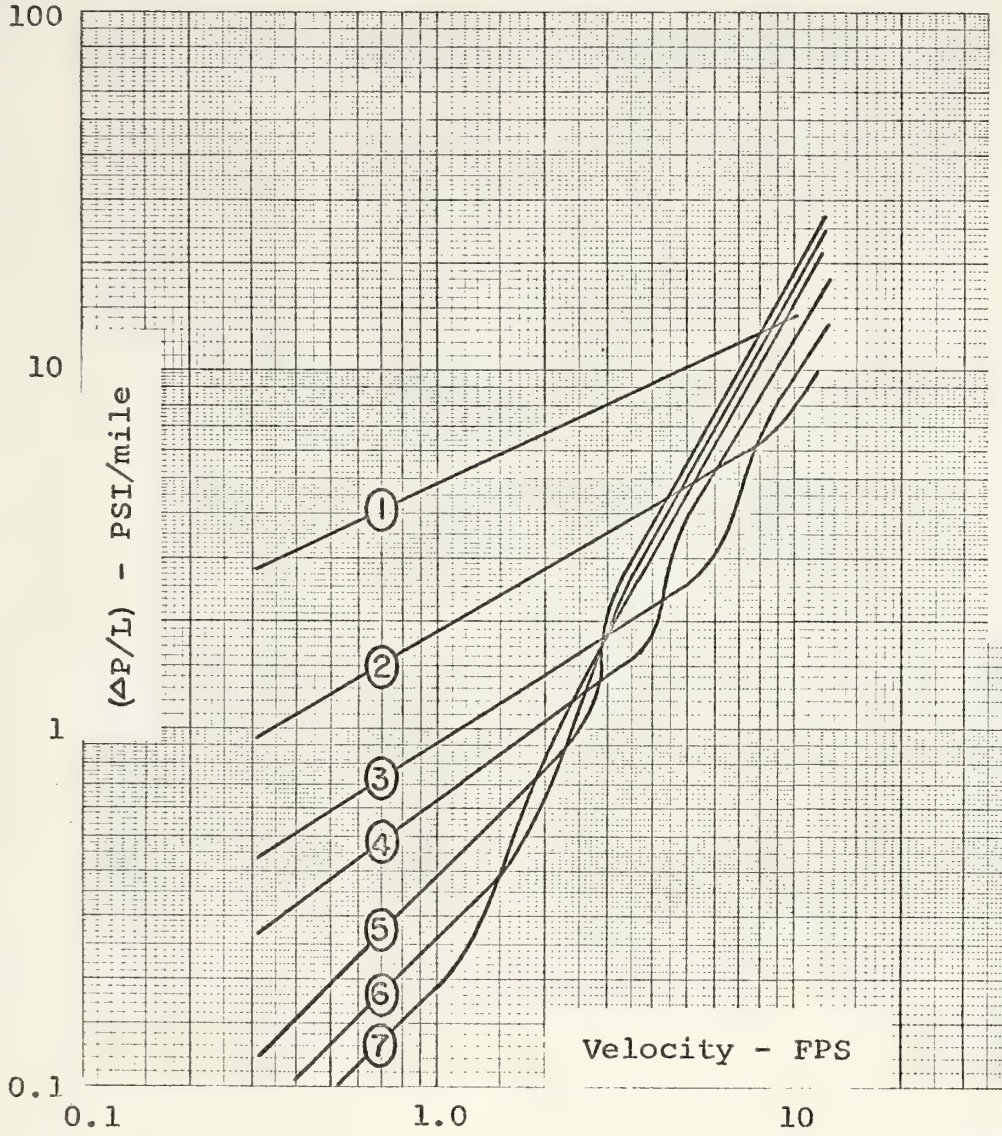


FIGURE 53

Calculated Pipeline Flow Behavior
of Thixotropic Model
For Various Flow States

Pressure Drop versus Average
Flow Velocity in a
Six Inch Pipeline at 60°F

1. Initial Gradient - Quick Quenched Case
2. Initial Gradient - Slowly Cooled Case
3. Final Gradient - Quick Quenched Case
4. Final Gradient - Slowly Cooled Case
5. Maximum Gradient - Sheared While Cooling
6. Initial Gradient - Sheared While Cooling
7. Pressure Gradient of CWO Oil

Inspection of Figure (53) reveals a wide variation in the calculated pressure gradients, which in turn is dependent solely on the fluid handling method. In all probability, for purposes of design, the quick quenched condition would be used since it corresponds to a maximum in rheological behaviour. However, this condition is probably not encountered in the field and a more realistic situation is afforded by either the slowly cooled or continuously sheared condition.

## RECOMMENDATIONS FOR FUTURE STUDIES

1. The Theory of Thixotropic Behaviour(1) should be modified to include provision for one or more rate decay constants.
2. A new viscometer should be constructed in order to extend testing periods and to improve shear stress measuring accuracy.
3. Numerical and/or curve fitting techniques should be investigated as methods for prediction of the limiting shear stress.

# CONCLUSIONS

The rheological behaviour of a non-Newtonian thixotropic model composed of a partially refined wax in a light lubricating oil has been investigated at 60°F. The rheological characteristics of the model are attributed to a loosely bonded network of wax clusters or crystals which form within the model at this temperature.

Utilizing the specialized network formation characteristics of the model, two separately distinct network systems were formed at 60°F and each individually shear tested. The two resulting sets of thixotropic decay data were correlated with a recent Theory of Thixotropic Behaviour(1). Correlation of the experimental data in terms of the latter theory proved satisfactory for one set of thixotropic data (overall average prediction error of 1.8 percent) but unsatisfactory for the second data set (overall average error of 5 percent, but maximum errors of up to 13.2 percent) The primary reason for the inadequacy of the correlation in the latter instance was due to the presence of a reproducible "secondary effect" superimposed on the conventional decay process.

Thus, although the Theory of Thixotropic Behaviour(1) is adequate for correlation of certain specific thixotropic measurements, further development of the Theory is required to extend its application to a wide variety of thixotropic systems.

NOMENCLATURE

| | |
|---|---|
| A | Flow area, $ft.^2$; constant in Arrhenius Equation(32); flow parameter defined in Equation (4). |
| (A) | Concentration of original networks |
| a | Torsion wire constant, $lb_f/ft^2$/degree |
| B | Flow parameter defined in Equation (4) |
| $B_1$ | Constant in Krieger and Maron Equation (15) |
| $B_2$ | Constant in Krieger and Maron Equation (15) |
| (B) | Concentration of network fragments |
| b | Slope of semilogarithmic plot of $k_A$ versus 1/T, $^oR$ |
| C | Constant in Equation of Thixotropic Behaviour as defined by Equation (43) |
| D | Differential operator, d/dt |
| D | Bob deflection, degrees |
| E | Dimensionless group in Energy Equation (39) and defined in APPENDIX FOUR |
| F | Applied deforming force, $lb_f$ |
| f | Flow resistance of network segment |
| G | Torsion wire moment, $lb_f$ - ft |
| h | Bob immersion depth, ft |
| k | Fluid consistency index, $lb_m/ft\ sec^{2-n}$; fluid thermal conductivity, $BTU/hr.ft^2\ ^oF$ |
| $k_A$ | Thixotropic decay rate constant |
| $k_B$ | Thixotropic growth rate constant |
| N | Cup speed, RPS |

| | |
|---|---|
| $N_i$ | Number of carbon storms per molecule |
| $\overline{N}$ | Dimensionless group in Energy Equation (39) and defined in APPENDIX FOUR |
| n | Slope of logarithmic plot of shear stress versus cup speed, $lb_f/ft^2/RPS$ |
| r | Radius, ft |
| $r_1$ | Radius of bob, ft |
| $r_2$ | Radius of cup, ft |
| T | Temperature, $^oF$ and $^oR$ |
| $T_{BW}$ | Bob wall temperature, $^oF$ |
| $T_{CW}$ | Cup wall temperature, $^oF$ |
| $T_{CF}$ | Cooling fluid temperature, $^oF$ |
| t | Time, minutes and seconds |
| V | Velocity, ft/sec |
| w | Angular velocity, radians/sec |
| y | Plate separation, ft |
| $\frac{dv}{dy}$ | Shear rate, $sec^{-1}$ |
| $\frac{dv}{dr}$ | Shear rate, $sec^{-1}$ |

Greek Letters

| | |
|---|---|
| $\alpha$ | Flow parameter defined in Equation (9) |
| $\alpha'$ | Proportionality constant in Equation (21) |
| $\beta$ | Flow parameter defined in Equation (9) |

| | |
|---|---|
| $\delta$ | Fluid deformation, ft |
| $\Theta$ | Dimensionless group in Energy Equation (39) and defined in APPENDIX FOUR |
| $\mu$ | Viscosity, $lb_m/ft.sec$ |
| $\mu_N$ | Newtonian viscosity, $lb_m/ft.sec$ |
| $\mu_a$ | Apparent Newtonian viscosity, $lb_m/ft.sec$ |
| $\mu_p$ | Plastic viscosity, $lb_m/ft.sec$ |
| $\mu_o$ | Apparent Newtonian viscosity at zero shear rate, $lb_m/ft.sec.$ |
| $\rho$ | Density, $lb_m/ft^3$ |
| $\tau$ | Shear Stress, $lb_f/ft^2$ |
| $\tau_y$ | Yield value shear stress, $lb_f/ft^2$ |
| $\tau_s$ | Structural shear stress, $lb_f/ft^2$ |
| $\tau_o$ | Shear stress at zero time, $lb_f/ft^2$ |
| $\tau_\infty$ | Limiting shear stress at infinite time, $lb_f/ft^2$ |
| $\tau_\mu$ | Shear stress due to Newtonian component, $lb_f/ft^2$ |
| $\tau_{so}$ | Structural shear stress at zero time, $lb_f/ft^2$ |
| $\tau_{s1}$ | Structural shear stress at one minute, $lb_f/ft^2$ |
| $\tau_{s\infty}$ | Limiting structural shear stress at infinite time, $lb_f/ft^2$ |
| $\frac{d\delta}{dt}$ | Deformation rate, ft/sec |

# BIBLIOGRAPHY


1. Ritter, R.A.: A Theory of Thixotropic Behavior; Ph.D. Thesis, University of Alberta, Edmonton, Alberta (1961)

2. Metzner, A.B.: Advances in Chemical Engineering; Volume 1, Academic Press, New York (1956)

3. Dodge, D.W. and Metzner, A.B.: "Turbulent Flow of Non-Newtonian Systems"; AIChE Journal, 2, 189 (1959)

4. Shaver, R.G. and Merrill, E.W.: "Turbulent Flow of Pseudoplastic Solutions in Straight Cylindrical Tubes";AIChE Journal,2, 181 (1959)

5. Metzner, A.B.: "Recent Developments in the Engineering Aspects of Rheology"; Rheologica Acta, Band 1, Nr 2-3, 205 (1958 - 1961)

6. Scott-Blair, G.W.: A Survey of General and Applied Rheology; Second Edition, Sir Isaac Pitman and Sons, London (1948)

7. Von Wozer, J.R., Lyons, J.W., Kim, K.Y. and Colwell, R.E.: Viscosity and Flow Measurement; Interscience Publishers, New York (1963)

* 8. Eyring, H. and Powell: Nature, 154, 427 (1944)

9. Reiner, M.: Deformation, Strain and Flow; Interscience Publishers, Interscience Publishers, New York (1960)

*10. Slattery, J.C.: Ph.D. Thesis, University of Wisconsin, (1959)

11. Winning, M.D.: Rheological Properties Pipeline Flow Clay Slurries; M.Sc. Thesis in Chemical Engineering, University of Alberta, Edmonton, Alberta (1948)

12. Winning, M.D.: Private Communication; (1962)

13. Hauser, E.A.: The Colloid Science of Important Clay Minerals; Clay and Clay Minerals; Publication 395 (edited by W.O. Milligan), NAS-NRC (1955)

14. Billington, E.W.: "Some Measurements of the Elastic and Viscous Properties of Thixotropic Fluids";Proc. Phys. Soc., 76, 127 (1960)

*15. Pyrce-Jones, W: J. Sci. Instruments, 18, 39 (1941)

16. Ackroyd, G.C. and Aubrey, K.V.: Some Observations on the Flow Properties of Residual Fuel Oils from Petroleum; Proceedings of the Second International Congress on Rheology; (Edited by V.G.W. Harrison), Butterworths Scientific Publications, London (1954)

17. Ferry, J.D.: Viscoelastic Properties of Polymers, First Edition, John Wiley and Sons, Inc., New York (1961)

*18. Poiseuille, J.: "Mem Savants Etrangers"; 9, 433 (1846)

19. Phillippoff, W. and Gaskins, F.H.: "The Capillary Experiment in Rheology"; Trans. Soc. Rheology, Vol. w, 263 (1958)

20. Bagley, E.B.: "The Separation of Elastic and Viscous Effects in Polymer Flow"; Trans. Soc. Rheology, Vol. 5, 355 (1961)

21. Wilkinson, W.L.: Non-Newtonian Fluids; First Edition, Pergamon Press, London (1960)

22. Pawlowski, J.: "Determination of the Friction Law of a Non-Newtonian Fluid From Viscosity Measurements Made in a Rotational Viscometer"; Kolloid-Zeitschrift, 130, 129 (1953)

23. Krieger, I.M. and Maron, S.H.: "Direct Determination of theFlow Curves of Non-Newtonian Fluids. III. Standardized Treatment of Viscometric Data"; J. Appl. Physics, 25, 72 (1954)

24. Billington, E.W.: "Some Measurements on the Time Dependence of the Viscosity of Thixotropic Fluids"; Proc. Phys. Soc., 75, 40 (1960)

25. Jones, S.P. and Ryson, J.K.: "The Rheology of a Lubricating Oil at Temperatures Below the Pour Point"; J. Colloid Sci., 7, 272 (1952)

26. Green, H.: Industrial Rheology and Rheological Structures; John Wiley and Sons, Inc., New York (1949)

27. Utsugi, H. Kim, K., Ree, T., and Eyring, H.: "Thixotropic Property of Lubricating Grease"; NLGI Spokesman, 25, 125 (1961)

28. Vela, S. and Fredrickson, A.G.: "On Stress Relaxing Solids. II. Relaxation Effects in Periodic Flow and in Unsteady Flow"; (To be published in Chem. Eng. Sci.) Preprint, Chemical Engineering Department, University of Minnesota (1961)

29. Frisch, H.L. and Simha, R.: "The Viscosity of Colloidal and Macromolecular Solutions"; Rheology; Volume I, (Edited by F.R. Eirich), Academic Press, Inc., New York (1956)

*30. Einstein, A.: Ann. Physik, 17, 549 (1905)

*31. Simha, R.: J. of Research Natl. Bur. Standards, 42, 405 (1949)

*32. Riseman, J. and Ullman, R.: J. Chem. Phys., 19, 578 (1951)

33. Storey, B.T. and Merril, E.W.: J. Polymer Sci., 33, 361 (1958)

34. Goodeve, C.F.: "A General Theory of Thixotropy and Viscosity"; Trans. Far. Soc., 35, 342 (1939)

35. Weltman, R.N.: "Rheology of Pastes and Paints"; Rheology; Volume 3 (Edited by F.R. Eirich), Academic Press, Inc., New York (1960)

36. Denny, D.A. and Brodkey, R.S.: "Kinetic Interpretation of Non-Newtonian Flow"; J. of Appl. Phys., 33, 2270 (1962)

37. Glasstone, S., Laidler, K.J. and Eyring, H.: The Theory of Rate Processes; McGraw-Hill Book Company, Inc.,New York (1941)

38. Bondi, A.: "Particle Kinetics in Gels"; Proceedings of the Second International Congress on Rheology; Butterworths Scientific Publications, London (1954)

39. Beale, R.: "The Flow of Waxy Oils and Other Non-Newtonian Liquids"; Science of Petroleum; Volume II (Edited by Dunstan, A.E.), Oxford University Press, London (1938)

40. A.S.T.M. Committee D-2: A.S.T.M. Standards on Petroleum Products and Lubricants; Test D97-47, American Society of Testing Materials, Philadelphia (1949)

41. Armour Research Foundation of Illinois Institute of Technology: Document 20716 (Unclassified); (Prepared for Wright Air Development Center under contract A.F. 33(038)-1644); On file at Defence Research Board, Ottawa, Canada

42. Van der Tempel, M: "Mechanical Properties of Plastic-Disperse Systems at Very Small Deformations"; J. of Coll. Sci., 16, 284 (1961)

43. van Olphen, H: Forces Between Suspended Bentonite Particles; Clay and Clay Minerals; (Edited by A Swineford), Publication 456, NAS-NRC (1956)

44. Bulter, R.M. and MacLeod, D.M.: "Solid-Liquid Equilibria in Wax Crystallization"; Canadian Journal of Chemical Engineering, April, 53 (1961)

45. Edwards, R.T.: "Crystal Habit of Paraffin Wax"; Ind. Eng. Chem., 49, 757 (1957)

46. Clarke, E.W.: "Crystal Types of Pure Hydrocarbons in the Paraffin Wax Range"; Ind. Eng. Chem., 43, 2526 (1951)

47. Villiers-Fisher, J.: Design of a Concentric Cylinder Viscometer; M.Sc. Thesis in Chemical Engineering, University of Alberta (1951)

48. Oka, S.: *The Principles of Rheology; Rheology, Volume III, (Edited by F.R. Eirich), Academic Press, New York (1960)

49. Bagley, H.D.: Flow Characteristics of Crude Oils; M.Sc. Thesis in Chemical Engineering, University of Alberta, Edmonton, Alberta (1955)

50. Schlichting, H.: Boundary Layer Theory; Fourth Edition, McGraw-Hill Book Company, New York (1960) 430

51. Merrill, E.W., Mickley, H.S. and Raw, A.: "Instability in Couette Flow of Solutions of Macromolecules"; Journal of Fluid Mechanics, 13, 86 (1962)

52. Bird, R.B., Stewart, W.E. and Lightfoot, E.N.: Transport Phenomena; John Wiley and Sons, Inc., New York (1960)

53. Lodge, A.S.: "Rheological Properties of Concentrated Polymer Solutions: (1) Growth of Pressure Fluctuations During Prolonged Shear Flow"; Polymer, 2, 195 (1961)

54. McLaughlin: "Cluster Formation in Relation to the Viscosity of Melts in the Pre-Freezing Region"; Trans. Far. Soc., 54, 1804 (1958)

55. Personal Communication: Wax Reserch Lab, Imperial Oil Production Research and Technical Services Lab, Calgary, Alberta

56. Bisschops, J.: "Gelation of Concentrated Polyacrylonitrile Solutions. II"; J. of Pol. Sci., 17, 89 (1955)

57. Govier, G.W. and Ritter, R.A.: "Pipeline Flow Characteristics of Crude Oils"; Paper Presented June 19, 1963 at the Sixth World Petroleum Congress, Frankfurt am Main, Germany

---

* Original reference unavailable to author

# APPENDIX ONE

## AIR CIRCULATION AND REFRIGERATION SYSTEMS

General Equipment Design Basis

Preliminary to equipment design, a literature survey was conducted to find a circulating air bath system which, when coupled to a refrigeration system, would complement the temperature control requirements (i.e. high sensitivity over a fairly wide range of temperatures ). Such a system has been described by Rasi*.

The system described utilized an intermediate heat transfer fluid between a refrigeration system and a recirculating air system. The advantage of such a system is that since the temperature of the intermediate heat transfer fluid may be set at a temperature level between that of the refrigeration coil and the circulating air, excellent temperature control and control system stability is obtained. This design principle appeared admirably suited to the viscometer air bath requirements and served as the basis for subsequent equipment design considerations.

Addition to Existing Cabinet

This addition was constructed so as to provide a compact internal air flow recycle system. As with the original cabinet, the addition was fabricated with 2 inch cork sandwiched between two layers of 1/2 inch plywood.

The top of the cabinet, which supports the air circulation fan drive motor, is removable to provide access to the circulation fan.

The flow channel divider (3/4 inch plywood) is supported by two sliding bolts, and if desired, may be either tilted upwards to provide direct access

---

* Razi, A: "Quelques Considerations sur L'Automatisation des Installations Frigorifiques" International Institute of Refrigeration, Proceedings of Meetings, Commissions 3-4-5 (Moscow, September, 1958), Dunod, Paris; p. 125.

to the main cabinet back, or, removed entirely for maintenance. Air cooling coils are mounted on the outer face of the divider; a 500 watt heater (Appendix 2) is mounted on the inner face.

Refrigeration System

The major piece of equipment in the refrigeration system is the Tecumseh 2-HP Low Temperature refrigeration unit. The manufacturers specifications of this unit are:

| Coil Temperature (°F) | Coil Pressure | Capacity (BTU/HR) |
|---|---|---|
| -40 | 11"V | 4050 |
| -30 | 5.5"V | 5860 |
| -20 | 0.6 psig | 8325 |
| -10 | 4.5 psig | 11190 |
| 0 | 9.2 psig | 14800 |
| 10 | 14.6 psig | 19080 |

The above data refers to operation with Freon-12.

A schematic diagram of the assembled refrigeration and varsol circulation system is shown in Figure (1-A). In operation, the bimetallic strip temperature sensing device is adjusted to the desired varsol circulation temperature. When this device detects a temperature increase above the set point temperature, a time-delay relay is activated and after a 25 second delay, the solenoid valve (d) is opened and liquid Freon-12 is flashed across the expansion valve into the expansion coil. Since the coil pressure increases, the differential back-pressure regulator on the refrigerator is activated and the compressor begins operation. The compressor will continue to operate until the varsol bath temperature drops below the set point temperature, at which time: (i) the contacts on the bimetallic strip device will separate; (ii) the solenoid valve will close (after a 25 second

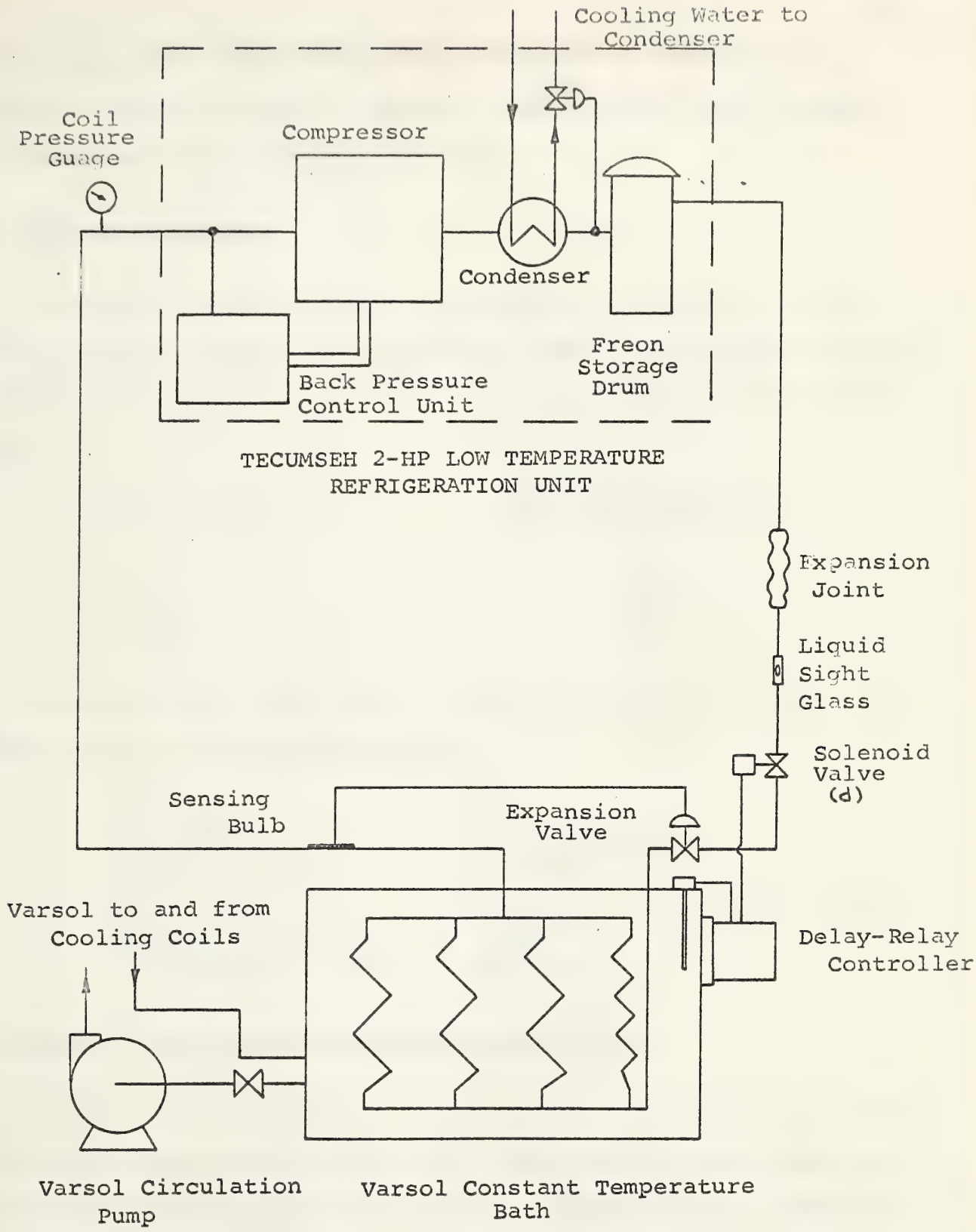


FIGURE 1-A Schematic of Assembled Refrigeration System

delay); and, (iii) the coil pressure will be drawn down until the back pressure regulator attains its set point. When this last stage is reached, the compressor will automatically shut off.

Air Recirculation System

The air recirculation system is composed of a circulation fan and a set of air cooling coils mounted on the back side of the flow channel divider. The flow characteristics of the circulation fan, as driven by a 1/2 HP motor are:

| SCFM at 1725 RPM | Static Pressure (in $H_2O$) |
|---|---|
| 902 | 0 |
| 855 | 1/4 |
| 782 | 1/2 |
| 678 | 3/4 |
| 571 | 1 |

The finned tube coils (two) are standard manufactured "booster" coils each with the following pertinent details:

| | | |
|---|---|---|
| Fins/inch | = | 8 |
| Fin diameter | = | 1.4 inches |
| Tube diameter | = | 0.675 inches O.D. |
| Finned tube length | = | 21 inches |
| No. of tubes | = | 7 |
| Geometrical spacing | = | triangular, 1.55" center to center |
| Surface area per coil | = | 59 $ft^2$ |
| Cooling fluid flow path | = | parallel |

Performance of Air Circulation and Refrigeration System

The air circulation and refrigeration system was designed for operation with the circulating varsol bath at $0^{\circ}F$. The accompanying graph (Figure 1-B) reveals the dynamic cooling characteristics of the air bath at a varsol circulation temperature of $0^{\circ}F$.

With the present set-up, if test temperatures lower than $30^{\circ}F$ are required, a Freon-12 expansion coil should be added to the present varsol air cooling coils.

FIGURE 1-B

Dynamic Cooling Characteristics
of Air Bath System

Cabinet Temperature versus Time

Varsol Circulation Temperature = 0°F
Ambient Room Temperature = 85°F

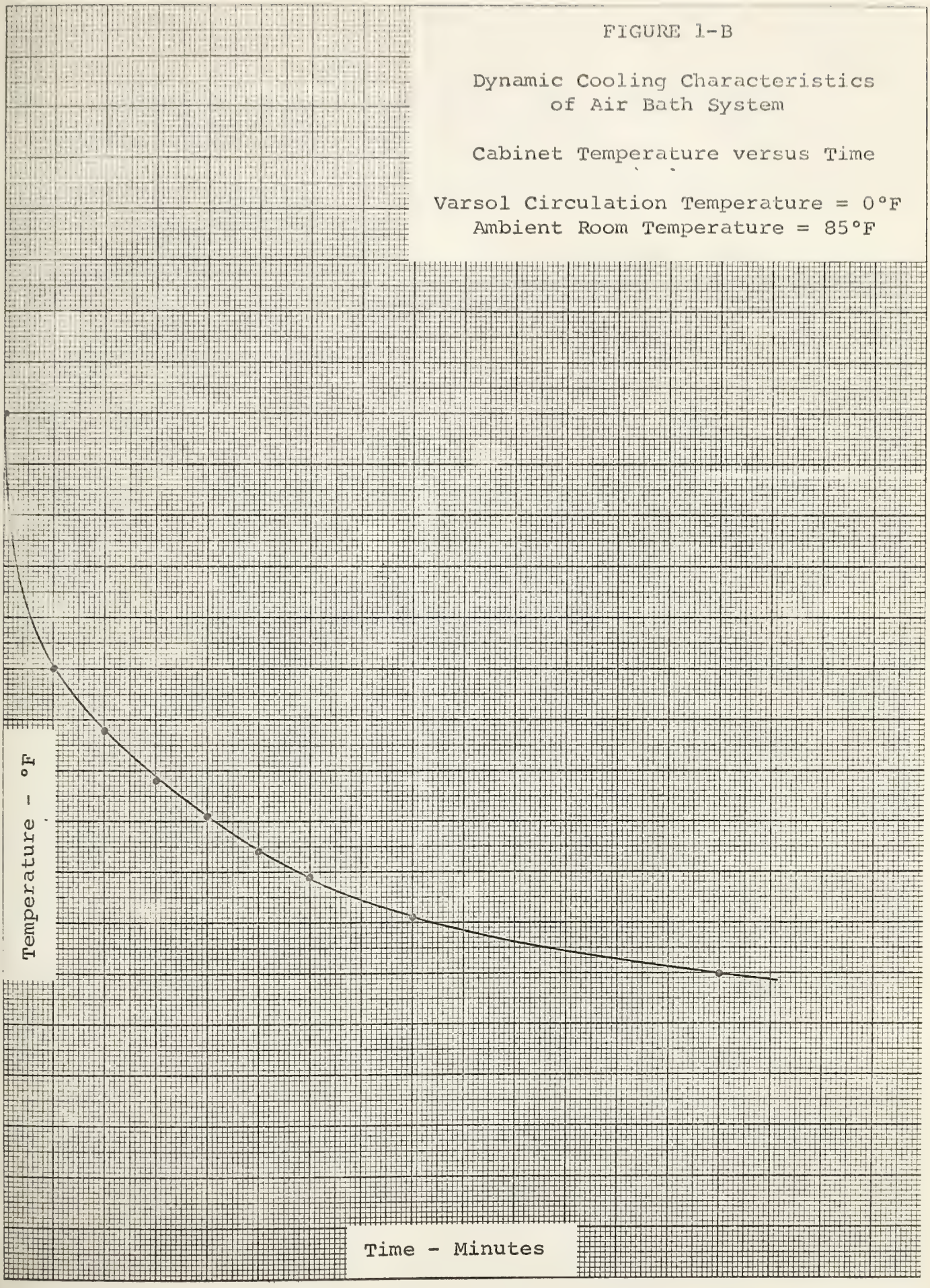

# APPENDIX TWO

## CABINET TEMPERATURE CONTROL SYSTEM

The most difficult equipment design problem encountered was that of designing a cabinet temperature control system which would regulate the air flow control louver. The design requisites for such a control system were (i) inexpensive construction, (ii) high sensitivity and (iii) capability of continuous operation for extended periods of time.

The finally chosen system is shown schematically in Figure(2-A), and may be seen to consist essentially of:

1. Two thermistor-actuated amplifier relays*;
2. A reversing 1/20 HP motor.

The sensitivity of the thermistor setup is excellent, being generally $\pm 0.10^{\circ}F$; in general, this control range was attained in the experimental setup.

In practice, the control system operated as an on-off controller since the temperature lag in the cabinet was sufficiently high to eliminate the inherent floating speed characteristics of the controller.

A detailed description of controller operation is beyond the scope of this manuscript; if necessary, sufficient operational detail may be deduced from Figure (2-A).

---

* R7 081A,C VERSA-TRAN Transistorized Amplifier Relay, Minneapolis-Honeywell Regulator Company, Toronto 17, Ontario.

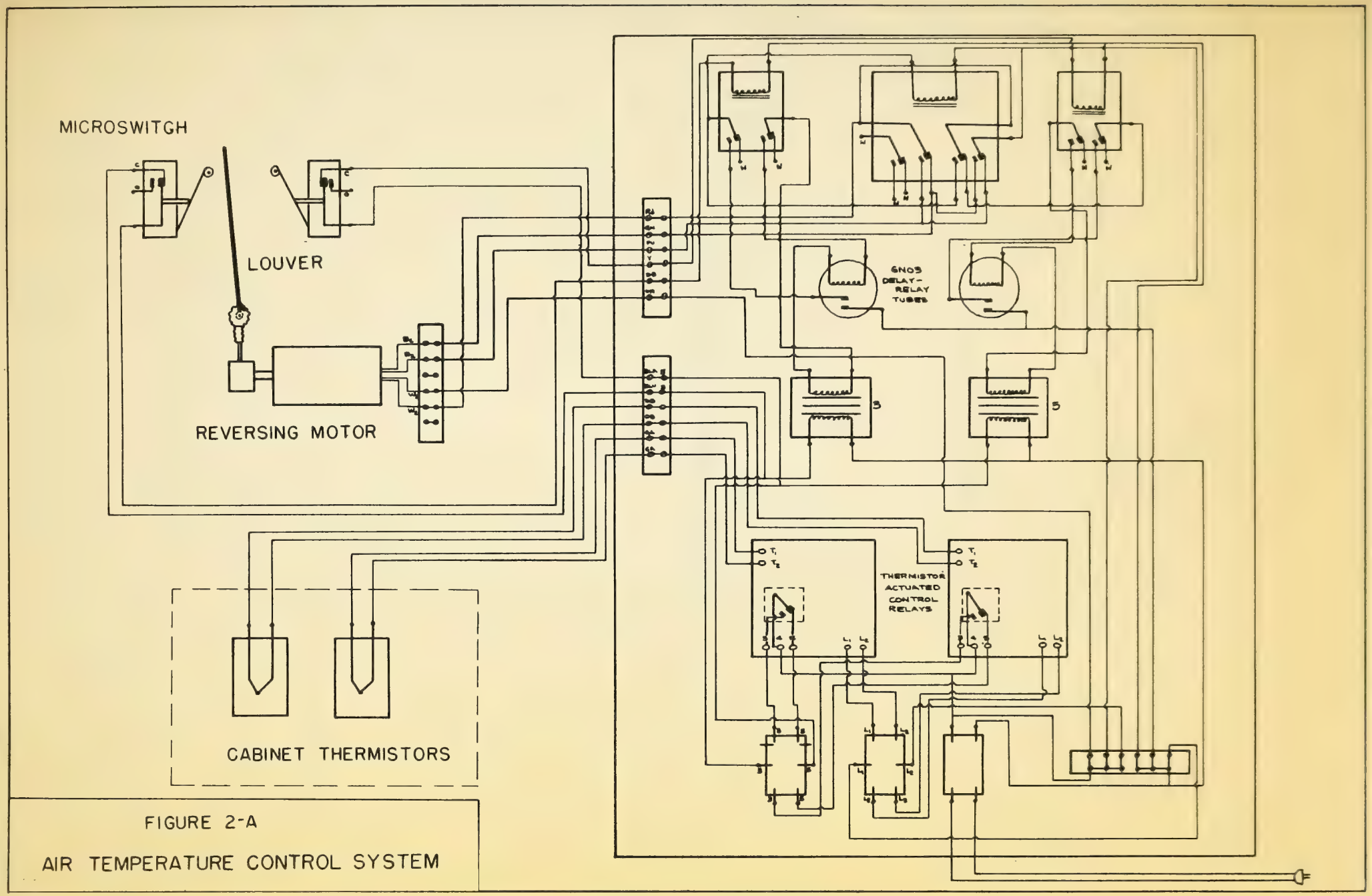


FIGURE 2-A

AIR TEMPERATURE CONTROL SYSTEM

# APPENDIX THREE

## EXPERIMENTAL EQUIPMENT CALIBRATIONS

Torsion Wires

The action of a tangential force, such as shear stress on the bob wall of a rotational viscometer, causes the bob to rotate which in turn produces an opposing torque in the suspension wire. Provided the wire is not deformed beyond its elastic limit, the deflection of the bob (D) is directly proportional to the applied shear stress, $\tau$. This relationship may be represented by:

$$\tau = aD$$

where the constant "a" is a function of the properties and diameter of the wire and the geometry of the system. Thus calibration of the torsion wires involves the evaluation of "a" and may be accomplished by either of two methods.

The first procedure requires measurement of the shear modulus of the wire which is then related to the constant "a" through the dimensions of the wire. Normally the shear modulus of the wire is obtained by means of a torsion pendulum(1). A second and more common method is by measuring the deflection of the bob when a Newtonian fluid of known viscosity is sheared at several predetermined speeds. Although both methods give essentially identical results, only the latter method was used in this investigation. In explanation, this procedure was deemed sufficient since the experimental program only required re-use of torsion wires which had previously(1) been rigorously calibrated.

The calibration equation used to determine "a" was:

$$a = \frac{4Nr_2^2\mu\pi}{(r_2^2 - r_1^2)g_c D}$$

where: $\mu$ = viscosity of oil, $lb_m/ft\text{-}sec$

$N$ = cup rotational speed, RPS

$r_1$ = radius of bob, ft.

$r_2$ = cup radius, ft.

$g_c$ = gravitational conversion factor, $lb_m\text{-}ft/lb_F\text{-}sec^2$

$D$ = bob or torsion wire deflection, degrees

Each wire was calibrated with three different standard oils over a wide range of shear rates and bob deflections using a maximum equivalent bob immersion depth of 4.225 inches. Generally no difficulties were encountered, except for calibration of the No. 28 wire with the 4.58 CP oil, during which bob oscillation was so severe that only a tentative calibration constant was obtained.

It may be noted by inspection of TABLE (3-A) that maximum individual deviation between any two calibration runs was 2.9 percent which is comparable to results reported by previous investigators(1).

Bob Thermocouples

The calibration curve(1) of the bob thermocouples was checked using a standard thermometer. There was essentially no detectable difference between the temperature as measured by either device over the temperature range investigated ($32^{\circ}F$ to $70^{\circ}F$). Consequently, no temperature correction was applied to any experimental results.

TABLE 3-A

TORSION WIRE CALIBRATIONS

| Standard Oil (centipoises) | Wire Number No. 24 | No. 26 | No. 28 |
|---|---|---|---|
| 4.508 | | | $(1.80 \times 10^{-4})$* |
| 19.14 | | $6.12 \times 10^{-4}$ | $1.87 \times 10^{-4}$ |
| 56.37 | $14.25 \times 10^{-4}$ | $6.26 \times 10^{-4}$ | $1.92 \times 10^{-4}$ |
| 93.67 | $14.23 \times 10^{-4}$ | $6.22 \times 10^{-4}$ | |
| 147.8 | $14.31 \times 10^{-4}$ | | |
| % Max Ind. Deviation | 0.6% | 2.2% | 2.9% |
| Average Wire Constant | $14.26 \times 10^{-4}$ | $6.20 \times 10^{-4}$ | $1.89 \times 10^{-4}$ |
| % Max Dev. From Average | 0.4% | 1.3% | 1.6% |
| Pendulum(1) | $13.7 \times 10^{-4}$ | $6.05 \times 10^{-4}$ | $1.86 \times 10^{-4}$ |
| Oil(2) | --- | $6.18 \times 10^{-4}$ | --- |
| % Deviation (Pendulum) | 3.9% | 2.4% | 1.6% |
| % Deviation (Oil) | --- | 0.3% | --- |

* Run ommitted from average due to calibration difficulties
(1) As obtained by Ritter (1) by torsion pendulum
(2) As obtained by Ritter (1) using standard oils

Cabinet Temperature Control System

The cabinet temperature control system, once set by calibration with a standard thermometer, did not display any noticeable drift. However, to ensure detection of any drift, a calibrated thermometer ($\pm 0.1^{\circ}F$) was permanently installed in the cabinet adjacent to the control thermistor. This arrangement provided an instantaneous visual check of cabinet temperature.

Aminco Bath Temperature Control System

The Aminco temperature control bath is provided with a mercury-relay control system which, in conjunction with an extremely sensitive ($\pm 0.05^{\circ}F$) bimetallic strip temperature sensing device, provides excellent control of the viscometer cup temperature. However, each time the bath temperature is intentionally changed, the bimetallic thermostat must be readjusted to the set-point temperature by a trial and error method. This procedure requires that an accurate mercury filled thermometer, or similar device, be used to measure instantaneous bath temperatures. An ASTM calibrated ($0^{\circ}$ to $120^{\circ}F$) thermometer was used for this purpose.

Stopwatch

A selected stopwatch with a reproducibility and calibrated accuracy of $\pm 0.2$ percent was used for all experimental runs. No correction was applied to any time measurements.

Voltmeter - Cup Speed Calibration

As has previously been described, the rotating viscometer cup is

gear connected to a small D.C. generator whose output is visually displayed on a digital voltmeter. This set-up performed admirably, providing an accurate representation of instantaneous cup velocity. The transient voltage stabilizer was not adjusted during the experimental program, so that the calibration curve shown in Figure (3-A) was representative of cup velocity at all times during the experimental program. As may be noted, the calibration curve was checked several times during the experimental program, but no essential deviation from the initial calibration was measured.

The calibration procedure involved setting the cup speed to an arbitrary control setting via the external Graham drive dial mechanism, recording the resultant stabilized voltage, and measuring the total number of cup revolutions over a specified time period with a mechanical-electrical counter. This procedure was repeated at various cup speeds until sufficient points were obtained to define a calibration curve.

FIGURE 3-A

Calibration Curve of Cup Speed
versus
Digital Voltmeter Output

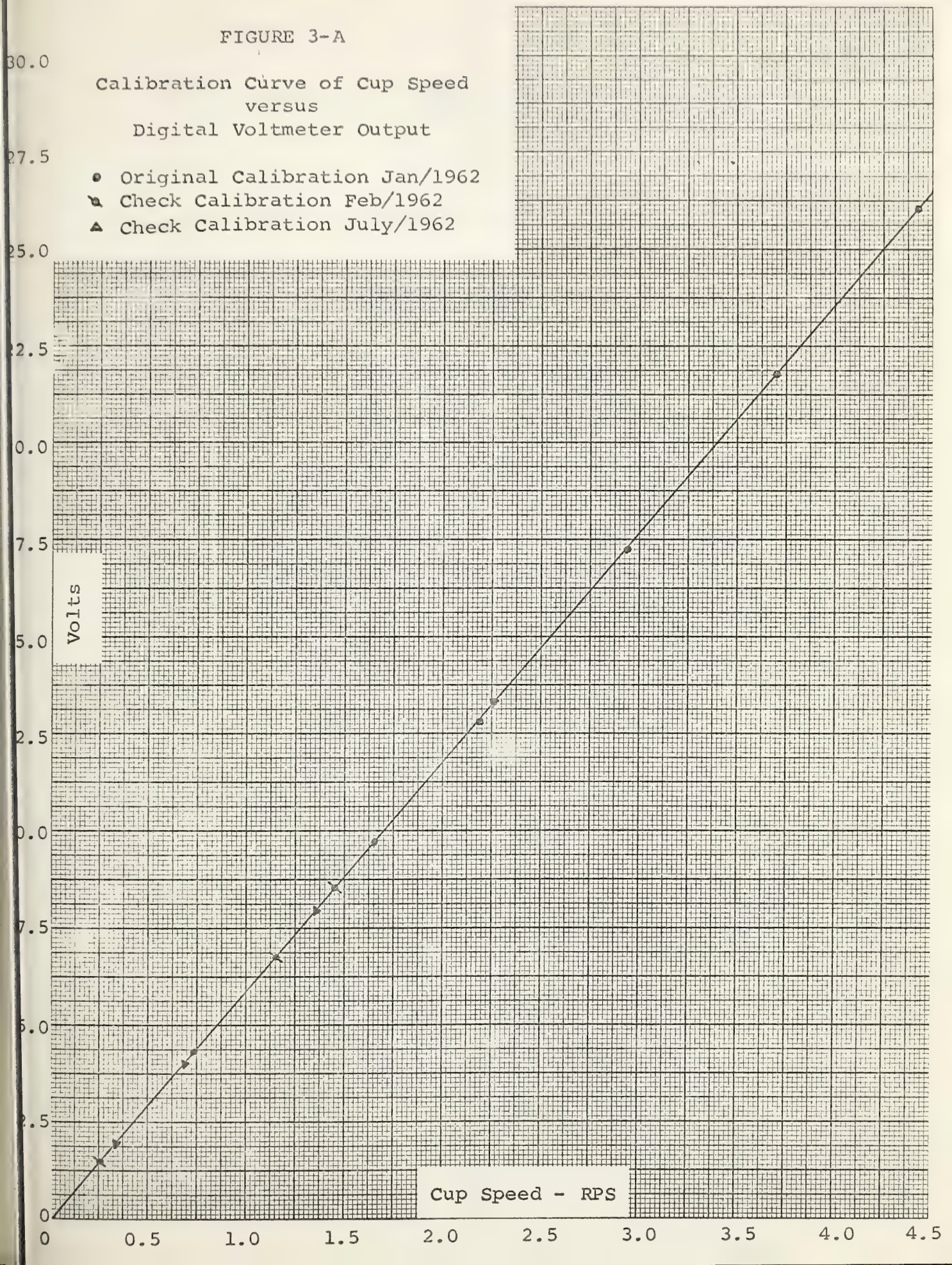

# APPENDIX FOUR

## SAMPLE HEATING EFFECTS DURING SHEAR

## Evaluation of the Temperature Gradient in a Fluid Sheared in a Rotational Viscometer

Evaluation of the steady-state sheared fluid temperature gradient is essentially equivalent to solving the energy equation in terms of the transport properties of the sheared fluid. For the coaxial case, this equation in cylindrical co-ordinates is:

$$\mu \left[ r \frac{d}{dr} \left( \frac{v}{r} \right) \right]^2 + \frac{k}{r} \frac{d}{dr} \left( r \frac{dT}{dr} \right) = 0 \qquad (1)$$

where: $\mu$ = fluid viscosity

$v$ = velocity of sheared fluid

$k$ = thermal conductivity of sheared fluid

Assuming the effect of temperature on the fluid physical properties $\mu$, $\rho$, and $C_p$ has negligible influence on the velocity profile, the velocity distribution across the annulus may be written as:*

$$v = \frac{w \left( r - \frac{K^2 r_2^2}{r} \right)}{(1 - K^2)} \qquad (2)$$

where $w$ = angular velocity of cup

$K = r_1/r_2$

Substituting (2) into (1) and performing the required differentiation, the following is obtained:

$$\frac{k}{r} \frac{d}{dr} \left( r \frac{dT}{dr} \right) + \frac{4w^2 \mu K^4 r_2^4}{(1 - K^2)^2 r^4} = 0 \qquad (3)$$

which upon substitution of the following dimensionless quantities:

---

* Bird, R.B., Stewart, W.E., and Lightfoot, E.N., "Transport Phenomena" John Wiley and Sons Inc., New York, (1960), 325.

$$E = \frac{r}{r_2} \qquad \Theta = \frac{T - T_K}{T_c - T_K}$$

$$\bar{N} = \frac{\mu r_2^2 w^2 K^4}{(T_c - T_K)(1 - K^2)^2 k} = B_r \frac{K^4}{(1 - K^2)^2}$$

where: $T_c$ = temperature of cup wall

$B_r$ = Brinkman number

becomes:

$$\frac{1}{E} \frac{d}{dE}\left(E \frac{d\Theta}{dE}\right) = -4\bar{N} \frac{1}{E^4} \qquad (4)$$

This then is the dimensionless differential equation describing the temperature profile in the sheared fluid across the annulus.

The solution of this equation differs from the solution by Bird et al, since the boundary conditions for the present experimental set-up may be approximated as:

$$\frac{d\Theta}{dE} = 0 \qquad \text{at } E = K \qquad (B.C.1)$$

$$E = 1 \qquad \text{at } \Theta = 1 \qquad (B.C.2)$$

Directly integrating (4):

$$E \frac{d\Theta}{dE} = \frac{2\bar{N}}{E^2} + C_1 \qquad (5)$$

which upon application of B.C.1, reduces to:

$$E \frac{d\Theta}{dE} = \frac{2\bar{N}}{E^2} - \frac{2\bar{N}}{K^2} \qquad (6)$$

Integrating (6):

$$\Theta = \frac{-\bar{N}}{E^2} - \frac{2\bar{N}}{K^2} \ln(E) + C_2 \qquad (7)$$

which upon application of B.C.2 yields:

$$\Theta = \frac{-\bar{N}}{E^2} - \frac{2\bar{N}}{K^2} \ln(E) + N + 1 \qquad (8)$$

Equation (8) is an expression for the temperature profile across the annulus. Since the maximum temperature in the annulus is of interest, Equation (8) may be simplified and expressed so as to permit evaluation of that temperature. Hence:

$$(Br)^{-1} = \left(\frac{1}{K^2} + \frac{2}{K^2} \ln K - 1\right) \frac{K^4}{(1 - K^2)^2} \qquad (9)$$

Evaluating the constants in the above equation in terms of the geometrical factors of the viscometer:

$$K = 0.900 \quad \frac{K^4}{(1 - K^2)^2} = 18.20$$

$$Br = \frac{\mu w_2 r_2^2}{k(T_c - T_K)} = (5.38 \times 10^{-3}) \frac{\mu w^2}{k(T_c - T_K)}$$

Substituting these values into (9), and simplifying:

$$T_K = T_c + \left(\frac{\mu w^2}{k}\right)(1.96 \times 10^{-3}) \qquad (10)$$

The above equation requires an estimation of the value of $T_c$ for the temperature control arrangement in the Alberta viscometer. A schematic diagram of the viscometer sample temperature control arrangement is given below:

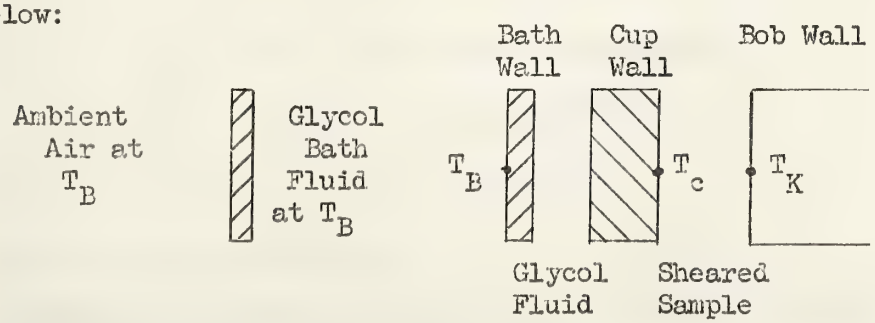

For all practical purposes, the above may be considered as one-dimensional heat transfer. Then:

Heat generated in sheared fluid $= \tau \left(\frac{dv}{dr}\right) = \mu\left(\frac{dv}{dr}\right)^2$ and

$$\mu\left(\frac{dv}{dr}\right)^2 = \frac{(T_B - T_C)A}{\frac{1}{h_{GF}} + \frac{CW}{k_S} + \frac{GB}{k_C}}$$

where: $\Delta CW$, $\Delta GB$ = the respective thicknesses of the cup and glycol bath walls

$k_S$, $k_C$ = the thermal conductivities of steel and copper, respectively

$h_{GF}$ = the heat transfer coefficient through the glycol film when the cup is rotating

$(dv/dr)$ = the shear rate of the sheared fluid

$A$ = the available heat transfer area

Further, the glycol transfer coefficient may be approximated as*:

$$h_{GF} = 7.60 \left(\frac{D_e}{k}\right)$$

Consider then a fluid with the following properties being sheared in the viscometer:

$$\mu = 7.85 \times 10^{-2} \text{ lb}_m\text{ft}^{-1}\text{sec}^{-1}$$

$$k = 8.2 \times 10^{-3} \text{ BTU hr}^{-1}\text{ft}^{-1}\,^{o}\text{F}^{-1}$$

and at the shear and heat transfer conditions of:

$$N = 4.50 \text{ RPS}$$

$$w = 28.0 \text{ radions/sec}$$

$$(dv/dr) = 300 \text{ sec}^{-1}$$

$$A = 0.200 \text{ ft}^2$$

---

* Knudsen, J.G. and Katz, D.L.: "Fluid Dynamics and Heat Transfer"; McGraw-Hill, New York (1958) p. 384.

Then if $T_B = 60.0^{\circ}F$:

$$T_K = 60.0 + \left(\frac{\mu w^2}{k}\right)(1.96 \times 10^{-3})$$

$$+ \mu\left(\frac{dv}{dr}\right)^2 \left(\frac{1}{h_{GF}} + \frac{CW}{k_S} + \frac{GB}{k_C}\right) \frac{1}{A}$$

Upon substitution into this expression, and with consideration to conversion to appropriate units, the following temperature was calculated:

$$T_K = 60.25^{\circ}F$$

This temperature represents the maximum temperature in the sheared oil; and thereby, provides an upper bound to the temperature increase within the oil.

Experimental Run

An experimental run was conducted by shearing a 117 cp oil at 4.5 RPS for two hours at $60^{\circ}F$. The bob deflection associated with the test decreased 0.25 percent during the first five minutes of the test and stabilized at a constant value for the remainder of the test period.

The temperature coefficient of the oil may be approximated as:

bob deflection in oil at $70.0^{\circ}F = 164^{\circ}$ at 4.60 RPS

bob deflection in oil at $60.0^{\circ}F = 199^{\circ}$ at 4.60 RPS

Hence, for the range considered, a change in bob deflection of 1 degree is equivalent to an "average" temperature change within the oil of about $0.29^{\circ}F$. Thus, for the total change in bob deflection ($0.5^{\circ}$) noted at $60^{\circ}F$, the equivalent average temperature increase in the oil was about $0.15^{\circ}F$. This value provides an approximate check on the magnitude of the upper temperature bound calculated in the previous section.

# APPENDIX FIVE

## PRELIMINARY TESTING SCHEDULES AND TEST RESULTS INVOLVING TEST SAMPLE REPRODUCTIBILITY

FIGURE 5-A

Preliminary Testing Schedule and Test Results

1000 c.c. 5.25% Parawax-CWO Dissolved at 180°F

Stored at Room Temperature

(A)

Reheat to 180°F;
Quench to 85°F for 15 minutes
Insert in Viscometer and slow cool to 60°F;
Cure at 60°F for one hour;
Test at 0.3 RPS

| Test | Yield Value | $T_1$* |
|---|---|---|
| 1 | $334 \times 10^{-4}$ | $584 \times 10^{-4}$ |
| 2 | $270 \times 10^{-4}$ | $532 \times 10^{-4}$ |
| 3 | $286 \times 10^{-4}$ | $534 \times 10^{-4}$ |
| 4 | $292 \times 10^{-4}$ | $508 \times 10^{-4}$ |

(B)

Reheat to 180°F;
Quench to 85°F and cure at 85°F;
Quench to 70°F in Viscometer;
Slow cool** to 60°F;
Cure at 60°F for one hour;
Test at 0.3 RPS

| Test | Cure Time at 85°F | Yield Value | $T_1$* |
|---|---|---|---|
| 1 | 9 hours | $1240 \times 10^{-4}$ | $885 \times 10^{-4}$ |
| 2 | 13 hours | $1330 \times 10^{-4}$ | $960 \times 10^{-4}$ |
| 3 | 64 hours | $845 \times 10^{-4}$ | $700 \times 10^{-4}$ |

Gross Sample Stored at 180°F

(C)

4 Samples withdrawn at same time;
All quenched to 85°F;
Slow cooled to 60°F in Viscometer;
Cure at 60°F for one hour;
Test at 0.3 RPS

| Test | Cure Time at 85°F | $T_1$* |
|---|---|---|
| 1 | 92 hours | $435 \times 10^{-4}$ |
| 2 | 96 hours | $435 \times 10^{-4}$ |
| 3 | 116 hours | $408 \times 10^{-4}$ |
| 4 | 140 hours | $388 \times 10^{-4}$ |

(D)

Sample withdrawn after 24 hours longer cure at 180°F than Series (C) Samples;
Subsequently treated as in Series (C)

| Test | Cure Time at 85°F | $T_1$* |
|---|---|---|
| 1 | 140 hours | $336 \times 10^{-4}$ |

---

* $T_1$ = measured shear stress after one minute of shear test

** = at about 0.43°F/minute

Discussion of Test Results

The incentives to the tests listed on the previous page were to determine experimental techniques which would permit either (i) re-use of one sample, or (ii) use of different samples on a once-through basis. It was recognized that an unknown"factor" was determining the subsequent rheological behaviour of the samples; the problem was to determine a technique to eliminate dependence upon this "factor".

Series (A) was a repetition of an earlier set of tests with 5.0% Parawax-Diol. This series indicated, as before, that re-use of one sample could not be attained.

Sample series (B) was an attempt to reduce, if possible, the experimental handling technique errors during the slow cooling period. It is interesting to note (i) the relative effect of sample cure time at 85°F (i.e. which indicates that sample degeneration occurs in a gross sample of 85°F) and (ii) the increase in sample shear stress at one minute as compared to sample series (A).

Sample series (C) was an attempt to store the gross sample at a temperature at which sample degeneration with time would be negligible. A comparison of Test (4) of sample series (C) and Test (1) of sample series (D) indicates that sample degeneration occurs at 180°F, albeit fairly slow.

An additional set of tests were conducted for sample storage at 250°F; the results were similar to the comparison between Test (C-4) and Test (D-1).

## Conclusions

The rheological behaviour of a test sample is dependent upon a "factor" which is a function of:

(i) Sample history before treatment - method of sample preparation; length of time for which sample has been stored; storage temperature.

(ii) Sample history during treatment - reheat and curing time and temperatures; cooling rate to test temperature.

# APPENDIX SIX

## CONSIDERATIONS DURING SAMPLE PREPARATION

It was noted that when individual test size samples (about 100 $cm^3$) were prepared and tested in the viscometer, a wide variation existed beteen the measured rheological flow curves. For example, the following shear stresses were measured for five separately prepared and tested samples:

| Sample | Shear Stress (At one minute) |
|---|---|
| A | $405 \times 10^{-4}$ $lb_f/ft^2$ |
| B | $383 \times 10^{-4}$ $lb_f/ft^2$ |
| C | $406 \times 10^{-4}$ $lb_f/ft^2$ |
| D | $423 \times 10^{-4}$ $lb_f/ft^2$ |
| E | $409 \times 10^{-4}$ $lb_f/ft^2$ |

The average correspondence between the above tests is about four percent, but maximum error between any two tests is as high as ten percent; where:

$$\text{error} = 100 \left[ \frac{(\text{shear stress})_i - (\text{shear stress})_j}{(\text{average shear stress})_{i,j}} \right]_{t=1}$$

Two observations on the test results appeared significant: (i) if individual test samples were to be prepared and tested, a considerable number of tests would have to be conducted before an average shear would be within an acceptable average error range; (ii) the average and maximum errors quoted above were considerably greater than experience indicated could be attributed to rheological test techniques. To elaborate on this latter point, the cumulative error was considered as due to four sources:

(1) Obtaining a representative wax sample to be dissolved in the CWO oil;

(2) Handling errors during sample preparation;

(3) Errors during sample handling sequence;

(4) Rheological testing error.

Experience with test samples from a time-continual degenerating gross sample indicated that the probable maximum error due to sources (2), (3) and (4)was only about one-half the measured error. Hence, it appeared the major source of error was due to wax sampling. If this source of error could be reduced, then in all probability, the overall maximum and average errors would be reduced, which in turn would decrease the number of required tests at each specified shear rate.

A probable error reduction technique was to increase the size of the wax sample, thereby requiring the preparation of a homogeneous gross wax-oil mixture from which a test size sample could be selected and tested. Consider then, if two identically sized gross samples were prepared (say A and B) and a test sample $A_i$ taken from A, what is an estimate of the size of A such that the flow curves of $A_i$ and $B_i$ would not differ by more than three percent? An estimate of the lower bound size of A may be made if it is assumed all error was due to the wax sampling step.

Statistically, it is necessary to determine the number of test size wax samples N such that the homogeneous gross sample mean $\bar{x}$ will not differ from $\mu$, the mean of the "infinite" wax population by more than a specified standard error $|\delta|$. Assuming random sampling of an infinite wax population, then the distribution of m, the mean of a random sample may be stated* as:

---

* Kenny and Keeping: Mathematics of Statistics; Part Two, Third Edition, D. Van Nostrand Company, Inc., Toronto (1954).

$$t = \frac{(\bar{x} - \mu)\ N}{\sigma} \qquad (1)$$

where: $t$ = the normally distributed statistic;

$\sigma$ = the standard variance

Hence, considering the previous experimental results, if a standard error $|\delta|$ of 2.0 percent is chosen with a 95.0 percent probability, then from tables:

$$t = 1.96$$

$$(\bar{x} - \mu) = 0.020(405) = 8.1$$

$$\sigma \cong \sqrt{166} = 12.9$$

Hence, substituting these values in Equation (1):

$$N = \left[\frac{(1.96)(12.9)}{8.1}\right]^2 = 10$$

Thus, if wax sampling were the sole source of error, the equivalent of 10 separate wax samples dissolved to yield a homogeneous wax-oil mixture should yield a test sample ($A_i$) having a rheological flow curve within 2 percent of the gross wax sample mean. A test sample ($B_i$) from a second separately prepared and identically sized gross sample would also have a flow curve with 2 percent of gross wax sample mean, and hence, within 4 percent of $A_i$. However, the probable error between $A_i$ and $B_i$ is only $0.6745(4.0)=2.7$ percent.

As a sequel to the above calculations, subsequent testing of samples from two separately prepared wax-oil gross mixtures, each containing the equivalent to 11 test size wax-oil samples, resulted in rheological decay

curves which differed by less than three percent. Hence, despite restrictive simplifications and assumptions, the analysis would appear to indicate a satisfactory lower bound gross sample size.

# TABULATED EXPERIMENTAL RHEOLOGICAL TEST DATA

Viscosity of CWO-Oil

| Temperature (°F) | Viscosity (cp) |
|---|---|
| 120 | 6.21 |
| 110 | 7.26 |
| 100 | 8.60 |
| 90 | 10.00 |
| 80 | 12.25 |
| 70 | 15.25 |
| 60 | 19.1 |
| 50 | 24.2 |
| 40 | 32.2 |
| 30 | 42.0 |

Viscosity of 5.25% Parawax-CWO Oil

| Temperature (°F) | Viscosity (cp) |
|---|---|
| 110 | 7.1 |
| 100 | 8.4 |
| 90 | 9.7 |
| 80 | 11.9 |

## Yield Value Tests

### Sample Quick Quenched From 85°F to 60°F

| Temperature (°F) | Cure Time | Torsion Wire Constant | Bob Deflection To Yield (Degrees) | Shear Stress ($lb_f/ft^2$) |
|---|---|---|---|---|
| 70 | 1 hour | $1.89 \times 10^{-4}$ | 2 | $3.78 \times 10^{-4}$ |
| 65 | 1 hour | $6.20 \times 10^{-4}$ | 30.5 | $1.90 \times 10^{-2}$ |
| 60 | 1 hour | $1.43 \times 10^{-3}$ | 126 | $1.80 \times 10^{-1}$ |
| 50 | 1 hour | $3.65 \times 10^{-3}$ | 267 | $9.75 \times 10^{-1}$ |
| 40 | 1 hour | $1.05 \times 10^{-1}$ | 124 | $13.1 \times 10^{-1}$ |
| 30 | 1 hour | $1.05 \times 10^{-2}$ | 193 | $20.0 \times 10^{-1}$ |

## Incremental Volume Change of CWO-Oil and 5.25% Parawax - CWO Oil Systems As a Function of Temperature

| 5.25% Parawax-CWO | | CWO | |
|---|---|---|---|
| Temperature (°F) | Δ(Volume)* ($cm^3$) | Temperature (°F) | Δ(Volume)* ($cm^3$) |
| 99.0 | 0.00 | 99.0 | 0.000 |
| 93.5 | 0.19 | 92.0 | 0.205 |
| 87.8 | 0.34 | 85.0 | 0.390 |
| 81.7 | 0.52 | 78.1 | 0.580 |
| 77.5 | 0.65 | 70.5 | 0.780 |
| 73.5 | 0.84 | 63.3 | 0.965 |
| 70.0 | 1.00 | 56.0 | 1.150 |
| 68.0 | 1.11 | 50.0 | 1.310 |
| 63.2 | 1.25 | 43.0 | 1.48 |
| 59.2 | 1.40 | | |
| 54.7 | 1.56 | | |
| 50.0 | 1.72 | | |
| 45.0 | 1.87 | | |
| 44.8 | 1.88 | | |

* Reference volume = $100^3$cm at 98°F

THIXOTROPIC DECAY DATA - SLOW COOLED SAMPLES

0.300 RPS

| TIME (min:sec) | RUN NUMBER ONE 0.299 RPS | | TIME (min:sec) | RUN NUMBER TWO 0.300 RPS | |
|---|---|---|---|---|---|
| | Bob Deflection (Degrees) | Shear Stress $x10^4$ ($lb_f/ft^2$) | | Bob Deflection (Degrees) | Shear Stress $x10^4$ ($lb_f/ft^2$) |
| :10 | 99.5(1) | 622 | :10 | 96.5(1) | 603 |
| :15 | 94.5 | 591 | :15 | 91.5 | 572 |
| :20 | 91.2 | 570 | :20 | 88.5 | 553 |
| :25 | 88.4 | 553 | :25 | 86.5 | 541 |
| :30 | 87.0 | 544 | :30 | 85.0 | 531 |
| :40 | 85.0 | 531 | :40 | 82.4 | 515 |
| :50 | 82.3 | 514 | :50 | 80.5 | 503 |
| 1:00 | 80.2 | 501 | 1:00 | 79.5 | 497 |
| 1:15 | 79.2 | 495 | 1:15 | 78.0 | 488 |
| 1:30 | 77.3 | 483 | 1:30 | 76.3 | 477 |
| 1:45 | 76.4 | 478 | 1:45 | 74.7 | 467 |
| 2:00 | 75.4 | 471 | 2:00 | 74.5 | 466 |
| 2:15 | 74.2 | 464 | 2:15 | 74.2 | 464 |
| 2:30 | 73.5 | 459 | 2:30 | 72.5 | 453 |
| 2:45 | 72.3 | 452 | 2:45 | 73.7 | 454 |
| 3:00 | 72.1 | 451 | 3:00 | 72.2 | 451 |
| 3:15 | 71.5 | 447 | 3:15 | 71.0 | 444 |
| 3:30 | 70.9 | 443 | 3:30 | 71.3 | 446 |
| 3:45 | 70.6 | 441 | 3:45 | 70.7 | 442 |
| 4:00 | 70.3 | 439 | 4:00 | 69.5 | 434 |
| 4:15 | 69.9 | 437 | 4:15 | 69.5 | 434 |
| 4:30 | 69.6 | 435 | 4:30 | 70.0 | 438 |
| 4:45 | 69.2 | 433 | 4:45 | 69.0 | 431 |
| 5:00 | 69.0 | 431 | 5:00 | 69.5 | 434 |
| 5:30 | 68.3 | 427 | 5:30 | -- | - |
| 6:00 | 68.1 | 426 | 6:00 | -- | - |
| 6:30 | 67.5 | 422 | 6:30 | -- | - |
| 7:00 | 67.0 | 419 | 7:00 | -- | - |
| 7:30 | 66.8 | 417 | 7:30 | -- | - |
| 8:00 | 66.5 | 416 | 8:00 | 67.0 | 419 |
| 8:30 | 65.9 | 412 | 8:30 | 66.7 | 417 |
| 9:00 | 65.8 | 411 | 9:00 | 66.5 | 416 |
| 9:30 | 65.9 | 412 | 9:30 | -- | - |
| 10:00 | 66.2 | 414 | 10:00 | 66.0 | 413 |
| 10:30 | -- | - | 10:30 | 65.6 | 410 |
| 11:00 | 65.3 | 408 | 11:00 | 65.3 | 408 |
| 11:30 | 64.5 | 403 | 11:30 | 65.2 | 408 |
| 12:00 | 64.5 | 403 | 12:00 | 64.9 | 406 |
| 13:00 | 64.0 | 400 | 13:00 | 64.5 | 403 |
| 14:00 | 63.5 | 397 | 14:00 | 64.3 | 402 |
| 15:00 | 63.5 | 397 | 15:00 | 64.2 | 402 |
| 16:00 | 63.1 | 394 | 16:00 | 63.9 | 399 |

0.300 RPS - (Continued)

| | | | | | |
|---|---|---|---|---|---|
| 17:00 | 63.0 | 394 | 17:00 | 63.7 | 398 |
| 18:00 | 62.6 | 391 | 18:00 | 63.4 | 396 |
| 19:00 | 62.3 | 389 | 19:00 | 63.0 | 394 |
| 20:00 | 61.8 | 386 | 20:00 | 62.8 | 393 |
| 21:00 | 61.8 | 386 | 21:00 | 62.3 | 389 |
| 22:00 | 61.6 | 385 | 22:00 | 62.0 | 388 |
| 23:00 | 61.3 | 383 | 23:00 | 61.8 | 386 |
| 24:00 | 61.3 | 383 | 24:00 | 61.6 | 385 |
| 25:00 | 61.0 | 381 | 25:00 | 61.5 | 384 |
| 26:00 | 60.8 | 380 | 26:00 | 62.0 | 388 |
| 27:00 | 60.5 | 378 | 27:00 | 62.0 | 388 |
| 28:00 | 60.3 | 377 | 28:00 | 61.5 | 384 |
| 29:00 | 60.0 | 375 | 29:00 | 61.2 | 382 |
| 30:00 | 59.9 | 374 | 30:00 | 61.5 | 384 |
| 32:00 | 59.6 | 373 | 31:00 | 61.2 | 383 |
| 34:00 | 59.0 | 369 | 32:00 | 60.8 | 380 |
| 36:00 | 58.9 | 368 | 35:00 | 60.2 | 376 |
| 38:00 | 58.5 | 366 | 38:00 | 59.7 | 373 |
| 45:00 | 58.0 | 363 | 41:00 | 59.5 | 372 |
| 50:00 | 57.8 | 361 | 44:00 | 59.0 | 370 |
| 55:00 | 57.4 | 459 | 48:00 | 58.7 | 367 |
| 60:00 | 57.1 | 357 | 50:00 | 58.5 | 366 |
| 65:00 | 56.8 | 355 | 55:00 | 58.3 | 364 |
| 71:00 | 56.4 | 353 | 60:00 | 58.0 | 363 |
| 75:00 | 56.0 | 350 | 65:00 | 57.4 | 359 |
| 80:00 | 55.7 | 348 | 70:00 | 57.5 | 359 |
| 87:00 | 55.4 | 346 | 75:00 | 57.0 | 356 |
| 92:00 | 55.1 | 344 | 80:00 | 57.0 | 356 |
| 97:00 | 54.9 | 343 | 85:00 | 56.9 | 356 |
| 104:00 | 54.2 | 338 | 90:00 | 56.8 | 355 |
| 127:00 | 53.1 | 332 | | | |
| 135:00 | 53.2 | 333 | | | |
| 145:00 | 53.0 | 331 | | | |
| 155:00 | 52.5 | 328 | | | |
| 172:00 | 52.2 | 326 | | | |
| 183:00 | 52.0 | 325 | | | |
| 195:00 | 51.4 | 321 | | | |
| 210:00 | -- | - | | | |
| 227:00 | 50.7 | 317 | | | |
| 234:00 | 50.8 | 318 | | | |
| 246:00 | 50.8 | 318 | | | |

(1) No. 26 torsion wire

THIXOTROPIC DECAY DATA - SLOW COOLED SAMPLES

0.800 RPS

| TIME (min:sec) | RUN NUMBER ONE 0.798 RPS | | TIME (min:sec) | | |
|---|---|---|---|---|---|
| | Bob Deflection (Degrees) | Shear Stress $x10^4$ ($lb_f/ft^2$) | | Bob Deflection (Degrees) | Shear Stress $x10^4$ ($lb_f/ft^2$) |
| :10 | 180.0(1) | 1116 | 21:00 | 121.0 | 756 |
| :15 | 177.0 | 1097 | 22:00 | 120.4 | 753 |
| :20 | 171.5 | 1063 | 23:00 | 120.3 | 752 |
| :25 | 169.0 | 1048 | 24:00 | 120.2 | 751 |
| :30 | 164.5 | 1020 | 25:00 | 119.8 | 749 |
| :40 | 159.8 | 991 | 26:00 | 119.7 | 748 |
| :50 | 156.5 | 970 | 27:00 | 119.3 | 746 |
| 1:00 | 154.0 | 955 | 28:00 | 118.8 | 743 |
| 1:15 | 151.0 | 936 | 29:00 | 118.3 | 739 |
| 1:30 | 148.5 | 921 | 31:00 | 118.1 | 738 |
| 1:45 | 146.2 | 906 | 32:00 | 118.2 | 739 |
| 2:00 | 144.2 | 894 | 34:00 | 117.8 | 731 |
| 2:15 | 143.2 | 888 | 36:00 | 116.8 | 730 |
| 2:30 | 141.5 | 884 | 38:00 | 116.6 | 729 |
| 2:45 | 140.5 | 878 | 40:00 | 116.3 | 727 |
| 3:00 | 140.0 | 875 | 42:00 | 115.9 | 724 |
| 3:15 | 138.8 | 868 | 45:00 | 115.3 | 721 |
| 3:30 | 138.2 | 864 | 46:00 | 115.1 | 719 |
| 3:45 | 137.0 | 856 | 48:00 | 114.6 | 716 |
| 4:00 | 136.2 | 851 | 50:00 | 114.3 | 714 |
| 4:15 | 135.8 | 849 | 55:00 | 113.7 | 711 |
| 4:30 | 134.7 | 843 | 60:00 | 112.8 | 705 |
| 4:45 | 134.1 | 838 | 65:00 | 112.1 | 701 |
| 5:00 | 133.7 | 836 | 70:00 | 111.5 | 697 |
| 5:30 | 133.1 | 832 | 75:00 | 111.1 | 694 |
| 6:00 | 132.0 | 825 | 80:00 | 110.9 | 693 |
| 6:30 | 130.6 | 816 | 87:00 | 110.3 | 689 |
| 7:00 | 130.1 | 813 | 91:00 | 109.8 | 686 |
| 7:30 | 129.7 | 811 | 95:00 | 109.5 | 684 |
| 8:00 | 128.9 | 806 | 101:00 | 108.7 | 679 |
| 8:30 | 128.3 | 802 | 110:00 | 107.9 | 674 |
| 9:00 | 127.7 | 797 | 120:00 | 107.7 | 673 |
| 9:30 | 127.1 | 794 | 132:00 | 107.0 | 669 |
| 10:00 | 126.9 | 793 | 140:00 | 106.3 | 665 |
| 10:30 | 126.7 | 792 | 150:00 | 105.8 | 661 |
| 11:00 | 126.1 | 789 | 160:00 | 105.3 | 658 |
| 11:30 | 125.8 | 786 | 170:00 | 105.1 | 657 |
| 12:00 | 125.4 | 784 | 180:00 | 104.7 | 654 |
| 13:00 | 124.9 | 781 | 190:00 | 104.2 | 651 |
| 14:00 | 124.3 | 777 | 200:00 | 103.7 | 648 |
| 15:00 | 123.7 | 773 | 210:00 | 103.5 | 647 |
| 16:00 | 123.2 | 770 | 223:00 | 103.0 | 644 |
| 17:00 | 122.7 | 767 | 234:00 | 102.5 | 641 |
| 18:00 | 122.3 | 764 | 240:00 | 102.3 | 639 |
| 19:00 | 122.0 | 763 | 250:00 | 102.1 | 638 |
| 20:00 | 121.4 | 759 | 260:00 | 101.7 | 636 |

(1) No.26 torsion wire

THIXOTROPIC DECAY DATA - SLOW COOLED SAMPLES

2.0 RPS

| TIME (min:sec) | RUN NUMBER ONE 1.99 RPS | | TIME (min:sec) | RUN NUMBER TWO 2.00 RPS | |
|---|---|---|---|---|---|
| | Bob Deflection (Degrees) | Shear Stress $x10^4$ ($lb_f/ft^2$) | | Bob Deflection (Degrees) | Shear Stress $x10^4$ ($lb_f/ft^2$) |
| :10 | 148.6(1) | 2119 | :10 | 140.5(1) | 2004 |
| :15 | 141.6 | 2019 | :15 | 137.0 | 1954 |
| :20 | 138.6 | 1976 | :20 | 133.5 | 1904 |
| :25 | 135.1 | 1927 | :25 | 131.4 | 1874 |
| :30 | 132.6 | 1891 | :30 | 129.1 | 1841 |
| :40 | 128.6 | 1834 | :40 | 125.8 | 1794 |
| :50 | 125.8 | 1794 | :50 | 123.6 | 1763 |
| 1:00 | 123.8 | 1765 | 1:00 | 121.7 | 1735 |
| 1:15 | 121.4 | 1731 | 1:15 | 119.7 | 1707 |
| 1:30 | 118.8 | 1694 | 1:30 | 118.3 | 1687 |
| 1:45 | 117.5 | 1675 | 1:45 | 117.2 | 1671 |
| 2:00 | 115.9 | 1653 | 2:00 | 115.9 | 1653 |
| 2:15 | 115.1 | 1641 | 2:15 | 114.7 | 1636 |
| 2:30 | 114.4 | 1631 | 2:30 | 114.2 | 1629 |
| 2:45 | 113.6 | 1620 | 2:45 | 113.4 | 1617 |
| 3:00 | 112.7 | 1607 | 3:00 | 112.5 | 1604 |
| 3:15 | 112.0 | 1597 | 3:15 | 111.7 | 1593 |
| 3:30 | 110.9 | 1582 | 3:30 | 111.1 | 1584 |
| 3:45 | 110.5 | 1576 | 3:45 | 110.6 | 1577 |
| 4:00 | 110.0 | 1569 | 4:00 | 109.7 | 1564 |
| 4:15 | 109.0 | 1554 | 4:15 | 109.4 | 1560 |
| 4:30 | 108.4 | 1545 | 4:30 | 108.7 | 1550 |
| 4:45 | 107.7 | 1535 | 4:45 | 108.2 | 1543 |
| 5:00 | 107.2 | 1528 | 5:00 | 107.9 | 1539 |
| 5:30 | 106.5 | 1518 | 5:30 | 107.2 | 1529 |
| 6:00 | 105.9 | 1510 | 6:00 | 106.5 | 1519 |
| 6:30 | 105.1 | 1499 | 6:30 | 105.9 | 1510 |
| 7:00 | 104.5 | 1490 | 7:00 | 105.4 | 1503 |
| 7:30 | 103.7 | 1479 | 7:30 | 105.0 | 1497 |
| 8:00 | --- | -- | 8:00 | 104.3 | 1487 |
| 8:30 | 102.8 | 1466 | 8:30 | 104.0 | 1483 |
| 9:00 | 102.4 | 1460 | 9:00 | 103.7 | 1479 |
| 9:30 | 101.8 | 1454 | 9:30 | 103.3 | 1473 |
| 10:00 | 101.6 | 1451 | 10:00 | 103.0 | 1469 |
| 10:30 | 101.3 | 1447 | 10:30 | 102.7 | 1465 |
| 11:00 | 101.0 | 1445 | 11:00 | 102.3 | 1459 |
| 11:30 | 100.7 | 1441 | 12:00 | 101.9 | 1453 |
| 12:00 | 100.4 | 1438 | 13:00 | 101.5 | 1446 |
| 13:00 | 100.0 | 1425 | 14:00 | 100.9 | 1437 |
| 14:00 | --- | -- | 15:00 | 100.8 | 1436 |
| 15:00 | 99.0 | 1411 | 16:00 | 100.4 | 1432 |

2.0 RPS - (Continued)

| | | | | | |
|---|---|---|---|---|---|
| 16:00 | 98.4 | 1403 | 17:00 | 100.0 | 1426 |
| 17:00 | 98.1 | 1399 | 18:00 | 99.6 | 1420 |
| 18:00 | 97.7 | 1393 | 19:00 | 99.2 | 1414 |
| 19:00 | 97.1 | 1385 | 20:00 | 98.0 | 1410 |
| 20:00 | 96.6 | 1378 | 21:00 | 98.6 | 1406 |
| 21:00 | 96.3 | 1374 | 22:00 | 98.3 | 1402 |
| 22:00 | 96.0 | 1370 | 23:00 | 98.1 | 1399 |
| 23:00 | 95.7 | 1366 | 24:00 | 97.8 | 1395 |
| 24:00 | 95.5 | 1363 | 25:00 | 97.5 | 1391 |
| 25:00 | 95.2 | 1358 | 26:00 | 97.3 | 1387 |
| 26:00 | 94.8 | 1352 | 30:00 | 96.2 | 1386 |
| 27:00 | 94.5 | 1348 | 33:00 | 95.5 | 1376 |
| 28:00 | 94.3 | 1345 | 36:00 | 94.9 | 1367 |
| 29:00 | 94.0 | 1341 | 39:00 | 94.2 | 1357 |
| 30:00 | 93.7 | 1336 | 45:00 | 93.3 | 1344 |
| 31:00 | 93.6 | 1335 | 53:00 | 91.9 | 1310 |
| 32:00 | 93.6 | 1335 | 55:00 | 91.8 | 1309 |
| 33:00 | 93.4 | 1332 | 62:00 | 91.2 | 1300 |
| 34:00 | 93.3 | 1331 | 70:00 | 90.4 | 1289 |
| 35:00 | 93.2 | 1329 | 75:00 | 90.2 | 1286 |
| 36:00 | 93.0 | 1326 | 82:00 | 89.5 | 1276 |
| 37:00 | 92.8 | 1323 | 92:00 | 88.9 | 1267 |
| 39:00 | 92.2 | 1315 | 105:00 | 88.6 | 1263 |
| 41:00 | 91.7 | 1308 | 120:00 | 88.2 | 1257 |
| 43:00 | 91.3 | 1302 | 141:00 | 87.5 | 1248 |
| 45:00 | 91.1 | 1299 | 180:00 | 86.2 | 1229 |
| 49:00 | 90.6 | 1292 | | | |
| 50:00 | 90.4 | 1289 | | | |
| 55:00 | 89.7 | 1279 | | | |
| 60:00 | 89.3 | 1273 | | | |
| 65:00 | 89.2 | 1271 | | | |
| 70:00 | 88.7 | 1264 | | | |
| 74:00 | 88.5 | 1262 | | | |
| 75:00 | 88.4 | 1261 | | | |
| 80:00 | 88.0 | 1256 | | | |
| 87:00 | 87.6 | 1250 | | | |
| 92:00 | 87.3 | 1246 | | | |
| 97:00 | 87.0 | 1243 | | | |
| 102:00 | 86.7 | 1236 | | | |
| 108:00 | 86.4 | 1232 | | | |
| 116:00 | 86.0 | 1226 | | | |
| 125:00 | 85.7 | 1222 | | | |
| 132:00 | 85.4 | 1218 | | | |
| 146:00 | 84.9 | 1211 | | | |
| 165:00 | 84.6 | 1207 | | | |
| 179:00 | 84.2 | 1201 | | | |
| 190:00 | 83.9 | 1197 | | | |
| 217:00 | 83.6 | 1193 | | | |
| 222:00 | 83.4 | 1189 | | | |
| 246:00 | 83.1 | 1185 | | | |

(1) No. 24 torsion wire

THIXOTROPIC DECAY DATA - SLOW COOLED SAMPLES

4.5 RPS

| TIME (min:sec) | RUN NUMBER ONE 4.50 RPS | | TIME (min:sec) | RUN NUMBER TWO 4.50 RPS | |
|---|---|---|---|---|---|
| | Bob Deflection | Shear Stress $x10^4$ ($lb_f/ft^2$) | | Bob Deflection | Shear Stress $x10^4$ ($lb_f/ft^2$) |
| :10 | 95.0(1) | 3468 | :10 | 96.7(1) | 3530 |
| :15 | 91.5 | 3340 | :15 | 93.7 | 3420 |
| :20 | 89.2 | 3256 | :20 | 91.7 | 3347 |
| :25 | 87.9 | 3208 | :25 | 90.0 | 3285 |
| :30 | 86.8 | 3168 | :30 | 88.7 | 3238 |
| :40 | 84.5 | 3084 | :40 | 86.7 | 3165 |
| :50 | 83.1 | 3033 | :50 | 85.1 | 3106 |
| 1:00 | 81.8 | 2986 | 1:00 | 83.7 | 3055 |
| 1:15 | 80.5 | 2038 | 1:15 | 82.3 | 3004 |
| 1:30 | 79.2 | 2891 | 1:30 | 81.2 | 2964 |
| 1:45 | 78.5 | 2865 | 1:45 | 80.3 | 2931 |
| 2:00 | 77.8 | 2840 | 2:00 | 79.6 | 2905 |
| 2:15 | 76.9 | 2807 | 2:15 | 78.6 | 2869 |
| 2:30 | 76.3 | 2785 | 2:30 | 78.0 | 2847 |
| 2:45 | 75.8 | 2767 | 2:45 | 77.6 | 2832 |
| 3:00 | 75.2 | 2745 | 3:00 | 77.0 | 2810 |
| 3:15 | 74.7 | 2727 | 3:15 | 76.4 | 2788 |
| 3:30 | 74.2 | 2708 | 3:30 | 76.2 | 2781 |
| 3:45 | 74.0 | 2701 | 3:45 | 75.8 | 2766 |
| 4:00 | 73.8 | 2694 | 4:00 | 75.4 | 2751 |
| 4:15 | 73.7 | 2691 | 4:15 | 74.9 | 2733 |
| 4:30 | 73.2 | 2672 | 4:30 | 74.6 | 2723 |
| 4:45 | 72.8 | 2657 | 4:45 | 74.6 | 2723 |
| 5:00 | 72.6 | 2650 | 5:00 | 74.2 | 2708 |
| 5:30 | 72.3 | 2639 | 5:30 | 73.7 | 2690 |
| 6:00 | 71.8 | 2621 | 6:00 | 73.2 | 2672 |
| 6:30 | 71.4 | 2606 | 6:30 | 73.0 | 2665 |
| 7:00 | 71.1 | 2595 | 7:00 | 72.5 | 2647 |
| 7:30 | 70.8 | 2584 | 7:30 | 72.3 | 2640 |
| 8:00 | 70.5 | 2573 | 8:00 | 71.9 | 2625 |
| 8:30 | 70.2 | 2562 | 8:30 | 71.6 | 2613 |
| 9:00 | 70.0 | 2555 | 9:00 | 71.5 | 2610 |
| 9:30 | 69.8 | 2548 | 9:30 | 71.2 | 2598 |
| 10:00 | 69.5 | 2537 | 10:00 | 71.0 | 2591 |
| 10:30 | 69.3 | 2530 | 10:30 | 70.7 | 2581 |
| 11:00 | 69.2 | 2526 | 11:00 | 70.5 | 2574 |
| 12:00 | 68.7 | 2508 | 12:00 | 70.2 | 2563 |
| 13:00 | 68.4 | 2497 | 13:00 | 69.8 | 2548 |
| 14:00 | 68.1 | 2486 | 14:00 | 69.5 | 2537 |
| 15:00 | 67.9 | 2479 | 15:00 | 69.2 | 2526 |
| 16:00 | 67.6 | 2467 | 16:00 | 68.9 | 2515 |

4.5 RPS - (Continued)

| | | | | | |
|---|---|---|---|---|---|
| 17:00 | 68.7 | 2508 | 17:00 | 68.6 | 2504 |
| 18:00 | 67.0 | 2445 | 18:00 | 68.4 | 2497 |
| 19:00 | 66.8 | 2438 | 19:00 | 68.1 | 2486 |
| 20:00 | 66.6 | 2431 | 20:00 | 67.9 | 2478 |
| 21:00 | 66.4 | 2424 | 21:00 | 67.8 | 2474 |
| 23:00 | 66.0 | 2409 | 22:00 | 67.4 | 2459 |
| 25:00 | 65.7 | 2398 | 23:00 | 67.4 | 2459 |
| 27:00 | 65.4 | 2387 | 24:00 | 67.1 | 2448 |
| 29:00 | 65.2 | 2380 | 25:00 | 66.9 | 2442 |
| 31:00 | 65.0 | 2373 | 26:00 | 66.6 | 2431 |
| 33:00 | 64.7 | 2362 | 27:00 | 66.4 | 2424 |
| 37:00 | 64.2 | 2344 | 28:00 | 66.3 | 2420 |
| 43:00 | 63.5 | 2318 | 29:00 | 66.2 | 2416 |
| 48:00 | 63.2 | 2307 | 30:00 | 65.9 | 2405 |
| 53:00 | 62.9 | 2296 | 33:00 | 65.6 | 2494 |
| 57:00 | 62.7 | 2289 | 36:00 | 65.1 | 2476 |
| 60:00 | 62.4 | 2278 | 39:00 | 64.8 | 2465 |
| 66:00 | 62.2 | 2271 | 42:00 | 64.5 | 2354 |
| 71:00 | 61.9 | 2259 | 45:00 | 64.2 | 2343 |
| 77:00 | 61.6 | 2248 | 50:00 | 63.9 | 2332 |
| 83:00 | 61.1 | 2230 | 55:00 | 63.4 | 2314 |
| 86:00 | 60.9 | 2223 | 60:00 | 63.1 | 2303 |
| 97:00 | 60.4 | 2205 | 65:00 | 62.9 | 2296 |
| 107:00 | 60.4 | 2205 | 70:00 | 62.7 | 2289 |
| 120:00 | 60.1 | 2194 | 75:00 | 62.4 | 2278 |
| 129:00 | 59.9 | 2187 | 80:00 | 62.1 | 2267 |
| 150:00 | 58.9 | 2151 | 85:00 | 62.1 | 2267 |
| 156:00 | 58.9 | 2151 | 91:00 | 62.0 | 2263 |
| 166:00 | 58.8 | 2146 | 95:00 | 61.7 | 2252 |
| 184:00 | 58.6 | 2139 | 100:00 | 61.6 | 2248 |
| 194:00 | 58.5 | 2136 | | | |
| 209:00 | 58.3 | 2129 | | | |
| 220:00 | 58.3 | 2128 | | | |
| 230:00 | 58.2 | 2125 | | | |
| 240:00 | 58.1 | 2121 | | | |

(1) No. 22 torsion wire

SLOW COOLED SAMPLE SHEAR STRESS GROWTH DATA

0.3 RPS

| TIME (min:sec) | PREVIOUS CUP SPEED 0.8 RPS(1) | | TIME (min:sec) | PREVIOUS CUP SPEED 2.0 RPS(2) | |
|---|---|---|---|---|---|
| | Bob Deflection (Degrees) | Shear Stress $x10^4$ ($lb_f/ft^2$) | | Bob Deflection (Degrees) | Shear Stress $x10^4$ ($lb_f/ft^2$) |
| :10 | 38.7(3) | 240 | :10 | 13.4(4) | 191 |
| 1:00 | 38.7 | 240 | 1:00 | 13.4 | 191 |
| 2:00 | 38.7 | 240 | 2:00 | 13.6 | 194 |
| 3:00 | 38.7 | 240 | 3:00 | 13.6 | 194 |
| 4:00 | 39.0 | 242 | 4:00 | 13.6 | 194 |
| 6:00 | 39.2 | 243 | 6:00 | 13.6 | 194 |
| 8:00 | 39.2 | 243 | 9:00 | 13.8 | 197 |
| 11:00 | 39.3 | 244 | 12:00 | 13.9 | 198 |
| 16:00 | 39.6 | 246 | 13:00 | 13.9 | 198 |
| 18:00 | 39.5 | 245 | 15:00 | 13.9 | 198 |
| 21:00 | 39.7 | 246 | 17:00 | 13.9 | 198 |
| 24:00 | 39.7 | 246 | 19:00 | 13.8 | 197 |
| 28:00 | 39.7 | 246 | 24:00 | 13.9 | 198 |
| 36:00 | 39.8 | 247 | 30:00 | 14.0 | 200 |
| 40:00 | 39.9 | 247 | 34:00 | 14.1 | 201 |
| 43:00 | 40.0 | 248 | 41:00 | 14.1 | 201 |
| 46:00 | 40.1 | 249 | 46:00 | 14.1 | 201 |
| 49:00 | 40.5 | 251 | 50:00 | 14.1 | 201 |
| 53:00 | 40.3 | 250 | 57:00 | 14.1 | 201 |
| 56:00 | 40.4 | 250 | 60:00 | 14.2 | 202 |
| 60:00 | 40.4 | 250 | 65:00 | 14.2 | 202 |
| | | | 70:00 | 14.2 | 202 |

(1) After 260 minutes shear at 0.8 RPS
(2) After 250 minutes shear at 2.0 RPS
(3) No. 26 torsion wire
(4) No. 24 torsion wire

SLOW COOLED SAMPLE SHEAR STRESS GROWTH DATA

0.3 RPS

| TIME (min:sec) | PREVIOUS CUP SPEED 4.5 RPS (1) | |
|---|---|---|
| | Bob Deflection (Degrees) | Shear Stress $x10^4$ ($lb_f/ft^2$) |
| :10 | 3.7(2) | 135 |
| 1:00 | 3.7 | 135 |
| 2:00 | 3.7 | 135 |
| 3:00 | 3.7 | 135 |
| 4:00 | 3.7 | 135 |
| 6:00 | 3.8 | 139 |
| 8:00 | 3.9 | 142 |
| 10:00 | 3.9 | 142 |
| 12:00 | 3.9 | 142 |
| 17:00 | 4.0 | 146 |
| 19:00 | 4.0 | 146 |
| 22:00 | 4.0 | 146 |
| 24:00 | 4.0 | 146 |
| 27:00 | 4.0 | 146 |
| 30:00 | 4.0 | 146 |
| 35:00 | 4.0 | 146 |
| 40:00 | 4.0 | 146 |
| 45:00 | 4.1 | 150 |
| 50:00 | 4.1 | 150 |
| 55:00 | 4.1 | 150 |
| 60:00 | 4.1 | 150 |

(1) After 240 minutes shear at 4.5 RPS
(2) No. 22 torsion wire

SLOW COOLED SAMPLE SHEAR STRESS GROWTH DATA

0.8 RPS

| TIME (min:sec) | PREVIOUS CUP SPEED 2.0 RPS[1] | | TIME (min:sec) | PREVIOUS CUP SPEED 4.5 RPS[2] | |
|---|---|---|---|---|---|
| | Bob Deflection (Degrees) | Shear Stress $x10^4$ ($lb_f/ft^2$) | | Bob Deflection (Degrees) | Shear Stress $x10^4$ ($lb_f/ft^2$) |
| :10 | 35.1[3] | 500 | :10 | 10.2[4] | 372 |
| 1:00 | 35.1 | 500 | 1:00 | 10.2 | 372 |
| 2:00 | 35.1 | 500 | 2:00 | 10.2 | 372 |
| 3:00 | 35.2 | 501 | 3:00 | 10.2 | 372 |
| 4:00 | 35.3 | 503 | 4:00 | 10.2 | 372 |
| 5:00 | 35.4 | 504 | 6:00 | 10.2 | 372 |
| 6:00 | 35.4 | 504 | 8:00 | 10.2 | 372 |
| 7:00 | 35.5 | 505 | 10:00 | 10.3 | 376 |
| 8:00 | 35.5 | 505 | 12:00 | 10.3 | 376 |
| 9:00 | 35.5 | 505 | 14:00 | 10.3 | 376 |
| 10:00 | 35.5 | 505 | 16:00 | 10.3 | 376 |
| 12:00 | 35.5 | 505 | 18:00 | 10.3 | 376 |
| 14:00 | 35.6 | 507 | 20:00 | 10.3 | 376 |
| 16:00 | 35.7 | 508 | 25:00 | 10.3 | 376 |
| 18:00 | 35.7 | 508 | 30:00 | 10.4 | 380 |
| 20:00 | 35.8 | 510 | 35:00 | 10.4 | 380 |
| 22:00 | 35.8 | 510 | 40:00 | 10.4 | 380 |
| 24:00 | 35.8 | 510 | 45:00 | 10.4 | 380 |
| 28:00 | 35.9 | 511 | 50:00 | 10.4 | 380 |
| 30:00 | 36.0 | 512 | 55:00 | 10.4 | 380 |
| 32:00 | 36.0 | 512 | 60:00 | 10.4 | 380 |
| 34:00 | 36.0 | 512 | | | |
| 36:00 | 36.0 | 512 | | | |
| 38:00 | 36.1 | 514 | | | |
| 40:00 | 36.1 | 514 | | | |
| 45:00 | 36.1 | 514 | | | |
| 50:00 | 36.1 | 514 | | | |
| 55:00 | 36.2 | 515 | | | |
| 60:00 | 36.1 | 514 | | | |

(1) After 180 minutes shear at 2.0 RPS
(2) After 240 minutes shear at 4.5 RPS
(3) No. 24 torsion wire
(4) No. 22 torsion wire

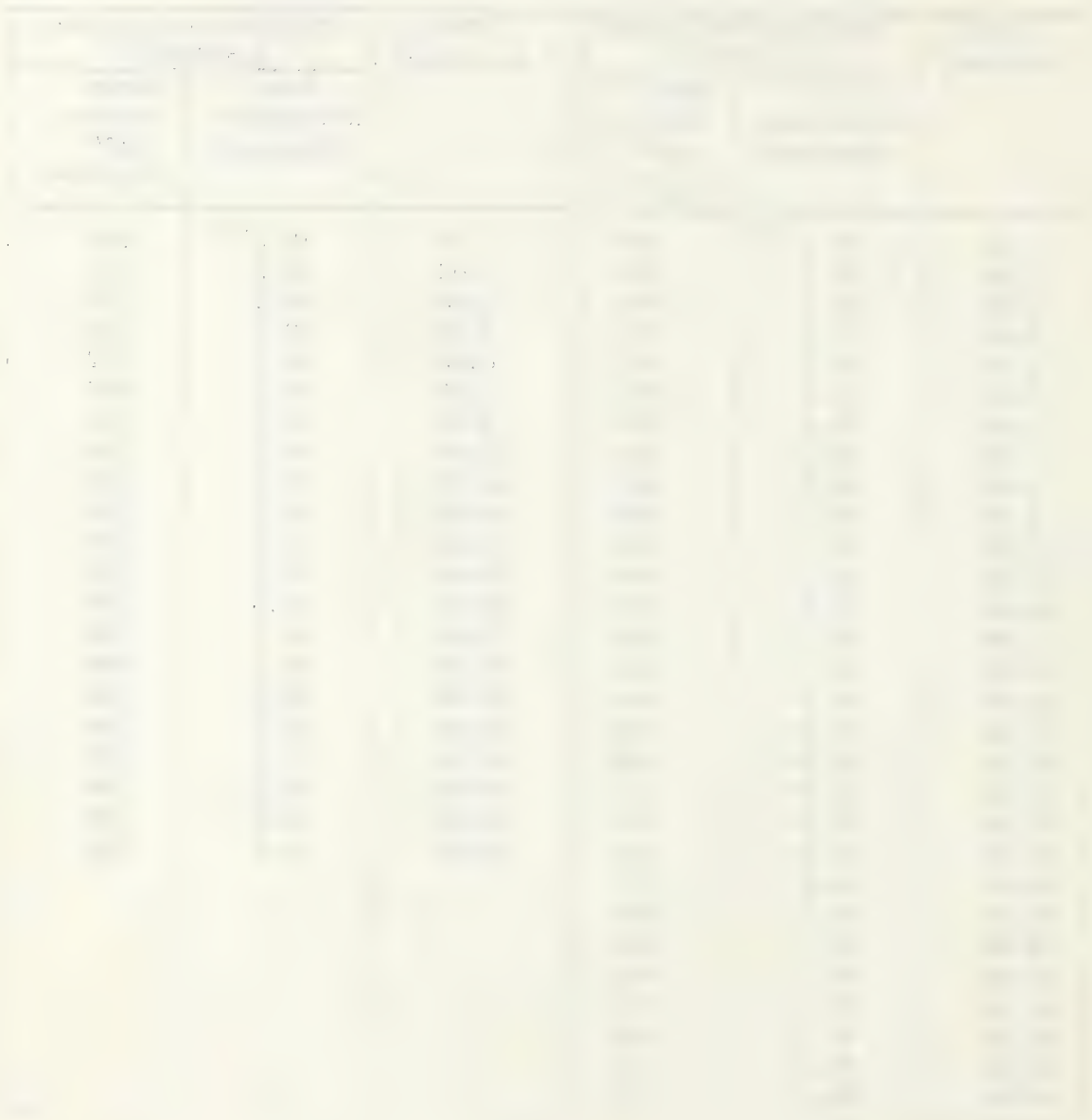

SLOW COOLED SAMPLE SHEAR STRESS GROWTH DATA

2.0 RPS

| TIME (min:sec) | PREVIOUS CUP SPEED 4.5 RPS(1) | |
|---|---|---|
| | Bob Deflection (Degrees) | Shear Stress $x10^4$ ($lb_f/ft^2$) |
| :10 | 24.8(2) | 905 |
| 1:00 | 24.8 | 905 |
| 2:00 | 24.9 | 909 |
| 3:00 | 24.8 | 905 |
| 4:00 | 24.8 | 905 |
| 5:00 | 24.8 | 905 |
| 6:00 | 25.0 | 912 |
| 7:00 | 25.0 | 912 |
| 8:00 | 25.0 | 912 |
| 9:00 | 25.0 | 912 |
| 10:00 | 25.0 | 912 |
| 11:00 | 25.0 | 912 |
| 13:00 | 25.0 | 912 |
| 15:00 | 25.0 | 912 |
| 17:00 | 25.0 | 912 |
| 19:00 | 25.0 | 912 |
| 21:00 | 25.0 | 912 |
| 25:00 | 25.0 | 912 |
| 30:00 | 25.0 | 912 |
| 35:00 | 25.0 | 912 |
| 40:00 | 25.0 | 912 |
| 45:00 | 25.0 | 912 |
| 50:00 | 25.0 | 912 |

(1) After 240 minutes shear at 4.5 RPS
(2) No. 22 torsion wire

THIXOTROPIC DECAY DATA - QUICK QUENCHED SAMPLES

0.3 RPS

| TIME (min:sec) | RUN NUMBER ONE 0.301 RPS | | TIME (min:sec) | RUN NUMBER TWO 0.299 RPS | |
|---|---|---|---|---|---|
| | Bob Deflection (Degrees) | Shear Stress $x10^4$ ($lb_f/ft^2$) | | Bob Deflection (Degrees) | Shear Stress $x10^4$ ($lb_f/ft^2$) |
| :10 | 103.5(1) | 1475 | :10 | -- | -- |
| :15 | 96.0 | 1370 | :15 | 94.0(1) | 1340 |
| :20 | 91.0 | 1295 | :20 | 88.0 | 1255 |
| :25 | 86.5 | 1232 | :25 | -- | -- |
| :30 | 84.5 | 1205 | :30 | 83.0 | 1185 |
| :40 | 81.5 | 1160 | :40 | 80.0 | 1140 |
| :50 | 78.0 | 1110 | :50 | 76.5 | 1090 |
| 1:00 | 76.0 | 1083 | 1:00 | 74.3 | 1060 |
| 1:15 | 73.5 | 1048 | 1:15 | 71.8 | 1025 |
| 1:30 | 71.0 | 1012 | 1:30 | 69.7 | 994 |
| 1:45 | 70.0 | 997 | 1:45 | 68.7 | 980 |
| 2:00 | 69.0 | 984 | 2:00 | 67.1 | 956 |
| 2:15 | 67.5 | 962 | 2:15 | 66.2 | 942 |
| 2:30 | 66.7 | 950 | 2:30 | 65.2 | 930 |
| 2:45 | 65.9 | 939 | 2:45 | 64.7 | 921 |
| 3:00 | 65.3 | 930 | 3:00 | 64.0 | 911 |
| 3:15 | 65.3 | 930 | 3:15 | 63.1 | 900 |
| 3:30 | 64.5 | 919 | 3:30 | 63.0 | 898 |
| 3:45 | 63.5 | 905 | 3:45 | 62.7 | 894 |
| 4:00 | 63.0 | 896 | 4:00 | 62.3 | 888 |
| 4:15 | 62.7 | 893 | 4:15 | 62.0 | 883 |
| 4:30 | 62.3 | 888 | 4:30 | 61.9 | 881 |
| 4:45 | 61.7 | 879 | 4:45 | 61.7 | 879 |
| 5:00 | 61.3 | 875 | 5:00 | 61.7 | 879 |
| 5:30 | 61.3 | 875 | 5:30 | -- | - |
| 6:00 | 61.2 | 874 | 6:00 | 62.0 | 883 |
| 6:30 | 60.5 | 862 | 6:30 | 62.0 | 883 |
| 7:00 | 60.1 | 856 | 7:00 | 62.0 | 883 |
| 7:30 | 59.8 | 852 | 7:30 | 61.5 | 876 |
| 8:00 | 59.0 | 840 | 8:00 | 60.7 | 865 |
| 8:30 | 59.0 | 840 | 8:30 | 60.0 | 855 |
| 9:00 | 58.3 | 830 | 9:00 | 59.3 | 845 |
| 9:30 | 57.8 | 824 | 9:30 | 58.7 | 836 |
| 10:00 | 57.2 | 815 | 10:00 | 58.4 | 831 |
| 10:30 | 57.2 | 815 | 10:30 | 57.8 | 823 |
| 11:00 | 56.8 | 809 | 11:00 | 57.5 | 819 |
| 12:00 | 56.0 | 798 | 12:00 | 56.4 | 803 |
| 13:00 | 55.0 | 784 | 12:30 | 56.0 | 798 |
| 14:00 | 54.5 | 776 | 13:00 | 56.0 | 798 |
| 15:00 | 53.2 | 758 | 14:00 | 54.8 | 780 |

0.3 RPS - (Continued)

| | | | | | |
|---|---|---|---|---|---|
| 16:00 | 52.0 | 741 | 15:00 | 53.5 | 762 |
| 17:00 | 51.3 | 731 | 16:00 | 52.8 | 752 |
| 18:00 | 50.5 | 720 | 17:00 | 52.2 | 744 |
| 20:00 | 49.7 | 708 | 18:00 | 51.3 | 730 |
| 21:00 | 49.5 | 705 | 19:00 | 50.5 | 719 |
| 22:00 | 49.2 | 700 | 20:00 | 50.2 | 715 |
| 23:00 | 48.8 | 695 | 21:00 | 49.4 | 704 |
| 24:00 | 48.5 | 691 | 22:00 | 49.1 | 699 |
| 25:00 | 48.0 | 684 | 23:00 | 48.5 | 690 |
| 27:00 | 47.3 | 674 | 24:00 | 47.8 | 680 |
| 28:00 | 46.8 | 666 | 25:00 | 47.4 | 675 |
| 29:00 | 46.5 | 662 | 27:00 | 46.3 | 659 |
| 30:00 | 46.3 | 659 | 29:00 | 45.5 | 648 |
| 31:00 | 46.0 | 655 | 31:00 | 44.8 | 638 |
| 32:00 | 45.8 | 652 | 33:00 | 44.0 | 626 |
| 33:00 | 45.6 | 649 | 35:00 | 43.3 | 616 |
| 34:00 | 45.1 | 642 | 37:00 | 43.3 | 616 |
| 35:00 | 44.7 | 637 | 39:00 | 42.5 | 605 |
| 36:00 | 44.4 | 632 | 41:00 | 41.9 | 596 |
| 37:00 | 44.2 | 629 | 43:00 | 41.6 | 592 |
| 38:00 | 44.0 | 626 | 45:00 | 41.2 | 586 |
| 39:00 | 43.7 | 622 | 47:00 | 41.2 | 586 |
| 42:00 | 42.7 | 608 | 50:00 | 40.7 | 580 |
| 45:00 | 41.9 | 596 | 55:00 | 40.1 | 571 |
| 48:00 | 41.6 | 593 | 60:00 | 39.5 | 562 |
| 51:00 | 40.7 | 579 | 65:00 | 39.1 | 556 |
| 55:00 | 40.2 | 572 | 70:00 | 38.7 | 551 |
| 60:00 | 39.6 | 564 | 75:00 | 38.4 | 547 |
| 65:00 | 39.3 | 560 | 82:00 | 38.0 | 541 |
| 70:00 | 38.8 | 553 | 85:00 | 37.8 | 538 |
| 75:00 | 38.4 | 546 | 90:00 | 37.6 | 535 |
| 80:00 | 38.1 | 542 | 97:00 | 37.4 | 533 |
| 86:00 | 37.6 | 535 | 100:00 | 37.3 | 531 |
| 90:00 | 37.0 | 527 | | | |
| 96:00 | 36.9 | 525 | | | |
| 100:00 | 36.8 | 524 | | | |
| 130:00 | 35.7 | 508 | | | |
| 140:00 | 35.3 | 503 | | | |
| 152:00 | 34.7 | 494 | | | |
| 160:00 | 34.4 | 490 | | | |
| 170:00 | 34.2 | 487 | | | |
| 180:00 | 34.0 | 484 | | | |
| 195:00 | 34.0 | 484 | | | |
| 210:00 | 33.6 | 478 | | | |
| 227:00 | 33.5 | 477 | | | |
| 240:00 | 33.4 | 476 | | | |

(1) No. 24 torsion wire

THIXOTROPIC DECAY DATA - QUICK QUENCHED SAMPLES

0.8 RPS

| TIME (min:sec) | RUN NUMBER ONE 0.802 RPS | | TIME (min:sec) | RUN NUMBER TWO 0.800 RPS | |
|---|---|---|---|---|---|
| | Bob Deflection (Degrees) | Shear Stress $x10^4$ ($lb_f/ft^2$) | | Bob Deflection (Degrees) | Shear Stress $x10^4$ ($lb_f/ft^2$) |
| :10 | 150.5(1) | 2141 | :10 | 154.8(1) | 2205 |
| :15 | 143.5 | 2042 | :15 | 146.3 | 2082 |
| :20 | 139.5 | 1990 | :20 | 142.3 | 2023 |
| :25 | 136.5 | 1945 | :25 | 138.8 | 1976 |
| :30 | 133.8 | 1907 | :30 | 135.8 | 1932 |
| :40 | 130.4 | 1860 | :40 | 131.2 | 1870 |
| :50 | 128.0 | 1825 | :50 | 128.8 | 1832 |
| 1:00 | 126.2 | 1800 | 1:00 | 126.8 | 1805 |
| 1:15 | 123.4 | 1760 | 1:15 | 123.8 | 1763 |
| 1:30 | 120.9 | 1722 | 1:30 | 121.1 | 1728 |
| 1:45 | 118.6 | 1690 | 1:45 | --- | -- |
| 2:00 | 117.0 | 1679 | 2:00 | 118.1 | 1682 |
| 2:15 | 115.5 | 1648 | 2:15 | 116.5 | 1660 |
| 2:30 | 114.3 | 1630 | 2:30 | 114.9 | 1637 |
| 2:45 | 112.9 | 1609 | 2:45 | 114.2 | 1627 |
| 3:00 | 112.0 | 1597 | 3:00 | 112.3 | 1600 |
| 3:15 | 110.6 | 1578 | 3:15 | 111.6 | 1590 |
| 3:30 | 109.9 | 1570 | 3:30 | 110.3 | 1572 |
| 3:45 | 108.9 | 1551 | 3:45 | 109.9 | 1567 |
| 4:00 | 108.2 | 1541 | 4:00 | 109.3 | 1559 |
| 4:15 | 107.0 | 1525 | 4:15 | 108.8 | 1552 |
| 4:30 | 106.3 | 1515 | 4:30 | 109.3 | 1559 |
| 4:45 | 105.4 | 1502 | 4:45 | 108.3 | 1543 |
| 5:00 | 104.5 | 1490 | 5:00 | 107.8 | 1536 |
| 5:30 | 102.9 | 1468 | 5:30 | 106.1 | 1512 |
| 6:00 | 101.4 | 1448 | 6:00 | 104.7 | 1492 |
| 6:30 | 100.5 | 1432 | 6:30 | 102.5 | 1461 |
| 7:00 | 98.9 | 1408 | 7:00 | 100.8 | 1437 |
| 7:30 | 98.0 | 1395 | 7:30 | 98.8 | 1408 |
| 8:00 | 97.0 | 1380 | 8:00 | 97.1 | 1384 |
| 8:30 | 95.8 | 1363 | 8:30 | 95.7 | 1364 |
| 9:00 | 94.7 | 1350 | 9:00 | 95.0 | 1354 |
| 9:30 | 94.0 | 1340 | 9:30 | 93.5 | 1333 |
| 10:00 | 93.0 | 1325 | 10:00 | 92.5 | 1318 |
| 10:30 | 92.0 | 1310 | 10:30 | 91.5 | 1304 |
| 11:00 | 91.2 | 1300 | 11:00 | 90.5 | 1290 |
| 12:00 | 90.0 | 1281 | 12:00 | 89.1 | 1270 |
| 13:00 | 88.3 | 1257 | 13:00 | 87.4 | 1246 |
| 14:00 | 87.0 | 1240 | 14:00 | 86.3 | 1230 |
| 15:00 | 85.8 | 1221 | 15:00 | -- | -- |
| 16:00 | 84.8 | 1210 | 16:00 | 83.8 | 1194 |

0.800 RPS - (continued)

| | | | | | |
|---|---|---|---|---|---|
| 17:00 | 84.0 | 1199 | 17:00 | 83.3 | 1187 |
| 18:00 | 83.0 | 1183 | 18:00 | 82.6 | 1177 |
| 19:00 | 82.3 | 1173 | 19:00 | 81.8 | 1166 |
| 20:00 | 82.0 | 1169 | 20:00 | 81.2 | 1157 |
| 21:00 | 80.5 | 1148 | 21:00 | 80.4 | 1146 |
| 22:00 | 80.5 | 1148 | 22:00 | 80.0 | 1140 |
| 23:00 | 79.5 | 1133 | 23:00 | 79.4 | 1132 |
| 24:00 | 78.9 | 1124 | 24:00 | 79.1 | 1128 |
| 25:00 | 78.5 | 1119 | 25:00 | 78.7 | 1122 |
| 26:00 | 78.3 | 1116 | 26:00 | 78.1 | 1114 |
| 27:00 | 77.5 | 1104 | 27:00 | 77.5 | 1105 |
| 28:00 | 77.2 | 1100 | 28:00 | 77.1 | 1099 |
| 29:00 | 76.9 | 1096 | 29:00 | 76.9 | 1096 |
| 30:00 | 76.5 | 1090 | 30:00 | 76.7 | 1093 |
| 31:00 | 76.2 | 1086 | 31:00 | 76.2 | 1086 |
| 32:00 | 76.0 | 1083 | 32:00 | 75.8 | 1080 |
| 33:00 | 75.7 | 1079 | 33:00 | 75.4 | 1074 |
| 34:00 | 75.4 | 1075 | 34:00 | 75.2 | 1071 |
| 36:00 | 74.9 | 1067 | 35:00 | 74.9 | 1067 |
| 37:00 | 74.7 | 1064 | 36:00 | 74.7 | 1064 |
| 40:00 | 74.0 | 1055 | 37:00 | 74.5 | 1062 |
| 43:00 | 73.5 | 1048 | 40:00 | 73.6 | 1049 |
| 46:00 | 73.0 | 1041 | 43:00 | 73.0 | 1041 |
| 50:00 | 72.5 | 1034 | 46:00 | 72.1 | 1028 |
| 55:00 | 71.9 | 1025 | 50:00 | 71.6 | 1021 |
| 61:00 | 71.2 | 1015 | 56:00 | 70.7 | 1007 |
| 65:00 | 70.8 | 1009 | 60:00 | 70.1 | 999 |
| 70:00 | 70.2 | 1001 | 65:00 | 69.8 | 995 |
| 76:00 | 69.8 | 996 | 70:00 | 69.3 | 988 |
| 80:00 | 69.2 | 988 | 77:00 | 68.9 | 982 |
| 86:00 | 68.5 | 976 | 80:00 | 68.7 | 979 |
| 90:00 | 68.2 | 972 | 86:00 | 68.5 | 976 |
| 117:00 | 66.8 | 952 | 90:00 | 68.2 | 972 |
| 130:00 | 65.9 | 939 | 95:00 | 67.8 | 966 |
| 140:00 | 65.4 | 932 | 100:00 | 67.6 | 963 |
| 150:00 | 65.2 | 929 | | | |
| 160:00 | 64.9 | 925 | | | |
| 174:00 | 64.5 | 920 | | | |
| 192:00 | 64.0 | 912 | | | |
| 210:00 | 63.5 | 905 | | | |
| 225:00 | 63.0 | 898 | | | |
| 240:00 | 62.8 | 895 | | | |
| 250:00 | 62.5 | 891 | | | |

(1) No. 24 torsion wire

THIXOTROPIC DECAY DATA - QUICK QUENCHED SAMPLES

2.0 RPS

| TIME (min:sec) | RUN NUMBER ONE 2.00 RPS | | TIME (min:sec) | RUN NUMBER TWO 2.00 RPS | |
|---|---|---|---|---|---|
| | Bob Deflection (Degrees) | Shear Stress $x10^4$ ($lb_f/ft^2$) | | Bob Deflection (Degrees) | Shear Stress $x10^4$ ($lb_f/ft^2$) |
| :10 | 90.5(1) | 3303 | :10 | 92.8(1) | 3387 |
| :15 | 88.0 | 3212 | :15 | 88.8 | 3241 |
| :20 | 86.0 | 3139 | :20 | 86.3 | 3150 |
| :25 | 84.3 | 3076 | :25 | 85.0 | 3102 |
| :30 | 83.3 | 3040 | :30 | 83.3 | 3040 |
| :40 | 81.3 | 2967 | :40 | 81.3 | 2967 |
| :50 | 79.0 | 2883 | :50 | 79.8 | 2913 |
| 1:00 | 77.5 | 2829 | 1:00 | 78.3 | 2858 |
| 1:15 | 75.3 | 2748 | 1:15 | 75.8 | 2767 |
| 1:30 | 72.5 | 2646 | 1:30 | 74.8 | 2730 |
| 1:45 | 71.9 | 2626 | 1:45 | 73.6 | 2686 |
| 2:00 | 69.3 | 2529 | 2:00 | 72.6 | 2650 |
| 2:15 | 68.0 | 2482 | 2:15 | 71.0 | 2592 |
| 2:30 | 66.9 | 2441 | 2:30 | 69.1 | 2522 |
| 2:45 | 66.0 | 2409 | 2:45 | 67.9 | 2478 |
| 3:00 | 65.2 | 2380 | 3:00 | 66.7 | 2435 |
| 3:15 | 64.5 | 2354 | 3:15 | 65.8 | 2402 |
| 3:45 | 63.3 | 2310 | 3:45 | 63.9 | 2332 |
| 4:00 | 63.0 | 2299 | 4:00 | 63.2 | 2307 |
| 4:15 | 62.5 | 2281 | 4:15 | 62.6 | 2285 |
| 4:30 | 62.0 | 2263 | 4:30 | 62.2 | 2270 |
| 4:45 | 61.5 | 2245 | 4:45 | 61.5 | 2245 |
| 5:00 | 61.3 | 2238 | 5:00 | 61.0 | 2227 |
| 5:30 | 60.7 | 2216 | 5:30 | 60.2 | 2198 |
| 6:00 | 60.2 | 2198 | 6:00 | 59.4 | 2169 |
| 6:30 | 59.5 | 2172 | 6:30 | 58.9 | 2151 |
| 7:00 | 59.0 | 2154 | 7:00 | 58.5 | 2136 |
| 7:30 | 58.7 | 2143 | 7:30 | 57.8 | 2110 |
| 8:00 | 58.3 | 2128 | 8:00 | 57.5 | 2099 |
| 8:30 | 57.9 | 2114 | 8:30 | 57.0 | 2081 |
| 9:00 | 57.5 | 2099 | 9:00 | 56.8 | 2074 |
| 9:30 | 57.2 | 2088 | 9:30 | 56.6 | 2066 |
| 10:00 | 56.9 | 2077 | 10:00 | 56.1 | 2048 |
| 10:30 | 56.6 | 2066 | 10:30 | 55.8 | 2037 |
| 11:00 | 56.4 | 2059 | 11:00 | 55.7 | 2033 |
| 12:00 | 55.9 | 2040 | 12:00 | 55.4 | 2022 |
| 13:00 | 55.5 | 2025 | 13:00 | 55.1 | 2011 |
| 14:00 | 55.2 | 2014 | 14:00 | 54.6 | 1993 |
| 15:00 | 54.7 | 1996 | 15:00 | 54.2 | 1978 |

2.0 RPS - (continued)

| | | | | | |
|---|---|---|---|---|---|
| 16:00 | 54.2 | 1978 | 16:00 | 53.9 | 1967 |
| 17:00 | 54.0 | 1971 | 17:00 | 53.5 | 1953 |
| 18:00 | 53.7 | 1960 | 18:00 | 53.2 | 1942 |
| 19:00 | 53.3 | 1945 | 19:00 | 53.1 | 1939 |
| 20:00 | 52.8 | 1927 | 20:00 | 52.8 | 1928 |
| 21:00 | 52.7 | 1923 | 21:00 | 52.6 | 1920 |
| 22:00 | 52.5 | 1916 | 22:00 | 52.3 | 1909 |
| 23:00 | 52.2 | 1905 | 23:00 | 52.2 | 1905 |
| 24:00 | 52.0 | 1897 | 24:00 | 51.9 | 1894 |
| 25:00 | 51.9 | 1893 | 25:00 | 51.7 | 1887 |
| 26:00 | 51.7 | 1886 | 26:00 | 51.6 | 1883 |
| 27:00 | 51.5 | 1880 | 27:00 | 51.5 | 1880 |
| 28:00 | 51.4 | 1876 | 28:00 | 51.4 | 1877 |
| 29:00 | 51.3 | 1873 | 29:00 | 51.2 | 1870 |
| 30:00 | 51.2 | 1870 | 30:00 | 51.0 | 1862 |
| 31:00 | 51.0 | 1863 | 32:00 | 50.8 | 1855 |
| 32:00 | 51.0 | 1863 | 35:00 | 50.4 | 1840 |
| 33:00 | 50.9 | 1860 | 37:00 | 50.2 | 1833 |
| 34:00 | 50.7 | 1851 | 39:00 | 50.0 | 1826 |
| 35:00 | 50.4 | 1840 | 41:00 | 49.7 | 1815 |
| 36:00 | 50.4 | 1840 | 43:00 | 49.5 | 1807 |
| 37:00 | 50.3 | 1836 | 45:00 | 49.3 | 1799 |
| 38:00 | 50.3 | 1836 | 48:00 | 49.1 | 1791 |
| 39:00 | 50.2 | 1832 | 50:00 | 48.9 | 1784 |
| 40:00 | 50.0 | 1825 | 54:00 | 48.6 | 1773 |
| 41:00 | 49.8 | 1818 | 57:00 | 48.3 | 1762 |
| 44:00 | 49.7 | 1814 | 60:00 | 48.1 | 1755 |
| 47:00 | 49.5 | 1806 | 65:00 | 47.7 | 1741 |
| 50:00 | 49.2 | 1795 | 70:00 | 47.5 | 1734 |
| 55:00 | 48.6 | 1773 | 75:00 | 47.3 | 1726 |
| 60:00 | 48.3 | 1762 | 82:00 | 47.1 | 1718 |
| 65:00 | 47.8 | 1744 | 90:00 | 46.5 | 1696 |
| 70:00 | 47.5 | 1733 | 95:00 | 46.4 | 1694 |
| 75:00 | 47.3 | 1727 | 100:00 | 46.2 | 1686 |
| 82:00 | 46.9 | 1712 | 105:00 | 46.0 | 1678 |
| 89:00 | 46.7 | 1705 | 110:00 | 45.9 | 1674 |
| 93:00 | 46.5 | 1697 | 124:00 | 45.5 | 1660 |
| 111:00 | 45.9 | 1675 | 150:00 | 44.6 | 1628 |
| 139:00 | 45.1 | 1646 | 172:00 | 44.2 | 1613 |
| 147:00 | 44.7 | 1632 | | | |
| 162:00 | 44.5 | 1624 | | | |
| 182:00 | 44.0 | 1606 | | | |
| 190:00 | 43.8 | 1599 | | | |
| 195:00 | 43.6 | 1592 | | | |
| 212:00 | 43.5 | 1589 | | | |
| 220:00 | 43.3 | 1580 | | | |
| 230:00 | 43.2 | 1577 | | | |
| 240:00 | 43.1 | 1573 | | | |

(1) No. 22 torsion wire

THIXOTROPIC DECAY DATA - QUICK QUENCHED SAMPLES

4.5 RPS

| TIME (min:sec) | RUN NUMBER ONE 4.50 RPS | | TIME (min:sec) | RUN NUMBER TWO 4.50 RPS | |
|---|---|---|---|---|---|
| | Bob Deflection (Degrees) | Shear Stress $x10^4$ ($lb_f/ft^2$) | | Bob Deflection (Degrees) | Shear Stress $x10^4$ ($lb_f/ft^2$) |
| :10 | 143.5(1) | 5240 | :10 | 146.5(1) | 5340 |
| :15 | 139.0 | 5070 | :15 | 141.5 | 5160 |
| :20 | 135.5 | 4950 | :20 | 137.5 | 5015 |
| :25 | 133.5 | 4865 | :25 | 134.5 | 4900 |
| :30 | 131.0 | 4780 | :30 | 133.0 | 4850 |
| :40 | 128.5 | 4690 | :40 | 130.0 | 4745 |
| :50 | 126.5 | 4620 | :50 | 129.0 | 4705 |
| 1:00 | 124.3 | 4540 | 1:00 | 128.3 | 4680 |
| 1:15 | 121.5 | 4440 | 1:15 | 127.0 | 4635 |
| 1:30 | 119.6 | 4360 | 1:30 | 124.5 | 4545 |
| 1:45 | 118.0 | 4310 | 1:45 | 119.7 | 4365 |
| 2:00 | 115.3 | 4210 | 2:00 | 115.5 | 4220 |
| 2:15 | 112.0 | 4090 | 2:15 | 111.0 | 4052 |
| 2:30 | 108.0 | 3940 | 2:30 | 108.3 | 3960 |
| 2:45 | 106.7 | 3890 | 2:45 | 105.8 | 3860 |
| 3:00 | 104.5 | 3820 | 3:00 | 104.0 | 3795 |
| 3:15 | 103.5 | 3780 | 3:15 | 102.5 | 3740 |
| 3:30 | 102.3 | 3740 | 3:30 | 101.3 | 3700 |
| 3:45 | 101.0 | 3685 | 3:45 | 100.3 | 3661 |
| 4:00 | 99.9 | 3650 | 4:00 | 99.3 | 3625 |
| 4:15 | 99.3 | 3620 | 4:15 | 98.5 | 3596 |
| 4:30 | 98.5 | 3590 | 4:30 | 97.7 | 3567 |
| 4:45 | 98.0 | 3575 | 4:45 | -- | -- |
| 5:00 | 97.5 | 3555 | 5:00 | 96.8 | 3534 |
| 5:30 | 96.5 | 3520 | 5:30 | 95.6 | 3490 |
| 6:00 | 95.5 | 3480 | 6:00 | 94.7 | 3457 |
| 6:30 | 94.7 | 3460 | 6:30 | 93.9 | 3428 |
| 7:00 | 94.3 | 3440 | 7:00 | 93.2 | 3403 |
| 7:30 | 93.5 | 3410 | 7:30 | 92.5 | 3376 |
| 8:00 | 93.0 | 3394 | 8:00 | 92.2 | 3365 |
| 8:30 | 92.4 | 3372 | 8:30 | 91.5 | 3339 |
| 9:00 | 91.9 | 3354 | 9:00 | 91.2 | 3328 |
| 9:30 | 91.4 | 3336 | 9:30 | 90.5 | 3302 |
| 10:00 | 91.2 | 3330 | 10:00 | 90.3 | 3295 |
| 10:30 | 90.5 | 3305 | 10:30 | 90.0 | 3285 |
| 11:00 | 90.3 | 3298 | 11:00 | 89.5 | 3267 |
| 12:00 | 89.7 | 3276 | 12:00 | 89.0 | 3249 |
| 13:00 | 88.9 | 3246 | 13:00 | 88.5 | 3231 |
| 14:00 | 88.5 | 3231 | 14:00 | 88.0 | 3213 |
| 15:00 | 87.8 | 3205 | 15:00 | 87.6 | 3198 |

4.5 RPS - (continued)

| | | | | | |
|---|---|---|---|---|---|
| 16:00 | 87.3 | 3187 | 16:00 | 87.6 | 3198 |
| 17:00 | 86.9 | 3172 | 17:00 | 87.3 | 3187 |
| 18:00 | 86.7 | 3165 | 18:00 | 86.9 | 3172 |
| 19:00 | 86.4 | 3150 | 19:00 | 86.3 | 3150 |
| 20:00 | -- | -- | 20:00 | 85.9 | 3135 |
| 21:00 | 86.0 | 3139 | 21:00 | 85.5 | 3120 |
| 22:00 | 85.7 | 3128 | 22:00 | 85.2 | 3109 |
| 23:00 | 85.6 | 3124 | 23:00 | 84.8 | 3094 |
| 24:00 | 85.3 | 3113 | 24:00 | 84.5 | 3083 |
| 25:00 | 85.1 | 3106 | 25:00 | 84.2 | 3072 |
| 26:00 | 84.9 | 3100 | 26:00 | 84.1 | 3068 |
| 27:00 | 84.8 | 3096 | 27:00 | 84.0 | 3063 |
| 28:00 | 84.6 | 3089 | 28:00 | 83.7 | 3052 |
| 29:00 | 84.5 | 3085 | 30:00 | 83.3 | 3037 |
| 31:00 | 84.3 | 3078 | 34:00 | 82.5 | 3008 |
| 32:00 | 83.9 | 3063 | 36:00 | 82.1 | 2993 |
| 33:00 | 83.8 | 3060 | 42:00 | 81.5 | 2971 |
| 34:00 | 83.7 | 3056 | 52:00 | 80.0 | 2920 |
| 36:00 | 83.4 | 3045 | 57:00 | 79.8 | 2913 |
| 38:00 | 83.3 | 3041 | 62:00 | 79.5 | 2902 |
| 40:00 | 83.0 | 3029 | 70:00 | 79.1 | 2887 |
| 42:00 | 82.8 | 3021 | 84:00 | 78.5 | 2865 |
| 44:00 | 82.5 | 3010 | 90:00 | 78.0 | 2847 |
| 46:00 | 82.2 | 2999 | 100:00 | 77.4 | 2825 |
| 48:00 | 82.0 | 2992 | 105:00 | 77.1 | 2814 |
| 50:00 | 81.6 | 2977 | 116:00 | 76.8 | 2803 |
| 53:00 | 81.5 | 2973 | 135:00 | 76.5 | 2792 |
| 57:00 | 81.2 | 2962 | 140:00 | 76.2 | 2781 |
| 62:00 | 80.6 | 2940 | 150:00 | 75.7 | 2763 |
| 66:00 | 80.2 | 2925 | 163:00 | 75.1 | 2741 |
| 73:00 | 79.3 | 2892 | 172:00 | 75.1 | 2741 |
| 78:00 | 79.0 | 2884 | 180:00 | 74.8 | 2730 |
| 81:00 | 78.8 | 2877 | | | |
| 88:00 | 78.5 | 2866 | | | |
| 95:00 | 78.3 | 2859 | | | |
| 101:00 | 78.0 | 2847 | | | |
| 116:00 | 77.5 | 2829 | | | |
| 125:00 | 77.0 | 2811 | | | |
| 138:00 | 75.8 | 2767 | | | |
| 158:00 | 75.4 | 2752 | | | |
| 165:00 | 75.0 | 2738 | | | |
| 180:00 | 74.9 | 2734 | | | |

(1) No. 22 torsion wire

QUICK QUENCHED SAMPLE SHEAR STRESS GROWTH DATA

0.3 RPS

| TIME (min:sec) | PREVIOUS CUP SPEED 0.8 RPS(1) | | TIME (min:sec) | PREVIOUS CUP SPEED 0.8 RPS(2) | |
|---|---|---|---|---|---|
| | Bob Deflection (Degrees) | Shear Stress $x10^4$ ($lb_f/ft^2$) | | Bob Deflection (Degrees) | Shear Stress $x10^4$ ($lb_f/ft^2$) |
| :15 | 24.1(3) | 343 | :15 | 26.4(4) | 376 |
| :30 | 24.0 | 342 | :30 | 26.4 | 376 |
| :45 | 24.0 | 342 | :45 | 26.4 | 376 |
| 1:00 | 24.1 | 343 | 1:00 | 26.4 | 376 |
| 2:00 | 24.0 | 342 | 2:00 | 26.4 | 376 |
| 3:00 | 24.2 | 344 | 3:00 | 26.4 | 376 |
| 3:30 | 24.0 | 342 | 4:00 | 26.4 | 376 |
| 4:30 | 23.9 | 341 | 5:00 | 26.5 | 378 |
| 5:30 | 24.0 | 342 | 7:00 | 26.6 | 379 |
| 7:00 | 24.0 | 342 | 10:00 | 26.9 | 383 |
| 9:00 | 24.1 | 343 | 12:00 | 27.0 | 385 |
| 11:00 | 24.3 | 346 | 14:00 | 27.2 | 388 |
| 13:30 | 24.5 | 349 | 16:00 | 27.3 | 389 |
| 17:00 | 24.5 | 349 | 18:00 | 27.3 | 389 |
| 20:00 | 24.5 | 349 | 20:00 | 27.5 | 392 |
| 26:00 | 25.0 | 356 | 22:00 | 27.7 | 395 |
| 29:00 | 25.1 | 358 | 25:00 | 27.7 | 395 |
| 32:00 | 25.3 | 361 | 27:00 | 27.8 | 396 |
| 37:00 | 25.3 | 361 | 30:00 | 27.9 | 398 |
| 39:00 | 25.5 | 363 | 34:00 | 28.0 | 399 |
| 43:00 | 25.4 | 362 | 37:00 | 28.0 | 399 |
| 46:00 | 25.5 | 363 | 41:00 | 27.9 | 398 |
| 50:00 | 25.5 | 363 | 44:00 | 27.9 | 398 |
| 52:30 | 25.6 | 365 | 50:00 | 28.3 | 403 |
| 55:00 | 25.8 | 368 | 55:00 | 28.5 | 406 |
| 57:30 | 25.8 | 368 | 60:00 | 28.6 | 407 |
| 60:00 | 25.8 | 368 | | | |
| 62:30 | 25.7 | 366 | | | |
| 65:00 | 25.7 | 366 | | | |
| 67:30 | 25.7 | 366 | | | |
| 70:00 | 25.7 | 366 | | | |

(1) After 240 minutes shear at 0.8 RPS
(2) After 100 minutes shear at 0.8 RPS
(3) No. 24 torsion wire
(4) No. 24 torsion wire

QUICK QUENCHED SAMPLE SHEAR STRESS GROWTH DATA

0.3 RPS

| TIME (min:sec) | PREVIOUS CUP SPEED 2.0 RPS(1) | | TIME (min:sec) | PREVIOUS CUP SPEED 4.5 RPS(2) | |
|---|---|---|---|---|---|
| | Bob Deflection (Degrees) | Shear Stress $x10^4$ ($lb_f/ft^2$) | | Bob Deflection (Degrees) | Shear Stress $x10^4$ ($lb_f/ft^2$) |
| :15 | 6.6(3) | 241 | :15 | 4.9(4) | 179 |
| 1:00 | 6.6 | 241 | 1:00 | 4.9 | 179 |
| 2:00 | 6.7 | 245 | 2:00 | 5.0 | 183 |
| 2:30 | 6.7 | 245 | 3:00 | 5.0 | 183 |
| 3:30 | 6.7 | 245 | 4:00 | 5.3 | 193 |
| 5:00 | 6.7 | 245 | 6:00 | 5.3 | 193 |
| 7:00 | 6.8 | 248 | 8:00 | 5.4 | 197 |
| 10:00 | 6.9 | 252 | 10:00 | 5.5 | 201 |
| 12:00 | 6.9 | 252 | 12:00 | 5.5 | 201 |
| 14:30 | 6.9 | 252 | 14:00 | 5.6 | 204 |
| 17:00 | 7.0 | 256 | 16:00 | 5.6 | 204 |
| 19:00 | 7.0 | 256 | 18:00 | 5.6 | 204 |
| 21:00 | 7.1 | 259 | 20:00 | 5.7 | 208 |
| 24:00 | 7.0 | 256 | 22:00 | 5.7 | 208 |
| 27:00 | 7.0 | 256 | 25:00 | 5.8 | 212 |
| 30:00 | 7.1 | 259 | 30:00 | 5.9 | 215 |
| 35:00 | 7.1 | 259 | 35:00 | 6.0 | 219 |
| 37:00 | 7.2 | 263 | 40:00 | 6.0 | 219 |
| 41:00 | 7.2 | 263 | 45:00 | 6.0 | 219 |
| 45:30 | 7.3 | 266 | 50:00 | 6.1 | 223 |
| 49:00 | 7.3 | 266 | 55:00 | 6.1 | 223 |
| 53:00 | 7.3 | 266 | 60:00 | 6.1 | 223 |
| 57:00 | 7.3 | 266 | | | |
| 60:00 | 7.3 | 266 | | | |
| 65:00 | 7.4 | 270 | | | |
| 71:00 | 7.4 | 270 | | | |
| 75:00 | 7.5 | 274 | | | |
| 80:00 | 7.5 | 274 | | | |
| 90:00 | 7.7 | 281 | | | |
| 95:00 | 7.7 | 281 | | | |
| 100:00 | 7.7 | 281 | | | |

(1) After 240 minutes shear at 2.0 RPS
(2) After 180 minutes shear at 4.5 RPS
(3) No. 22 torsion wire
(4) No. 22 torsion wire

QUICK QUENCHED SAMPLE SHEAR STRESS GROWTH DATA

0.8 RPS

| TIME (min:sec) | PREVIOUS CUP SPEED 2.0 RPS(1) | | TIME (min:sec) | PREVIOUS CUP SPEED 4.5 RPS(2) | |
|---|---|---|---|---|---|
| | Bob Deflection (Degrees) | Shear Stress x $10^4$ ($lb_f/ft^2$) | | Bob Deflection (Degrees) | Shear Stress x$10^4$ ($lb_f/ft^2$) |
| :15 | 17.0(3) | 621 | :15 | 13.5(4) | 493 |
| 2:00 | 17.0 | 621 | :30 | 13.5 | 493 |
| 4:00 | 17.1 | 624 | 1:30 | 13.6 | 496 |
| 6:00 | 17.3 | 631 | 2:00 | 13.6 | 496 |
| 9:30 | 17.3 | 631 | 3:00 | 13.6 | 496 |
| 12:00 | 17.3 | 631 | 4:00 | 13.8 | 504 |
| 13:30 | 17.4 | 635 | 6:00 | 14.0 | 511 |
| 16:30 | 17.4 | 635 | 8:30 | 14.1 | 515 |
| 18:00 | 17.5 | 639 | 11:00 | 14.1 | 515 |
| 21:00 | 17.5 | 639 | 14:30 | 14.1 | 515 |
| 24:00 | 17.6 | 642 | 17:00 | 14.3 | 522 |
| 27:00 | 17.5 | 639 | 19:30 | 14.4 | 526 |
| 30:00 | 17.5 | 639 | 22:00 | 14.5 | 529 |
| 33:00 | 17.6 | 642 | 24:30 | 14.6 | 533 |
| 36:00 | 17.6 | 642 | 27:00 | 14.6 | 533 |
| 39:00 | 17.6 | 642 | 31:00 | 14.7 | 537 |
| 40:00 | 17.6 | 642 | 33:30 | 14.6 | 533 |
| | | | 35:00 | 14.7 | 537 |
| | | | 37:30 | 14.7 | 537 |
| | | | 40:00 | 14.7 | 537 |
| | | | 43:00 | 14.8 | 540 |
| | | | 46:00 | 14.9 | 544 |
| | | | 49:30 | 14.9 | 544 |
| | | | 52:00 | 15.0 | 548 |
| | | | 55:00 | 14.9 | 544 |
| | | | 57:00 | 14.9 | 544 |
| | | | 60:00 | 14.9 | 544 |

(1) After 180 minutes shear at 2.0 RPS
(2) After 180 minutes shear at 4.5 RPS
(3) No. 22 torsion wire
(4) No. 22 torsion wire

QUICK QUENCHED SAMPLE SHEAR STRESS GROWTH DATA

2.0 RPS

| TIME (min:sec) | PREVIOUS CUP SPEED 4.5 RPS(1) | |
|---|---|---|
| | Bob Deflection (Degrees) | Shear Stress $x10^4$ ($lb_f/ft^2$) |
| :15 | 32.8 | 1197 |
| 1:00 | 32.8 | 1197 |
| 2:00 | 32.8 | 1197 |
| 3:00 | 32.9 | 1200 |
| 4:00 | 32.9 | 1200 |
| 7:00 | 33.0 | 1204 |
| 9:00 | 33.1 | 1208 |
| 12:00 | 33.2 | 1212 |
| 15:00 | 33.4 | 1219 |
| 18:00 | 33.5 | 1223 |
| 21:00 | 33.7 | 1230 |
| 24:00 | 33.8 | 1234 |
| 30:00 | 33.8 | 1234 |
| 34:00 | 33.8 | 1234 |
| 38:00 | 33.9 | 1237 |
| 42:00 | 34.0 | 1241 |
| 45:00 | 34.1 | 1245 |
| 48:00 | 34.0 | 1241 |
| 51:00 | 34.1 | 1245 |
| 54:00 | 34.1 | 1245 |
| 57:00 | 34.2 | 1248 |
| 62:00 | 34.3 | 1252 |
| 65:00 | 34.4 | 1256 |
| 69:00 | 34.4 | 1256 |
| 74:00 | 34.4 | 1256 |
| 76:00 | 34.5 | 1259 |
| 82:00 | 34.6 | 1263 |

(1) After 180 minutes shear at 4.5 RPS
(2) No. 22 torsion wire

# APPENDIX EIGHT

## SENSITIVITY ANALYSIS OF CORRELATION OF EXPERIMENTAL DATA USING THEORY OF THIXOTROPIC BEHAVIOUR (RITTER)

The correlation equation of the Theory of Thixotropic Behaviour(1) may be written as:

$$\log \left(\frac{\tau_s - \tau_{s\infty}}{\frac{\tau_{so}^2}{\tau_{s\infty}} - \tau_s}\right) = -k_A \left(\frac{\tau_{so} + \tau_{s\infty}}{\tau_{so} - \tau_{s\infty}}\right) \log t - \log \left(\frac{\tau_{so}^2/\tau_{s\infty} - \tau_{sl}}{\tau_{sl} - \tau_{s\infty}}\right)$$

Hence, on log-log coordinates, the above equation describes a linear relationship between the quantities

$$\left(\frac{\tau_s - \tau_{s\infty}}{\tau_{so}^2/\tau_{s\infty} - \tau_s}\right) \qquad \text{and } t$$

with a slope of

$$-k_A \left(\frac{\tau_{so} + \tau_{s\infty}}{\tau_{so} - \tau_{s\infty}}\right)$$

Correlation of experimental data in terms of the above equation requires an estimate of $\tau_o$, $\tau_\infty$, and for some thixotropic materials, an estimate of $\tau_\mu$. Unlike the absolutely experimentally measured values of $\tau$, these three quantities are experimentally indeterminable in that they must be secondarily derived from experimental data. Consequently, data processing techniques must be used. The question then is, if an error is made in estimation of any of these derivable quantities, what is the subsequent effect upon the predicted linear relationship?

An attempt was made to answer this question on an analytical basis, but the resultant equations were too cumbersome. Hence, subsequent effort was devoted to direct analysis of an experimentally measured set of thixotropic data. This data is given below:

| Time (minutes) | Shear Stress x $10^{4}$ ($lb_f/ft^2$) |
|---|---|
| 0.17 | 1475 |
| 0.25 | 1385 |
| 0.50 | 1275 |
| 1.0 | 1160 |
| 2.0 | 1070 |
| 5.0 | 970 |
| 10.0 | 910 |
| 20.0 | 860 |
| 50.0 | 790 |
| 100.0 | 740 |

It should be noted that the above data does not correspond to any tabulated results in this manuscript, being part of an earlier unreported investigational series. This fact is no consequence since the important consideration is that of relative effect.

Specifically, the following cases were treated:

(1) The limiting shear stress ( $\tau_\infty = 650 \times 10^{-4}$) and the Newtonian component ($\tau_\mu = 305 \times 10^{-4}$) were assumed to have been evaluated precisely; the initial shear stress was assumed to have three possible values ( $\tau_o = 1660$, 1710, and $1610 \times 10^{-4}$, respectively).

(2) The initial shear stress ($\tau_o = 1660 \times 10^{-4}$) and the Newtonian component ($\tau_\mu = 305 \times 10^{-4}$) were assumed to have been evaluated precisely; the limiting shear stress was assumed to have four possible values ( $\tau_\infty = 550$, 600, 650, $700 \times 10^{-4}$, respectively).

(3) The initial and limiting shear stresses (1660 and $650 \times 10^{-4}$, respectively) were assumed to have been evaluated precisely; the Newtonian component was assumed to have three possible values ($\tau_\mu = 200$, 250 and $305 \times 10^{-4}$, respectively).

The results corresponding to correlation of the experimental data for these three cases are shown in Figures (8-A), (8-B) and (8-C), respectively.

The thixotropic rate decay constants, $k_A$ were calculated for each case by the formula;

$$k_A = -\left(\frac{\tau_{so} - \tau_{s\infty}}{\tau_{so} + \tau_{s\infty}}\right)(\text{slope of linear section of curve}) \qquad (2)$$

or in shorter terms:

$$k_{A_i} = M_i S_i \qquad (3)$$

where $M_i$ and $S_i$ refer to the respective quantities in Equation (2).

The tabulated values of $k_A$ are:

| CASE 1 | | CASE 2 | | CASE 3 | |
|---|---|---|---|---|---|
| $\tau_o \times 10^4$ | $k_A$ | $\tau_\infty \times 10^4$ | $k_A$ | $\tau_\mu \times 10^4$ | $k_A$ |
| 1610 | 0.186 | 550 | 0.178 | 200 | 0.169 |
| 1660 | 0.187 | 600 | 0.180 | 250 | 0.179 |
| 1710 | 0.188 | 650 | 0.187 | 305 | 0.187 |
| | | 700 | 0.197 | | |

Discussion of Results:

The effect of a possible variation in $\tau_o$ is to simultaneously laterally shift and tilt the curve describing the experimentally correlated data. Alternately, the motion may be considered a rotation about a point somewhere to the extreme right. The effect of such motion upon the calculated values of $k_A$ is slight, since although the individual curve slope changes for each case, a compensating change in $M_i$ is introduced.

The effect of a possible variation in $\tau_\infty$ is considerably more pronounced than that of a variation in $\tau_o$. Consider the range of values of $\tau_\infty$ (i.e. $550 \times 10^{-4}$ to $700 \times 10^{-4}$) used. Then, if the curves describing

the experimental data are examined in sequence, starting at a value of $\tau_\infty$ equal to $550 \times 10^{-4}$, it will be noted that not only does the slope of the experimental plot increase as $\tau_\infty$ decreases, but also that the plot gradually degenerates into a curve. The effect of such behaviour on the subsequently calculated values of $k_A$ is apparent after investigation of the previous table.

The effect of a variation in $\tau_\mu$ on the experimental data plots is similar to that of a variation in $\tau_o$ (i.e. a lateral shift and tilt). However, since $M_i$ increases significantly faster than $S_i$ decreases as $\tau_\mu$ increases, calculated values of $k_A$ increase correspondingly.

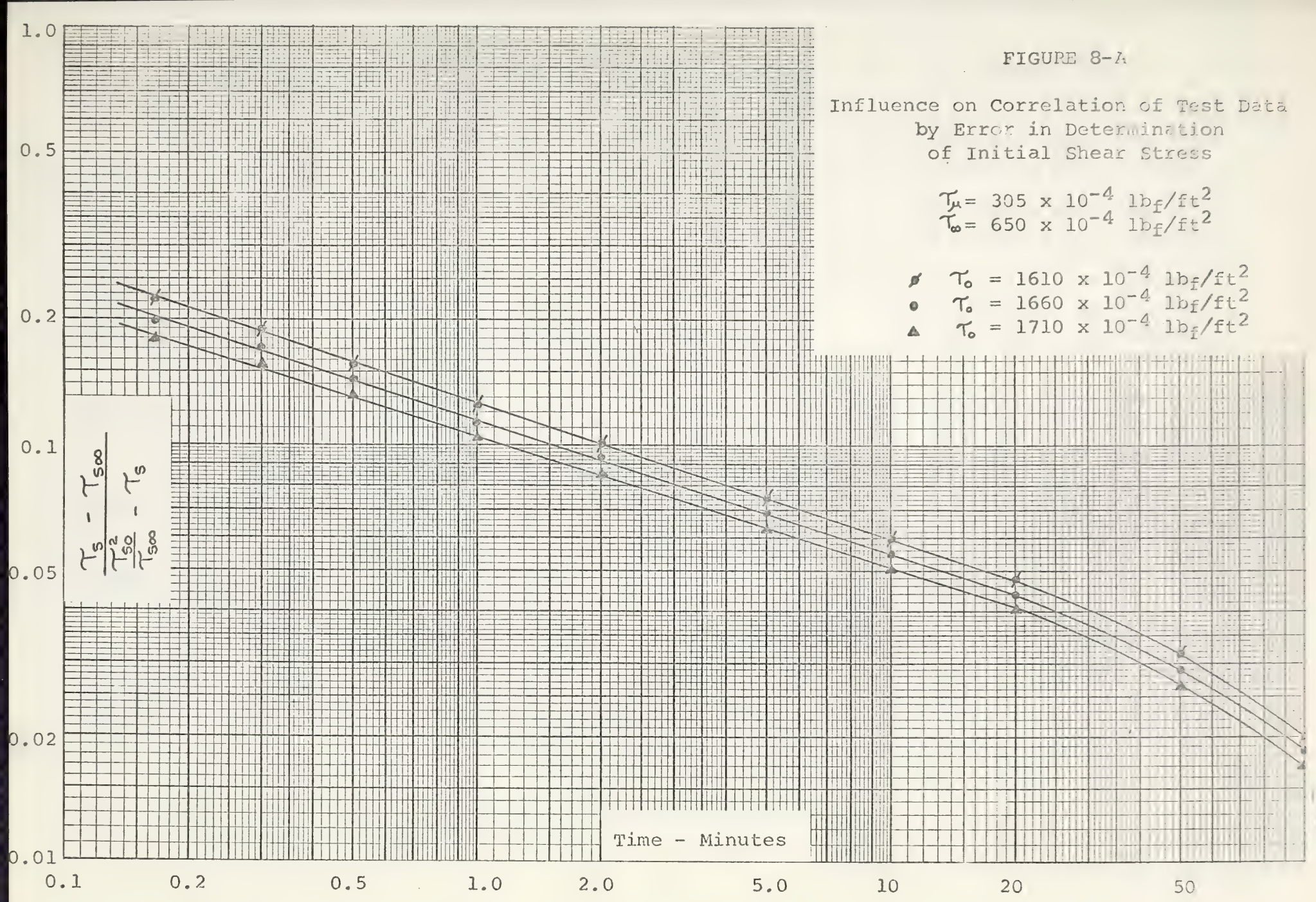


FIGURE 8-A

Influence on Correlation of Test Data by Error in Determination of Initial Shear Stress

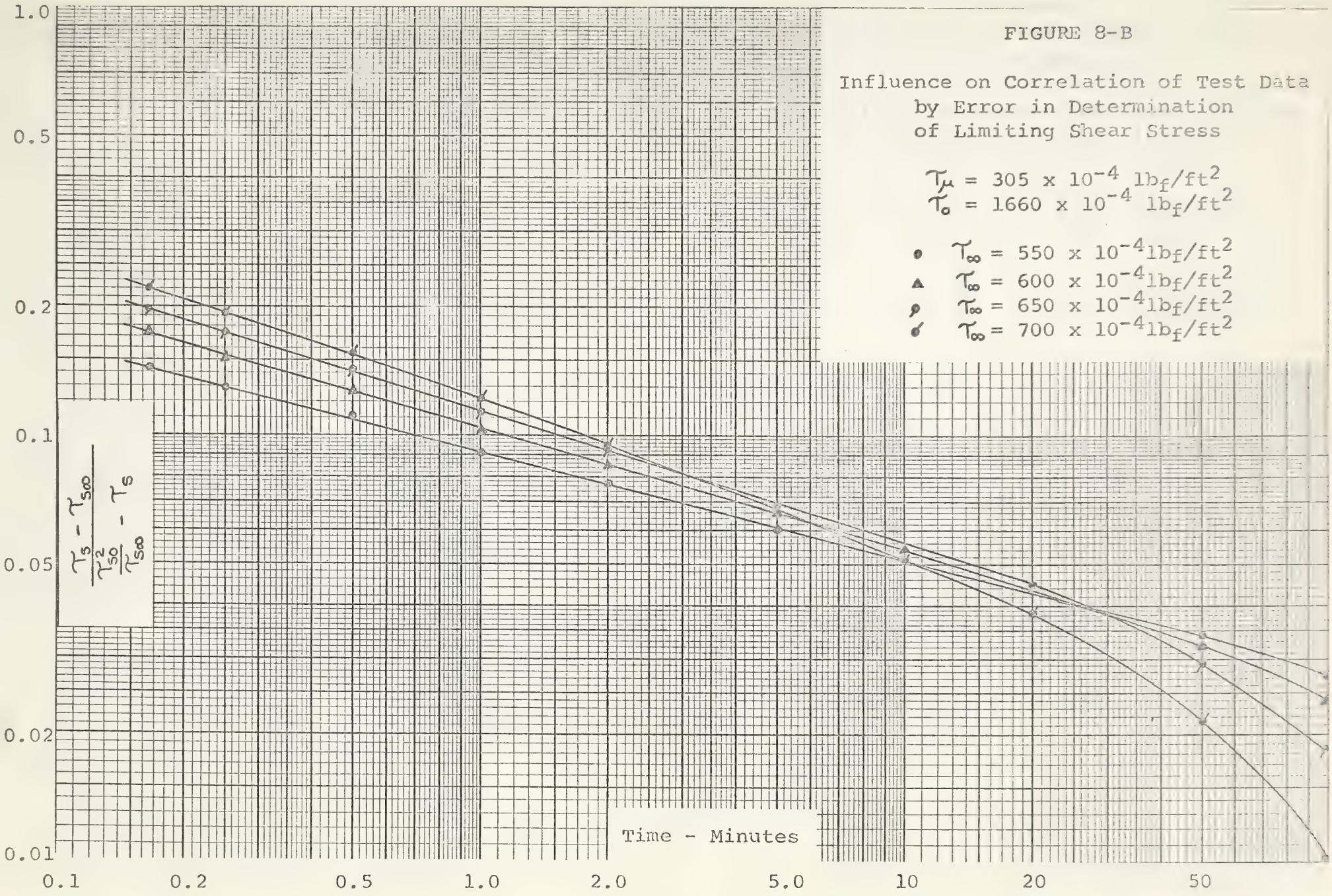


FIGURE 8-B

Influence on Correlation of Test Data
by Error in Determination
of Limiting Shear Stress

$\tau_\mu = 305 \times 10^{-4}$ lb$_f$/ft$^2$
$\tau_o = 1660 \times 10^{-4}$ lb$_f$/ft$^2$

- $\tau_\infty = 550 \times 10^{-4}$ lb$_f$/ft$^2$
- $\tau_\infty = 600 \times 10^{-4}$ lb$_f$/ft$^2$
- $\tau_\infty = 650 \times 10^{-4}$ lb$_f$/ft$^2$
- $\tau_\infty = 700 \times 10^{-4}$ lb$_f$/ft$^2$

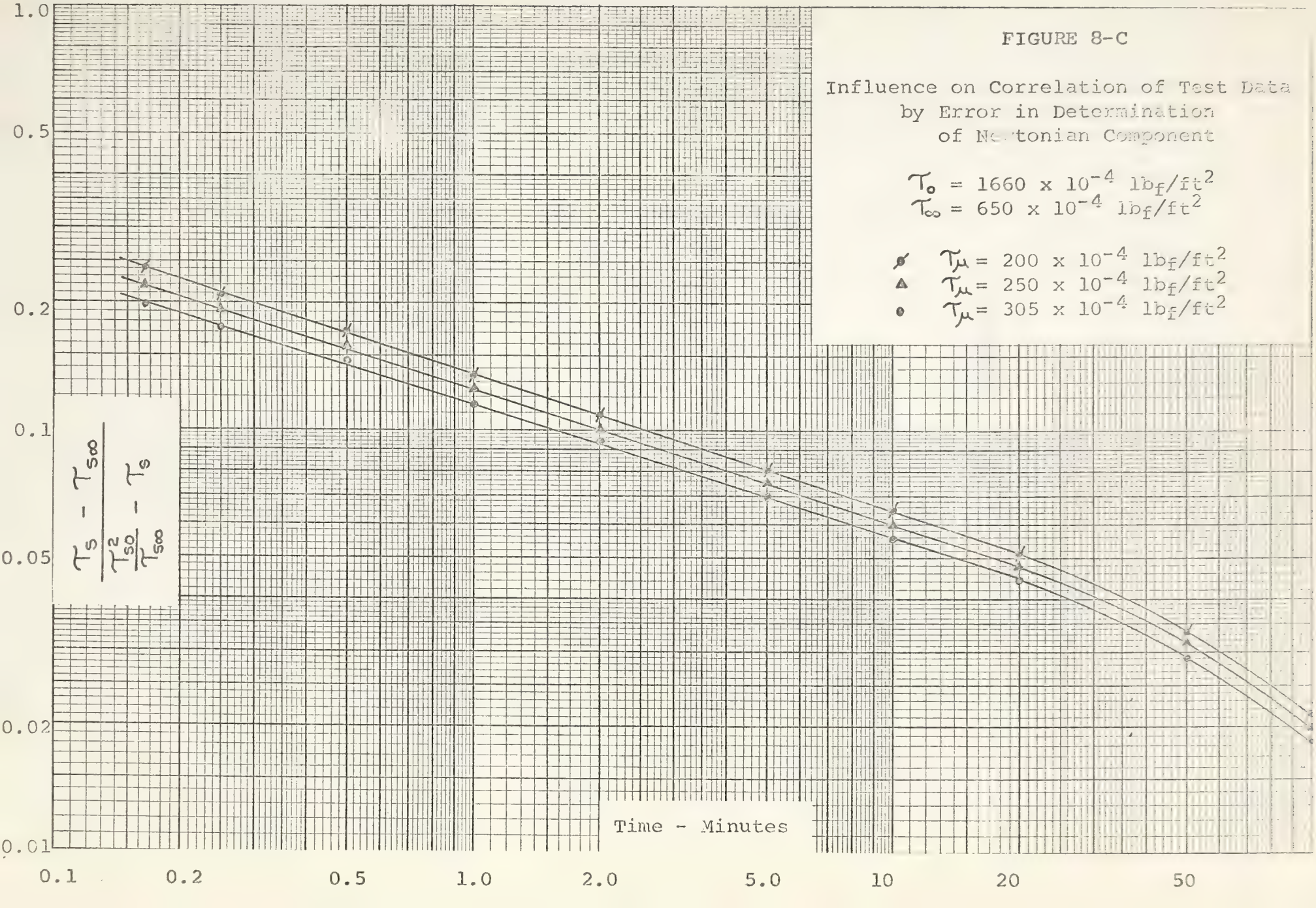
FIGURE 8-C
Influence on Correlation of Test Data by Error in Determination of Newtonian Component
$\tau_o = 1660 \times 10^{-4}$ lb$_f$/ft$^2$
$\tau_\infty = 650 \times 10^{-4}$ lb$_f$/ft$^2$
$\tau_\mu = 200 \times 10^{-4}$ lb$_f$/ft$^2$
$\tau_\mu = 250 \times 10^{-4}$ lb$_f$/ft$^2$
$\tau_\mu = 305 \times 10^{-4}$ lb$_f$/ft$^2$
$\frac{\tau_s - \tau_{s\infty}}{\frac{\tau_{s0}^2}{\tau_{s\infty}} - \tau_s}$
Time - Minutes
1.0
0.5
0.2
0.1
0.05
0.02
0.01
0.1
0.2
0.5
1.0
2.0
5.0
10
20
50

# APPENDIX NINE

## PROCESSED AND COMPUTED RHEOLOGICAL DATA

SLOW COOLED SAMPLES

PROCESSED AND COMPUTED RHEOLOGICAL DATA

| Time (min) | Cup Speed | | | | | | | |
|---|---|---|---|---|---|---|---|---|
| | 0.3 RPS | | 0.8 RPS | | 2.0 RPS | | 4.5 RPS | |
| | $\tau^*$ | $(\frac{dv}{dr})$ | $\tau^*$ | $(\frac{dv}{dr})$ | $\tau^*$ | $(\frac{dv}{dr})$ | $\tau^*$ | $(\frac{dv}{dr})$ |
| 0.000 | 720 | 21.45 | 1307 | 57.2 | 2360 | 143.0 | 3920 | 322.0 |
| 0.167 | 612 | 21.32 | 1134 | 56.87 | 2070 | 142.2 | 3495 | 319.9 |
| 0.30 | 567 | 21.24 | 1070 | 56.65 | 1955 | 141.6 | 3330 | 318.7 |
| 0.50 | 538 | 21.23 | 1020 | 56.64 | 1862 | 141.6 | 3200 | 318.5 |
| 1.0 | 500 | 21.21 | 955 | 56.57 | 1753 | 141.4 | 3025 | 318.2 |
| 2.0 | 465 | 21.19 | 897 | 56.51 | 1655 | 141.3 | 2865 | 317.9 |
| 5.0 | 433 | 21.17 | 836 | 56.46 | 1545 | 141.1 | 2680 | 317.6 |
| 10.0 | 408 | 21.15 | 796 | 56.40 | 1465 | 141.0 | 2565 | 317.3 |
| 20.0 | 387 | 21.15 | 760 | 56.40 | 1390 | 141.0 | 2450 | 317.3 |
| 40.0 | 367 | 21.13 | 726 | 56.34 | 1325 | 140.8 | 2350 | 316.9 |
| 75.0 | 352 | 21.13 | 690 | 56.34 | 1270 | 140.8 | 2260 | 316.9 |
| 200.0 | 325 | 21.11 | 649 | 56.29 | 1210 | 140.7 | 2155 | 316.6 |
| 250.0 | 318 | 21.0 | 638 | 56.26 | 1195 | 140.7 | 2135 | 316.5 |
| $\infty$ | 250 | 21.0 | 520 | 56.2 | 1025 | 140.5 | 1860 | 316.0 |

25 $Sec^{-1}$ Shear Rate

| Time (min) | $\tau^*$ | $\tau^*_s$ | $\tau^*_s - \tau^*_s$ | $(\frac{\tau_{so}^2}{\tau_{s\infty}} - \tau_s)^*$ | $\frac{\tau_s - \tau_{s\infty}}{\frac{\tau_{so}^2}{\tau_{s\infty}} - \tau_s}$ |
|---|---|---|---|---|---|
| 0.000 | 793 | | | | |
| 0.167 | 670 | 575 | 387 | 2015 | 0.1925 |
| 0.30 | 630 | 535 | 347 | 2055 | 0.1690 |
| 0.50 | 595 | 500 | 312 | 2090 | 0.1490 |
| 1.0 | 555 | 460 | 272 | 2130 | 0.1280 |
| 2.0 | 520 | 425 | 237 | 2165 | 0.1095 |
| 5.0 | 483 | 388 | 200 | 2202 | 0.0908 |
| 10.0 | 457 | 362 | 174 | 2228 | 0.0780 |
| 20.0 | 435 | 340 | 152 | 2250 | 0.0675 |
| 40.0 | 413 | 318 | 130 | 2272 | 0.0571 |
| 75.0 | 398 | 303 | 115 | 2287 | 0.0503 |
| 250.0 | 355 | 260 | 72 | 2230 | 0.0309 |
| $\infty$ | 283 | | | | |

$\tau^*_{so}$ = 698 $\tau^*_{s\infty}$ = 188 $\tau^*_{\mu}$ = 95

---

* All quantities to be multiplied by $10^{-4}$.

60 $Sec^{-1}$ Shear Rate

| Time (min) | $\tau^*$ | $\tau^*_s$ | $\tau^*_s - \tau^*_{s\infty}$ | $\left(\frac{\tau_{so}^2}{\tau_{s\infty}} - \tau_s\right)^*$ | $\frac{\tau_s - \tau_{s\infty}}{\frac{\tau_{so}^2}{\tau_{s\infty}} - \tau_s}$ |
|---|---|---|---|---|---|
| 0.000 | 1370 | | | | |
| 0.167 | 1175 | 945 | 633 | 3220 | 0.197 |
| 0.30 | 1120 | 890 | 578 | 3275 | 0.177 |
| 0.50 | 1060 | 830 | 518 | 3335 | 0.155 |
| 1.0 | 995 | 765 | 453 | 3400 | 0.133 |
| 2.0 | 935 | 705 | 393 | 3460 | 0.1138 |
| 5.0 | 870 | 640 | 328 | 3525 | 0.0930 |
| 10.0 | 825 | 595 | 283 | 3570 | 0.0792 |
| 20.0 | 790 | 560 | 248 | 3605 | 0.0687 |
| 40.0 | 750 | 520 | 208 | 3645 | 0.0570 |
| 75.0 | 720 | 490 | 178 | 3675 | 0.0484 |
| 250.0 | 660 | 430 | 118 | 3735 | 0.0315 |
| $\infty$ | 542 | | | | |

$\tau^*_{so}$ = 1140 $\tau^*_{s\infty}$ = 312 $\tau^*_{\mu}$ = 230

150 $Sec^{-1}$ Shear Rate

| Time (min) | $\tau^*$ | $\tau^*_s$ | $\tau^*_s - \tau^*_{s\infty}$ | $\left(\frac{\tau_{so}^2}{\tau_{s\infty}} - \tau_s\right)^*$ | $\frac{\tau_s - \tau_{s\infty}}{\frac{\tau_{so}^2}{\tau_{s\infty}} - \tau_s}$ |
|---|---|---|---|---|---|
| 0.000 | 2425 | | | | |
| 0.167 | 2145 | 1570 | 1075 | 5330 | 0.2020 |
| 0.30 | 2040 | 1465 | 970 | 5435 | 0.1785 |
| 0.50 | 1450 | 1375 | 880 | 5525 | 0.1590 |
| 1.0 | 1840 | 1265 | 770 | 5635 | 0.1370 |
| 2.0 | 1725 | 1150 | 655 | 5750 | 0.1140 |
| 5.0 | 1610 | 1035 | 540 | 5865 | 0.0920 |
| 10.0 | 1540 | 965 | 470 | 5935 | 0.0792 |
| 20.0 | 1460 | 885 | 390 | 6015 | 0.0648 |
| 40.0 | 1400 | 825 | 330 | 6075 | 0.0543 |
| 75.0 | 1350 | 775 | 280 | 6125 | 0.0457 |
| 250.0 | 1250 | 675 | 180 | 6226 | 0.0289 |
| $\infty$ | 1070 | | | | |

$\tau^*_{so}$ = 1850 $\tau^*_{s\infty}$ = 495 $\tau^*_{\mu}$ = 575

---

* All quantities to be multiplied by $10^{-4}$

300 Sec$^{-1}$ Shear Rate

| Time (min) | $\tau^*$ | $\tau^*_s$ | $\tau^*_s - \tau^*_{s\infty}$ | $(\frac{\tau_{so}^2}{\tau_{s\infty}} - \tau_s)^*$ | $\frac{\tau_s - \tau_{s\infty}}{\frac{\tau_{so}^2}{\tau_{s\infty}} - \tau_s}$ |
|---|---|---|---|---|---|
| 0.000 | 3750 | | | | |
| 0.167 | 3350 | 2190 | 1550 | 8290 | 0.187 |
| 0.30 | 3200 | 2040 | 1400 | 8440 | 0.166 |
| 0.50 | 3100 | 1940 | 1300 | 8540 | 0.152 |
| 1.0 | 2920 | 1760 | 1120 | 8720 | 0.1285 |
| 2.0 | 2750 | 1590 | 950 | 8890 | 0.107 |
| 5.0 | 2575 | 1415 | 775 | 9065 | 0.0855 |
| 10.0 | 2480 | 1320 | 680 | 9160 | 0.0742 |
| 20.0 | 2350 | 1190 | 550 | 9290 | 0.0593 |
| 40.0 | 2250 | 1090 | 450 | 9390 | 0.0479 |
| 75.0 | 2170 | 1010 | 370 | 9470 | 0.0391 |
| 250.0 | 2050 | 990 | 350 | 9490 | 0.0369 |
| $\infty$ | 1800 | | | | |

$\tau^*_{so}$ = 2590 $\tau^*_{s\infty}$ = 640 $\tau^*_{\mu}$ = 1160

---

* All quantities to be multiplied by $10^{-4}$

# ERROR ANALYSIS - SLOW COOLED SAMPLES

**Prediction Equations:**

| Shear Rate | Correlation Equation |
|---|---|
| 25 $sec^{-1}$ | $\log M = -0.245 \log t - 0.886$ |
| 60 $sec^{-1}$ | $\log M = -0.247 \log t - 0.886$ |
| 150 $sec^{-1}$ | $\log M = -0.244 \log t - 0.886$ |
| 300 $sec^{-1}$ | $\log M = -0.234 \log t - 0.886$ |

where: $$M = \left(\frac{\tau_s - \tau_{s\infty}}{\frac{\tau_{so}^2}{\tau_{s\infty}} - \tau_s}\right)$$

25 $sec^{-1}$

| Time (min) | M | $\tau^*_{Pred}$ | $\tau^*_{Exp}$ | \|Error\| % |
|---|---|---|---|---|
| 0.5 | 0.154 | 602 | 595 | 1.2 |
| 5.0 | 0.0874 | 476 | 483 | 1.5 |
| 20.0 | 0.0625 | 424 | 435 | 2.5 |
| 75.0 | 0.0451 | 387 | 398 | 2.8 |
| 250.0 | 0.0336 | 361 | 355 | 1.7 |
| | | | Average = | 1.9 |

60 $sec^{-1}$

| M | $\tau^*_{Pred}$ | $\tau^*_{Exp}$ | \|Error\| % |
|---|---|---|---|
| 0.154 | 1055 | 1060 | 0.5 |
| 0.0871 | 871 | 870 | 2.2 |
| 0.0620 | 767 | 790 | 2.9 |
| 0.0448 | 708 | 720 | 1.7 |
| 0.0332 | 666 | 660 | 0.9 |
| | | Average = | 1.6 |

150 $sec^{-1}$

| Time (min) | M | $\tau^*_{Pred}$ | $\tau^*_{Exp}$ | \|Error\| % |
|---|---|---|---|---|
| 0.5 | 0.154 | 1923 | 1950 | 1.4 |
| 5.0 | 0.0874 | 1585 | 1610 | 1.6 |
| 20.0 | 0.0625 | 1447 | 1460 | 0.9 |
| 75.0 | 0.0451 | 1347 | 1350 | 0.2 |
| 250.0 | 0.0337 | 1279 | 1250 | 2.2 |
| | | | Average = | 1.3 |

300 $sec^{-1}$

| M | $\tau^*_{Pred}$ | $\tau^*_{Exp}$ | \|Error\| % |
|---|---|---|---|
| 0.153 | 3105 | 3100 | 0.2 |
| 0.0890 | 2608 | 2575 | 1.3 |
| 0.0645 | 2395 | 2350 | 2.0 |
| 0.0474 | 2245 | 2170 | 3.4 |
| 0.0357 | 2140 | 2050 | 4.4 |
| | | Average = | 2.3 |

**Overall Average Error = 1.8%**

---

* All quantities to be multiplied by $10^{-4}$

QUICK QUENCHED SAMPLES - UNSMOOTHED EXPERIMENTAL DATA CASE

PROCESSED AND COMPUTED RHEOLOGICAL DATA

| Time (min) | Cup Speed | | | | | | | |
|---|---|---|---|---|---|---|---|---|
| | 0.3 RPS | | 0.8 RPS | | 2.0 RPS | | 4.5 RPS | |
| | $\tau^*$ | $(\frac{dv}{dr})$ | $\tau^*$ | $(\frac{dv}{dr})$ | $\tau^*$ | $(\frac{dv}{dr})$ | $\tau^*$ | $(\frac{dv}{dr})$ |
| 0.000 | 1750 | 27.2 | 2400 | 60.0 | 3600 | 144.0 | 5825 | 312.0 |
| 0.167 | 1450 | 23.0 | 2170 | 59.3 | 3320 | 142.9 | 5300 | 313.2 |
| 0.30 | 1310 | 22.7 | 2020 | 58.7 | 3190 | 141.9 | 5020 | 312.3 |
| 0.50 | 1200 | 21.8 | 1920 | 58.2 | 3040 | 141.9 | 4820 | 311.4 |
| 1.0 | 1070 | 20.5 | 1800 | 57.4 | 2840 | 141.9 | 4620 | 309.1 |
| 2.0 | 970 | 20.7 | 1680 | 58.4 | 2580 | 143.4 | 4220 | 309.1 |
| 5.0 | 880 | 20.8 | 1500 | 58.0 | 2240 | 143.2 | 3550 | 314.7 |
| 10.0 | 830 | 21.6 | 1320 | 59.1 | 2070 | 141.8 | 3320 | 311.5 |
| 20.0 | 710 | 22.2 | 1160 | 56.9 | 1930 | 139.8 | 3150 | 314.7 |
| 40.0 | 610 | 21.4 | 1055 | 56.1 | 1810 | 138.9 | 3000 | 312.6 |
| 75.0 | 550 | 21.0 | 985 | 55.8 | 1720 | 138.3 | 2880 | 311.2 |
| 200.0 | 480 | 20.7 | 905 | 55.3 | 1600 | 137.4 | 2720 | 309.4 |
| 250.0 | 470 | 20.7 | 890 | 55.2 | 1570 | 138.0 | - | - |
| $\infty$ | 350 | 20.5 | 680 | 55.0 | 1275 | 138.0 | 2250 | 309 |

25 $Sec^{-1}$ Shear Rate

| Time (min) | $\tau^*$ | $\tau^*_s$ | $\tau^*_s - \tau^*_{s\infty}$ | $(\frac{\tau_{so}^2}{\tau_{s\infty}} - \tau_s)^*$ | $\frac{\tau_s - \tau_{s\infty}}{\frac{\tau_{so}^2}{\tau_{s\infty}} - \tau_s}$ |
|---|---|---|---|---|---|
| 0.000 | 1680 | | | | |
| 0.167 | 1500 | 1405 | 1100 | 6805 | 0.162 |
| 0.30 | 1365 | 1270 | 965 | 6940 | 0.139 |
| 0.50 | 1275 | 1180 | 875 | 7030 | 0.125 |
| 1.0 | 1180 | 1085 | 780 | 7125 | 0.109 |
| 2.0 | 1075 | 980 | 675 | 7230 | 0.0933 |
| 5.0 | 980 | 885 | 580 | 7325 | 0.0792 |
| 10.0 | 880 | 785 | 480 | 7425 | 0.0646 |
| 20.0 | 750 | 655 | 350 | 7555 | 0.0464 |
| 40.0 | 664 | 569 | 264 | 7641 | 0.0345 |
| 75.0 | 615 | 520 | 215 | 7690 | 0.0280 |
| 200.0 | 543 | 448 | 143 | 7762 | 0.0184 |
| $\infty$ | 400 | | | | |

$\tau^*_{so}$ = 1585 $\tau^*_{s\infty}$ = 305 $\tau^*_{\mu}$ = 95

---

* All quantities to be multiplied by $10^{-4}$

60 $Sec^{-1}$ Shear Rate

| Time (min) | $\tau^*$ | $\tau^*_s$ | $\tau^*_s - \tau^*_{s\infty}$ | $(\frac{\tau_{so}^2}{\tau_{s\infty}} - \tau_s)^*$ | $\frac{\tau_s - \tau_{s\infty}}{\frac{\tau_{so}^2}{\tau_{s\infty}} - \tau_s}$ |
|---|---|---|---|---|---|
| 0.000 | 2400 | | | | |
| 0.167 | 2200 | 1970 | 1475 | 7500 | 0.192 |
| 0.30 | 2050 | 1820 | 1325 | 7650 | 0.173 |
| 0.50 | 1950 | 1720 | 1225 | 7750 | 0.158 |
| 1.0 | 1845 | 1615 | 1120 | 7855 | 0.143 |
| 2.0 | 1700 | 1470 | 975 | 8000 | 0.122 |
| 5.0 | 1520 | 1290 | 795 | 8180 | 0.0972 |
| 10.0 | 1330 | 1100 | 605 | 8370 | 0.0722 |
| 20.0 | 1200 | 970 | 475 | 8500 | 0.0558 |
| 40.0 | 1100 | 870 | 375 | 8600 | 0.0435 |
| 75.0 | 1035 | 805 | 310 | 8665 | 0.0356 |
| 200.0 | 955 | 725 | 230 | 8745 | 0.0263 |
| $\infty$ | 725 | | | | |

$\tau^*_{so}$ = 2170 $\tau^*_{s\infty}$ = 495 $\tau^*_{\mu}$ = 230

150 $Sec^{-1}$ Shear Rate

| Time (min) | $\tau^*$ | $\tau^*_s$ | $\tau^*_s - \tau^*_{s\infty}$ | $(\frac{\tau_{so}^2}{\tau_{s\infty}} - \tau_s)^*$ | $\frac{\tau_s - \tau_{s\infty}}{\frac{\tau_{so}^2}{\tau_{s\infty}} - \tau_s}$ |
|---|---|---|---|---|---|
| 0.000 | 3700 | | | | |
| 0.167 | 3400 | 2825 | 2050 | 9775 | 0.210 |
| 0.30 | 3300 | 2725 | 1950 | 9875 | 0.198 |
| 0.50 | 3150 | 2575 | 1800 | 10025 | 0.180 |
| 1.0 | 2930 | 2355 | 1580 | 10245 | 0.154 |
| 2.0 | 2650 | 2075 | 1300 | 10525 | 0.123 |
| 5.0 | 2300 | 1725 | 950 | 10875 | 0.0872 |
| 10.0 | 2140 | 1565 | 790 | 11035 | 0.0716 |
| 20.0 | 2025 | 1450 | 675 | 11150 | 0.0606 |
| 40.0 | 1900 | 1325 | 550 | 11275 | 0.0487 |
| 75.0 | 1800 | 1225 | 450 | 11375 | 0.0396 |
| 200.0 | 1690 | 1115 | 340 | 11485 | 0.0295 |
| $\infty$ | 1350 | | | | |

$\tau^*_{so}$ = 3125 $\tau^*_{s\infty}$ = 775 $\tau^*_{\mu}$ = 575

---

All quantities must be multiplied by $10^{-4}$

300 $Sec^{-1}$ Shear Rate

| Time (min) | $\tau^*$ | $\tau^*_s$ | $\tau^*_s - \tau^*_{s\infty}$ | $(\frac{\tau_{so}^2}{\tau_{s\infty}} - \tau_s)^*$ | $\frac{\tau_s - \tau_{s\infty}}{\frac{\tau_{so}^2}{\tau_{s\infty}} - \tau_s}$ |
|---|---|---|---|---|---|
| 0.000 | 5650 | | | | |
| 0.167 | 5130 | 3970 | 2955 | 15880 | 0.186 |
| 0.30 | 4900 | 3740 | 2725 | 16110 | 0.169 |
| 0.50 | 4700 | 3540 | 2525 | 16310 | 0.155 |
| 1.0 | 4550 | 3390 | 2375 | 16460 | 0.144 |
| 2.0 | 4160 | 3000 | 1985 | 16850 | 0.118 |
| 5.0 | 3460 | 2300 | 1285 | 17550 | 0.073 |
| 10.0 | 3240 | 2080 | 1065 | 17770 | 0.060 |
| 20.0 | 3060 | 1900 | 885 | 17950 | 0.0493 |
| 40.0 | 2900 | 1740 | 725 | 18110 | 0.0400 |
| 75.0 | 2800 | 1640 | 625 | 18210 | 0.0344 |
| 200.0 | 2650 | 1490 | 475 | 18360 | 0.0259 |
| $\infty$ | 2175 | | | | |

$\tau^*_{so}$ = 4490 $\tau^*_{s\infty}$ = 1015 $\tau^*_{\mu}$ = 1160

---

* All quantities must be multiplied by $10^{-4}$

ERROR ANALYSIS - QUICK QUENCHED SAMPLES

UNSMOOTHED EXPERIMENTAL DATA CASE

Prediction Equations:

Shear Rate

| Shear Rate | Correlation Equation |
|---|---|
| 25 $sec^{-1}$ | log M = -0.313 log t - 0.892 |
| 60 $sec^{-1}$ | log M = -0.324 log t - 0.892 |
| 150 $sec^{-1}$ | log M = -0.349 log t - 0.892 |
| 300 $sec^{-1}$ | log M = -0.325 log t - 0.892 |

where: $$M = \left(\frac{\tau_s - \tau_{s\infty}}{\frac{\tau_{so}^2}{\tau_{s\infty}} - \tau_s}\right)$$

25 $sec^{-1}$

| Time (min) | M | $\tau^*_{Pred}$ | $\tau^*_{Exp}$ | \|Error\| % |
|---|---|---|---|---|
| 0.5 | 0.159 | 1485 | 1275 | 16.5 |
| 5.0 | 0.0775 | 975 | 980 | 0.5 |
| 20.0 | 0.0503 | 778 | 750 | 3.7 |
| 75.0 | 0.0332 | 653 | 615 | 6.1 |
| 200.0 | 0.0244 | 588 | 543 | 8.3 |
| $t_m$* | 0.0624 | 864 | 880 | 1.8 |
| | | | Average = | 6.1 |

60 $sec^{-1}$

| M | $\tau^*_{Pred}$ | $\tau^*_{Exp}$ | \|Error\| % |
|---|---|---|---|
| 0.160 | 1970 | 1950 | 1.1 |
| 0.0760 | 1358 | 1520 | 10.6 |
| 0.0487 | 1143 | 1200 | 5.6 |
| 0.0318 | 1001 | 1035 | 3.4 |
| 0.0230 | 927 | 955 | 2.9 |
| | | Average = | 4.7 |

150 $sec^{-1}$

| Time (min) | M | $\tau^*_{Pred}$ | $\tau^*_{Exp}$ | \|Error\| % |
|---|---|---|---|---|
| 0.5 | 0.163 | 3025 | 3150 | 4.0 |
| 5.0 | 0.073 | 2155 | 2300 | 6.3 |
| 20.0 | 0.0452 | 1862 | 2025 | 8.0 |
| 75.0 | 0.0286 | 1680 | 1800 | 6.7 |
| 200.0 | 0.0210 | 1590 | 1690 | 5.9 |
| $t_m$* | 0.128 | 2685 | 2930 | 8.3 |
| | | | Average = | 6.5 |

300 $sec^{-1}$

| M | $\tau^*_{Pred}$ | $\tau^*_{Exp}$ | \|Error\| % |
|---|---|---|---|
| 0.161 | 4722 | 4700 | 0.5 |
| 0.0758 | 3500 | 3460 | 1.1 |
| 0.0485 | 3045 | 3060 | 0.5 |
| 0.0316 | 2750 | 2800 | 1.8 |
| 0.0230 | 2595 | 2650 | 2.1 |
| 0.129 | 4320 | 4550 | 5.1 |
| | | Average = | 1.8 |

Overall Average Error = 4.9%

---

* All quantities to be multiplied by $10^{-4}$

QUICK QUENCHED SAMPLES - SMOOTHED EXPERIMENTAL DATA CASE

PROCESSED AND COMPUTED RHEOLOGICAL DATA

| Time (min) | Cup Speed | | | | | | | |
|---|---|---|---|---|---|---|---|---|
| | 0.3 RPS | | 0.8 RPS | | 2.0 RPS | | 4.5 RPS | |
| | $\tau^*$ | $(\frac{dv}{dr})$ | $\tau^*$ | $(\frac{dv}{dr})$ | $\tau^*$ | $(\frac{dv}{dr})$ | $\tau^*$ | $(\frac{dv}{dr})$ |
| 0.000 | 1750 | 22.8 | 2600 | 59.8 | 3960 | 144.0 | 6300 | 310.0 |
| 0.167 | 1450 | 22.8 | 2170 | 59.8 | 3320 | 144.0 | 5300 | 310.0 |
| 0.30 | 1310 | 22.3 | 2020 | 58.6 | 3110 | 144.0 | 4920 | 313.0 |
| 0.50 | 1200 | 21.8 | 1900 | 58.2 | 2940 | 143.0 | 4640 | 317.0 |
| 1.0 | 1070 | 21.8 | 1740 | 57.8 | 2710 | 143.0 | 4250 | 320.0 |
| 2.0 | 970 | 21.7 | 1590 | 57.8 | 2490 | 144.0 | 3920 | 318.0 |
| 5.0 | 850 | 21.5 | 1400 | 57.2 | 2240 | 142.0 | 3550 | 319.0 |
| 10.0 | 760 | 21.5 | 1270 | 57.2 | 2070 | 141.5 | 3320 | 317.0 |
| 20.0 | 675 | 21.5 | 1150 | 56.7 | 1930 | 140.0 | 3150 | 314.0 |
| 40.0 | 605 | 21.3 | 1055 | 56.2 | 1810 | 140.0 | 3000 | 314.0 |
| 75.0 | 550 | 20.9 | 985 | 55.7 | 1720 | 140.0 | 2880 | 313.0 |
| 200.0 | 480 | 20.7 | 905 | 55.2 | 1600 | 138.0 | 2720 | 311.0 |
| $\infty$ | 350 | 20.6 | 680 | 54.9 | 1275 | 137.0 | 2250 | 309.0 |

25 Sec$^{-1}$ Shear Rate

| Time (min) | $\tau^*$ | $\tau^*_s$ | $\tau^*_s - \tau^*_{s\infty}$ | $(\frac{\tau_{so}^2}{\tau_{s\infty}} - \tau_s)^*$ | $\frac{\tau_s - \tau_{s\infty}}{\frac{\tau_{so}^2}{\tau_{s\infty}} - \tau_s}$ |
|---|---|---|---|---|---|
| 0.000 | 1800 | | | | |
| 0.167 | 1500 | 1405 | 1100 | 8145 | 0.1350 |
| 0.30 | 1380 | 1285 | 980 | 8265 | 0.1185 |
| 0.50 | 1275 | 1180 | 875 | 8370 | 0.1045 |
| 2.0 | 1040 | 945 | 640 | 8605 | 0.0745 |
| 5.0 | 915 | 820 | 515 | 8730 | 0.0590 |
| 10.0 | 820 | 725 | 420 | 8825 | 0.0477 |
| 20.0 | 730 | 635 | 330 | 8915 | 0.0370 |
| 40.0 | 660 | 565 | 260 | 8985 | 0.0290 |
| 75.0 | 610 | 515 | 210 | 9035 | 0.0233 |
| 200.0 | 540 | 445 | 140 | 9105 | 0.0154 |
| $\infty$ | 400 | | | | |

$\tau^*_{so}$ = 1705 $\tau^*_{s\infty}$ = 305 $\tau^*_{\mu}$ = 95

---

* All quantities must be multiplied by $10^{-4}$

60 Sec$^{-1}$ Shear Rate

| Time (min) | $\tau^*$ | $\tau^*_s$ | $\tau^*_s - \tau^*_{s\infty}$ | $(\frac{\tau_{so}^2}{\tau_{s\infty}} - \tau_s)^*$ | $\frac{\tau_s - \tau_{s\infty}}{\frac{\tau_{so}^2}{\tau_{s\infty}} - \tau_s}$ |
|---|---|---|---|---|---|
| 0.000 | 2600 | | | | |
| 0.167 | 2170 | 1940 | 1445 | 9410 | 0.1535 |
| 0.30 | 2050 | 1820 | 1325 | 9530 | 0.139 |
| 0.50 | 1915 | 1680 | 1185 | 9670 | 0.123 |
| 1.0 | 1760 | 1530 | 1035 | 9820 | 0.1052 |
| 2.0 | 1615 | 1385 | 890 | 9965 | 0.0892 |
| 5.0 | 1425 | 1195 | 700 | 10155 | 0.0689 |
| 10.0 | 1310 | 1080 | 585 | 10270 | 0.0570 |
| 20.0 | 1190 | 960 | 465 | 10390 | 0.0447 |
| 40.0 | 1090 | 860 | 365 | 10490 | 0.0348 |
| 75.0 | 1025 | 795 | 300 | 10555 | 0.0284 |
| 200.0 | 945 | 715 | 220 | 10635 | 0.0207 |
| $\infty$ | 725 | | | | |

$\tau^*_{so}$ = 2370 $\tau^*_{s\infty}$ = 495 $\tau^*_{\mu}$ = 230

150 Sec$^{-1}$ Shear Rate

| Time (min) | $\tau^*$ | $\tau^*_s$ | $\tau^*_s - \tau^*_{s\infty}$ | $(\frac{\tau_{so}^2}{\tau_{s\infty}} - \tau_s)^*$ | $\frac{\tau_s - \tau_{s\infty}}{\frac{\tau_{so}^2}{\tau_{s\infty}} - \tau_s}$ |
|---|---|---|---|---|---|
| 0.000 | 4020 | | | | |
| 0.167 | 3400 | 2825 | 2050 | 12475 | 0.164 |
| 0.30 | 3200 | 2625 | 1850 | 12675 | 0.146 |
| 0.50 | 3010 | 2435 | 1660 | 12865 | 0.129 |
| 1.0 | 2800 | 2225 | 1450 | 13075 | 0.111 |
| 2.0 | 2550 | 1975 | 1200 | 13325 | 0.0900 |
| 5.0 | 2310 | 1735 | 960 | 13565 | 0.0708 |
| 10.0 | 2150 | 1575 | 800 | 13725 | 0.0582 |
| 20.0 | 2010 | 1435 | 660 | 13865 | 0.0478 |
| 40.0 | 1900 | 1325 | 550 | 13975 | 0.0394 |
| 75.0 | 1800 | 1225 | 450 | 14075 | 0.0320 |
| 200.0 | 1700 | 1125 | 350 | 14175 | 0.0247 |
| $\infty$ | 1350 | | | | |

$\tau^*_{so}$ = 3445 $\tau^*_{s\infty}$ = 775 $\tau^*_{\mu}$ = 575

---

* All quantities must be multiplied by $10^{-4}$

300 $Sec^{-1}$ Shear Rate

| Time (min) | $\tau^*$ | $\tau^*_s$ | $\tau^*_s - \tau^*_{s\infty}$ | $\left(\frac{\tau_{so}^2}{\tau_{s\infty}} - \tau_s\right)$ | $\frac{\tau_s - \tau_{s\infty}}{\frac{\tau_{so}^2}{\tau_{s\infty}} - \tau_s}$ |
|---|---|---|---|---|---|
| 0.000 | 6175 | | | | |
| 0.167 | 5160 | 4000 | 2985 | 20800 | 0.144 |
| 0.30 | 4800 | 3640 | 2625 | 21160 | 0.1245 |
| 0.50 | 4500 | 3340 | 2325 | 21460 | 0.1085 |
| 1.0 | 4120 | 2960 | 1945 | 21840 | 0.0890 |
| 2.0 | 3800 | 2640 | 1625 | 22160 | 0.0735 |
| 5.0 | 3420 | 2260 | 1245 | 22540 | 0.0553 |
| 10.0 | 3200 | 2040 | 1025 | 22760 | 0.0452 |
| 20.0 | 3020 | 1860 | 845 | 22940 | 0.0368 |
| 40.0 | 2920 | 1760 | 745 | 23040 | 0.0324 |
| 75.0 | 2790 | 1630 | 615 | 23170 | 0.0266 |
| 200.0 | 2640 | 1480 | 465 | 23320 | 0.0200 |
| $\infty$ | 2175 | | | | |

$\tau^*_{so}$ = 5015 $\tau^*_{s\infty}$ = 1015 $\tau^*_{\mu}$ = 1160

---

* All quantities must be multiplied by $10^{-4}$

ERROR ANALYSIS - QUICK QUENCHED SAMPLES

SMOOTHED EXPERIMENTAL DATA CASE

Prediction Equations:

| Shear Rate | Correlation Equation |
|---|---|
| 25 $sec^{-1}$ | log M = -0.270 log t - 1.022 |
| 60 $sec^{-1}$ | log M = -0.287 log t - 1.022 |
| 150 $sec^{-1}$ | log M = -0.296 log t - 1.022 |
| 300 $sec^{-1}$ | log M = -0.286 log t - 1.022 |

where: $$M = \left(\frac{\tau_s - \tau_{s\infty}}{\frac{\tau_{so}^2}{\tau_{s\infty}} - \tau_s}\right)$$

25 $sec^{-1}$

| Time (min) | M | $\tau^*_{Pred}$ | $\tau^*_{Exp}$ | \|Error\| % |
|---|---|---|---|---|
| 0.5 | 0.1145 | 1345 | 1275 | 5.5 |
| 5.0 | 0.0614 | 933 | 980 | 4.8 |
| 20.0 | 0.0423 | 777 | 750 | 3.6 |
| 75.0 | 0.0297 | 666 | 612 | 8.8 |
| 200.0 | 0.0228 | 603 | 540 | 11.5 |
| $t_m$* | 0.051 | 847 | 880 | 3.8 |
| | | | Average = | 6.3 |

60 $sec^{-1}$

| M | $\tau^*_{Pred}$ | $\tau^*_{Exp}$ | \|Error\| % |
|---|---|---|---|
| 0.116 | 1860 | 1950 | 4.6 |
| 0.0597 | 1340 | 1525 | 13.2 |
| 0.0403 | 1146 | 1200 | 4.5 |
| 0.0276 | 1014 | 1035 | 2.1 |
| 0.0208 | 948 | 945 | 0.3 |
| | | Average = | 5.0 |

150 $sec^{-1}$

| Time (min) | M | $\tau^*_{Pred}$ | $\tau^*_{Exp}$ | Error % |
|---|---|---|---|---|
| 0.5 | 0.117 | 2870 | 3150 | 8.9 |
| 5.0 | 0.0588 | 2157 | 2300 | 6.2 |
| 20.0 | 0.0393 | 1897 | 2020 | 6.1 |
| 75.0 | 0.0266 | 1725 | 1800 | 4.2 |
| 200.0 | 0.0199 | 1635 | 1700 | 3.8 |
| $t_m$* | 0.095 | 2605 | 2925 | 10.9 |
| | | | Average = | 6.7 |

300 $sec^{-1}$

| M | $\tau^*_{Pred}$ | $\tau^*_{Exp}$ | \|Error\| % |
|---|---|---|---|
| 0.116 | 4660 | 4700 | 0.9 |
| 0.0596 | 3510 | 3450 | 1.7 |
| 0.0404 | 3100 | 3070 | 0.9 |
| 0.0278 | 2820 | 2800 | 0.7 |
| 0.0209 | 2680 | 2630 | 1.8 |
| 0.095 | 4240 | 4570 | 7.4 |
| | | Average = | 2.2 |

Overall Average Error = 5.0%

---

* All quantities to be multiplied by $10^{-4}$

# APPENDIX TEN

## TABULATED CALCULATIONS FOR PIPELINE FLOW OF THIXOTROPIC MODEL

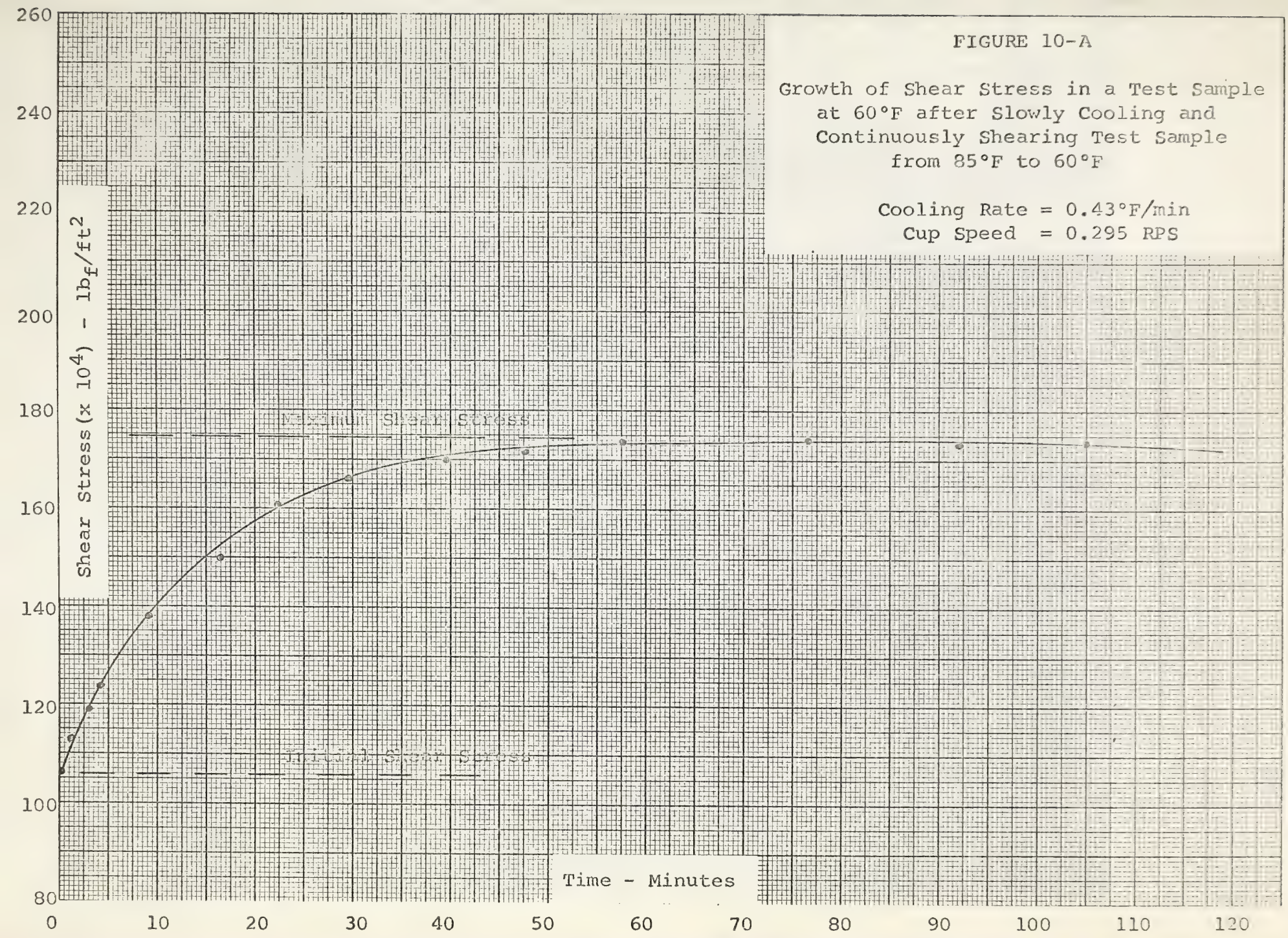
FIGURE 10-A
Growth of Shear Stress in a Test Sample at 60°F after Slowly Cooling and Continuously Shearing Test Sample from 85°F to 60°F
Cooling Rate = 0.43°F/min
Cup Speed = 0.295 RPS
Shear Stress (x $10^4$) - $lb_f/ft^2$
Maximum Shear Stress
Limited Shear Stress
Time - Minutes
260
240
220
200
180
160
140
120
100
80
0
10
20
30
40
50
60
70
80
90
100
110
120

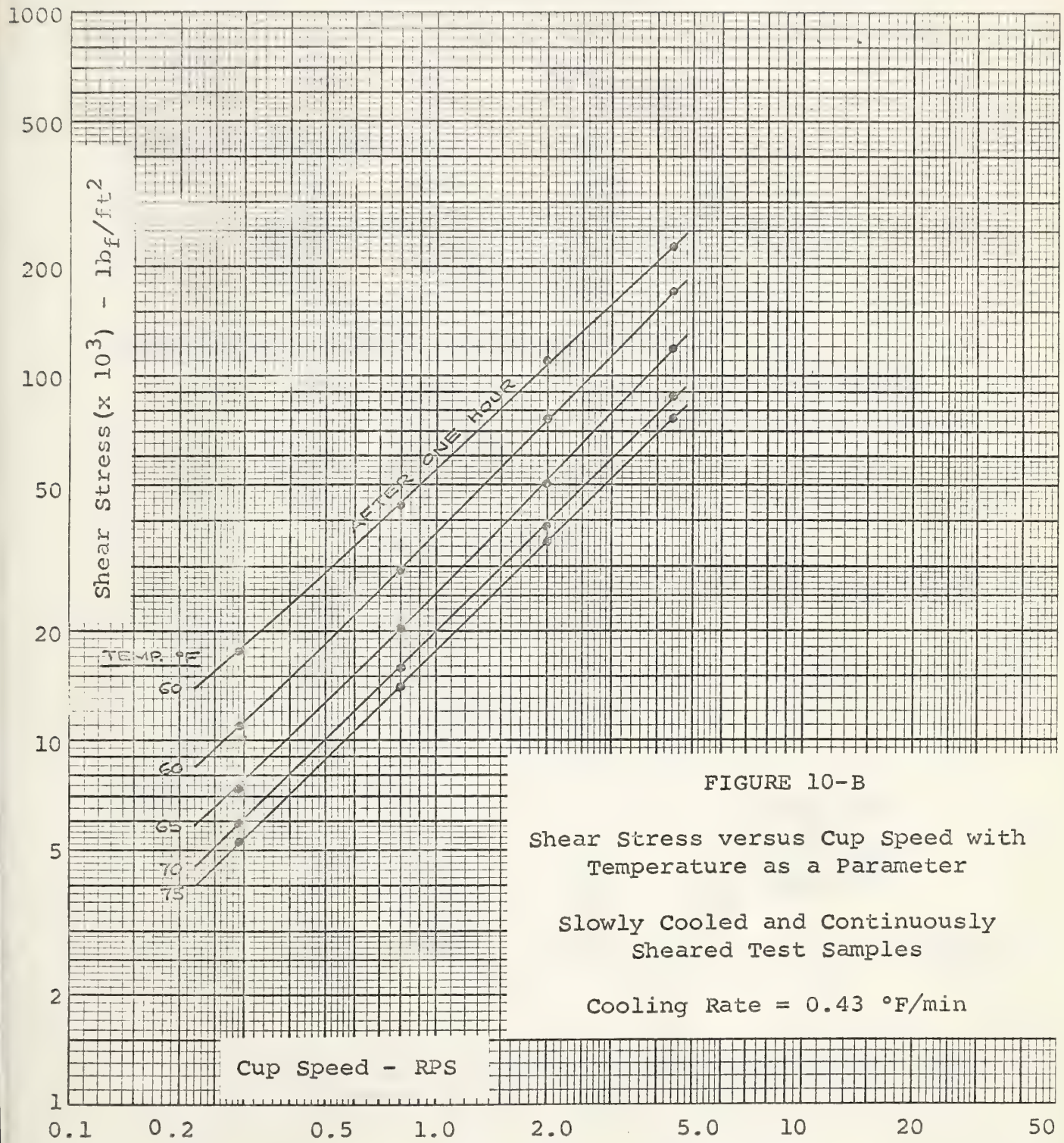


FIGURE 10-B

Shear Stress versus Cup Speed with Temperature as a Parameter

Slowly Cooled and Continuously Sheared Test Samples

Cooling Rate = 0.43 °F/min

## SUMMARIZED DATA ON PIPELINE FLOW OF MODEL

(5.25% Parawax in CWO)

| Velocity (fps) | $N_{RE}$ | f | $(\frac{\Delta P}{L})_{psi/mile}$ | |
|---|---|---|---|---|
| **Solvent Oil (CWO) Case:** | | | | $\mu$ = 19.1 cp |
| 0.5 | 1,040 | 0.0154 | 0.97 | $\rho$ = 53.4 $lb_m/ft^3$ |
| 1.0 | 2,080 | 0.0077 | 1.94 | |
| 2.0 | 4,160 | 0.0098(1) | 9.52 | ← v = 1.01 fps (Transition) |
| 5.0 | 10,400 | 0.0075(1) | 45.5 | |
| 10.0 | 20,800 | 0.0064(1) | 156.0 | |
| **Sheared While Cooling to Test Temperature: t = 0** | | | | $\mu$ = 27.4 cp |
| 0.5 | 725 | 0.022 | 1.33 | $\rho$ = 53.4 $lb_m/ft^3$ |
| 1.0 | 1,450 | 0.011 | 2.67 | |
| 2.0 | 2,900 | 0.0090(1) | 8.76 | ← v = 1.45 fps (Transition) |
| 5.0 | 7,250 | 0.0084(1) | 51.0 | |
| 10.0 | 14,500 | 0.0072(1) | 172.0 | |
| **t = 60 minutes** | | | | $\mu$ = 41.0 cp |
| | | | | $\rho$ = 53.4 $lb_m/ft^3$ |
| 0.5 | 485 | 0.0330 | 2.02 | |
| 1.0 | 970 | 0.0165 | 4.0 | |
| 2.0 | 1,940 | 0.0083 | 8.0 | ← v = 2.16 fps (Transition) |
| 3.5 | 3,400 | 0.010 (1) | 29.7 | |
| 5.0 | 4,850 | 0.0095(1) | 57.5 | |
| 10.0 | 9,700 | 0.0079(1) | 192.0 | |
| **Slow Cooled Case: t = 0** | | | | b = 3460 x $10^{-4}$ |
| | | | | s = 0.62 |
| 0.5 | 77.5 | 0.209 | 12.7 | $\rho$ = 53.4 $lb_m/ft^3$ |
| 1.0 | 202 | 0.0793 | 19.2 | $N_{RE} = 202v^{1.389}$ |
| 2.0 | 531 | 0.0303 | 29.5 | |
| 5.0 | 1,890 | 0.0084 | 51.0 | |
| 10.0 | 4,950 | - | - | ← v = 7.0 fps (Transition) |

(1) Obtained from friction factor plot - Knudsen and Katz "Fluid Dynamics and Heat Transfer" McGraw-Hill (1958) p.176

| V | $N_{RE}$ | f | $(\frac{\Delta P}{L})$ | |
|---|---|---|---|---|
| | | t = ∞ | | b = 852 x $10^{-4}$ |
| | | | | s = 0.742 |
| 0.5 | 360 | 0.0443 | 3.9 | ρ = 53.4 lbm/ft$^3$ |
| 1.0 | 600 | 0.0266 | 6.5 | $N_{RE}$ = 600 $v^{1.258}$ |
| 2.0 | - | - | - | |
| 3.0 | - | - | 14.7 | |
| 5.0 | 4,540 | 0.0065(2) | 39.7 | ← v = 3.58 fps (Transition) |
| 10.0 | 10,900 | 0.0050(2) | 122 | |

Quick Quenched Case: t = 0

| | | | | |
|---|---|---|---|---|
| | | | | b = |
| | | | | s = 0.450 |
| 0.5 | 26.6 | 0.602 | 36.7 | ρ = 53.4 lbm/ft$^3$ |
| 1.0 | 77.0 | 0.209 | 50.7 | $N_{RE}$ = 77$v^{1.55}$ |
| 2.0 | 223 | 0.0717 | 69.5 | |
| 5.0 | 925 | 0.0173 | 105 | |
| 10.0 | 2,740 | 0.00582 | 141 | ← v = 10.6 fps (Transition) |
| | | t = ∞ | | b = 1450 x $10^{-4}$ |
| | | | | s = 0.675 |
| 0.5 | 167 | 0.096 | 5.83 | ρ = 53.4 lbm/ft$^3$ |
| 1.0 | 418 | 0.0384 | 9.34 | $N_{RE}$ = 418$v^{1.325}$ |
| 2.0 | 1,050 | 0.0152 | 14.8 | |
| 4.0 | 2,640 | 0.00605(2) | 23.5 | |
| 7.0 | 5,520 | 0.0050 (2) | 59.6 | ← v = 4.45 fps (Transition) |
| 12.0 | 11,200 | 0.0038 (2) | 133.5 | |

(2) As obtained from friction factor plot of Shaver-Merrill(4)

B29818